

Dissecting Toll-like receptor 3 function in pancreatic regeneration and neoplastic transformation

Ludwig Alexander Kübelsbeck

Vollständiger Abdruck der von der Fakultät für Medizin der Technischen Universität München zur Erlangung des akademischen Grades eines Doktors der Naturwissenschaften (Dr. rer. nat.) genehmigten Dissertation.

Vorsitz: Prof. Dr. Hana Algül

Prüfer*innen der Dissertation:

1. Prof. Dr. Bernhard Holzmann
2. Prof. Angelika Schnieke, Ph.D.

Die Dissertation wurde am 28.03.2023 bei der Technischen Universität München eingereicht und durch die Fakultät für Medizin am 16.05.2023 angenommen.

Eidesstattliche Erklärung

Hiermit erkläre ich, dass ich die vorliegende Arbeit selbstständig und ohne fremde Hilfe verfasst habe. Die Stellen der Arbeit, die anderen Quellen im Wortlaut oder Sinn entnommen wurden, sind durch Angabe der Quelle kenntlich gemacht. Dies gilt auch für Abbildungen.

Ort, Datum

Unterschrift

Table of contents

| | |
|---|-------------|
| List of figures | IV |
| List of tables | V |
| Summary | VI |
| Zusammenfassung | VIII |
| 1 Introduction | 1 |
| 1.1 Acute pancreatitis (AP) | 1 |
| 1.1.1 General information | 1 |
| 1.1.2 Etiology and risk factors for AP | 1 |
| 1.1.3 Pathophysiology | 2 |
| 1.1.4 Regeneration of the exocrine pancreas / Acinar-to-ductal metaplasia (ADM) | 3 |
| 1.1.5 Microenvironment in AP | 4 |
| 1.1.6 Therapy | 6 |
| 1.1.7 Recurrent episodes of AP and chronic pancreatitis (CP) | 6 |
| 1.2 Pancreatic ductal adenocarcinoma (PDAC) | 8 |
| 1.2.1 General information about cancer | 8 |
| 1.2.2 PDAC: etiology and risk factors | 8 |
| 1.2.3 Genetic drivers | 9 |
| 1.2.4 PDAC Carcinogenesis | 10 |
| 1.2.5 PDAC microenvironment | 13 |
| 1.2.6 Therapy of PDAC | 18 |
| 1.2.7 Mouse models to study acute pancreatitis and PDAC | 18 |
| 1.3 Function of the immune system in tissue regeneration and cancer | 23 |
| 1.3.1 Immune therapy for PDAC | 25 |
| 1.3.2 Toll-like receptor 3 (TLR3) | 26 |
| 1.4 Aims | 31 |
| 2 Materials and methods | 32 |
| 2.1 Materials | 32 |
| 2.2 Methods | 32 |
| 2.2.1 Mouse strains and <i>in vivo</i> procedures | 32 |
| 2.2.2 Histological methods | 37 |
| 2.2.3 Molecular biological methods | 39 |
| 2.2.4 Cell biological methods | 44 |
| 2.2.5 Protein biochemical methods | 50 |

| | | |
|----------|---|------------|
| 3 | Results | 53 |
| 3.1 | Myeloid cell TLR3 is critical for pancreatic regeneration after acute pancreatitis in mice | 53 |
| 3.1.1 | Work preceding this thesis | 53 |
| 3.1.2 | Increased expression of ADM markers in global <i>Tlr3</i> -deficient mice after AP | 55 |
| 3.1.3 | TLR3 signaling has no direct effect on acinar transdifferentiation <i>in vitro</i> | 56 |
| 3.1.4 | Increased cytokine expression in global <i>Tlr3</i> -deficient mice after AP | 57 |
| 3.1.5 | Generation of Hoxb8-ER/FL immune progenitor cell lines to study the effect of TLR3 in myeloid cell <i>in vitro</i> | 59 |
| 3.1.6 | Myeloid cell TLR3 induces immune cell clearance after acute pancreatitis | 62 |
| 3.1.7 | TLR3-dependent cell death is induced in the late phase of acute pancreatitis | 63 |
| 3.1.8 | <i>Casp8</i> deficiency has no effect on pancreatic regeneration after acute pancreatitis in mice | 65 |
| 3.1.9 | TLR3 induces cell death of macrophages alternatively via induction of caspase-dependent or RIPK1-dependent pathways | 66 |
| 3.1.10 | Exosomal dsRNA as a new potential ligand for TLR3 activation | 68 |
| 3.2 | Myeloid cell TLR3 limits inflammation-induced carcinogenesis but does not affect oncogene-driven carcinogenesis in the pancreas | 70 |
| 3.2.1 | Oncogene-driven pancreatic carcinogenesis is unaffected by <i>Tlr3</i> deficiency | 70 |
| 3.2.2 | Myeloid cell-specific TLR3 signaling inhibits pancreatitis-driven carcinogenesis | 78 |
| 3.3 | TLR3 in human PDAC | 92 |
| 3.3.1 | Generation of a <i>TLR3</i> -deficient human tumor cell line using the CRISPR/Cas9 system | 93 |
| 3.3.2 | TLR3 is unable to induce cell death of AsPC-1 cells <i>in vitro</i> | 94 |
| 3.3.3 | TLR3 regulates cytokine expression in human tumor cell lines | 95 |
| 4 | Discussion | 97 |
| 4.1 | Myeloid cell TLR3 is important for pancreatic regeneration after acute pancreatitis | 97 |
| 4.1.1 | Immunoregulatory function of myeloid cell TLR3 in pancreatic regeneration | 97 |
| 4.1.2 | Mechanism for TLR3-dependent induction of macrophage cell death | 100 |
| 4.2 | Cell-specific function of TLR3 in oncogene-driven and pancreatitis-driven carcinogenesis | 102 |
| 4.2.1 | Maternal imprinting of the Pdx1-Flp transgene in the dual recombinase system | 103 |
| 4.2.2 | Myeloid cell TLR3 in oncogene-driven carcinogenesis | 103 |
| 4.2.3 | Myeloid cell TLR3 limits inflammation-driven carcinogenesis | 105 |
| 4.3 | TLR3 in human PDAC | 108 |
| 5 | Conclusion and Outlook | 111 |
| 6 | References | 114 |
| 7 | Appendix | 141 |

| | | |
|------|---|-----|
| 7.1 | Description of preinvasive pancreatic lesions | 141 |
| 7.2 | Chemicals | 143 |
| 7.3 | Enzymes | 145 |
| 7.4 | Buffer | 145 |
| 7.5 | Commercial kits | 146 |
| 7.6 | Consumables | 146 |
| 7.7 | Technical equipment | 147 |
| 7.8 | Cell culture reagents | 148 |
| 7.9 | Oligonucleotides for RT-qPCR | 150 |
| 7.10 | Primary and secondary antibodies | 152 |
| 7.11 | Optimized genotyping PCR protocols | 155 |

List of figures

| | |
|---|----|
| Figure 1: Regeneration of the exocrine pancreas after acute pancreatitis. _____ | 4 |
| Figure 2: The complex interplay of injured acinar cells and the immune system in the initial phase of acute pancreatitis. _____ | 5 |
| Figure 3: H&E-stained preinvasive pancreatic lesions at various grades. _____ | 11 |
| Figure 4: The function of the microenvironment in PDAC carcinogenesis. _____ | 17 |
| Figure 5: Mechanism of Cre/loxP-dependent deletion, insertion, and inversion of genetic element 19 | |
| Figure 6: Model of dsRNA binding by TLR3. _____ | 27 |
| Figure 7: Overview of the TLR3-regulated signal transduction pathways after binding of dsRNA. _____ | 28 |
| Figure 8: Mouse model to study the cell-specific function of TLR3 in acute pancreatitis. _____ | 53 |
| Figure 9: Global <i>Tlr3</i> deficiency causes induction of ductal markers and reduction of acinar cell-specific markers after AP. _____ | 56 |
| Figure 10: TLR3 signaling has no direct effect on the transdifferentiation of acinar cells <i>in vitro</i> . _____ | 57 |
| Figure 11: TLR3 in myeloid cells regulates cytokine expression at day 2 after AP induction. _____ | 58 |
| Figure 12: Establishment of the Hoxb8-ER/FL <i>in vitro</i> culture system for the <i>in vitro</i> generation of differentiated macrophages. _____ | 60 |
| Figure 13: Endosomal TLR3 in WT Hoxb8-ER/FL macrophages induces NF- κ B signaling and the expression of proinflammatory cytokines. _____ | 61 |
| Figure 14: TLR3 signaling induces cell death of murine macrophages <i>in vitro</i> . _____ | 62 |
| Figure 15: Bulk pancreas RNA sequencing confirms the TLR3-dependent induction of cell death pathways in the late phase of tissue regeneration after AP. _____ | 64 |
| Figure 16: Myeloid cell-specific <i>Casp8</i> deficiency does not affect pancreatic regeneration after acute pancreatitis in mice. _____ | 65 |
| Figure 17: Mechanistic characterization of TLR3-mediated cell death in macrophages. _____ | 67 |
| Figure 18: Exosomal dsRNA represents a potential source of TLR3 ligands. _____ | 69 |
| Figure 19: Global or partial <i>Tlr3</i> deficiency had no effect on oncogene-driven pancreatic carcinogenesis in the KPF model. _____ | 72 |
| Figure 20: <i>Tlr3</i> deficiency did not affect the activation of tumor-related signal transduction pathways. _____ | 74 |
| Figure 21: <i>Tlr3</i> deficiency did not affect oncogene-driven carcinogenesis in the KPPF model. _____ | 75 |
| Figure 22: TLR3 signaling in myeloid cells limits expression of <i>Cd3</i> and <i>Foxp3</i> in KPPF tumors. _____ | 77 |
| Figure 23: <i>Tlr3</i> deficiency promotes lesion formation at day 7 after pancreatitis induction in the KF mouse model. _____ | 79 |
| Figure 24: Myeloid cell-specific TLR3 signaling inhibits pancreatitis-driven carcinogenesis at day 21. _____ | 80 |

| | |
|---|----|
| Figure 25: Pancreatitis-associated serum marker levels are unaffected by global or partial <i>Tlr3</i> deficiency. _____ | 81 |
| Figure 26: Myeloid cell-specific TLR3 limits the infiltration of macrophages and neutrophils at day 7 of pancreatitis-driven carcinogenesis. _____ | 82 |
| Figure 27: Activation of pro-tumorigenic signal transduction pathways by <i>Tlr3</i> deficiency at day 7 of pancreatitis-induced carcinogenesis. _____ | 85 |
| Figure 28: Myeloid TLR3 limits the formation and progression of pancreatic lesions at day 21 of inflammation-driven carcinogenesis. _____ | 87 |
| Figure 29: Global <i>Tlr3</i> -deficient mice express low levels of acinar lineage markers and high levels of proliferative markers at day 21 of pancreatitis-induced carcinogenesis. _____ | 88 |
| Figure 30: The regulatory effect of myeloid TLR3 on the lesion microenvironment does not persist until day 21 of pancreatitis-driven carcinogenesis. _____ | 89 |
| Figure 31: Myeloid TLR3 inhibits activation of pro-tumorigenic signal transduction pathways. ____ | 91 |
| Figure 32: TLR3 in human PDAC. _____ | 92 |
| Figure 33: Generation of <i>TLR3</i> -deficient AsPC-1 cells by CRISPR/Cas9. _____ | 94 |
| Figure 34: TLR3 signaling has no effect on cell viability of AsPC-1 cells. _____ | 95 |
| Figure 35: TLR3 signaling induces cytokine expression in AsPC-1 cells. _____ | 96 |

List of tables

| | |
|--|----|
| Table 1: Overview of the different mouse strains used in the project. _____ | 33 |
| Table 2: Primer sequences used for genotyping. _____ | 34 |
| Table 3: Conditions of the PCR steps for genotyping. _____ | 35 |
| Table 4: Conditions of the steps for qPCR. _____ | 41 |
| Table 5: Components for the PCR amplification of genomic fragments by Phusion Hot Start II DNA Polymerase prior to the T7 endonuclease assay. _____ | 42 |
| Table 6: Conditions of the PCR reaction using Phusion Hot Start II DNA Polymerase. _____ | 42 |
| Table 7: Conditions for hybridizing PCR products prior to potential digestion by T7 endonuclease. 43 | |
| Table 8: Composition of the progenitor outgrowth medium. _____ | 46 |
| Table 9: Composition of the culture medium for the 3D culture of primary acinar cell clusters. ____ | 49 |
| Table 10: Correlation of the Flp activity and the gender of the experimental mice. Flp activity was proven by PCR detection of recombined <i>FSF-Kras^{G12D}</i> . _____ | 70 |
| Table 11: Correlation of the Flp activity and the gender of the Flp inheriting parents. _____ | 71 |

Summary

The immune system is manifoldly involved in the regeneration of the pancreas after acute pancreatitis (AP), as well as in the initiation and progression of pancreatic ductal adenocarcinoma (PDAC). TLR3 is an endosomal receptor for double-stranded RNA. Components of the TLR3 pathway are mutated in 40% of patients with PDAC and high expression of *TLR3* correlates with reduced patient survival. The aim of the present work was to dissect the cell-specific influence of TLR3 on pancreatic regeneration after AP and PDAC carcinogenesis.

In mice with global *Tlr3* deficiency ($TLR3^{OFF}$), caerulein-induced AP led to enhanced formation and persistence of acinar-to-ductal metaplasia (ADM), regarded as a precancerous alteration of the pancreas. This regenerative defect was associated with a sustaining high number of immune cells in the pancreas, predominantly macrophages. The exclusive expression of *Tlr3* in myeloid cells ($TLR3^{Mye}$) was sufficient to rescue the regenerative defect and to normalize the immune cell infiltration. The *in vitro* stimulation of the TLR3 pathway induced cell death of macrophages, a previously unknown mechanism for the termination of the immune response after AP. RNA expression analysis confirmed the induction of apoptosis-associated markers by TLR3 in wild-type mice in the terminal phase of pancreatic regeneration.

Based on the immunomodulatory function of TLR3 after AP, we examined the cell-specific effect of TLR3 in oncogenic KRAS-dependent, as well as in pancreatitis-induced PDAC carcinogenesis. Global or partial *Tlr3* deficiency did not affect spontaneous KRAS-driven formation and progression of pancreatic lesions in the KPF ($Kras^{G12D}$, $Trp53^{+/FRT}$, $Pdx1-Flp$) mouse model. TLR3 in myeloid cells limited the intratumoral infiltration of $CD3^+$ and $Foxp3^+$ immune cells in KPPF ($Kras^{G12D}$, $Trp53^{FRT/FRT}$, $Pdx1-Flp$) mice, which was not manifested in altered mouse survival.

In the highly inflammatory context of pancreatitis-induced carcinogenesis in KF ($Kras^{G12D}$, $Pdx1-Flp$) mice, expression of *Tlr3* in myeloid cells (KFT^{Mye}) limited pancreatic lesion formation and progression compared with global *Tlr3* deficient mice (KFT^{OFF}) or mice with exclusive expression of *Tlr3* in pancreatic epithelial cells (KFT^{Epi}). TLR3 in myeloid cells limited the recruitment of macrophages and neutrophil granulocytes at day 7 after the induction of inflammation, combined with the reduced activation of the p-ERK pathway and decreased proliferation of pancreatic exocrine cells, compared with KFT^{OFF} and KFT^{Epi} mice. At day 21, KFT^{OFF} mice had an increased lesion area and progressed carcinogenesis, associated with a

high expression of *Il-6* and activation of the protumorigenic p-STAT3 and p-ERK pathways. Exclusive expression of *Tlr3* in myeloid cells was sufficient to abrogate the effect of global *Tlr3* deficiency.

The *in vitro* stimulation of the human PDAC cell line AsPC-1 with the TLR3 agonist poly(I:C) revealed the TLR3-dependent modulation of cytokine expression, thus illustrating a potential modulation of the tumor microenvironment also in human PDAC. This underlines the relevance of the results of the mouse models for human PDAC patients.

On the one hand, the present work displays the key role of TLR3 in myeloid cells in pancreatic regeneration after AP. On the other hand, the results show the immunoregulatory modulation of the tumor microenvironment by TLR3 in myeloid cells to limit inflammation-induced PDAC carcinogenesis. The results highlight the versatile therapeutic potential of TLR3 agonists for targeted modulation of the immune response in inflammatory and malignant diseases.

Zusammenfassung

Das Immunsystem ist vielseitig involviert an der Regeneration des Pankreas nach akuter Pankreatitis (AP), sowie bei der Entstehung und Progression des Pankreaskarzinoms (PDAC). TLR3 ist ein endosomaler Rezeptor für doppelsträngige RNA. Komponenten des TLR3 Signalwegs sind bei 40% der Patienten mit PDAC mutiert und eine hohe Expression von *TLR3* korreliert mit verringertem Überleben der Patienten. Ziel der vorliegenden Arbeit war die zellspezifische Charakterisierung des Einflusses von TLR3 auf die Pankreasregeneration nach AP und auf die PDAC Karzinogenese.

Eine globale *Tlr3*-Defizienz ($TLR3^{OFF}$) führte bei Caerulein-induzierter AP in Mäusen zu einer erhöhten Bildung und Persistenz von *Acinar-to-ductal metaplasia* (ADM), die als präkanzeröse Veränderung des Pankreas betrachtet werden. Der regenerative Defekt war verbunden mit einer anhaltend hohen Anzahl an Immunzellen im Pankreas, vor allem Makrophagen. Die exklusive Expression von *Tlr3* in myeloiden Zellen ($TLR3^{Mye}$) war ausreichend zur Behebung des Regenerationsdefekts und zur Normalisierung der Immunzellinfiltration. Die Stimulation des TLR3 Signalwegs führte bei Makrophagen *in vitro* zur Induktion des Zelltods, einen bisher unbekanntem Mechanismus zur Termination der Immunantwort nach AP. Die RNA-Expressionsanalyse bestätigte die Induktion von Apoptose-assoziierten Markern durch TLR3 bei Wildtyp-Mäusen in der terminalen Phase der Pankreasregeneration.

Aufbauend auf den Ergebnissen der immunmodulatorischen Funktion von TLR3 nach AP erfolgte die Untersuchung der zellspezifischen Funktion von TLR3 bei der KRAS-Onkogen-abhängigen, sowie der Pankreatitis-induzierten PDAC Karzinogenese. Globale oder partielle *Tlr3*-Defizienzen hatten keine Auswirkung auf die spontane, KRAS-getriebene Bildung und Progression von Läsionen im KPF (*Kras*^{G12D}, *Trp53*^{+/^{FRT}}, *Pdx1-Flp*) Mausmodell. TLR3 in myeloiden Zellen limitierte die intratumorale Infiltration von *CD3*⁺ und *Foxp3*⁺ Immunzellen bei KPPF (*Kras*^{G12D}, *Trp53*^{FRT/^{FRT}}, *Pdx1-Flp*) Mäusen, dies manifestierte sich jedoch nicht in einem veränderten Überleben der Mäuse. Im hochinflammatorischen Kontext der Pankreatitis-induzierten Karzinogenese bei KF (*Kras*^{G12D}, *Pdx1-Flp*) Mäusen limitierte die Expression von *Tlr3* in myeloiden Zellen (KFT^{Mye}) die Bildung und Progression von Pankreasläsionen, verglichen mit Mäusen mit globaler *Tlr3*-Defizienz (KFT^{OFF}) oder exklusiver Expression von *Tlr3* in pankreatischen Epithelzellen (KFT^{Epi}). TLR3 in myeloiden Zellen limitierte die Rekrutierung von Makrophagen und neutrophilen Granulozyten an Tag 7 nach Induktion der Inflammation, verbunden mit einer Limitierung der Aktivierung des p-ERK Signalwegs und verringerter

Proliferation von exokrinen Pankreaszellen, verglichen mit KFT^{OFF} und KFT^{Epi} Mäusen. An Tag 21 war die erhöhte Läsionsfläche und Progression der Karzinogenese bei KFT^{OFF} Mäusen verbunden mit der Expression von *Il-6* und Aktivierung des protumorigenen p-STAT3 und des p-ERK Signalwegs. Exklusive Expression von *Tlr3* in myeloiden Zellen war ausreichend, um den Effekt globaler *Tlr3*-Defizienz aufzuheben. Die *in vitro* Stimulation der humanen PDAC Zelllinie AsPC-1 mit dem TLR3 Agonisten poly(I:C) zeigte die Modulation der Zytokinexpression durch TLR3, verdeutlicht damit eine potenzielle Modulation des Tumormikroenvironments auch bei humanem PDAC und untermauert die Relevanz der Ergebnisse der Mausmodelle für humane PDAC-Patienten.

Die vorliegende Arbeit konnte somit zum einen eine Schlüsselrolle von TLR3 in myeloiden Zellen bei der Regeneration des Pankreas nach AP aufdecken. Zum anderen zeigen die Ergebnisse eine Modulation des Tumormikroenvironments durch TLR3 zur Limitierung der Inflammations-induzierten PDAC Karzinogenese. Somit unterstreichen die Ergebnisse der vorliegenden Arbeit das vielseitige therapeutische Potenzial von TLR3 Agonisten zur gezielten Modulation der Immunantwort bei entzündlichen und malignen Erkrankungen.

1 Introduction

1.1 Acute pancreatitis (AP)

1.1.1 General information

Acute pancreatitis (AP) is a suddenly occurring, potentially life-threatening inflammatory disorder of the pancreas caused by the premature activation of digestive enzymes resulting in pancreatic autodigestion (Pförringer, 1899; Xue et al., 2014; Murtaugh and Keefe, 2015; Lee and Papachristou, 2019). Among gastrointestinal diseases, AP is the most common reason for hospitalization, with an increasing incidence rate (Peery et al., 2012; Xiao et al., 2016; Krishna et al., 2017). The meta-analysis from Xiao et al. estimated a global incidence rate of 34 cases per 100,000 persons for AP (Xiao et al., 2016). Typical symptoms include pain in the upper abdominal area in the epigastric and periumbilical regions, along with symptoms of nausea and vomiting (Caroll et al., 2007). The diagnosis of AP is made when 2 of the following 3 criteria are present: (I) characteristic abdominal pain, (II) increased serum levels of the pancreatic enzymes amylase and lipase more than 3 times higher than the basal level and (III) signs of pancreatitis confirmed by imaging techniques (Weiss et al., 2019).

The overall mortality for AP is 5% (interstitial pancreatitis: 3%, necrotizing pancreatitis: 17%; Banks and Freeman, 2006). The mortality rate in AP highly depends on the presence of an additional infection of the pancreas (Banks and Freeman, 2006). In infected necrotizing pancreatitis, mortality is highest at 30%, while in sterile necrotizing pancreatitis the mortality rate is 12% (Banks and Freeman, 2006).

1.1.2 Etiology and risk factors for AP

The most prevalent risk factors for AP are gallstones and alcohol abuse, underlying 30-50% of cases (Caroll et al., 2007; Weiss et al., 2019). For women, gallstones are causative in 50% of cases, whereas in men, alcohol is predominantly etiologic for the development of AP (Weiss et al., 2019). Additional risk factors include hypertriglyceridemia, smoking, abdominal trauma, genetic predisposition, and infections (Mounzer and Whitcomb, 2013; Weiss et al., 2019).

1.1.3 Pathophysiology

Intra vitamous self-digestion of the pancreas was hypothesized as the cause of AP more than 100 years ago (Pförriinger, 1899). However, the exact pathogenesis of AP has not yet been fully uncovered.

In the initial phase of AP, zymogenes like trypsin are activated intracellularly in acinar cells (Saluja et al., 1999; Lerch and Gorelick, 2000). Mutations in genes of pancreatic digestive enzymes are correspondingly associated with an inherited genetic predisposition to AP (Whitcomb, 2010). The premature activation of pancreatic digestive enzymes initiates acinar cell injury, inflammation, hemorrhage, edema, and necrosis (Xue et al., 2014).

Pancreatic self-digestion provokes intrapancreatic inflammation and the recruitment of immune cells (Kong et al., 2018). Danger-associated molecular patterns (DAMPs) are molecular structures that are associated with tissue damage or infections and are recognized by conserved pattern recognition receptors (PRRs) of the innate immune system triggering the immediate activation of the immune system upon recognition of danger signals (Hoque et al., 2012). Pancreatic self-digestion releases DAMPs, which are detected by PRR and initiate intrapancreatic inflammation and immune cell recruitment (Hoque et al., 2011; Hoque et al., 2012; Watanabe et al., 2017). For example, DNA from injured acinar cells is detected in the early phase of AP by the endosomal PRR TLR9 in macrophages, inducing the subsequent inflammatory response (Hoque et al., 2011). Additionally, injured acinar cells secrete cytokines to directly recruit and activate immune cells (Lee and Papachristou, 2019).

The finely balanced, precisely regulated immune response is of pivotal importance in AP. Excessive activation of the inflammatory cascade causes systemic complications in 10-20% of AP patients, termed systemic inflammatory response syndrome (SIRS; Banks and Freeman, 2006). SIRS can progress to multiple organ failure, the major cause of AP mortality (Johnson and Abu-Hilal, 2004). In contrast, compensatory immune-inhibitory mechanisms in the late phase of the disease can lead to the so-called compensatory anti-inflammatory response syndrome (CARS), resulting in local complications or sepsis (Veit et al., 2014). The complex interplay of pro- and anti-inflammatory mechanisms in AP requires precise regulation of the immune response.

1.1.4 Regeneration of the exocrine pancreas / Acinar-to-ductal metaplasia (ADM)

The molecular processes involved in the regeneration of the exocrine pancreas have been the subject of extensive research efforts during the past decades. Sarles et al. reported the increased formation of ductal structures and the reduced number of normal acinar cells in alcohol-induced pancreatitis in rats (Sarles et al., 1971). Similarly, ductal-like tubular complexes of undefined origin were observed in human chronic pancreatitis and during regeneration of the pancreas after caerulein-induced AP in rats (Bockman et al., 1982; Elsässer et al., 1986). Already at that time, morphological changes in acinar cells were noticed and it was postulated that the tubular complexes are not formed by proliferating ductal cells but originate from de-differentiating acinar cells (Bockman et al., 1982). This concept of reversible de-differentiation of acinar cells to ductal-like progenitor cells is to date established as acinar-to-ductal metaplasia (ADM, Fig. 1). During the regeneration of the exocrine pancreas, acinar cells recapitulate features of undifferentiated pancreatic progenitor cells in early organogenesis (Jensen et al., 2005). It is assumed that during pancreatic regeneration, the ductal-like progenitor structures proliferate and finally redifferentiate to terminally differentiated, functional acinar cells (Kong et al., 2018; Zhou and Melton, 2018). Accordingly, the regenerative capacity of the pancreas after AP is limited by the genetic deletion of factors that are important for maintaining acinar cell differentiation (Figura et al., 2014; Krah et al., 2015). This is associated with the inhibition of acinar cell redifferentiation and the persistence of ADM structures (Figura et al., 2014; Krah et al., 2015).

While ADM is known for decades as a mechanism involved in the regeneration process of the pancreas after pancreatitis, recent evidence highlighted the crucial role of ADM as an initial step of pancreatic carcinogenesis (Wagner et al., 2000; Kopp et al., 2012). Wagner et al. revealed in a mouse model with pancreas-specific expression of *Tgf α* that hyperproliferative tubular neoplasms originate from acinar cells and progress to invasive tumors with ductal morphology (Wagner et al., 2000). Pancreatic carcinogenesis is described in detail in chapter 1.2.4.

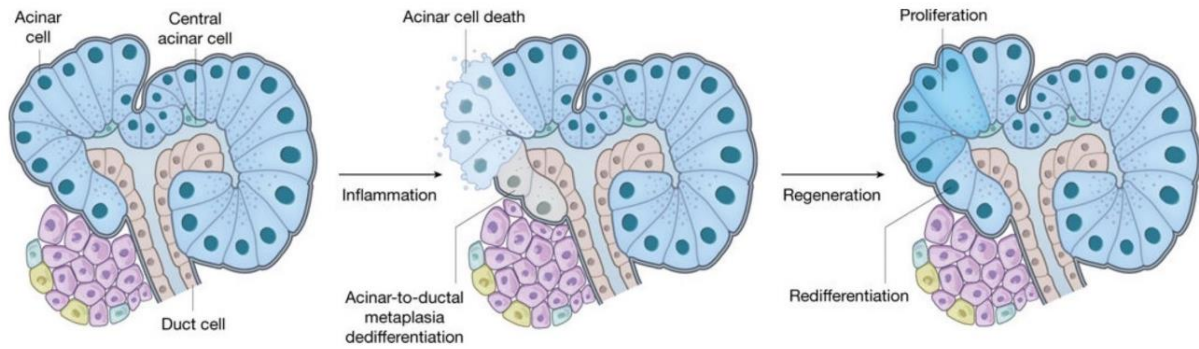


Figure 1: Regeneration of the exocrine pancreas after acute pancreatitis. Acute pancreatitis leads to acinar cell death and the induction of inflammation. During the regeneration of the exocrine pancreas, acinar cells reversibly de-differentiate to ductal-like progenitor cells, a process termed acinar-to-ductal metaplasia. These structures are characterized by their ductal morphology and the expression of genes that are typically expressed during early pancreatic organogenesis. These ductal-like progenitor cells proliferate and differentiate into functional acinar cells, to re-establish the pancreatic parenchyma after AP. Figure from Zhou and Melton 2018.

The regeneration of the pancreas after AP ends with the termination of the immune response, resolution of residual inflammation, and the redifferentiation of ductal-like progenitor cells to acinar cells to re-establish the pancreatic parenchyma (Kong et al., 2018).

1.1.5 Microenvironment in AP

The immune system is extensively involved in the pathogenesis of AP (Fig. 2). In the initial phase of AP, neutrophilic granulocytes infiltrate the pancreas (Gukovskaya et al., 2002; Zheng et al., 2013). In murine models, the depletion of neutrophils was reported to reduce the severity of AP (Gukovskaya et al., 2002; Abdulla et al., 2011). Neutrophils stimulate the premature activation of trypsin via NADPH oxidase (Gukovskaya et al., 2002). In addition, neutrophilic extracellular traps (NETs) increase the inflammation in AP (Merza et al., 2015).

Following neutrophils, monocytes/macrophages are recruited to the pancreas (Habtezion, 2015). Macrophages are of central importance in AP with versatile functions (Liou et al., 2013; Folias et al., 2014; Habtezion, 2015; Sandler et al., 2018). In AP, macrophages are the most abundant immune cells in the pancreas (Folias et al., 2014; Sandler et al., 2018). The degree of macrophage activation is a critical determinant for the severity of AP, with excessive activation of macrophages leading to increased inflammation and severity of AP (McKay et al., 1996; Xue et al., 2014). Activated macrophages secrete cytokines to recruit other immune cells and to promote pancreatic inflammation (Criscimanna et al., 2014; Das et al., 2015). Using isolated monocytes from the blood of AP patients, a direct correlation between AP severity and the secretion of TNF, IL-6, and IL-8 by monocytes was demonstrated (McKay et al., 1996). Further, macrophages can directly induce ADM by secretion of TNF and CCL5 (Liou et al., 2013). Folias et al. showed that *in vivo* depletion of macrophages by clodronate liposomes reduces the formation of ADM and improves pancreatic regeneration after AP (Folias et al., 2014). MCP1 inhibitors prevent the recruitment of macrophages and reduce

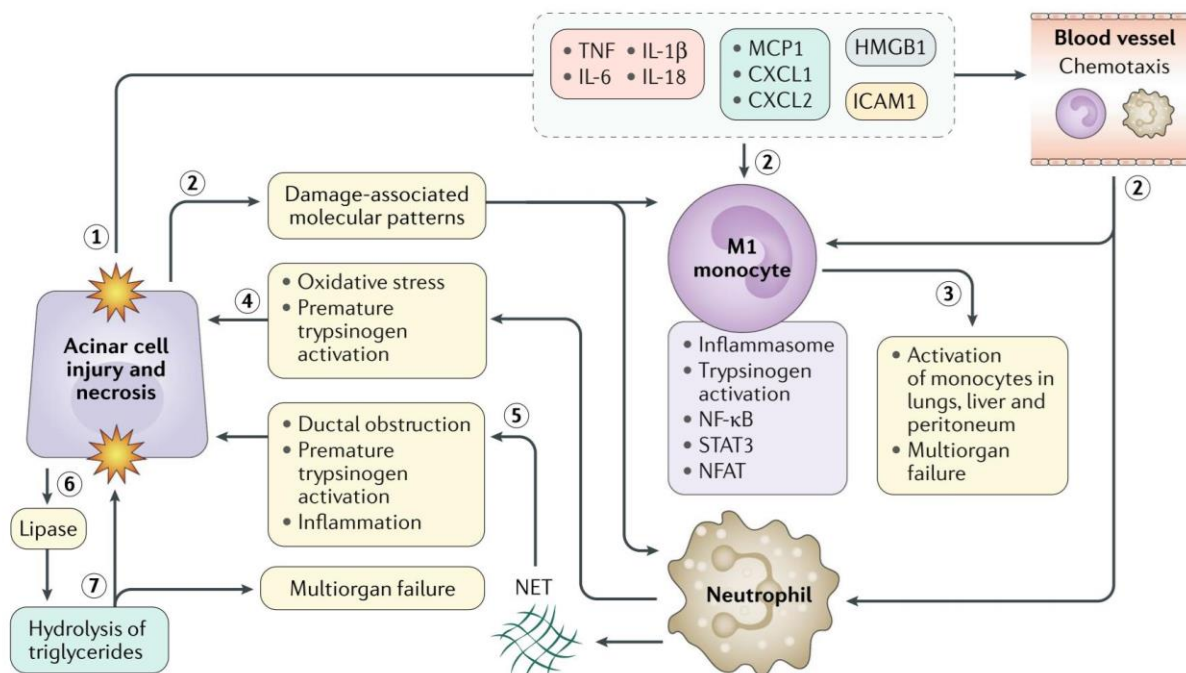


Figure 2: The complex interplay of injured acinar cells and the immune system in the initial phase of acute pancreatitis. Acinar cell injury and necrosis leads to the liberation of danger-associated molecular patterns (e.g. dsRNA, HMGB1), the secretion of proinflammatory cytokines (e.g. TNF, IL-1 β , IL-6, IL-8) and chemokines (e.g. MCP1, CXCL1, CXCL2), and the upregulation of adhesion molecules (ICAM1) to recruit immune cells to the pancreas (1) and to subsequently activate the immune response (2), via NF- κ B and STAT3 signaling. Activated macrophages enhance the immune reaction through the recruitment and activation of further immune cells into the pancreas. Additionally, immune cells in other organs are activated which can potentially lead to remote organ injury and multiorgan failure (3). Activated neutrophils can potentiate the premature activation of trypsin (4) via NADPH oxidase-mediated oxidative stress (Gukovskaya 2002) and can release neutrophil extracellular traps (NETs) causing ductal obstruction and inflammation (5). Figure adapted from Lee and Papachristou 2019.

acinar cell damage leading to a decreased severity of AP (Bhatia et al., 2005).

Besides macrophages and neutrophils, CD4⁺ T cells and dendritic cells (DCs) are infiltrating the pancreas in AP (Demols et al., 2000; Bedrosian et al., 2011). Nude mice are lacking T cells, leading to reduced severity of AP (Demols et al., 2000). *In vivo* depletion of DCs causes larger lesion areas and increased necrosis of exocrine cells, demonstrating the protective influence of DCs on the pancreas in AP (Bedrosian et al., 2011).

1.1.6 Therapy

AP patients are treated symptomatically with analgesia, close monitoring, nutritional support, and fluid replacement to prevent hypovolemia caused by vomiting, diaphoresis, and increased vascular permeability (Banks and Freeman, 2006). In a meta-analysis, enteral nutrition compared to parenteral nutrition was shown to result in significantly fewer infections, reduced need for surgical intervention, and a reduced length of hospital stay, while mortality was unaffected (Marik and Zaloga, 2004). Further, necrotic areas of the pancreas can be surgically resected in necrotizing AP or chronic pancreatitis (Murtaugh and Keefe, 2015).

Causal therapy approaches for the treatment of AP patients are missing. Despite the central etiologic role of proteases in AP, a meta-analysis of studies on the therapeutic use of protease inhibitors showed that they fail to reduce mortality (Singh and Chari, 2005). Given the key involvement of the immune system in the pathogenesis of AP, targeting the immune system provides a potential option for therapeutic interventions. Maintaining the balance between complications from systemic inflammation, such as multiple organ failure after SIRS, and complications from compensatory immunosuppression, such as sepsis after CARS, requires a profound knowledge of the regulation of the immune system in the different phases of AP for the development of precise individualized therapy approaches (Veit et al., 2014).

1.1.7 Recurrent episodes of AP and chronic pancreatitis (CP)

Acute pancreatitis is not only a life-threatening disease but can also result in recurrent episodes of AP (Petrov and Yadav, 2019). About 21% of patients with AP experience recurrent

episodes of AP and 36% of patients with recurrent AP develop chronic pancreatitis (CP), a progressive inflammatory, fibrotic disease leading to dysfunction of the exocrine and endocrine system of the pancreas (Kleeff et al., 2017; Petrov and Yadav, 2019). The main symptoms of CP are severe abdominal pain, which occurs either attack-like, resembling the symptoms of AP, or is present as constant pain (Braganza et al., 2011). In addition, CP can lead to endocrine and exocrine insufficiency of the pancreas and a substantially impaired quality of life for patients (Kleeff et al., 2017). CP represents a major risk factor for the development of pancreatic cancer (Lowenfels et al., 1993; Kirkegård et al., 2017). CP patients have an 8-fold increased probability of developing PDAC 5 years after the diagnosis of CP (Kirkegård et al., 2017).

1.2 Pancreatic ductal adenocarcinoma (PDAC)

1.2.1 General information about cancer

Cancer is a leading cause of death worldwide, with an annual global incidence rate of 19,3 million cases and approximately 10 million deaths in the year 2020 (Sung et al., 2021). One out of five persons develops cancer during lifetime (Sung et al., 2021). Most tumors arise from the malignant transformation of epithelial cells, termed carcinomas.

The causative factors for cancer development are diverse, ultimately leading to the activation of genes that promote tumor progression, so-called oncogenes, and the inactivation of genes with tumor preventive function, termed tumor suppressor genes. These initial genetic changes provide tumor cells with a selective growth advantage over non-transformed cells, enabling the formation and progression of neoplastic lesions (Nowell, 1976). Genetic instability provokes further mutations, which prevail in case of a resulting growth advantage and thus result in the accumulation of genetic mutations in tumor cells (Nowell, 1976; Vogelstein et al., 1988). Thereby, tumor cells acquire essential qualities that enable invasive tumor growth and metastatic dissemination (Hanahan and Weinberg, 2011). These ‘hallmarks of cancer’ include sustaining proliferation, evading growth suppression, resistance to cell death, angiogenesis, replicative immortality, and invasive growth (Hanahan and Weinberg, 2011). The high genomic instability and tumor-promoting inflammation are underlying mechanisms of tumor development (Hanahan and Weinberg, 2011). Additionally, changes in tumor cell metabolism and immune evasion are important concepts for tumor growth (Hanahan and Weinberg, 2011).

1.2.2 PDAC: etiology and risk factors

According to the GLOBOCAN statistics, pancreatic cancer is the 7th leading cause of cancer-related deaths worldwide with an annual global incidence rate of 496,000 almost equal to the mortality rate of 466,000 (Sung et al., 2021). The incidence rate and mortality rate are 4-5 times higher in highly developed countries, with the highest incidence in Europe (Sung et al., 2021). Overall, pancreatic cancer is causative for 4.7% of all cancer-related deaths and is expected to become the 2nd leading cause of cancer-related deaths by 2030 (Rahib et al., 2014; Sung et al., 2021). The 5-year overall survival rate slightly increased within recent years to 9% but is still the lowest among all cancer types, demonstrating the urgent need for

a better understanding of the fundamental molecular pathways for the development of novel therapeutic strategies (Rawla et al., 2019; Miller et al., 2020). 90% of all pancreatic tumors are classified as pancreatic ductal adenocarcinoma (PDAC), originating from cells of the exocrine pancreas (Hidalgo et al., 2015).

The etiology of PDAC is multifactorial. The most important risk factors include smoking (Kuzmickiene et al., 2013), chronic pancreatitis, obesity, diabetes mellitus, and genetic predisposition (Shi et al., 2008; Li et al., 2009; Solomon et al., 2012; Rawla et al., 2019).

Obesity in early adulthood correlates with an increased risk for early onset pancreatic cancer (Li et al., 2009). It is estimated that a genetic predisposition underlies 10% of pancreatic cancer cases (Shi et al., 2008). Germline mutations in the genes *BRCA1*, *BRCA2*, *CDKN2A*, or *APC* increase the risk for pancreatic cancer (Solomon et al., 2012).

1.2.3 Genetic drivers

The most frequently mutated genes in human PDAC are *KRAS* (89.8%), *TP53* (66.1%), *SMAD4* (22.5%), and *CDKN2A* (18.5%; Cerami et al., 2012; Gao et al., 2013; Bailey et al., 2016). Based on RNA sequencing data of 456 human pancreatic cancer samples, Bailey et al. identified the most frequent genetic driver pathways: *KRAS*, *TGF β* , *WNT*, *NOTCH*, *ROBO/SLIT* signaling, G1/S transition, *SWI-SNF*, chromatin modification, DNA repair and RNA processing (Bailey et al., 2016).

Kirsten rat sarcoma viral oncogene homolog (*KRAS*) is a membrane-bound regulatory guanine triphosphatase (GTPase; Chang et al., 1982; Huang et al., 2021). In response to stimulation by growth signals, like the binding of EGF to the EGF receptor, guanine nucleotide exchange factors (GEFs) replace the *KRAS*-associated GDP by GTP, inducing conformational changes of *KRAS*, which enable the activation of downstream signal transduction pathways (Bos et al., 2007). *KRAS* activates the RAF-MEK-ERK and the PI3K-AKT-mTOR signaling pathways to promote cell proliferation, influence cell differentiation, inhibit apoptotic cell death, and regulate cell migration (Huang et al., 2021). GTPase activating proteins (GAPs) promote the intrinsic GTPase activity of *KRAS*, leading to the hydrolysis of GTP to GDP and thereby to the inactivation of the *KRAS* signal transduction (Bos et al., 2007). The majority of *KRAS* mutations in PDAC patients occur in codon 12, resulting in the amino acid exchange G12D or G12V (Almoguera et al., 1988; Witkiewicz et al., 2015). These oncogenic mutations prevent the intrinsic GTPase activity of *KRAS* leading to the inhibition of the negative-feedback

mechanism, which results in the constitutive activity of the KRAS signaling pathway and the permanent, uncontrolled activation of cell proliferation (Hanahan and Weinberg, 2011).

The tumor suppressor p53 is a tetrameric transcription factor composed of four identical subunits (Chan et al., 2004). Stress signals like DNA damage or aberrant growth signals activate p53, leading to the expression of target genes to induce cell cycle arrest (f. e. *CDKN1A*), senescence, or apoptosis (f. e. *PUMA*, *BAX*; Freed-Pastor and Prives, 2012). Germline mutations of *TP53* cause the autosomal-dominant inherited Li-Fraumeni syndrome, leading to a predisposition of tumor development at different entities at very early ages and a reduced life expectancy (Malkin et al., 1990). *TP53* is frequently mutated in pancreatic cancer (Scarpa et al., 1993; Witkiewicz et al., 2015; Bailey et al., 2016). The majority of mutations affect the DNA binding domain of p53 and are assumed to exert either a dominant-negative effect on the remaining p53 from the WT allele or to induce a pro-tumorigenic gain-of-function (Chan et al., 2004; Polireddy et al., 2019).

1.2.4 PDAC Carcinogenesis

Pancreatic carcinogenesis occurs through the formation of preinvasive precursor lesions. Based on morphologic characteristics, they are classified as pancreatic intraepithelial neoplasms (PanIN), intraductal papillary mucinous neoplasms (IPMNs), or mucinous cystic neoplasms (MCN; Hruban et al., 2001). Recently, another preinvasive precursor lesion with acinar cell origin was characterized, termed atypical flat lesions (AFL; Figura et al., 2017).

Based on histological criteria, PanIN structures are categorized as PanIN1A, PanIN1B, PanIN2, and PanIN3/carcinoma *in situ* (Appendix 7.1). The classification criteria of PDAC precursor lesions according to Hruban et al. 2001 are summarized in Figure 3 (Fig. 3, Appendix 7.1).

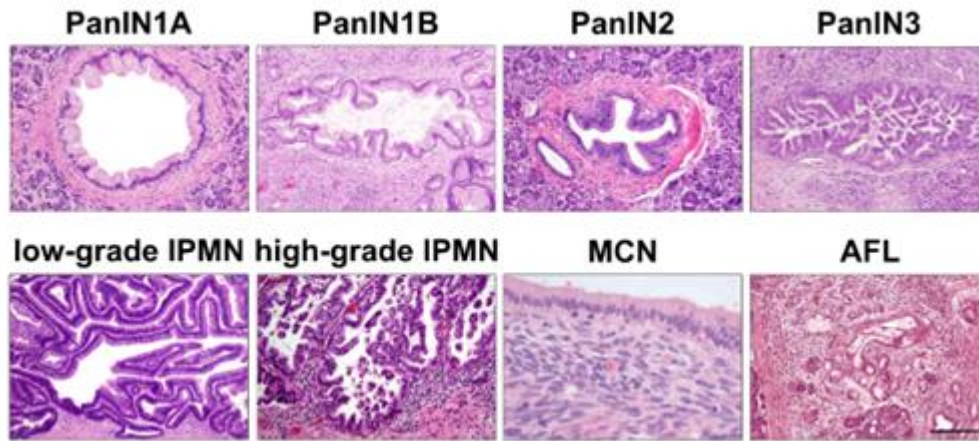


Figure 3: H&E-stained preinvasive pancreatic lesions at various grades. Pancreatic intraepithelial neoplasia 1A (PanIN1A) are flat epithelial lesions with tall columnar cells, basally located, round nuclei, and abundant supranuclear mucin. PanIN1B lesions are papillary, micropapillary, or basally pseudostratified. Other histological characteristics of PanIN1B are identical to PanIN1A. PanIN2 are papillary, mucinous epithelial lesions with nuclear abnormalities (loss of polarity, nuclear crowding, enlarged nuclei, pseudo stratification, hyperchromatism). PanIN1A, PanIN1B, and PanIN2 were collectively referred to as low-grade PanIN. PanIN3 (also classified as carcinoma *in situ* or high-grade PanIN) has usually a papillary or micropapillary architecture, resembling carcinoma without invasion through the basement membrane. Small epithelial clusters and lumina necrosis are present in the lumen of PanIN3 lesions. PanIN3 is associated with nuclear abnormalities, including abnormal mitosis. Intraductal papillary mucinous neoplasms (IPMNs) are mucinous epithelial neoplasms located in the main pancreatic duct or its major branches. IPMNs are usually larger than PanIN lesions. Mucinous cystic neoplasms (MCNs) are not connected to the main duct system and have a characteristic ovarian stroma surrounding the cyst. Atypical flat lesions (AFLs) are tubular, highly proliferative, ductal lesions, which arise in ADM areas. The stroma of AFLs is loose but highly cellular. The images were adapted from Basturk et al. 2015 (PanIN1A, PanIN1B, PanIN2, PanIN3, low-grade IPMN, high-grade IPMN, AFL) and Distler et al. 2014 (MCN). The classification was adapted from Hruban et al. 2001.

1.2.4.1 The cell of origin in PDAC

PDAC histologically displays a ductal morphology. However, recent findings indicate that oncogenically transformed acinar cells represent the cellular origin of PDAC (Murtaugh and Leach, 2007; Habbe et al., 2008; Kopp et al., 2012; Ferreira et al., 2017; Peng et al., 2019; Schlesinger et al., 2020). Oncogenic KRAS^{G12D} primarily induces the metaplastic transformation of acinar cells, whereas centroacinar cells and ductal cells are refractory to KRAS-induced oncogenic transformation (Kopp et al., 2012). Oncogenic KRAS initiates the irreversible transformation of acinar cells into ductal ADM structures (Habbe et al., 2008). The formation of ductal-like progenitor structures by de-differentiation of acinar cells has been described above for the regeneration of the exocrine pancreas after AP (Chapter 1.1.4). In contrast to the subsequent redifferentiation of ADM structures to acinar cells as in pancreatic regeneration, KRAS^{G12D} causes the persistence of ADM lesions and their progression to PanIN structures. Kopp and von Figura et al. demonstrated in a mouse model that exclusive expression of the oncogene *Kras*^{G12D} and the tracer *YFP* in pancreatic acinar cells causes the

development of YFP⁺, mucinous PanIN structures with ductal morphology, whereas ductal cell-specific expression of *Kras*^{G12D} only rarely resulted in PanIN formation (Kopp et al., 2012). Acinar cells were found to be approximately 100-fold more susceptible to oncogenic transformation by KRAS^{G12D} compared to ductal cells (Kopp et al., 2012). Using mice with acinar cell-specific expression of *Kras*^{G12D} and *tdTomato* as a tracer, Schlesinger et al. demonstrated by single-cell RNA sequencing and subsequent trajectory analysis the transformation of acinar cells to tdTomato⁺ metaplastic cells in the context of PDAC carcinogenesis (Schlesinger et al., 2020).

1.2.4.2 Pancreatic intraepithelial neoplasia

PanIN lesions are the most frequent type of preinvasive lesion in humans, characterized by their high expression of mucins (Distler et al., 2014). *MUC5AC*, for example, is highly expressed by low-grade and high-grade PanINs but is absent in normal duct structures (Distler et al., 2014). All PanIN grades are preinvasive structures that do not invade through the basement membrane (Hruban et al., 2001). The mutation of *KRAS* occurs initially in pancreatic carcinogenesis and, accordingly, is often detectable in early PanIN stages (Löhr et al., 2005). However, oncogenic *KRAS* is not sufficient for the development of invasive tumors. Progression from low-grade PanIN lesions to high-grade PanINs and PDAC requires the gradual acquisition of genetic mutations, leading to the activation of oncogenes and inactivation of tumor suppressor genes like *TP53*, *CDKN2A* or *SMAD4* (Storz and Crawford, 2020). While *CDKN2A* is frequently inactivated already in low-grade PanINs, mutations of *TP53* and *SMAD4* occur late in carcinogenesis (Distler et al., 2014). In parallel, the progression of PDAC carcinogenesis is associated with a microenvironmental shift from a proinflammatory environment present in the early stages of carcinogenesis, to a highly desmoplastic, immunosuppressive microenvironment in high-grade lesions and invasive tumors (Storz and Crawford, 2020).

1.2.4.3 Intraductal papillary mucinous neoplasm

IPMNs are mucinous, premalignant lesions that form in the main pancreatic duct or its major branches and are usually significantly larger than PanIN structures (Hruban et al., 2001). Main duct (MD)-IPMNs and branch duct (BD)-IPMNs are classified according to the localiza-

tion of the lesion (Distler et al., 2013). Based on histological and IHC characteristics (MUC1, MUC2, MUC5AC, nuclear CDX-2), IPMNs are subclassified into intestinal, pancreatobiliary, oncocytic, and gastric IPMNs (Distler et al., 2013). Invasive carcinomas arising from pancreatobiliary IPMNs correlate with significantly lower patient survival (Distler et al., 2013).

1.2.4.4 Mucinous cystic neoplasms

MCNs are infrequent precursor lesions, detected predominantly in women (95%) and mainly localized in the distal pancreas (97%; Crippa et al., 2008). Unlike IPMNs, MCNs are not connected to the main pancreatic duct (Distler et al., 2014). MCN lesions display an 'ovarian-like' stroma that characteristically expresses progesterone and estrogen receptors (Distler et al., 2014). The 5-year survival rate for patients with noninvasive MCN is 100%; for patients with invasive cancer associated with MCN, the 5-year survival rate is 57% (Crippa et al., 2008).

1.2.4.5 Atypical flat lesions

AFLs are infrequently occurring, highly proliferative ductal lesions, usually associated with a loose stroma that has a high cell content (Figura et al., 2017). AFLs arise in ADM areas and can be distinguished from ADM by their characteristic stromal reaction and the occurrence of cytological atypia (Basturk et al., 2015).

1.2.5 PDAC microenvironment

Recent findings in tumor biology are shifting the focus from an isolated view of the tumor as a mere accumulation of unregulated proliferating cells to a holistic understanding of the tumor as a complex interplay of tumor cells and the tumor microenvironment, consisting of infiltrating immune cells and the extracellular matrix (Dvorak, 1986; Werb, 1999). Due to the high stroma content, PDAC tumors consist of only about 30% of malignant cells (Karamitopoulou, 2019; Peng et al., 2019). The tumor microenvironment (TME) hereby represents a highly dynamic, reactive system with a decisive impact on tumor biology (Werb, 1999; Ligorio et al., 2019).

Rudolf Virchow first recognized high leukocyte infiltration in tumors over 150 years ago and, based on these observations, hypothesized a connection between inflammation and tumor-

igeneis (Virchow, 1864-1865). Tumor-promoting inflammation is to date broadly established as an important mechanism of carcinogenesis for many tumor entities, including PDAC (Coussens and Werb, 2002; Guerra et al., 2007; Hanahan and Weinberg, 2011). Fundamental mechanisms of tumor-promoting inflammation include the immune cell-mediated secretion of growth factors, survival factors to limit the cell death of tumor cells, proangiogenic factors, the remodeling of the extracellular matrix to facilitate invasive growth, and the secretion of signal transducers that induce epithelial-to-mesenchymal transition (EMT; Hanahan and Weinberg, 2011). The central role of the tumor-promoting inflammation led to the concept of tumors as wounds that do not heal (Dvorak, 1986).

Inflammation is decisively involved in the early stages of PDAC carcinogenesis. Chronic pancreatitis, for example, significantly increase the risk of PDAC (Lowenfels et al., 1993; Kirkegård et al., 2017). Guerra et al. demonstrated that activation of oncogenic KRAS in adult mice is insufficient to cause the formation of invasive PDAC, due to cellular senescence barriers (Guerra et al., 2007; Guerra et al., 2011). Interestingly, in the described model, the additional induction of mild inflammation was sufficient to overcome these senescence barriers and to enable the development of invasive PDAC (Guerra et al., 2007; Guerra et al., 2011).

1.2.5.1 The microenvironment in the early phase of carcinogenesis

Macrophages are the most abundant immune cells in early, preinvasive stages of carcinogenesis (Schlesinger et al., 2020). Oncogenic KRAS in metaplastic cells promotes the recruitment of macrophages in pancreatic precursor lesions (Liou et al., 2015). Recruited macrophages, in turn, stimulate the dedifferentiation process of acinar cells by the secretion of proinflammatory cytokines, including TNF and CCL5 (Liou et al., 2013). Thereby, macrophages promote pancreatic inflammation and the progression of carcinogenesis. In addition, macrophages secrete chemokines such as CXCL1, CXCL2, and CCL8 to recruit monocytes, neutrophils, T cells, NK cells, and B cells to the pancreas, to amplify the immune reaction (Schlesinger et al., 2020).

While in the early stages of tumorigenesis proinflammatory signal transducers promote the growth and progression of the neoplasia, in advanced PDAC immunosuppressive mecha-

nisms are crucial to prevent endogenous, antitumoral immune surveillance (Storz and Crawford, 2020). For example, in early carcinogenesis proinflammatory macrophages promote tumorigenesis, whereas in advanced PDAC, mainly immunosuppressive tumor-associated macrophages (TAMs) are present (Ino et al., 2013). PanIN lesions secrete IL-13 to directly mediate the transition of proinflammatory macrophages to immunosuppressive macrophages (Liou et al., 2017).

1.2.5.2 Tumor microenvironment (TME) in PDAC

Characteristically, the PDAC microenvironment is highly immunosuppressive, caused by a pronounced desmoplastic reaction, the upregulation of immune checkpoint regulators, and the high infiltration of immunosuppressive cells, including cancer-associated fibroblasts (CAFs), TAMs, Tregs and MDSCs (Knudsen et al., 2017).

High infiltration of macrophages, neutrophils, and an increased ratio of Tregs to CD4⁺ T cells correlate with shorter survival of PDAC patients, whereas a high infiltration of CD4⁺ T cells, CD8⁺ T cells, and proinflammatory macrophages correlates with longer survival (Hiraoka et al., 2006; Ino et al., 2013).

The tumor microenvironment (TME) in PDAC is highly heterogeneous (Fig. 4; Peng et al., 2019). Using scRNA sequencing of PDAC samples, Peng et al. reported the existence of different subclusters of malignant cells and different types of stromal cells within PDAC tumors (Peng et al., 2019). Subclustering of stromal cell clusters revealed the existence of 2 different subsets of CD4⁺ T cells, 3 subsets of CD8⁺ T cells, 6 subsets of B cells, 5 subsets of macrophages, and 8 subsets of fibroblasts in PDAC (Peng et al., 2019).

PDAC has a very high proportion of stroma, accounting for 50-80% of the tumor volume (Karamitopoulou, 2019). The extracellular matrix (ECM) within the stroma is primarily synthesized by CAFs and consists of collagen I, collagen IV, fibronectin, lamin, hyaluronan, glycosaminoglycan, growth factors, cytokines, and chemokines (Bachem et al., 2005; Storz and Crawford, 2020). The function of the ECM is multi-faceted (Weniger et al., 2018).

The dense tumor stroma complicates the surgical resection of PDAC and functions as a physical barrier to chemotherapeutics (Provenzano et al., 2012). The strong desmoplastic reaction elevates the interstitial fluid pressure, which can provoke the collapse of the microvas-

culature, preventing the perfusion of the tissue by chemotherapeutic agents and thus complicating the treatment of patients (Provenzano et al., 2012). On the other hand, the stroma also has tumor-preventive properties (Özdemir et al., 2014; Rhim et al., 2014). Rhim et al. showed that PDAC tumors with reduced stromal content were surprisingly more aggressive and associated with augmented tumor vascularization (Rhim et al., 2014). Consistently, a low stroma content, as well as a low infiltration of myofibroblasts in the TME in human PDAC correlates with shorter patient survival (Özdemir et al., 2014; Knudsen et al., 2017).

CAFs are the most abundant cells in the PDAC microenvironment (Peng et al., 2019). Fibroblasts are categorized as quiescent fibroblasts, anti-tumorigenic myofibroblasts, and pro-tumorigenic inflammatory fibroblasts, with high plasticity (Feldmann et al., 2021). The depletion of α SMA⁺ myofibroblasts was shown to lead to more undifferentiated, invasive PDAC tumors, combined with increased immunosuppression through increased recruitment of FOXP3⁺ Tregs (Özdemir et al., 2014). By genetic deletion of the transcription factor *Prrx1*, CAFs remain constitutively activated, exerting a strong influence on tumor biology and metastatic dissemination by modulating the differentiation of the tumor and the TME (Feldmann et al., 2021). Co-culture experiments of CAFs and PDAC cells with subsequent RNA sequencing revealed that CAFs promote epithelial-to-mesenchymal transition and proliferation of cancer cells via the activation of the MAPK and the STAT3 signaling pathways (Ligorio et al., 2019). On the other hand, tumor cells amplify the proliferation of fibroblasts, enabling the reciprocal expansion of the tumor and the microenvironment (Ligorio et al., 2019).

While CAFs are generally the most abundant cell type in the PDAC TME, macrophages are the most frequent immune cells in the microenvironment (Karamitopoulou, 2019; Peng et al., 2019). High tumor infiltration by TAMs correlates with poor prognosis in PDAC (Knudsen et al., 2017; Karamitopoulou, 2019). Consistently, the deletion of macrophages by clodronate liposomes significantly reduces the tumor burden in mice (Zhu et al., 2017). The function of TAMs in the TME are versatile, involving the secretion of chemokines to recruit additional immune cells, including immunosuppressive MDSCs and Tregs, the secretion of pro-inflammatory cytokines, and the remodeling of the ECM (Beatty et al., 2015; Peng et al., 2019). TAMs secrete proteases like cathepsin B and S to modulate the ECM, thereby promoting tumor growth, angiogenesis, and invasion in PDAC (Gocheva et al., 2010).

The high infiltration of immunosuppressive cells like Tregs and MDSCs amplifies the pronounced immunosuppression in PDAC (Siret et al., 2019). The infiltration of Tregs into the TME increases gradually during PDAC progression and correlates with reduced patient survival through inhibition of the anti-tumoral immune response (Hiraoka et al., 2006; Jang et al., 2017). Depletion of Tregs is sufficient to restore an effective immune response against tumor cells through the activation of cytotoxic CD8⁺ T cells and dendritic cells, leading to a significant reduction in tumor volume and prolonged survival of mice (Jang et al., 2017).

The highly desmoplastic, immunosuppressive TME contributes decisively to the therapy resistance of PDAC, by complicating surgical resection, limiting perfusion of chemotherapeutic agents, and by counteracting immunotherapy (Provenzano et al., 2012; Knudsen et al., 2017; Yamamoto et al., 2020; Principe et al., 2021). Accordingly, there is high interest in the understanding and the modulation of the TME, as a potential target of efficient therapeutic approaches.

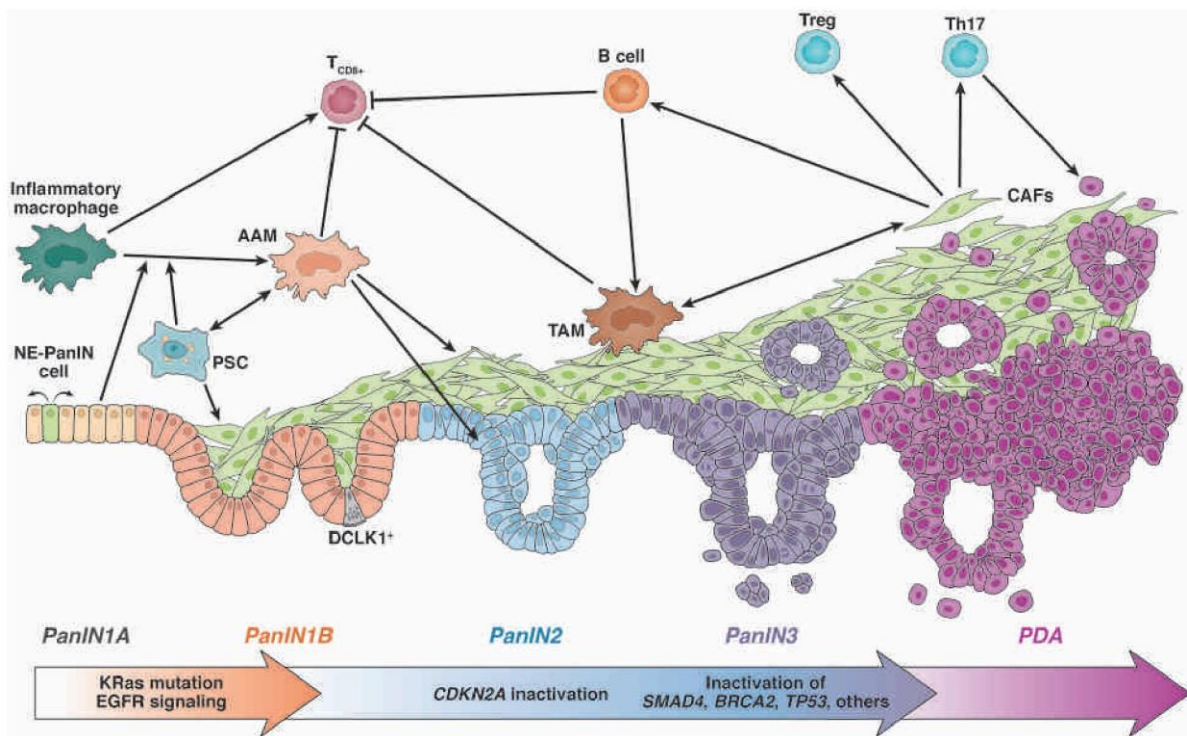


Figure 4: The function of the microenvironment in PDAC carcinogenesis. PDAC carcinogenesis involves the formation of different stages of low-grade (PanIN1A, PanIN1B, PanIN2) and high-grade (PanIN3) precursor lesions. Oncogenic KRAS and the upregulation of EGFR signaling initiate the irreversible de-differentiation of acinar cells into ADM structures and the progression to low-grade PanIN lesions. In the initial phase of carcinogenesis, ADM and low-grade PanINs recruit inflammatory macrophages, which are pivotal for amplifying the tumor-promoting inflammation and tumor growth. Low-grade PanINs and pancreatic stellate cells (PSCs) secrete cytokines to mediate the transition of inflammatory macrophages to alternatively activated macrophages (AAMs), which in turn promotes the expansion and progression of PanIN lesions and

the proliferation of fibroblasts. The progression of carcinogenesis is accompanied by an enhanced desmoplastic reaction, primarily mediated by fibroblasts, PSCs, and AAMs. AAMs and, in advanced stages of carcinogenesis, tumor-associated macrophages (TAMs) generate a tumor-promoting, immunosuppressive microenvironment by the recruitment of cancer-associated fibroblasts (CAFs) and the secretion of cytokines to inhibit the endogenous anti-tumoral immune response, for example, by inhibition of CD8⁺ T cells. CAFs enhance the immune suppression by the recruitment of Tregs and Th17 cells. The mutation of tumor suppressor genes like *CDKN2A*, *SMAD4*, *BRCA2*, or *TP53* causes the progression to high-grade dysplasia and PDAC. The figure is adapted from Storz and Crawford (2020).

1.2.6 Therapy of PDAC

PDAC is rapidly progressing and early metastatic, but commonly asymptomatic or associated with nonspecific symptoms at early stages. Accordingly, PDAC is usually diagnosed at advanced stages, often as a non-resectable primary tumor combined with metastasis (Hidalgo et al., 2015). In total, only 20% of patients are diagnosed with a surgically resectable tumor (Gillen et al., 2010). Patients with resected primary tumors generally have a significantly higher median survival of 22.4 months, compared to patients with surgically non-resectable tumors with a median survival of 9.5 months (Gillen et al., 2010). The cytostatics FOLFIRINOX (5-FU, leucovorin, irinotecan, oxaliplatin) and gemcitabine plus nab-paclitaxel are established for the treatment of patients with metastatic PDAC (Conroy et al., 2011; Kang et al., 2018). FOLFIRINOX and gemcitabine marginally extend patient survival but induce massive side effects leading to an impaired quality of life for the patients (Conroy et al., 2011).

1.2.7 Mouse models to study acute pancreatitis and PDAC

The missing therapy options for patients with non-resectable pancreatic cancer highlight the outstanding need for reliable model systems to dissect essential tumor-promoting molecular processes necessary for tumor growth and therapy resistance. Genetically engineered mouse models (GEMMs) enable the investigation of the full spectrum of carcinogenesis *ab initio* (Gabriel et al., 2020). Tumors evolve in presence of an intact immune system, mimicking clinical features like immunoediting (Lee et al., 2016). Additionally, GEMMs can be used to study the highly relevant mechanisms of immune cell recruitment and activation, as well as mechanisms of immune evasion (Lee et al., 2016).

1.2.7.1 The Cre/loxP system

The Cre (causes recombination) recombinase system was originally identified by Sternberg and Hamilton in bacteriophage P1 (Sternberg, N. and Hamilton, D., 1981). Cre catalyzes the site-specific recombination of two loxP (locus of crossing-over, P1) sequences, each consisting of two 13 bp inverted repeat sequences flanking a central 8 bp spacer sequence (Missirlis et al., 2006). Thereby, Cre-mediated recombination enables the insertion, deletion, or inversion of genetic elements (Fig. 5; Missirlis et al., 2006).

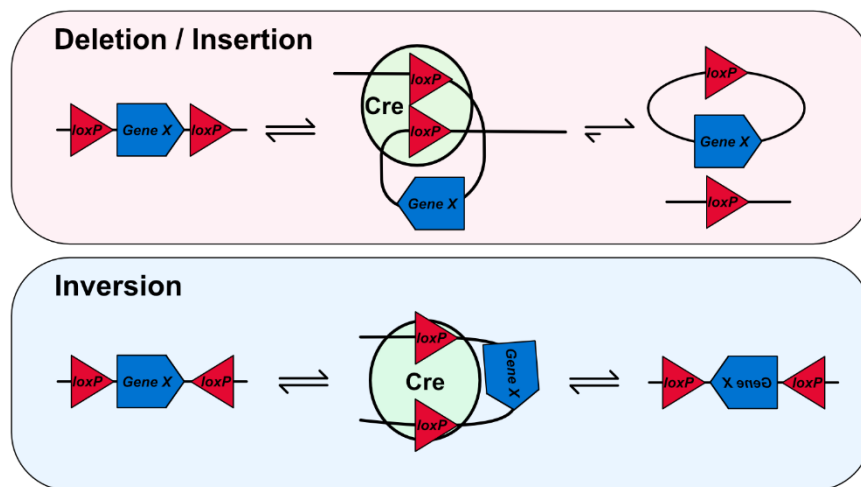


Figure 5: Mechanism of Cre/loxP-dependent deletion, insertion, and inversion of genetic elements. Cre catalyzes the site-specific recombination of two loxP sequences in spatial proximity. The recombination enables the deletion of genetic elements between the two loxP sites. The entropically unfavored backreaction leads to the insertion of genetic elements. Depending on the orientation of the loxP sequences, the Cre/loxP-system can also be used for the inversion of genetic elements.

Besides the Cre/loxP system, other, mechanistically similar recombination systems are known, for example, the Flp/FRT system derived from *Saccharomyces cerevisiae*, based on the Flp-catalyzed recombination of two 34 bp FRT sequences (Reynolds et al., 1987). Site-specific recombination systems are commonly used in GEMMs. The usage of tissue-specific promoters for the expression of the recombinase enables the recombination to take place exclusively in a certain tissue or cell type.

1.2.7.2 KC model

The KC ($Kras^{G12D}$, $Pdx1-Cre$) model developed by Hingorani et al. is the most established and most frequently used GEMM for PDAC (Hingorani et al., 2003). In this model, the most frequent mutation of *KRAS* in human PDAC is mimicked by the introduction of a point mutation at the endogenous gene locus of *Kras*, resulting in the amino acid substitution G12D (Hingorani et al., 2003). This point mutation inhibits the intrinsic GTPase activity, resulting in constitutively active KRAS signaling (see 1.2.3). A transcriptional termination element, flanked by two *loxP* sequences, was inserted upstream of the first exon of $Kras^{G12D}$ so that the transcription is systemically inhibited (Hingorani et al., 2003).

Pdx1 is expressed from day 8.5 in murine embryogenesis in the dorsal endoderm of the gut and is essential for the development of the pancreas (Offield et al., 1996). In the KC model, the promoter of *Pdx1* was coupled to the *Cre* gene sequence, which enables the exclusive expression of *Cre* in pancreatic progenitor cells during embryogenesis (Hingorani et al., 2003). Thereby, *Cre* catalyzes the deletion of the *loxP*-flanked transcriptional stop element in pancreatic progenitor cells to enable the expression of oncogenic $Kras^{G12D}$ exclusively in the pancreas (Hingorani et al., 2003).

KRAS^{G12D} evokes the formation of lesions with ductal morphology in the pancreas of KC mice, recapitulating all stages of PDAC carcinogenesis, associated with the recruitment of immune cells to the microenvironment and a pronounced desmoplastic reaction through infiltrating fibroblasts (Hingorani et al., 2003). KC mice form PanIN precursor lesions, which can progress to invasive, metastatic PDAC (Hingorani et al., 2003). In very rare cases, additional extrapancreatic tumors (mucocutaneous papillomas, intestinal metaplasia of the gastric epithelium, duodenal hyperplastic polyps) arise, presumably because of the expression of *Pdx1* in progenitor cells of the foregut endothelium during embryogenesis, leading to an extrapancreatic expression of $Kras^{G12D}$ (Hingorani et al., 2003).

1.2.7.3 KPC model

The KPC ($Kras^{G12D/+}$, $Trp53^{R172H/+}$, $Pdx1-Cre$) model represents a modification of the KC model leading to accelerated pancreatic carcinogenesis by the replacement of the endogenous allele for *Trp53* with a mutated allele ($Trp53^{R172H}$) regulated by a *loxP-stop-loxP* cassette up-

stream of the gene locus (Hingorani et al., 2005).

The amino acid substitution R172H is located in the DNA binding domain of Trp53 and corresponds to the human ortholog p53^{R175H}, which is the most frequent mutation of p53 in PDAC (Cerami et al., 2012; Freed-Pastor and Prives, 2012; Gao et al., 2013). Mechanistically, the mutation alters both, DNA binding and the interaction with other proteins, causing p53^{R172H} to exert novel, oncogenic functions (Cho et al., 1994; Freed-Pastor and Prives, 2012; Polireddy et al., 2019). In the KPC model, Cre recombinase catalyzes the pancreas-specific expression both of oncogenic *Kras*^{G12D} and *Trp53*^{R172H} (Hingorani et al., 2005).

Tumors arise in the KPC model at earlier time points and with an increased frequency, compared to the KC model (Hingorani et al., 2005). KPC mice reproduce clinical features of human PDAC including cachexia, ascites, abdominal distension, and metastasis in the lung, lymph node, liver, diaphragm, and adrenal glands (Hingorani et al., 2005). The mutation of *Trp53* causes a high degree of genetic instability, partly due to an increased number of centrosomes, causing abnormal mitotic figures and chromosomal instability (Hingorani et al., 2005). Accordingly, tumors from KPC mice exhibit a high mutation frequency with an average of 13 ± 7 somatic mutations per mouse and $32 \pm 13\%$ of the genes that are affected by copy gains and losses (Hingorani et al., 2005; Niknafs et al., 2019). The high frequency of genetic alterations causes a high heterogeneity of KPC-derived tumors (Niknafs et al., 2019).

1.2.7.4 Dual recombinase system

The recently published dual-recombinase system represents a fundamental improvement of the KC/KPC model (Schönhuber et al., 2014). A transgene with the promoter of *Pdx1*, regulating the expression of the mouse codon-optimized *Flp-o*, was transferred into C57BL/6 zygotes by nuclear injection, followed by the random integration of the fragment into the genome (Schönhuber et al., 2014). Flp catalyzes the pancreas-specific deletion of an *FRT*-site flanked transcriptional termination element to enable the expression of *Kras*^{G12D} exclusively in the pancreas (KF model: *Kras*^{G12D/+}, *Pdx1-Flp*; Schönhuber et al., 2014). The endogenous gene locus of *Trp53* was replaced by an *FRT*-flanked allele of *Trp53*, to accelerate tumor progression by the pancreas-specific, Flp-mediated heterozygous (KPF model) or homozygous (KPPF model) deletion of *Trp53* (Schönhuber et al., 2014). The carcinogenesis in the KF and KPF model proceeds analogously to the KC and KPC model, respectively, in terms of tumor

development, tumor progression, the formation of metastasis, and survival (Hingorani et al., 2005; Schönhuber et al., 2014).

The parallel usage of Flp/FRT and Cre/loxP in the dual-recombinase system enables the Flp-dependent, pancreas-specific activation of oncogenic *FSF-Kras^{G12D}* and the deletion of *Trp53*, while the Cre/loxP system offers the possibility to independently delete or re-express target genes to study their cell-specific role in carcinogenesis.

1.2.7.5 *Caerulein-induced acute pancreatitis in WT and Kras^{G12D}-expressing mice*

Formation of invasive PDAC requires the overcoming of senescence barriers by inactivation of tumor suppressor genes, for example, by mutation/deletion of *Trp53* in the KPC/KPF model or by inflammation (Hingorani et al., 2005; Guerra et al., 2007; Guerra et al., 2011; Lesina et al., 2011; Di Magliano and Logsdon, 2013).

Guerra et al. reported that the doxycycline-regulated activation of *Kras^{G12D}* in pancreatic acinar cells of 2-month-old adult mice was insufficient to cause PDAC formation within 6 months and 12 months after its activation (Guerra et al., 2007). In contrast, when these mice were challenged with mild pancreatitis, they developed the full spectrum of PDAC carcinogenesis, including the formation of high-grade PanIN lesions and invasive PDAC (Guerra et al., 2007). Pancreatitis-induced inflammation inhibits oncogene-induced senescence, enabling the development of invasive carcinomas (Guerra et al., 2011).

Lesina et al. demonstrated in the KC model that myeloid cells, particularly macrophages, induced STAT3 signaling in metaplastic cells via IL-6 trans-signaling to promote the progression of PanIN lesions to invasive PDAC, underscoring the central role of inflammation in pancreatic carcinogenesis (Lesina et al., 2011).

The secretagogue caerulein is derived from the skin of the Australian frog *Litoria caerulea* and acts as a derivative of cholecystokinin with approximately 10 times stronger effects (Lerch and Gorelick). Intraperitoneal injection of caerulein specifically induces pancreatic inflammation in mice in a controlled, reproducible experimental setting. In 1977, Lampel and Kern first described that rats evolved signs of acute pancreatitis after hourly administration of caerulein (Lampel and Kern, 1977). Caerulein induces an increased production of pancreatic digestive enzymes, ultimately leading to improper, premature activation of zymogenes by lysosomal cathepsin B within acinar cells, initiating the self-digestion of the exocrine pancre-

as (Murtaugh and Keefe, 2015). Simultaneously, ER stress caused by the overexpression of digestive enzymes and the resulting NF- κ B-dependent inflammation represents an alternative mechanism of caerulein-induced AP (Murtaugh and Keefe, 2015).

Caerulein-induced inflammation is used to study the mechanisms involved in acute pancreatitis in mice. Additionally, the administration of caerulein in mice with pancreas-specific expression of *Kras*^{G12D} represents a model system to investigate the complex interplay of the immune system and oncogenic transformed acinar cells in the context of inflammation-driven PDAC carcinogenesis (Morris et al., 2010; Guerra et al., 2011; Kong et al., 2018).

Caerulein-induced acute pancreatitis in wild-type mice is generally divided into three phases: The inflammatory phase 3 h to 36 h after caerulein injection is characterized by pancreatic edema, high inflammation caused by the extensive infiltration of immune cells, the presence of vacuolated acinar cells, and acinar cell death (Kong et al., 2018). ADM formation becomes pronounced at the end of the inflammatory phase (Kong et al., 2018). In the regenerative phase from day 2 until day 6, clearance of immune cells takes place, associated with the re-differentiation of ductal-like progenitor cells to acinar cells (Kong et al., 2018). Refinement occurs between days 7 and 14, during which residual inflammation is resolved and organ regeneration is completed (Kong et al., 2018).

In mice with pancreas-specific expression of oncogenic *Kras*, no distinct phases of caerulein-induced pancreatitis can be classified, neither histologically, nor based on transcriptome analysis (Kong et al., 2018). Caerulein injection in *Kras*^{G12D}-expressing mice induced an extensive, non-resolving immune response with strong inflammation and continuously increasing numbers of infiltrating immune cells (Guerra et al., 2011; Kong et al., 2018). Oncogenic *Kras*^{G12D} prevents the redifferentiation of ductal-like progenitor cells into acinar cells (Kong et al., 2018). The cells remain in a proliferative, de-differentiated state, resulting in the formation of pancreatic precursor lesions and the progression of carcinogenesis (Kong et al., 2018).

1.3 Function of the immune system in tissue regeneration and cancer

The immune system is decisively involved in tissue regeneration as well as in the endogenous tumor defense. In both cases, receptors of the innate immune system serve as molecu-

lar sensors of DAMPs, characteristically tissue damage-associated molecules released by necrotic cells (Visser et al., 2006; Julier et al., 2017). Macrophages, dendritic cells, and mast cells serve as sentinel cells pre-stationed in the tissue for the continuous monitoring of DAMPs (Visser et al., 2006). Detection of DAMPs induces the rapid, local activation of the immune response, leading to the recruitment of additional immune cells by secretion of pro-inflammatory cytokines and chemokines and the elimination of the etiological agent of inflammation to enable tissue repair (Visser et al., 2006).

Dysregulation of the termination of the immune response can cause chronic inflammatory disorders and promote cancer development (Visser et al., 2006; Serhan et al., 2007; Fullerton and Gilroy, 2016; Sugimoto et al., 2019).

A central function of the immune system is the immune surveillance, i.e. the detection and elimination of cancer cells based on the tumor-associated neo-antigens so that tumors are usually eliminated by the immune system before clinical manifestation (Burnet, 1970). Antigens presented in the MHC-I complex on tumor cells are different from those on non-transformed cells, due to the genetic instability and high mutation rate of tumor cells (Pardoll, 2015). The presentation of these neo-antigens on the cell surface enables the activation of T cells and leads to the elimination of tumor cells by the adaptive immune system. (Pardoll, 2015).

Shankaran et al. reported increased spontaneous and carcinogen-induced tumor formation in lymphocyte-deficient mice, compared to wild-type controls (Shankaran et al., 2001). The transplantation of tumors from immunodeficient mice into wild-type mice resulted in a complete regression in 40% of the mice (Shankaran et al., 2001). The experiment demonstrates that the immune system prevents tumor formation and that tumors arising from immunodeficient mice develop high immunogenicity compared to tumors that arise in presence of an intact immune system, a process called cancer immunoediting (Shankaran et al., 2001). Additionally, the experiment shows that the immune system is in general capable of eliminating tumor cells (Shankaran et al., 2001). Tumors inhibit the anti-tumoral activity of the immune system by the recruitment of immunosuppressive cells, like Tregs and MDSCs, and the secretion of anti-inflammatory cytokines, like TGF- β and IL-10 (Hanahan and Weinberg, 2011; Pardoll, 2015; Jang et al., 2017; Siret et al., 2019). Consistently, the high intra-tumoral infiltration of immunosuppressive macrophages and Tregs in PDAC correlates with significantly shorter patient survival (Ino et al., 2013).

The immunosuppressive TME in PDAC is a key contributor to tumor growth and therapy resistance (Provenzano et al., 2012; Knudsen et al., 2017; Yamamoto et al., 2020; Principe et al., 2021). Depletion of Tregs in mice with PDAC was demonstrated to result in significantly reduced tumor growth and prolonged survival (Jang et al., 2017). This effect was reversed when CD8⁺ T cells were additionally depleted or when IFN- γ was blocked (Jang et al., 2017). The results demonstrate that Tregs in the TME of PDAC promote tumor growth via suppression of IFN- γ secretion by CD8⁺ T cells, whereas depletion of Tregs was sufficient to restore an efficient antitumor immune response associated with prolonged survival of the mice (Jang et al., 2017).

1.3.1 Immune therapy for PDAC

In 2018, James Allison and Tasuku Honjo were awarded with the Nobel Prize in medicine for their pioneering work on the immune checkpoint inhibitors CTLA-4 and PD-1/PD-L1 (Huang and Chang, 2019). Tumor cells use PD-L1 and CTLA-4 to inactivate T cells as a central mechanism of tumor immune evasion (Huang and Chang, 2019). Based on the work of Dr. Honjo and Dr. Allison, therapeutic checkpoint inhibitors were developed using neutralizing antibodies against negative regulators of the immune system (Principe et al., 2021).

Especially in difficult-to-treat tumors, like advanced melanoma or PDAC, novel therapeutics based on the reactivation of the endogenous immune defense against tumors provide promising, new therapy options. For example, using neutralizing antibodies targeting CTLA-4, the 5-year overall survival rate of patients with advanced melanoma was increased from initially 10% (Garbe et al., 2011) to 20% (Schadendorf et al., 2015). In contrast, checkpoint inhibitors were ineffective for the treatment of PDAC, due to low efficiency associated with high toxicity and severe side effects (Royal et al., 2010; Brahmer et al., 2012; O'Reilly et al., 2019; Principe et al., 2021). For example, Ipilimumab (anti-CTLA-4) was inefficient for the therapy of patients with advanced pancreatic cancer in a phase 2 trial (Royal et al., 2010). The main reasons for the low efficiency of immunotherapy for the treatment of PDAC patients include the weak immunogenicity of the tumors, based on the lack of tumor-associated antigens and the highly immunosuppressive microenvironment, which prevents the efficient reactivation of the endogenous anti-tumoral immune response (Yamamoto et al., 2020; Principe et al., 2021). Augmentation of tumor immunogenicity might be achieved by the direct stimulation

of immune receptors, for example, by agonists of pattern recognition receptors to stimulate the immunosurveillance function of the innate immune system (Smith et al., 2018; Le Naour et al., 2020).

1.3.2 Toll-like receptor 3 (TLR3)

Toll-like receptors are evolutionarily conserved pattern recognition receptors (PRRs) of the innate immune system for the detection of pathogen-associated or endogenous DAMPs, leading to the activation of the immune response (Le Naour et al., 2020). Toll-like receptor 3 (TLR3) is an endosomal PRR responsible for the detection of viral dsRNA to induce the immediate, antiviral immune reaction to prevent viral spread (Alexopoulou et al., 2001). Further, TLR3 binds dsRNA released by necrotic cells after tissue injury to orchestrate the regeneration process, for example, by recruitment and activation of pro-regenerative immune cells (Karikó et al., 2004; Bsibsi et al., 2006; Cavassani et al., 2008; Nelson et al., 2015; Wang et al., 2018; Regel et al., 2019; Stöß et al., 2020).

TLR3 is not only expressed by immune cells, like macrophages and dendritic cells (Muzio et al., 2000; Murakami et al., 2014), but also by other cell types, including pancreatic epithelial cells (Regel et al., 2019).

TLR3 is synthesized in the endoplasmic reticulum and transported by UNC93B1 through the Golgi apparatus into endosomes (Garcia-Cattaneo et al., 2012). The full-length protein of TLR3 is proteolytically processed by cleavage of the signal peptide, as well as by cathepsin B- or H-dependent cleavage into an N- and C-terminal fragment, which remain associated within the endosome (Garcia-Cattaneo et al., 2012; Murakami et al., 2014).

The ectodomain of TLR3 forms a curved solenoid (inner diameter 42 Å, outer diameter 90 Å) with 15 glycosylation sites, 4 disulfide bridges, and 22 leucine-rich repeats, capped with characteristic motifs at the N-terminal site (LRR-NT) and C-terminal site (LRR-CT) of the ectodomain (Fig. 6A; Choe et al., 2005; Liu et al., 2008; Murakami et al., 2014). Hydrogen bonding networks formed by conserved asparagine residues stabilize the curved solenoid structure (Choe et al., 2005). The ectodomain of TLR3 does not interact with individual bases, but with the ribose phosphate backbone of dsRNA (Liu et al., 2008). Thereby, TLR3 does not exhibit sequence specificity (Liu et al., 2008). Ligands interact with both the N-terminal end

(LRR-NT to LRR-3, including the residues His39, His60, Arg64, Phe84, Ser86, His108, and Glu110) and the C-terminal end (LRR19 to LRR21, including the residues Asn515, Asn517, His539, Asn541, Arg544) of the ectodomain (Fig. 6B; Liu et al., 2008). Binding of dsRNA induces receptor dimerization of the C-terminal intracellular cytoplasmic Toll/IL-1 receptor (TIR) homology domains and tyrosine phosphorylation at Tyr759 and Tyr858 (Sarkar et al., 2007; Liu et al., 2008). This enables the recruitment of TRIF to the BB-loop in the TIR domain of TLR3 (Oshiumi et al., 2003; Choe et al., 2005; Liu et al., 2008). TRIF induces signal transduction via NF- κ B, AP-1, and IRF3 to activate the expression of proinflammatory cytokines and type-I interferons (Fig. 7; Doyle et al., 2002; Oshiumi et al., 2003). Further, TLR3 is able to induce cell death, which leads to the removal of virus-infected cells and tumor cells (Salaun et al., 2006; Weber et al., 2010). Mechanistically, TLR3 induces cell death via the formation of the so-called ripoptosome complex consisting of TRIF, RIPK1, CASP8, CASP10, FADD, cFLIP_L, and cFLIP_S (Feoktistova et al., 2011; Estornes et al., 2012). Depending on the molecular composition of the complex, TLR3 leads either to CASP8-dependent apoptosis or RIPK-dependent necrosis (Feoktistova et al., 2011).

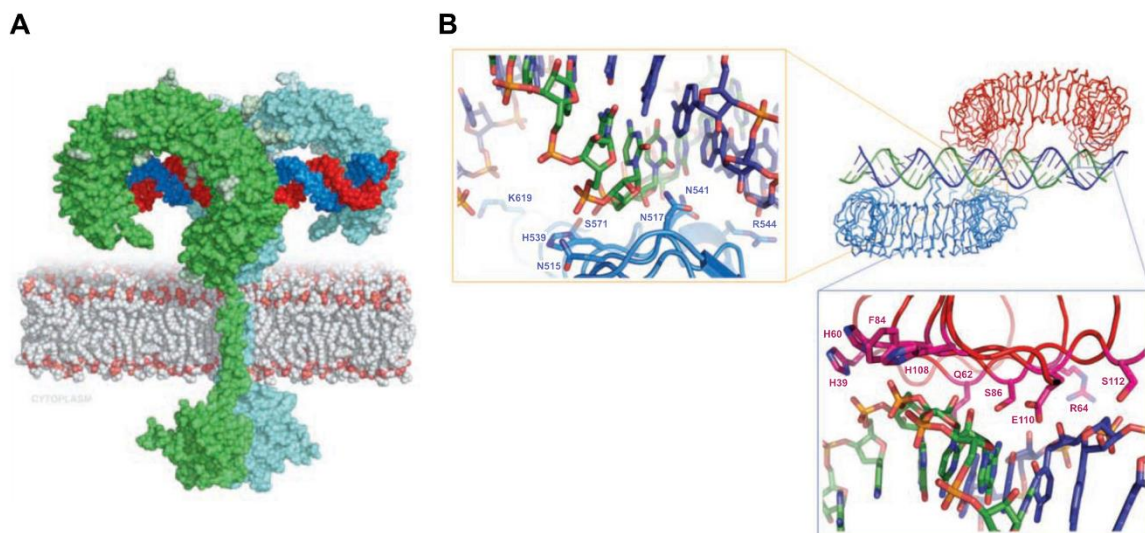


Figure 6: Model of dsRNA binding by TLR3. (A) Homology-modeled structure of dimerized TLR3 upon binding of dsRNA. The ectodomain of TLR3 forms a curved solenoid, which interacts with the ribose phosphate backbone of dsRNA. The interaction with dsRNA induces the dimerization of TLR3, which brings the C-terminal TIR domains in close spatial proximity to allow cytosolic signal transduction via the recruitment of TRIF. (B) dsRNA interacts with conserved amino acid residues at the C-terminal (yellow box) and N-terminal (grey box) site of the TLR3 ectodomain. Figures are adapted from Liu et al. 2008.

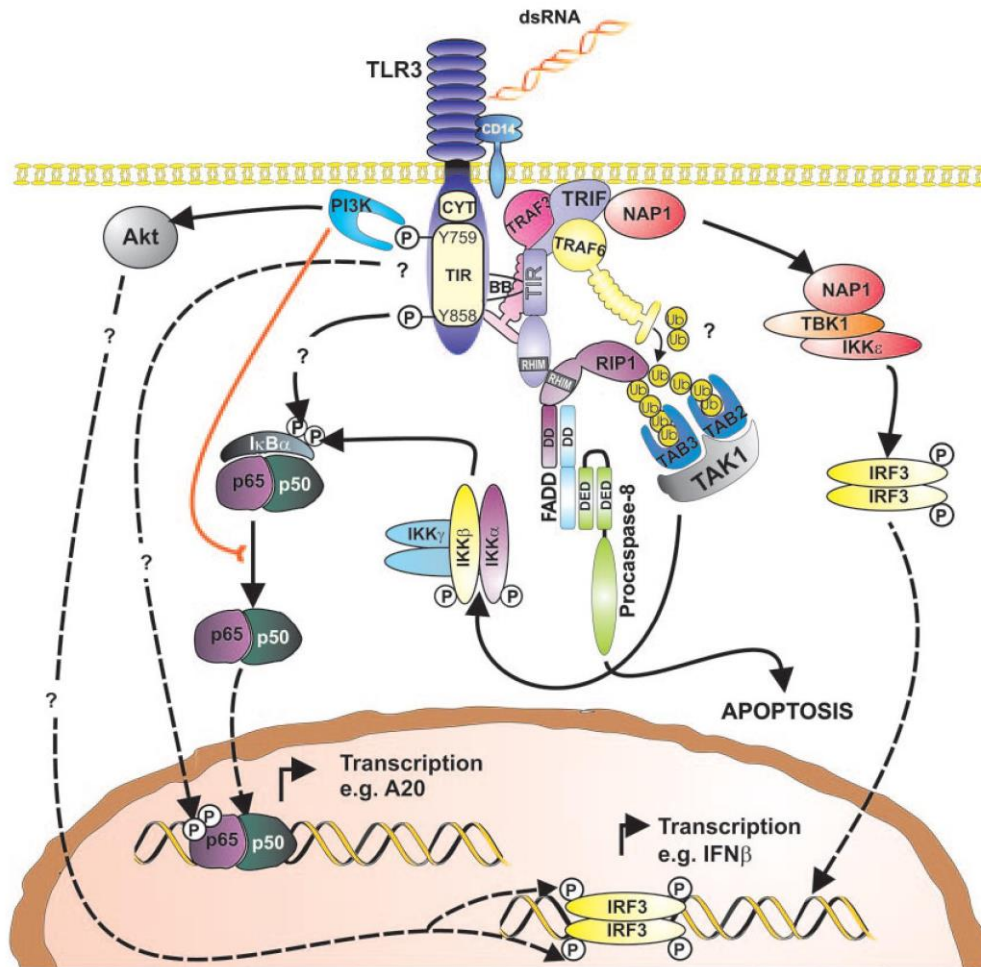


Figure 7: Overview of the TLR3-regulated signal transduction pathways after binding of dsRNA. Endosomal binding of dsRNA by the TLR3 ectodomain induces the dimerization of TLR3, which enables the cytoplasmic recruitment of TRIF to the C-terminal BB loop in the TIR domain of TLR3. TRIF recruits TRAF3 and NAP1, which leads to the activation of TBK1 and IKKε. TBK1 and IKKε phosphorylate IRF3, leading to its dimerization and nuclear translocation, to induce the expression of type-I interferons. Additionally, TRIF recruits the ubiquitin ligase TRAF6 and RIPK1, which potentially ubiquitinylates RIPK1. Ubiquitylated RIPK1 is bound by the ubiquitin receptor proteins TAB2 and TAB3, which activate TAK1. TAK1 phosphorylates IKKα and IKKβ, in the IKK complex. The IKK complex inactivates IκBα by phosphorylation, which allows the nuclear translocation of the NF-κB complex (p65/p50), leading to the expression of inflammation-associated target genes of NF-κB. Further, TLR3 induces cell death by TRIF-dependent recruitment of RIPK1, FADD, and procaspase 8. The figure is adapted from Vercammen et al. 2008.

1.3.2.1 *TLR3 in tissue regeneration processes*

The functions of TLR3 are versatile. TLR3 is not only involved in the detection of viral infections but also serves as a sensor of tissue damage by binding of dsRNA released from necrotic cells (Karikó et al., 2004; Bsibsi et al., 2006; Cavassani et al., 2008; Nelson et al., 2015; Wang et al., 2018; Regel et al., 2019; Stöß et al., 2020). Thus, TLR3 is involved in various regeneration processes with a multitude of cell- and tissue-specific functions.

Nelson et al. revealed the importance of TLR3 in wound-induced skin regeneration (Nelson et al., 2015). The dsRNA released by injured skin cells activates TLR3 to promote wound-induced hair neogenesis via its downstream effectors IL-6 and STAT3 (Nelson et al., 2015). TLR3 is functionally involved in the regeneration process after myocardial infarction (Wang et al., 2018). The infarct size is significantly increased in *Tlr3*-deficient mice, combined with reduced proliferation of cardiomyocytes (Wang et al., 2018). It was shown that TLR3 signaling stimulates the proliferation of cardiomyocytes via the activation of YAP1 (Wang et al., 2018).

In Astrocytes, inflammation activates TLR3 to stimulate the production of neuroprotective mediators that promote endothelial growth and enhance neuronal survival (Bsibsi et al., 2006).

Stöß et al. demonstrated the function of TLR3 in murine liver regeneration after partial hepatectomy (Stöß et al., 2020). *Tlr3*-deficient mice had defective liver regeneration, manifested by reduced liver-to-body weight ratios and the cell cycle arrest of hepatocytes (Stöß et al., 2020). TLR3 was shown to promote the regeneration process by inducing the secretion of uPA in hepatic stellate cells, which leads to the release of matrix-associated HGF to promote hepatocyte proliferation (Stöß et al., 2020).

1.3.2.2 *TLR3 in cancer*

TLR3 is expressed by tumor cells as well as by immune cells in the tumor microenvironment and has various cell-specific effects on tumorigenesis and progression (Chin et al., 2010; Ebihara et al., 2010; Chew et al., 2012b; Forte et al., 2012; Yu et al., 2012; Pradere et al., 2014).

In an *in vivo* melanoma model, TLR3 signaling was reported to promote the cell contact-dependent activation of NK cells by myeloid dendritic cells to enhance the NK cell-mediated

tumor regression (Ebihara et al., 2010). Further, TLR3 was demonstrated to exhibit an anti-tumor surveillance function of tumors induced by endogenous retroviruses (Yu et al., 2012). In a model system for metastatic lung cancer, TLR3 signaling was demonstrated to arrest tumor growth by the recruitment of dendritic cells, NKT cells, and CD8⁺ T cells (Forte et al., 2012). Using an orthotopically implanted prostate cancer model, it was shown that TLR3-dependent induction of proinflammatory pathways suppresses tumor growth and keeps tumors in a more differentiated state, mediated by a high infiltration of T lymphocytes and NK cells in the tumor microenvironment (Chin et al., 2010). In patients with hepatocellular carcinoma, high expression of *TLR3* was demonstrated to correlate with longer survival (Chew et al., 2012a). In a mouse model for liver cancer, TLR3-induced chemokines promoted the infiltration and activation of NK cells and T cells in the tumor microenvironment, associated with decreased tumor growth (Chew et al., 2012b).

1.3.2.3 Therapeutic modulation of TLR3 signaling

The examples in chapter 1.3.2.1 and chapter 1.3.2.2 highlight the multifaceted roles of TLR3 in tissue regeneration, carcinogenesis, and tumor progression. The specific induction of TLR3 signaling represents a potential target for new immunomodulatory therapeutics (Okada et al., 2011; Mehrotra et al., 2017; Smith et al., 2018; Le Naour et al., 2020). According to its cell-specific functions, therapeutic stimulation of TLR3 could act as an immunoadjuvant to modulate the immune response upon tissue damage or to enhance the endogenous anti-tumor immune response. Recently, an agonist of TLR3 was approved as adjuvants in influenza vaccines, mediating a strong induction of the immune response combined with low side effects (Wagner and Hildt, 2019). Mehrotra et al. documented the efficient production of tumor-specific T cell populations in pancreatic cancer patients treated with peptide-pulsed autologous dendritic cells combined with a TLR3 agonist as immunoadjuvant (Mehrotra et al., 2017). Further, induction of TLR3 signaling could be used to directly initiate cell death of tumor cells.

1.4 Aims

Understanding the multifaceted influence of the innate immune system on tissue regeneration and tumor carcinogenesis is critical for identifying novel potentially druggable pathways and for the development of novel immunomodulatory therapies. The function of the endosomal dsRNA receptor TLR3 in acute pancreatitis and PDAC carcinogenesis is largely unknown.

One aim of this thesis is to characterize the role of TLR3 in pancreatic regeneration after caerulein-induced acute pancreatitis in mice. By comparing mice with global or partial TLR3 deficiency, we aim to determine the cell-specific function of TLR3 in pancreatic regeneration after AP and subsequently characterize the underlying mechanism by using an *in vitro* model system.

Further, the cell-specific influence of TLR3 on Kras-dependent, oncogene-driven carcinogenesis, and inflammation-induced carcinogenesis will be determined using the dual recombinase mouse model. A particular focus is on characterizing the complex interplay between the tumor and immune cells in the microenvironment. To validate the relevance of the results for human patients, the function of TLR3 in human PDAC cell lines will be determined using the CRISPR/Cas9 system.

The overall aim of the present thesis is the characterization of TLR3 as a new potential therapeutic target in AP and PDAC.

2 Materials and methods

2.1 Materials

A list of the used chemicals (7.2), enzymes (7.3), buffers (7.4), commercial kits (7.5), consumables (7.6), technical equipment (7.7), cell culture reagents (7.8), oligonucleotides (7.9), and antibodies (7.10) is provided in the appendix.

2.2 Methods

2.2.1 Mouse strains and *in vivo* procedures

2.2.1.1 Mouse models

Systemic *Tlr3*-deficient mice (TLR3^{OFF}) were generated by the insertion of a *loxP*-site flanked transcriptional termination element between exon 3 and 4 of the endogenous *Tlr3* gene locus of C57BL/6N mice by homologous recombination, as described previously (Stöß et al., 2020). In presence of Cre recombinase, *Tlr3* expression is reactivated by the recombinase-mediated deletion of the transcriptional termination element, leading to the exclusive expression of *Tlr3* in Cre-expressing cells. Mice with myeloid cell-specific rescue of the *Tlr3* expression (TLR3^{Mye}) were generated by crossing mice with Cre knock-in allele in the gene locus of *lysozyme 2* (*LysM-Cre*; Clause et al., 1999) into the TLR3^{OFF} strain. Mice with an exclusive expression of *Tlr3* in pancreatic epithelial cells were obtained by crossing mice with a *pancreas transcription factor 1 alpha* (*Ptf1a*)-Cre knock-in allele (Kawaguchi et al., 2002) with the TLR3^{OFF} strain. C57BL/6N mice were used as wild-type controls. Pancreas-specific carcinogenesis was analyzed using mice with *Pdx1-Flp-o* transgene regulating the expression of a knock-in allele of oncogenic *FRT-stop-FRT-Kras*^{G12D} (*FSF-Kras*^{G12D}), provided by Dr. Dieter Saur (Klinikum rechts der Isar, Munich; Schönhuber et al., 2014). Oncogene-driven carcinogenesis was accelerated using mice with heterozygous or homozygous *FRT*-flanked *Trp53* allele leading to Flp-mediated deletion. Mice with *loxP* site-flanked exon 3 of the *Casp8* gene were developed by Dr. Stephen Hedrick (Beisner et al., 2005) and intercrossed with *LysM-Cre* mice for the myeloid cell-specific inactivation of *Casp8* (*Casp8*^{Mye}). All mouse strains were kept on the C57BL/6N background and maintained in a specified pathogen-free environment at the Klinikum rechts der Isar, Technical University of Munich (Germany). All mouse experiments

were authorized by the government of Upper Bavaria (license 55.2-1-54-2532-130-2016, 55.2-2532.Vet_02-19-56, 55.2-2532.Vet_02-19-55) and performed according to the guidelines and specifications. The health status of all experimental mice was monitored closely, as described in the licenses. An overview of the mouse strains used within this thesis is provided in table 1.

Table 1: Overview of the different mouse strains used in the project.

| Genotype | Strain | Experiment | <i>Kras</i>^{G12D} active/ <i>Trp53</i> inactive | <i>Tlr3</i> expression |
|--|-------------------------------|---|---|-------------------------------|
| WT | WT | Acute pancreatitis | - | Wild-type |
| <u><i>LSL-Tlr3</i></u> | TLR3 ^{OFF} | Acute pancreatitis | - | Global inactivation |
| <u><i>LysM-Cre; LSL-Tlr3</i></u> | TLR3 ^{Mye} | Acute pancreatitis | - | Only in myeloid cells |
| <i>Casp8</i> ^{fl/fl} | <i>Casp8</i> ^{fl/fl} | Acute pancreatitis | | Wild-type |
| <u><i>LysM-Cre, Casp8</i>^{fl/fl}</u> | <i>Casp8</i> ^{Mye} | Acute pancreatitis | | Wild-type |
| <i>Pdx1-Flp; FSF-Kras</i> ^{G12D} ; <i>Trp53</i> ^{+/^{FRT}} | KPFT ^{WT} | Oncogene-driven carcinogenesis | Pancreatic epithelium | Wild-type |
| <i>Pdx1-Flp; FSF-Kras</i> ^{G12D} ; <i>Trp53</i> ^{+/^{FRT}; <u><i>LSL-Tlr3</i></u>} | KPFT ^{OFF} | Oncogene-driven carcinogenesis | Pancreatic epithelium | Global inactivation |
| <i>Pdx1-Flp; FSF-Kras</i> ^{G12D} ; <i>Trp53</i> ^{+/^{FRT}; <u><i>LysM-Cre; LSL-Tlr3</i></u>} | KPFT ^{Mye} | Oncogene-driven carcinogenesis | Pancreatic epithelium | Only in myeloid cells |
| <i>Pdx1-Flp; FSF-Kras</i> ^{G12D} ; <i>Trp53</i> ^{FRT/^{FRT}} | KPPFT ^{WT} | Oncogene-driven carcinogenesis | Pancreatic epithelium | Wild-type |
| <i>Pdx1-Flp; FSF-Kras</i> ^{G12D} ; <i>Trp53</i> ^{FRT/^{FRT}; <u><i>LSL-Tlr3</i></u>} | KPPFT ^{OFF} | Oncogene-driven carcinogenesis | Pancreatic epithelium | Global inactivation |
| <i>Pdx1-Flp; FSF-Kras</i> ^{G12D} ; <i>Trp53</i> ^{FRT/^{FRT}; <u><i>LysM-Cre;</i></u> <i>LSL-Tlr3</i>} | KPPFT ^{Mye} | Oncogene-driven carcinogenesis | Pancreatic epithelium | Only in myeloid cells |
| <i>Pdx1-Flp; FSF-Kras</i> ^{G12D} | KFT ^{WT} | Inflammation- driven carcinogene- sis | Pancreatic epithelium | Wild-type |

| | | | | |
|---|--------------------|------------------------------------|-----------------------|-------------------------------------|
| <i>Pdx1-Flp; FSF-Kras^{G12D}; LSL-Tlr3</i> | KFT ^{OFF} | Inflammation-driven carcinogenesis | Pancreatic epithelium | Global inactivation |
| <i>Pdx1-Flp; FSF-Kras^{G12D}; LysM-Cre; LSL-Tlr3</i> | KFT ^{Mye} | Inflammation-driven carcinogenesis | Pancreatic epithelium | Only in myeloid cells |
| <i>Pdx1-Flp; FSF-Kras^{G12D}; Ptf1a-Cre; LSL-Tlr3</i> | KFT ^{Epi} | Inflammation-driven carcinogenesis | Pancreatic epithelium | Only in pancreatic epithelial cells |

2.2.1.2 Genotyping

Genotyping was performed with genomic DNA from ear biopsies taken from mice at the age of 21 days. To verify the activity of Flippase in mice with *Pdx1-Flp* and *FSF-Kras^{G12D}*, a pancreas biopsy was isolated when the mice were sacrificed and stored at -80 °C until further usage. Only mice with active Flippase, proven by polymerase chain reaction (PCR) detection of recombined *FSF-Kras^{G12D}* in the pancreas, were considered for further analysis.

The biopsies for genotyping were lysed at 55 °C for 3 h by proteinase K (Sigma-Aldrich) in DirectPCR Lysis Reagent (Viagen Biotech), followed by the inactivation of protease activity by incubation at 88 °C for 45 min and centrifugation at 21130 rcf for 1 min. Genotyping was performed with GoTaq G2 Hot Start Green master mix (Promega) according to the manufacturer's instructions. The sequences of the primers used for genotyping and the size of the PCR products are listed below (Table 2).

Table 2: Primer sequences used for genotyping.

| Target gene | Primer sequence (5' → 3') | Products |
|--------------------|---------------------------|--|
| <i>WT/LSL-Tlr3</i> | TGCCACAGGGTGAGGCATCG | <i>LSL-Tlr3</i> : 1203 bp wild-type <i>Tlr3</i> : 1051 bp |
| | TGGCTGCAGTCAGCTACGTTGT | |
| <i>LSL-Tlr3</i> | TGCCACAGGGTGAGGCATCG | <i>LSL-Tlr3</i> : 974 bp |
| | CCACCCTGGGGTTCGTGTCC | |
| <i>LysM-Cre</i> | CCCAGAAATGCCAGATTACG | <i>LysM-Cre</i> : 700 bp |
| | CTTGGGCTGCCAGAATTTCTC | |

| | | |
|---|-------------------------------|---|
| | TTACAGTCGGCCAGGCTGAC | |
| <i>Ptf1a-Cre</i> | GTCCAATTTACTGACCGTACACCAA | <i>Ptf1a-Cre</i> : 1300 bp |
| | CCTCGAAGGCGTCGTTGATGGACTGCA | |
| <i>Pdx1-Flp</i> | AACACACACTGGAGGACTGGCTAGG | <i>Pdx1-Flp</i> : 620 bp |
| | CGTTGTAAGGGATGATGGTGAAC | |
| | AGAGAGAAAATTGAAACAAGTGCAGGT | |
| | CAATGGTAGGCTCACTCTGGGAGATGATA | |
| <i>FSF-Kras^{G12D}</i> | CACCAGCTTCGGCTTCCTATT | <i>FSF-Kras^{G12D}</i> : 351 bp |
| | AGCTAATGGCTCTCAAAGGAATGTA | |
| | GCGAAGAGTTTGTCTCAACC | |
| <i>Trp53^{FRT}</i> | CAAGAGAACTGTGCCTAAGAG | <i>Trp53^{FRT}</i> : 300 bp |
| | CTTTCTAACAGCAAAGGCAAGC | |
| recombined <i>FSF-Kras^{G12D}</i> | TGTAGCAGCTAATGGCTCTCAA | recombined <i>FSF-Kras^{G12D}</i> : 196 bp |
| | AGAATACCGCAAGGGTAGGTGTTG | |
| <i>Casp8</i> | ATAATCCCCCAAATCCTCGCATC | <i>Casp8^{WT}</i> : 200 bp |
| | GGCTCACTCCCAGGGCTTCCT | <i>Casp8^{fl/fl}</i> : 300 bp |

The conditions of the PCR steps are given in table 3. Optimized PCR protocols were used for *Ptf1a-Cre*, *LysM-Cre*, *recombined FSF-Kras^{G12D}*, *LSL-Tlr3*, *WT/LSL-Tlr3* and *Casp8* (Appendix 7.11).

Table 3: Conditions of the PCR steps for genotyping.

| | Step | Temperature | Time |
|-----|----------------------|-------------|--------|
| | Initial denaturation | 94 °C | 5 min |
| 38x | Denaturation | 94 °C | 30 sec |
| | Annealing | 58 °C | 30 sec |
| | Elongation | 72 °C | 1 min |
| | Final elongation | 72 °C | 10 min |
| | Storage | 4 °C | ∞ |

The PCR products were separated by agarose gel electrophoresis in TAE buffer using a 2% agarose gel and visualized by Gel Doc XR (Bio-Rad Technologies) or UVP GelSolo (Analytik Jena).

2.2.1.3 *Caerulein-induced acute pancreatitis*

To analyze the cell type-specific function of TLR3 for pancreatic regeneration, acute pancreatitis was induced in 8-week-old female WT, TLR3^{OFF} and TLR3^{Mye} mice using a modified version of a previously described protocol (Jensen et al., 2005). Mice were fasting overnight prior to 8 hourly intraperitoneal injections of 2 µg/injection of the secretagogue caerulein (Bachem). Organs were collected 8 h, 24 h, 2 days, 5 days, 7 days, and 21 days after the first caerulein injection.

The cell-type specific function of TLR3 in inflammation-driven carcinogenesis was analyzed in 8- to 10-week-old KFT^{WT}, KFT^{OFF}, KFT^{Mye} and KFT^{Epi} mice according to a modified version of a previously described protocol (Carrière et al., 2009). Mice fasted overnight and were then treated with 6 hourly intraperitoneal injections of 2 µg/injection caerulein at day -2 and day 0. Organs were collected at day 7 and day 21. Casp8^{fl/fl} and Casp8^{Mye} mice were used to study the effect of *Casp8* deficiency in myeloid cells on pancreatic regeneration. Induction of acute pancreatitis in Casp8^{fl/fl} and Casp8^{Mye} mice was done using the same protocol as for inflammation-driven carcinogenesis in the KF mouse cohorts, with organ collection on day 2 and day 7.

2.2.1.4 *Serum analysis for amylase, lipase 2 and LDH*

Murine blood was isolated from vena cava caudalis, transferred to a tube (Microvette, Sarstedt), and centrifuged (10 000 rcf, 5 min). The plasma was incubated for 15 min at room temperature and centrifuged (3000 g, 5 min) to isolate the serum. The serum levels of amylase, LDH, and lipase 2 were measured using a cobas 8000 modular analyzer (Roche, Germany) at the Institute of Clinical Chemistry of the Technical University of Munich.

2.2.2 Histological methods

2.2.2.1 Tissue processing

Tissue samples for histology were fixed overnight in 3.5-3.7% PFA solution (Fischer) prior to dehydration by increasing concentrations of ethanol and the gradual replacement of ethanol by ROTICLEAR (Carl Roth). The organs were embedded in paraffin and stored at room temperature. For histological analysis, the paraffin blocks were cut into 2.5-3 μm thick sections with the microtome and fixed on glass slides.

2.2.2.2 Hematoxylin and eosin (H&E) staining

Hematoxylin and eosin (H&E) staining was used to highlight the tissue architecture for morphological analysis. The sections were first deparaffinized in ROTICLEAR (3x 5 min) and rehydrated through decreasing concentrations of ethanol (3x 3 min 100% EtOH, 3 min 96% EtOH, 3 min 70% EtOH, 3 min 50% EtOH, 2x 3 min ddH₂O). Slides were stained in hematoxylin solution (Carl Roth) for 5 min followed by the removal of excessive dye for 10 min in continuously exchanged H₂O. The slides were subsequently stained in eosin solution for 1 min. Excessive eosin was removed using 70% EtOH (10 sec) and 96% EtOH (15 sec). The sections were dehydrated in EtOH (3x 3 min 100%) and ROTICLEAR (3x 3 min) and mounted in Eukitt mounting medium (Sigma Aldrich). For morphological analysis, slides were scanned at the pathological institute at the Klinikum rechts der Isar.

2.2.2.3 Alcian blue staining

Alcian blue stains acidic mucopolysaccharides, which are expressed in the pancreas by PanIN lesions and was therefore used to evaluate pancreatic carcinogenesis. Sections were first deparaffinized and rehydrated, as described above (2.2.2.1), then stained for 30 min in Alcian blue solution (Alcian blue 8GX 1% (w/v), acetic acid 3% (v/v), pH 2.5). After washing for 5 min in continuously exchanged H₂O, sections were counterstained for 5 min in nuclear fast red solution (Vector) and washed again for 5 min in H₂O. Slides were dehydrated through increasing concentrations of EtOH (3 min 50% EtOH, 3 min 70% EtOH, 3 min 96% EtOH, 3x 3 min 100% EtOH), mounted, and scanned as described previously (2.2.2.1).

2.2.2.4 Immunohistochemistry

For immunohistochemical staining, the paraffin sections were first deparaffinized and rehydrated as described above (2.2.2.1). Heat-induced antigen retrieval was performed in citrate-based Antigen Unmasking Solution (Vector Laboratories) by first boiling the sections for 20 min in a microwave followed by subsequent cooling to room temperature for 30 min. Endogenous peroxidase activity was quenched by H₂O₂ (3%) for 10 min. After washing the slides with PBS plus 0.025% Triton-X 100 (2x 5 min), the PAP Pen (Vector Laboratories) was used to apply a hydrophobic barrier around the tissue. The slides were transferred to a wet chamber and incubated in 10% FCS in PBS for 1 h at room temperature. If a biotin-conjugated secondary antibody was subsequently used for staining, endogenous biotin was blocked by adding 80 µl/ml avidin solution (Vector Biolabs) to the blocking medium. After washing with PBS (2x 3 min), the slides were incubated with the primary antibody (diluted 1:250 in PBS with 5% FCS) at 4 °C overnight. If a biotin-conjugated secondary antibody was used, 80 µl/ml biotin solution (Vector Biolabs) was supplemented to the medium. The next day, the slides were washed with PBS (3x 3 min) prior to the incubation with the HRP-or biotin-conjugated secondary antibody (diluted 1:250 in PBS with 5% FCS) for 1 h at room temperature. For biotinylated secondary antibodies, 30 min prior to the end of the incubation period, the formation of the avidin-biotinylated enzyme complex (Vector Biolaboratories) was initiated at 4 °C according to the manufacturer's recommendations and, after washing with PBS (3x 3 min), added to the slides for 45 min at room temperature. The sections were washed with PBS (3x 3 min) and the staining was visualized by the addition of DAB substrate (Vector Laboratories). The staining was monitored microscopically and ended by the removal of the substrate. The slides were counterstained in hematoxylin for 3 min, washed with H₂O for 10 min, dehydrated through increasing concentrations of EtOH (3 min 50% EtOH, 3 min 70% EtOH, 3 min 96% EtOH, 3x 3 min 100% EtOH) and ROTICLEAR (3x 3 min), mounted under coverslips using Eukitt mounting medium (Sigma Aldrich), and scanned for quantification.

2.2.2.5 Immunofluorescence staining

Immunofluorescence staining was used to visualize the cellular localization of proteins of *in vitro* cultured cells. The coverslips were coated with 5 µg/ml fibronectin in PBS for at least 30 min at 37 °C and then washed with PBS. Cells were seeded directly on the coverslips and incubated overnight to allow cell adhesion prior to subsequent stimulation. For fixation, the medium was removed, the cells were washed with PBS, and fixed with 3% (w/v) PFA in PBS at room temperature for 20 min. After washing with PBS (3x 3 min), excessive PFA was inactivated by the addition of NH₄Cl (50 mM in PBS) for 20 min. The cells were permeabilized by incubation in 0,1% (v/v) Triton X-100 in PBS for 3 min and then washed with PBS (3x 3min). To reduce background signals by unspecific protein interactions, the cells were blocked in 2% (w/v) BSA in PBS for 1 h at room temperature. Subsequently, the cells were incubated with the primary antibodies (diluted 1:250 in 2% BSA in PBS) at 4 °C overnight in a wet chamber. The next day, unbound antibodies were removed by washing with PBS (3x 3min) and the fluorophore-conjugated secondary antibodies (diluted 1:200 in 2% BSA in PBS) and DAPI (diluted 1:5000 in 2% BSA in PBS) were added to the cells and incubated for 1 h at room temperature in absence of light. After washing with PBS (3x 3 min), the cells were mounted on slides in prewarmed glycerol gelatin. Immunofluorescence images were obtained using the AxioObserver Z1 microscope (Carl Zeiss).

2.2.3 Molecular biological methods

2.2.3.1 RNA Isolation from murine tissue

Murine tissue samples for RNA isolation were placed in RNAlater solution (Thermo Fisher Scientific) and stored at -80 °C until further usage. For the isolation of RNA from the murine pancreas, at least 25 mg of the tissue was mixed with 750 µl of TRIzol reagent (Thermo Fisher Scientific) and a metal bead, for subsequent mechanical tissue lysis at a frequency of 30/s for 3 min in the TissueLyser II (Qiagen). The lysate was mixed with 200 µl chloroform and incubated for 5 min on ice to enable RNA extraction into the hydrophilic phase. The phases were separated by centrifugation (15000 g, 20 min, 4 °C) and the upper phase was transferred to 350 µl ethanol (70%). The RNA extraction was subsequently performed with the RNeasy mini kit (Qiagen) according to the manufacturer's instructions. The RNA concentra-

tion was determined spectroscopically using the NanoDrop ND-1000 (Nanodrop-Technologies) and stored at -80 °C.

2.2.3.2 RNA isolation from cells

RNA isolation from cells was performed using the RNeasy mini kit (Qiagen). The concentration was determined by NanoDrop ND-1000 (Nanodrop-Technologies) and the isolated RNA was stored at -80 °C.

2.2.3.3 Reverse transcription quantitative PCR (RT-qPCR)

The reverse transcription of RNA to first-strand cDNA was performed prior to gene expression analysis via quantitative PCR (qPCR). A total amount of 1 µg RNA was reversely transcribed using the RevertAid RT Reverse Transcription Kit (Thermo Fisher Scientific). First, random hexamer primers (0.2 µg) and oio(dT)₁₈ primers (0.5 µg) were added to the RNA (1 µg) on ice. The total volume was adjusted to 12.5 µl by the addition of nuclease-free H₂O. The mixture was incubated for 10 min at 70 °C and immediately cooled on ice afterward. The reaction buffer, RiboLock RNase Inhibitor (20 U), dNTP mix (1 mM), and RevertAid Reverse Transcriptase (200 U) was added. The mixture was incubated first at room temperature for 10 min to allow primer annealing, then heated to 42 °C for 60 min for the synthesis of the first-strand cDNA. The reaction was terminated by incubation at 70 °C for 10 min. The cDNA was diluted 1:10 in nuclease-free H₂O and stored at -20 °C.

Quantitative PCR was performed in duplicates using the LightCycler 480 II instrument (Roche). In each cavity of a 96-well plate, 5 µl cDNA and 400 nM of each primer were added together with the Biozym Blue S'Green qPCR mix (Biozym Scientific) according to the manufacturer's specifications. The primer sequences are attached (see 7.9). The temperature and duration of the PCR steps are given in table 4.

Table 4: Conditions of the steps for qPCR.

| | Step | Temperature | Time |
|-----|----------------------|-------------|--------|
| | Initial denaturation | 95 °C | 2 min |
| 45x | Denaturation | 95 °C | 5 sec |
| | Annealing | 60 °C | 15 sec |
| | Elongation | 60 °C | 15 sec |
| | Storage | 4 °C | ∞ |

Data analysis was performed using the LightCycler 480 software (version 1.5, Roche). The gene expression was normalized to the expression of *Rsp13* or *Gapdh* for murine cDNA and to the expression of *HPRT* for cDNA from human cells.

2.2.3.4 T7 endonuclease assay

The T7 endonuclease assay was used to identify cells with CRISPR/Cas9-induced genetic modifications in the genomic target region, allowing the pre-screening of the clones prior to DNA sequencing. The cells were first detached from the cell culture plates by trypsin-EDTA (see 2.2.4.1), pelleted by centrifugation (500 g, 3 min) and lysed using the KAPA express extract Kit (Roche) following the manufacturer's instructions. The genomic locus that was targeted by the sgRNAs was amplified by PCR using the protocol described below (Table 5 and Table 6).

Table 5: Components for the PCR amplification of genomic fragments by Phusion Hot Start II DNA Polymerase prior to the T7 endonuclease assay.

| Component | Final concentration | Primer sequence (5' → 3') |
|-------------------------------------|---------------------|--|
| Phusion HF buffer | 1 x | |
| Forward Primer | 0.5 μm | sgRNA1: CAGAATCATGAGACAGACTTTGCCTTG sgRNA2: GTTTGCCTCTCTCGCTTTCTCCC |
| Reverse Primer | 0.5 μm | sgRNA1: CCCATGTAAAAGTTTTGAACCTCCAGC sgRNA2: GCCTGTCTTCCAGCAATCCTTCC |
| dNTP mix | 200 μm | |
| Template DNA | 2.5-10 ng/μl | |
| Phusion Hot Start II DNA Polymerase | 1 U/50 μl | |

Table 6: Conditions of the PCR reaction using Phusion Hot Start II DNA Polymerase.

| Step | Temperature | Time | |
|----------------------|------------------|--------|--------|
| Initial denaturation | 98 °C | 30 sec | |
| 35x | Denaturation | 98 °C | 15 sec |
| | Annealing | 60 °C | 30 sec |
| | Elongation | 72 °C | 60 sec |
| | Final Elongation | 72 °C | 5 min |
| Storage | 4 °C | ∞ | |

Synthesis of the correct PCR product was validated by agarose gel electrophoresis using a small test volume of the PCR product. For the digestion by T7 endonuclease I, an equal amount of the PCR product from the wild-type cell line and the respective clones was com-

bined in T7 endonuclease buffer and hybridized using the conditions described below (Table 7):

Table 7: Conditions for hybridizing PCR products prior to potential digestion by T7 endonuclease.

| Step | Temperature | Ramp rate | Time |
|----------------------|-------------|-------------|-------|
| Initial denaturation | 95 °C | | 5 min |
| Annealing | 95-85°C | -2 °C/sec | |
| | 85-25 °C | -0.1 °C/sec | |
| Storage | 4 °C | | ∞ |

The annealed PCR products were incubated with T7 endonuclease I (New England Biolabs, 1 µl/20 µl) at 37 °C for 30 min. The reaction was stopped by the addition of 1.5 µl EDTA (0.25 M) and analyzed by native polyacrylamide gel electrophoresis of the DNA fragments (see 2.2.3.5).

2.2.3.5 Native DNA PAGE

DNA polyacrylamide gel electrophoresis under native conditions was used to visualize size differences of small DNA fragments (50 – 500 bp). The DNA samples were separated in a 10% polyacrylamide gel in TBE buffer at 80 V. After the electrophoresis, the gel was stained in 5 µl/100 ml ethidium bromide in TBE buffer for 30 min at room temperature, washed with TBE buffer (2x 30 min), and visualized using the UVP ChemStudio imaging system (Analytik Jena).

2.2.3.6 DNA sequencing of the CRISPR/Cas9-targeted *TLR3* gene locus

To verify the CRISPR/Cas9-mediated gene knock-out, the *TLR3* gene locus of the AsPC-1 clones was amplified by Phusion Hot Start II DNA Polymerase (Thermo Fisher Scientific) using the protocol described in 2.2.3.4. The PCR product was diluted in nuclease-free H₂O to a final concentration of 10 ng/µl and sequenced by Eurofins Genomics (Ebersberg, Germany).

The sequencing results were evaluated using the free online program Synthego ICE analysis tool (<https://ice.synthego.com>).

2.2.4 Cell biological methods

2.2.4.1 Cell culture

All cell lines were cultured at 37 °C, with 5% CO₂ and a relative humidity of 95% in the BBD 6220 cell culture incubator (Heraeus). The human cell line HEK293T and the human PDAC cell line AsPC-1 were cultured in DMEM supplemented with 10% FCS, 1% L-glutamine, and 1% Penicillin-Streptomycin. Primary cell lines generated from murine tumors were cultured in RPMI 1640 medium with 10% FCS, 1% L-glutamine, and 1% Penicillin-Streptomycin. Cells were passaged before reaching confluency. Therefore, the cells were washed with PBS and incubated with trypsin-EDTA (Thermo Fisher Scientific) for 5 min at 37 °C. The reaction was stopped by the addition of FCS-containing culture medium and the cells were transferred to new cell culture dishes.

Hoxb8-ER/FL immune progenitor cells were cultivated as a suspension culture in 'progenitor outgrowth medium' as described in chapter 2.2.4.4.

2.2.4.2 Transfection of cells

HEK293T cells were transfected by calcium phosphate transfection at a confluency of 70-80% on a 10 cm cell culture dish. 15 µg of the plasmid DNA was diluted in H₂O to obtain a total volume of 360 µl and combined with 40 µl CaCl₂ (2.5 M). Afterwards, 400 µl of BES medium was added dropwise while mixing. The solution was incubated for 15 min at room temperature and then added dropwise to the cells. The cells were incubated overnight at 37 °C and the culture medium was replaced the next day.

2.2.4.3 Generation of conditioned medium

The FLT3L-conditioned medium was generated using a stably transfected B16 melanoma cell line. The FLT3L-secreting B16 cells were cultivated in RPMI 1640 medium (10% FCS, 1% L-

glutamine, 1% Penicillin-Streptomycin, 0.1% β -mercaptoethanol) until they reached confluency. The medium was replaced by fresh medium and the cells were further cultivated. The next day, the supernatant was collected, sterile filtered (pore size: 0.22 μ m, Starlab), and stored at -20 °C.

The murine fibroblast cell line L929 naturally secretes high levels of M-CSF. The cell line was used to generate the M-CSF-conditioned medium as described for the FLT3L-conditioned medium.

2.2.4.4 Generation of Hoxb8-ER/FL multipotent immune progenitor cell lines

Hoxb8-ER/FL immune progenitor cell lines were generated from murine, femoral bone marrow cells. The mice were euthanized by isoflurane and cervical dislocation, followed by the isolation of the femur. Both ends of the femur were cut off under sterile conditions in the Herasafe biological safety cabinet (Thermo Fisher Scientific) and the bone marrow cells were flushed with 10 ml RPMI 1640 medium with 10% FCS in a 15 ml conical tube using a syringe and a 27G cannula. The cells were pelleted (500 g, 3 min) and resuspended in 10 ml PBS with 1% FCS. To remove cell clusters and bone fragments, the suspension was filtered through a 100 μ m cell strainer. The cells were gently layered over 3 ml Biocoll (density 1.090) in a 15 ml conical tube and centrifuged for 10 min at 750 g without break. After centrifugation, the interphase was transferred to a 50 ml conical tube, washed with 45 ml PBS with 1% FCS and pellet by centrifugation (500 g, 3 min). The pellet was resuspended in RPMI 1640 medium, supplemented with 15% FCS, 1% L-glutamine, 1% Penicillin-Streptomycin, 5% FLT3L-conditioned medium, 10 ng/ml murine Interleukine-3, and 10 ng/ml murine Interleukine-6, and cultivated in 12-well plates with a cell density of $1.5-3 \times 10^6$ cells/well for 2-3 days. Then, the cells were pooled, centrifuged (500 g, 3 min), and resuspended in 'progenitor outgrowth medium' (Table 8).

Table 8: Composition of the progenitor outgrowth medium.

| Component | Percentage (v/v) / Concentration |
|----------------------------|----------------------------------|
| RPMI 1640 | |
| FCS (not heat inactivated) | 10% |
| L-Glutamine | 1% |
| Penicillin-Streptomycin | 1% |
| FLT3-conditioned medium | 5% |
| β -Mercaptoethanol | 0.1% |
| β -Estradiol | 1 μ M |

$2 \cdot 10^5$ cells/well were seeded in a 12-well plate and 1 ml of the Hoxb8-ER retrovirus-containing supernatant was added. To increase the infection efficiency, 1 μ l/ml Lipofectamine Transfection Reagent (Thermo Fisher Scientific) was added and the cells were incubated at 37 °C overnight. The next day, 1.5 ml/well of the medium was replaced by fresh progenitor outgrowth medium. During the following culture period, the medium was changed every 2-3 days. After 10 days, G418 (500 μ g/ml) was added for at least 7 days for the selection of virus infected cells. The *in vitro* differentiation upon withdrawal of β -estradiol from the medium was performed as described in 2.2.4.5 and the correct differentiation was verified by flow cytometry as described in chapter 2.2.4.6. The presence of Hoxb8-ER was determined by immunoblot detection of the protein complex based on the N-terminal HA-tag (see 2.2.5.4).

2.2.4.5 *In vitro* differentiation of Hoxb8-ER/FL immune progenitor cells to macrophages

The nuclear Hoxb8-ER complex keeps the immune progenitor cells in an undifferentiated state (Wang et al., 2006; Redecke et al., 2013). Withdrawal of β -estradiol from the culture medium prevents the nuclear import of the Hoxb8-ER complex and prevents its activity as

transcription factor, thereby enabling the differentiation of the cells in presence of differentiation stimuli.

For the differentiation of Hoxb8-ER/FL immune progenitor cells to macrophages, 2×10^6 cells were washed twice with PBS and resuspended in macrophage differentiation medium (RPMI 1640 with 10% FCS (not heat inactivated); 1% L-glutamine, 1% Penicillin-Streptomycin, 0.1% β -mercaptoethanol, 20% M-CSF-conditioned medium) and differentiated for 4 days at 37 °C. The medium was replaced by fresh medium on day 2. Correct differentiation was verified by flow cytometry (see 2.2.4.6).

2.2.4.6 Flow cytometry

Flow cytometry was used to verify the correct differentiation of *in vitro* differentiated macrophages by the detection of macrophage-specific cell surface markers. The differentiated macrophages were washed twice with PBS (Thermo Fisher Scientific) and incubated with trypsin-EDTA solution (Thermo Fisher Scientific) for 15 min at 37 °C to allow enzymatic cell detachment from the cell culture plates. Afterwards, the reaction was stopped by the addition of the macrophage differentiation medium (see 2.2.4.5). The cell suspension was transferred to a 15 ml conical tube and centrifuged (500 g, 3 min). To block unspecific signals, the cells were incubated for 15 min at 4 °C in anti-CD16/CD32 Fc-Block (BD Pharmingen), diluted 1:200 in PBS with 1% FCS.

After washing the cells in PBS with 1% FCS, the directly fluorescence-labeled primary antibodies for macrophage cell surface markers (diluted 1:200 in PBS containing 1% FCS) were incubated with the cells for at least 30 min at 4 °C. Unbound antibodies were removed by two subsequent washing steps in PBS with 1% FCS. The cells were resuspended in PBS with 1% FCS and analyzed by flow cytometry using the CytoFLEX flow cytometer (Beckman Coulter). Unspecific background fluorescence, cell debris and cell duplets were excluded from the analysis.

2.2.4.7 Annexin V FITC / Propidium iodide staining

The flow cytometric examination of cell death was performed using the Annexin V FITC / PI Dead Cell Apoptosis Kit (Thermo Fisher Scientific) according to the manufacturer's instructions using the CytoFLEX flow cytometer (Beckman Coulter).

2.2.4.8 MTT Assay

The MTT assay is a colorimetric measurement of metabolic cell activity based on the reduction of a tetrazolium salt by cellular NAD(P)H-dependent oxidoreductases and therefore used as an indicator for cell viability. 2×10^4 cells/well were seeded in a 96-well plate and stimulated as indicated. To analyze the metabolic cell activity, MTT solution was incubated with the cells for 4 h at 37 °C, followed by subsequent cell lysis and solubilization of the violet formazan crystals in MTT lysis buffer (0.1 M HCl, 10% SDS) at 37 °C overnight. The complex formation was quantified photometrically, based on the light absorbance at 580 nm.

2.2.4.9 CRISPR/Cas9-mediated gene knock-out

The plasmids psPAX2 (Addgene plasmid #12260; <http://n2t.net/addgene:12260>; RRID:Addgene_12260) and pMD2.G (Addgene plasmid #12259; <http://n2t.net/addgene:12259>; RRID:Addgene_12259) were gifts from Didier Trono. The plasmid lentiCas9-Blast (Addgene plasmid #52962; <http://n2t.net/addgene:52962>; RRID:Addgene_52962) and the plasmid lentiGuide-Puro (Addgene plasmid #52963; <http://n2t.net/addgene:52963>; RRID:Addgene_52963) were gifts from Feng Zhang. For CRISPR/Cas9-mediated gene knock-out of *TLR3*, two different sgRNAs were designed using an online sgRNA design tool (www.benchling.com) and cloned into the lentiviral plasmid lentiGuide-Puro. The work steps described in the following were executed in the S2 laboratory. Lentiviral particles were produced in HEK293T cells by transfection with the plasmids psPAX2, pMD2.G, and lentiCas9-Blast or lentiGuide-Puro. The virus-containing supernatant was collected 48 h and 72 h after transfection of the HEK293T cells, filtered using a 0.45 µm filter and stored at -80 °C until further usage. The human PDAC cell line AsPC-1 was first infected with the *Cas9*-encoding lentivirus. Two days after the infection, the medium was changed to fresh DMEM, supplemented with 10 µg/ml blasticidin S for the selection of in-

ected cells for 7 days. The selected cells were subsequently infected separately with the sgRNA-encoding lentiviruses. The medium was replaced two days after the infection by fresh DMEM containing 2 µg/ml Puromycin. After 5 days of selection, the cells were transferred to new cell culture plates at a low density and cultured until single colonies were macroscopically visible. The colonies were separated manually into new cell culture plates. *TLR3* deficiency was verified by sequencing.

2.2.4.10 3D culture of primary acinar cell clusters

The pancreas of 4- to 6-week-old mice was isolated, washed 3 times in cold HBSS, and cut into pieces of approximately 1 mm in size using a sterile scissor. The tissue fragments were digested with collagenase P (0.4 mg/ml, Roche) in HBSS for 10 min at 37 °C with gentle agitation. The digestion was stopped by the addition of 5% FCS in HBSS. The cells were pelleted (400 g, 2 min), washed twice with HBSS (5% FCS), and filtered through a 100 µm cell strainer. The cell suspension was layered over a 30% FCS solution to allow intact cell clusters to precipitate by low-speed centrifugation (180 g, 2 min). The acinar cell clusters were resuspended in Matrigel (Corning) with an equal volume of 3D culture media (Waymouth's media, 10% FCS, 1% Penicillin-Streptomycin, 1% L-glutamine, 100 µg/ml soybean trypsin inhibitor, 1 µg/ml dexamethasone), and seeded on collagen type 1-coated wells of a 24-well plate. After the polymerization of the Matrigel, the acinar cell culture medium was added (Table 9).

Table 9: Composition of the culture medium for the 3D culture of primary acinar cell clusters.

| Component | Percentage (v/v) / Concentration |
|---------------------------|---|
| Waymouth's medium | |
| FCS | 10% |
| L-Glutamine | 1% |
| Penicillin-Streptomycin | 1% |
| Soybean trypsin inhibitor | 100 µg/ml |
| Dexamethasone | 1 µg/ml |

2.2.4.11 Exosome isolation from cell culture supernatant

Exosomes were isolated from cell culture supernatant using the ExoQuick exosome isolation Kit (System Biosciences). KPF tumor cell lines were seeded with equal cell numbers in 6-well plates and cultivated in 2 ml cell culture medium overnight. Primary murine acinar cells were cultivated in 24-well plates as described in chapter 2.2.4.10.

Exosomes were isolated from the cell culture supernatant. After the removal of cell debris by centrifugation (1000 g, 5 min, 4 °C), 500 µl of the medium was combined with 126 µl exosome precipitation solution (ExoQuick exosome isolation Kit, System Biosciences) and incubated overnight at 4 °C. The next day, exosomes were precipitated by centrifugation (1500 g, 30 min, 4 °C). The pelleted exosomes were resuspended in 100 µl sterile PBS and directly used for quantification.

2.2.4.12 Exosome quantification

Exosome were quantified based on the activity of the exosomal acetyl-CoA acetylcholinesterase using the ExoCET exosome quantification Kit (System Biosciences) according to the manufacturer's instructions. To calculate the number of exosomes, the absorbances were compared to a standard curve with known exosome numbers and normalized to the volume of the medium used in the assay and the protein concentration as determined by NanoDrop ND-1000 (Nanodrop Technologies).

2.2.5 Protein biochemical methods

2.2.5.1 Protein isolation from murine tissue and cell lines

Murine tissue samples for protein isolation were immediately frozen in liquid nitrogen and stored at -80 °C until further usage. For protein isolation, a minimum of 25 mg of the tissue was lysed in 400 µl RIPA buffer containing 2 tablets/10 ml phosphatase inhibitor cocktail (Roche) and 2 tablets/10 ml protease inhibitor cocktail (Roche). Lysis efficiency was increased by the addition of a metal bead and mechanical tissue lysis at a frequency of 30/s for 3 min using the TissueLyser II (Qiagen). The lysate was sonicated (10x 15 sec, 4 °C) with the Bioruptor Sonicator (Diagenode) and rotated for 10 min at 4 °C. Cell debris was pelleted

by centrifugation (21130 rcf, 10 min, 4 °C). Complete protein denaturation was obtained using a combination of chemical denaturation, by diluting the lysate in Laemmli buffer, and heat-induced denaturation, by incubating the samples at 95 °C for 5 min. The lysates were stored at -20 °C.

For protein isolation from cell lines, the cells were first washed with PBS, then directly lysed by the addition of RIPA buffer with 2 tablets/10 ml phosphatase inhibitor cocktail (Roche) and 2 tablets/10 ml protease inhibitor cocktail (Roche). The lysate was transferred to a Safe Lock reaction tube (Eppendorf) using a cell scraper (Biochrom), sonicated, rotated, centrifuged, denatured, and stored as described above for tissue lysates.

2.2.5.2 *BCA assay*

The protein concentration was measured using the Pierce BCA Protein Assay Kit (Thermo Fisher Scientific) following the instructions of the manufacturer.

2.2.5.3 *Sodium dodecyl sulfate polyacrylamide gel electrophoresis (SDS-PAGE)*

Sodium dodecyl sulfate polyacrylamide gel electrophoresis (SDS-PAGE) was used to separate denatured proteins in an electric field according to their molecular weight. To achieve optimal separation of the proteins, a discontinuous SDS-PAGE, with stacking gel (5% acrylamide) and separating gel (12% acrylamide), was used. The SDS-PAGE was first performed at 80 V until the protein samples passed the stacking gel, then at 120 V using the Biometra P25T electrophoresis power supply (Analytik Jena).

2.2.5.4 *Immunoblot*

Immunoblot analysis was used for the quantification of specific proteins. Following the separation of the proteins by SDS-PAGE, the proteins were transferred to a 0.45 µm pore size nitrocellulose membrane (GE healthcare) using a semi-dry transblotting system at 12V for 1 h. The membrane was subsequently blocked in 5% BSA in PBS-Tw (see 7.4) for 1 h at room temperature to avoid unspecific binding of antibodies to the membrane. The primary anti-

bodies were diluted in PBS-Tw with 5% BSA and incubated with the membrane overnight at 4 °C. After washing the membrane with PBS-Tw (3x 10 min, RT), the HRP-conjugated secondary antibodies (diluted 1:4000 in PBS-Tw with 5% BSA) were incubated with the membrane for 1 h at room temperature. Unbound secondary antibodies were removed by subsequent washing with PBS-Tw (3x 10 min). Pierce ECL Western Blotting Substrate (Thermo Fisher Scientific) was used to visualize the antibody-enzyme complex bound proteins by chemiluminescence using the UPV ChemStudio visualization system (Analytik Jena).

3 Results

3.1 Myeloid cell TLR3 is critical for pancreatic regeneration after acute pancreatitis in mice

3.1.1 Work preceding this thesis

A conditionally *Tlr3*-deficient mouse line (TLR3^{OFF}), created by the insertion of a *loxP*-site flanked transcriptional termination element in the endogenous gene locus of *Tlr3*, was used to examine the cell-specific function of TLR3 in acute pancreatitis (AP) (Fig. 8A, 2.2.1.1; Stöß et al., 2020; Hidalgo-Sastre et al., 2021). *LysM-Cre* mice and TLR3^{OFF} mice were crossed for the Cre-mediated selective rescue of *Tlr3* expression in myeloid cells (TLR3^{Mye}). AP was induced by 8 hourly injections of caerulein (Fig. 8B, 2.2.1.3).

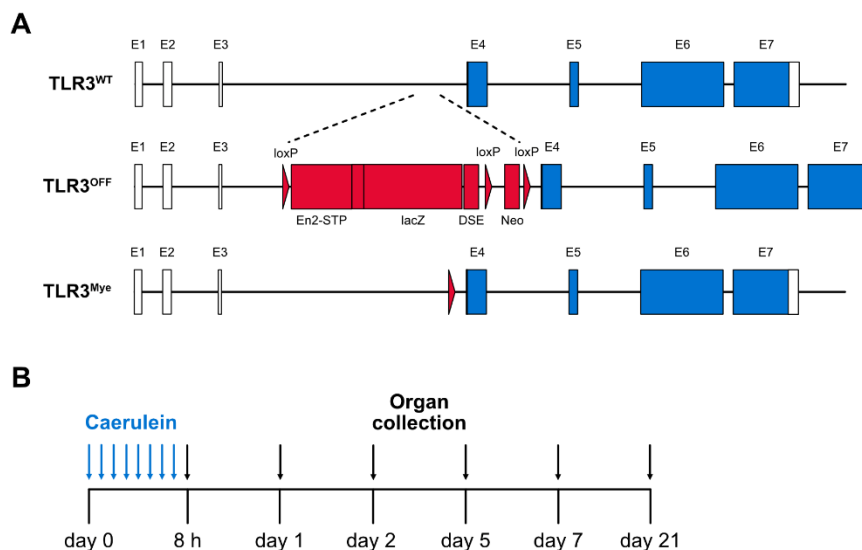


Figure 8: Mouse model to study the cell-specific function of TLR3 in acute pancreatitis. (A) Gene locus of *Tlr3* in WT, TLR3^{OFF}, and TLR3^{Mye} mice. The expression of *Tlr3* is blocked in TLR3^{OFF} mice by a *loxP*-site flanked transcriptional termination element (*En2-STP*) upstream of the start codon in exon 4. In TLR3^{Mye} mice, Cre-mediated recombination causes the myeloid cell-specific rescue of *Tlr3* expression. **(B)** Schematic representation of the protocol used to investigate the cell-specific function of TLR3 in acute pancreatitis induced by 8 hourly intraperitoneal injections of 2 µg/injection caerulein. Organs were collected at indicated time points after the first injection of caerulein.

At day 2 after caerulein treatment, acinar-to-ductal metaplasia (ADM) was histologically present, associated with a high number of intrapancreatic immune cells, predominantly macrophages. The pancreas of WT mice was fully regenerated at days 5 and 7 after AP induction with no histologically detectable ADM structures, associated with the clearance of tissue-resident immune cells back to the original baseline level.

While global or partial *Tlr3* deficiency had no influence on the early phase of acute pancreatitis, at day 2, TLR3^{OFF} mice had a significantly higher percentage of ADM area compared to WT mice. Immune cell infiltration of macrophages, T cells, and neutrophils was significantly increased in TLR3^{OFF} mice, indicative of an enhanced immune reaction. Remarkably, the number of macrophages and T cells remained at a persistently high level at day 5 in TLR3^{OFF} mice. ADM structures persisted until day 7 after acute pancreatitis induction as a consequence of the defective pancreatic regeneration caused by global *Tlr3* deficiency.

Strikingly, exclusive expression of *Tlr3* in myeloid cells partially rescued the regenerative defect caused by global *Tlr3* deficiency at day 2 and day 5, with a complete rescue at day 7. The immune cell infiltration in TLR3^{Mye} mice equaled the wild type. The results highlight the key role of myeloid cell-specific TLR3 signaling for pancreatic regeneration after AP. Myeloid cell TLR3 limited the number of tissue-resident immune cells and terminated the immune reaction to complete the regenerative process.

3.1.2 Increased expression of ADM markers in global *Tlr3*-deficient mice after AP

The current thesis continued on this work, first by characterizing the process of pancreatic regeneration by RT-qPCR and IHC staining for ductal cell markers (SOX9, KRT19) and the acinar cell marker CPA1.

Work conducted during the thesis shows that, at day 2, the increased ADM formation in $TLR3^{OFF}$ mice was associated with a significantly higher number of SOX9⁺ exocrine cells (Fig. 9A) and consistently an increased pancreatic expression of *Sox9* compared to WT and $TLR3^{Mye}$ mice (Fig. 9B). In accordance, the expression of *Krt19* was significantly increased in $TLR3^{OFF}$ mice and the KRT19⁺ area was higher in $TLR3^{OFF}$ mice compared to $TLR3^{Mye}$ mice. The expression of the acinar cell marker *Cpa1* was reduced in $TLR3^{OFF}$ mice compared to $TLR3^{Mye}$ mice, while there was no difference in the IHC staining of CPA1.

At day 5, the number of SOX9⁺ exocrine cells and the KRT19-stained area remained at a high level in $TLR3^{OFF}$ mice, in accordance with the histologically observed persistence of ADM structures. Compared to WT mice, the CPA1⁺ area was reduced in $TLR3^{OFF}$ mice. While there was no difference for the expression of *Sox9* and *Krt19* on RNA level at day 5, the expression of *Cpa1* was significantly reduced in $TLR3^{OFF}$ mice compared to WT and $TLR3^{Mye}$ mice.

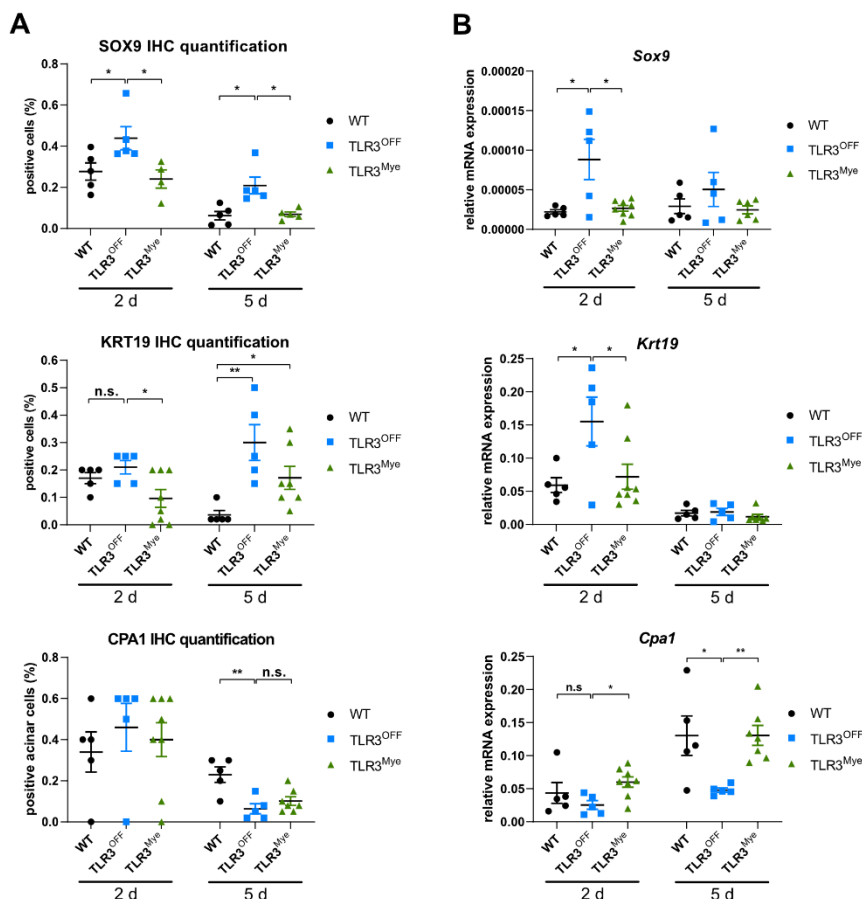


Figure 9: Global *Tlr3* deficiency causes induction of ductal markers and reduction of acinar cell-specific markers after AP. IHC-based (A) and RT-qPCR-based (B) quantification of the ductal markers SOX9 and KRT19 and the acinar cell-specific marker CPA1 in TLR3^{OFF} and TLR3^{Mye} mice compared to WT controls at day 2 and day 5 after AP induction. For the quantification of SOX9, five randomly distributed HPF (250 μ m x 250 μ m, 20x magnification) were analyzed. For KRT19 and CPA1, the staining of the whole pancreas was quantified. Data were analyzed using the unpaired t-test and are presented as mean \pm SEM. * $p < 0.05$, ** $p < 0.01$.

The IHC staining and RT-qPCR analysis for differentiation markers confirm the results of the H&E staining. The dedifferentiation of acinar cells to ductal-like progenitor cells was enhanced in TLR3^{OFF} mice and remained at a sustaining high level, indicative of a defective regenerative response after acute pancreatitis. The rescue of this phenotype by exclusive expression of *Tlr3* in myeloid cells highlights the importance of TLR3 in myeloid cells for pancreatic regeneration.

3.1.3 TLR3 signaling has no direct effect on acinar transdifferentiation *in vitro*

To characterize the function of TLR3 in ADM formation after AP, an *in vitro* model for studying the transdifferentiation of primary, murine acinar cells was established. Acinar cell clusters from WT mice were isolated and cultured in 3D. To study the influence of TLR3 signaling on acinar cells, transdifferentiation was examined in presence of the synthetic TLR3 agonist poly(I:C). At day 3, the acinar cell clusters spontaneously transdifferentiated to ductal-like spheroid structures, associated with the downregulation of the acinar cell-specific marker *Amy2* and the induction of the ductal marker *Krt19* (Fig. 10A, Fig. 10B, Fig. 10C). Induction of epithelial TLR3 signaling had no effect on acinar transdifferentiation. In contrast, the presence of EGF remarkably enhanced the transdifferentiation on day 3. Expression of *Tlr3* was significantly downregulated by *in vitro* cultured acinar cells at day 3 (Fig. 10D). The results from the *in vitro* experiment confirm that acinar cell-specific TLR3 signaling had no direct effect on the formation of ADM structures and thus supporting the previous observations that myeloid cell-specific TLR3 signaling was responsible for the defective pancreatic regeneration after AP.

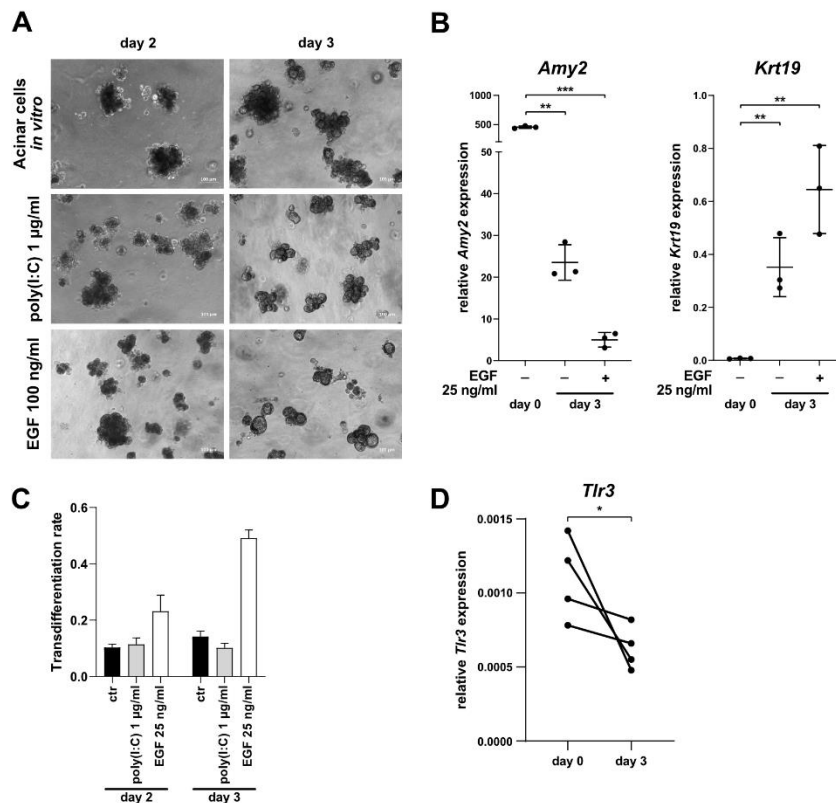


Figure 10: TLR3 signaling has no direct effect on the transdifferentiation of acinar cells *in vitro*. (A) Representative bright-field pictures of Matrigel-embedded murine WT acinar cell clusters on day 2 and day 3 in culture. TLR3 signaling was stimulated by 1 µg/ml poly(I:C). Stimulation with EGF (100 ng/ml) was used as a positive control. Acinar cell clusters formed ‘bunch-of-grape’ like structures, while transdifferentiated ductal-like clusters formed hollow spheres. Scale bars indicate 100 µm. (B) RT-qPCR-based quantification of the acinar cell-specific marker *Amy2* and the ductal marker *Krt19*. Data are presented as mean ± SEM and analyzed using the paired t-test. (C) Quantification of acinar cell transdifferentiation on day 2 and day 3. The percentage of transdifferentiated clusters per HPF was validated morphologically. Data are presented as mean ± SEM. (D) Expression of *Tlr3* of directly isolated acinar cells (d0) and transdifferentiated acinar cells after 3 days of *in vitro* culture (d3). Data were analyzed using the unpaired t-test. * p < 0.05, ** p < 0.01, *** p < 0.001.

3.1.4 Increased cytokine expression in global *Tlr3*-deficient mice after AP

To characterize the underlying molecular processes associated with defective pancreatic regeneration and the increased, sustaining high number of tissue-resident immune cells, the expression of inflammatory markers and cytokines was quantified by RT-qPCR at different time points after AP induction (24 h, day 2, day 5, day 7). At day 2, *TLR3*^{OFF} mice expressed significantly higher levels of the proinflammatory factors *Il-6* and *Tnf*, as well as higher levels of the immunosuppressive *Il-10* (Fig. 11). The expression of the monocyte recruiting factor *Ccl2* was increased in *TLR3*^{OFF} mice at day 2 compared to WT and *TLR3*^{Mye} mice, while there were no differences in the expression of the cytokines *Ccl3*, *Ccl4*, and *Ccl5*.

The RT-qPCR analysis of inflammatory markers cannot fully explain the observed increased and persistently high number of immune cells and the defective pancreatic regeneration caused by global *Tlr3* deficiency.

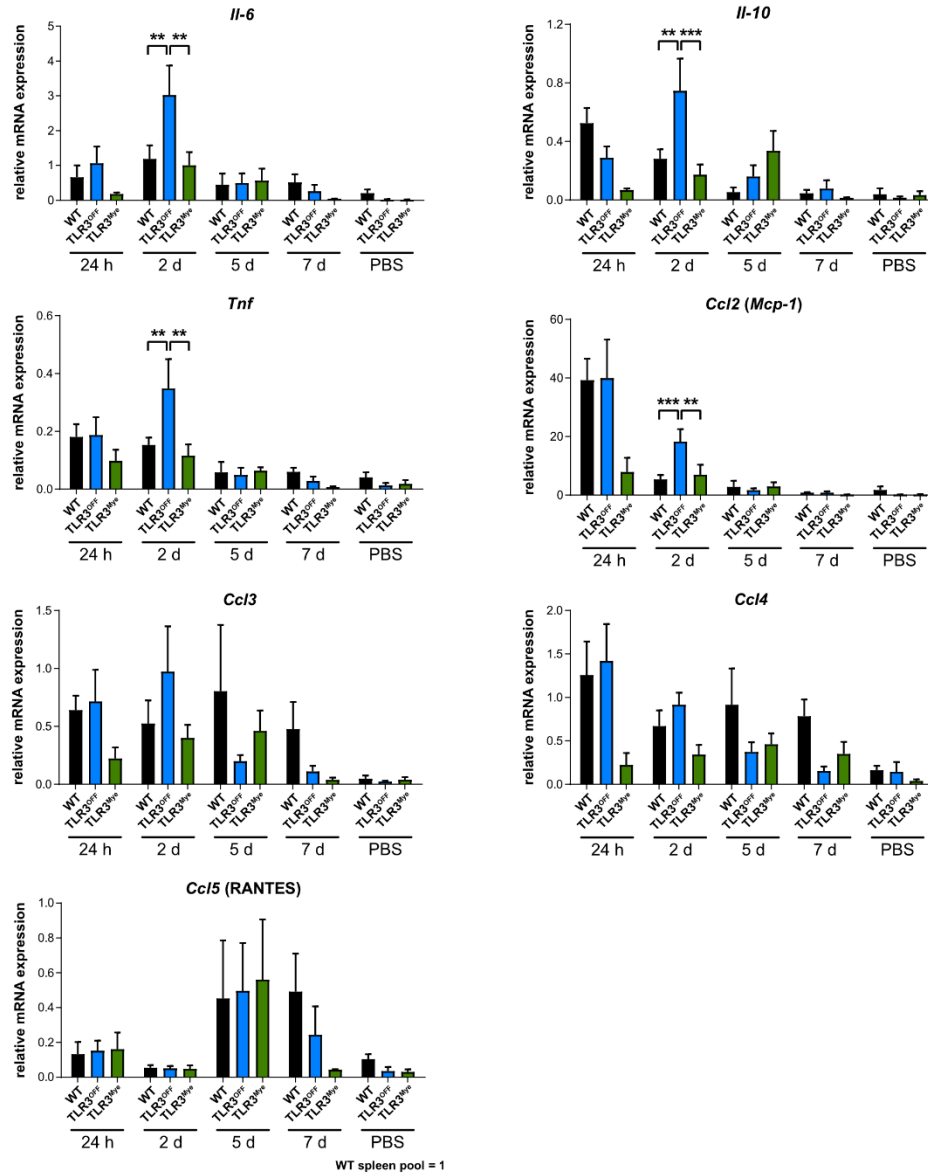


Figure 11: TLR3 in myeloid cells regulates cytokine expression at day 2 after AP induction. RT-qPCR-based quantification of the inflammatory cytokines *Il-6* and *Tnf*, the anti-inflammatory *Il-10*, and the immune cell recruiting cytokines *Ccl2*, *Ccl3*, *Ccl4*, and *Ccl5*. The expression was normalized to cDNA from a WT spleen pool. Data were analyzed using the two-way ANOVA test and are presented as mean \pm SEM. * p < 0.05, ** p < 0.01, *** p < 0.001.

3.1.5 Generation of Hoxb8-ER/FL immune progenitor cell lines to study the effect of TLR3 in myeloid cell *in vitro*

Macrophages are *Tlr3*-expressing myeloid-derived immune cells with outstanding importance for the regulation of the immune response (Murakami et al., 2014; Das et al., 2015). Additionally, it is known that macrophages can directly promote the transdifferentiation of acinar cells (Liou et al., 2013). Due to the persistently high number of macrophages in the tissues of TLR3^{OFF} mice and their key importance for orchestrating the immune response for tissue regeneration, the effect of TLR3 signaling in macrophages was examined.

For this purpose, an *in vitro* model for the expansion and differentiation of immune progenitor cells was established (Wang et al., 2006; Redecke et al., 2013). To keep the cells in an undifferentiated progenitor state, murine femoral bone marrow cells were retrovirally infected to express a complex of the transcription factor Hoxb8 covalently linked to a fragment of the estrogen receptor (Hoxb8-ER). Infected cells were selected based on the virally encoded neomycin resistance gene. The expression of the *Hoxb8-ER* complex was verified by immunoblot analysis based on the detection of the N-terminal HA-tag (Fig. 12A). Withdrawal of β -estradiol from the culture medium prevented the nuclear import of Hoxb8-ER and allowed for the differentiation of the progenitor cells to macrophages by M-CSF-conditioned media. The differentiation process was associated with the adhesion of the macrophages to the cell culture dish (Fig. 12B). The correct differentiation of the cells was confirmed by flow cytometric detection of the macrophage surface markers F4/80, CD115, and CD11b (Fig. 12C).

To examine the effect of TLR3 signaling on macrophages, a *Tlr3*-deficient Hoxb8-ER/FL immune progenitor cell line was generated from bone marrow cells of TLR3^{OFF} mice. To exclude potential effects of the *loxP* sites present in the *Tlr3* gene locus, a Hoxb8-ER/FL cell line was established from TLR3^{Mye} mice. *Tlr3* deficiency had no effect on the differentiation of macrophages, as demonstrated by flow cytometry for macrophage cell surface markers (Fig. 12C). *Tlr3* was not expressed by macrophages from TLR3^{OFF} mice (Fig. 12D). *Tlr3* expression of macrophages from WT mice equaled the *Tlr3* expression of macrophages from TLR3^{Mye} mice.

In summary, the *in vitro* system for the infinite expansion and differentiation of Hoxb8-ER/FL immune progenitor cells was successfully established. The *in vitro* generated macrophages were next stimulated with the synthetic TLR3 agonist poly(I:C), to study the effects of TLR3 signaling on macrophages.

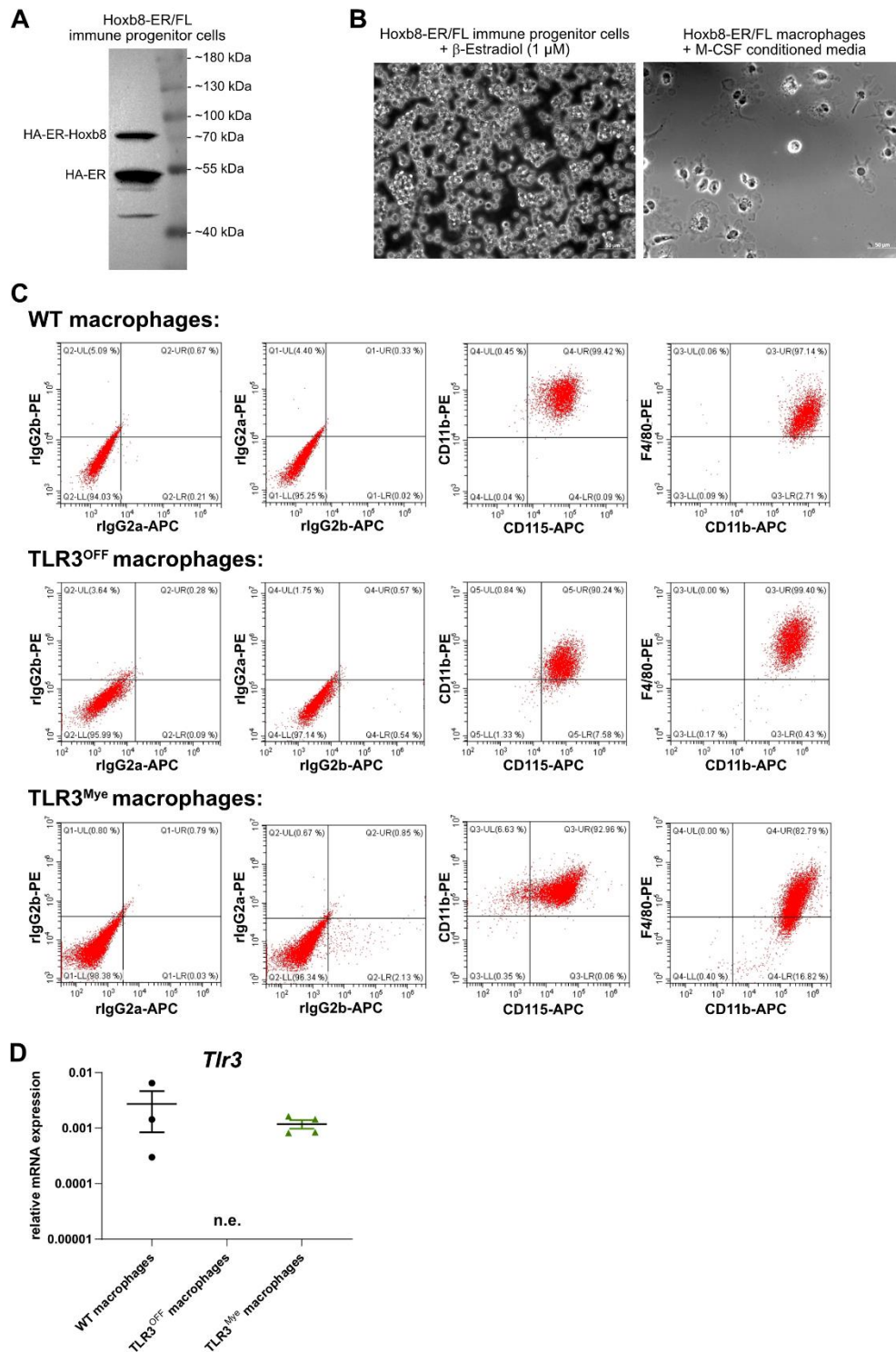


Figure 12: Establishment of the Hoxb8-ER/FL *in vitro* culture system for the *in vitro* generation of differentiated macrophages. (A) Representative immunoblot confirmation of the presence of the Hoxb8 fusion protein (molecular weight: 67 kDa) in a newly generated immune progenitor cell line by detection of the N-terminal HA-tag. The signal at approximately 55 kDa most likely originates from an N-terminal fragment of the HA-ER-Hoxb8 complex. (B) Phase contrast images of undifferentiated Hoxb8-ER/FL immune progenitor cells and M-CSF differentiated macrophages. In presence of β -estradiol, Hoxb8-ER/FL cells remain in an undifferentiated state, morphologically visible by the persistence of the cells as a suspension culture. M-CSF-induced differentiation promotes the adhesion of differentiated macrophages to the cell culture plate. Scale bars indicate 50 μ m. (C) Flow cytometric detection of the macrophage-specific cell surface markers F4/80, CD115, and CD11b by *in vitro* differentiated macrophages from Hoxb8-ER/FL immune progenitor cell lines established from WT, TLR3^{OFF}, and TLR3^{Mye} mice, compared to isotype controls. Cell duplicates and dead cells were excluded from the analysis. (D) *Tlr3* was expressed equally high in WT and TLR3^{Mye} macrophages, while it was not detectable in TLR3^{OFF} macrophages. Data are presented as mean \pm SEM. n.e. = not expressed.

In the Hoxb8-ER/FL macrophages from WT and TLR3^{Mye} mice, TLR3 was localized in endosomes (Fig. 13A). Induction of TLR3 signaling by stimulation with the TLR3 agonist poly(I:C) (100 ng/μl, 6 h) led to the nuclear translocation of p65/RelA, indicative of the activation of the NF-κB signal transduction pathway. Stimulation of WT Hoxb8-ER/FL macrophages with poly(I:C) induced the expression of proinflammatory factors (*Il-6*, *Tnf*, *Ccl5*, Fig. 13B). In contrast, poly(I:C) stimulation of TLR3^{OFF} macrophages had no effect on cytokine expression, confirming the absence of functional TLR3.

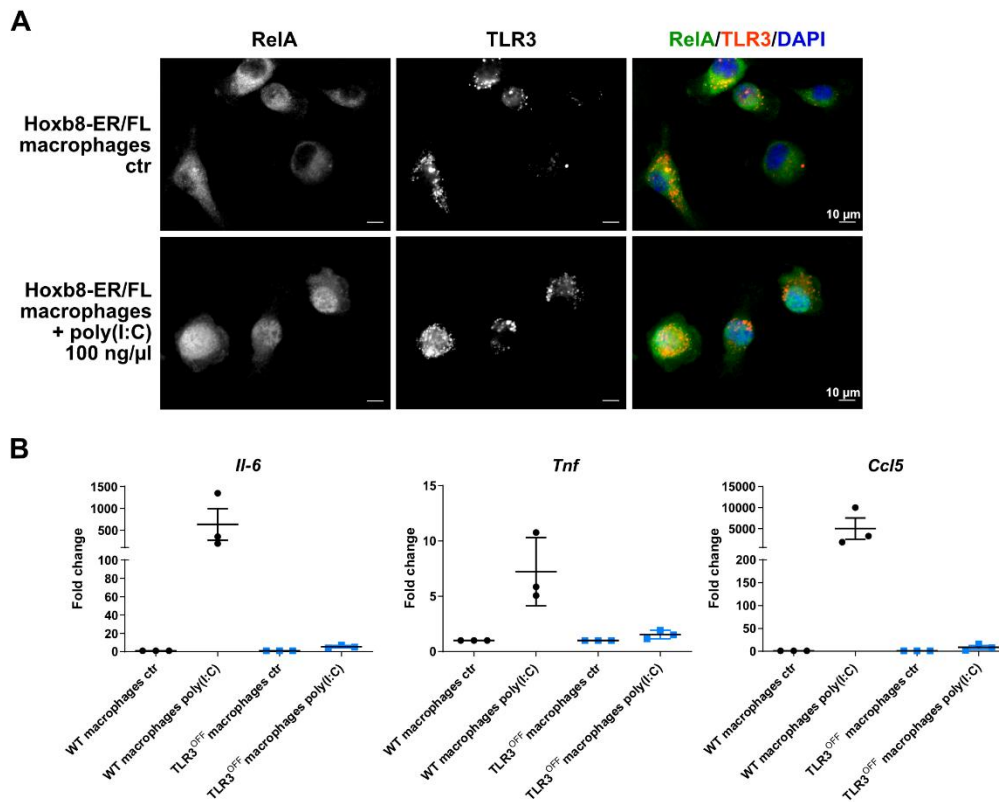


Figure 13: Endosomal TLR3 in WT Hoxb8-ER/FL macrophages induces NF-κB signaling and the expression of proinflammatory cytokines. (A) Representative immunofluorescence staining of p65/RelA and TLR3 in Hoxb8-ER/FL macrophages from WT mice. Poly(I:C) stimulated macrophages (6 h, 100 ng/μl, lower panels) were compared to untreated controls (upper panels). (B) RT-qPCR-based quantification of the expression of *Il-6*, *Tnf*, and *Ccl5* after stimulation of WT and TLR3^{OFF} macrophages with 100 ng/μl poly(I:C) for 6 h. Data are presented as mean ± SEM.

3.1.6 Myeloid cell TLR3 induces immune cell clearance after acute pancreatitis

Stimulation with poly(I:C) led to a dose-dependent reduction of macrophage cell viability after 48 h (Fig. 14A). Even low doses of poly(I:C) were sufficient to cause a significant reduction of the cell viability.

To verify the specificity of poly(I:C) for the induction of cell death via TLR3, the cell viability of macrophage lines from TLR3^{OFF} and TLR3^{Mye} mice was examined after poly(I:C) stimulation. The stimulation with poly(I:C) induced cell death only in *Tlr3*-expressing macrophage lines (WT and TLR3^{Mye}), while cell viability of TLR3^{OFF} macrophages was unaffected (Fig. 14B). The TLR3-dependent induction of cell death was associated with the formation of the 43 kDa and 18 kDa fragments of cleaved caspase 8 (Fig. 14C).

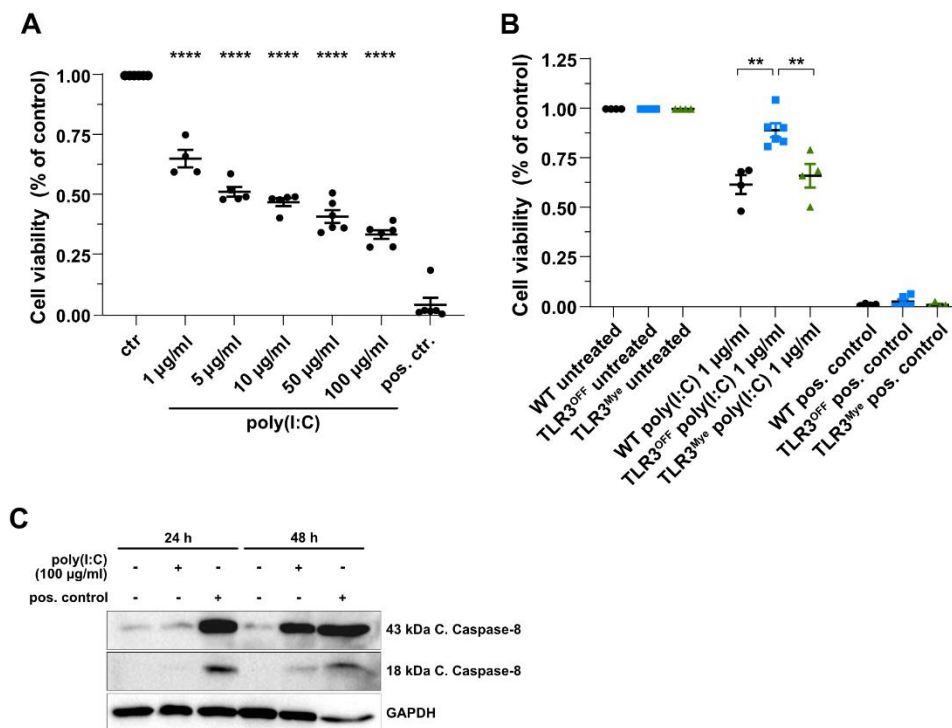


Figure 14: TLR3 signaling induces cell death of murine macrophages *in vitro*. (A) Dosage-dependent reduction of the cell viability of WT macrophages after 48 h of stimulation with the TLR3 agonist poly(I:C). The cell viability was quantified by MTT assay. (B) The cell viability of WT, TLR3^{OFF}, and TLR3^{Mye} macrophages after 48 h of stimulation with 1 µg/ml poly(I:C), measured by MTT assay. (C) The stimulation of WT macrophages with poly(I:C) (100 µg/ml) induced the formation of the 43 kDa and 18 kDa fragment of cleaved caspase 8. GAPDH was included as a loading control. (A, B, C) Brefeldin A (4.5 µg/ml) was used as a positive control for the induction of apoptosis. Data were analyzed using the unpaired t-test and are presented as mean ± SEM. * p < 0.05, ** p < 0.01, *** p < 0.001, **** p < 0.0001.

Macrophages are of key importance for orchestrating the immune reaction and for the resolution of the immune response after AP. Macrophages were demonstrated to be sensitive to TLR3-mediated induction of cell death, involving the formation of cleaved caspase 8. Mye-

loid cell TLR3 was shown to enable pancreatic regeneration by limiting the number of tissue-resident macrophages. TLR3-mediated termination of the immune reaction after AP seems to involve the resolution of macrophages by induction of cell death. This could finally lead to a clearance of the immune cells from the pancreas and thereby terminate the regeneration process.

3.1.7 TLR3-dependent cell death is induced in the late phase of acute pancreatitis

To identify TLR3-dependent signal transduction pathways involved in the late phase of pancreatic regeneration after AP, gene expression of WT and TLR3^{OFF} mice at day 2 and day 5 after AP induction was examined by bulk RNA sequencing of the pancreas. ANOVA-based clustering of differentially expressed genes revealed 5 distinct expression clusters (Fig. 15A). Genes of cluster 1 were expressed mainly at day 2 in the pancreas of WT mice. The genes included in this cluster are associated with the Molecular Signature Database (MSigDB) hallmark gene sets Myc targets V1, DNA repair, and apoptosis (Fig. 15B).

Cluster 3 includes genes associated with apoptosis. The bulk RNA sequencing results show the upregulation of apoptosis markers in the pancreas of WT mice mainly at day 5 after AP induction, whereas the cluster was only marginally expressed by TLR3^{OFF} mice.

At day 2 after AP induction, TLR3^{OFF} mice were characterized by the expression of cluster 4 (MSigDB hallmark gene sets: angiogenesis, Myc Targets V2, IL-6/JAK/STAT3 signaling) and cluster 5 (MSigDB hallmark gene sets: oxidative phosphorylation, unfolded protein response). At day 5 after AP, genes included in cluster 2 (MSigDB hallmark gene set: mTORC1 signaling) were upregulated in the pancreas of TLR3^{OFF} mice.

The associated expression clusters demonstrate the ongoing tissue regeneration and persistent immune reaction in the pancreas of TLR3^{OFF} mice on day 2 and day 5 after AP induction. The results confirm the observed impaired pancreatic regeneration caused by global *Tlr3* deficiency on RNA expression level. In contrast to the continuous expression of regeneration-associated gene clusters in TLR3^{OFF} mice, apoptosis-associated genes are upregulated in the pancreas of WT mice at day 5. Hence, the RNA sequencing results confirm the previously observed importance of TLR3-induced cell death for the termination of the immune response to allow proper tissue regeneration.

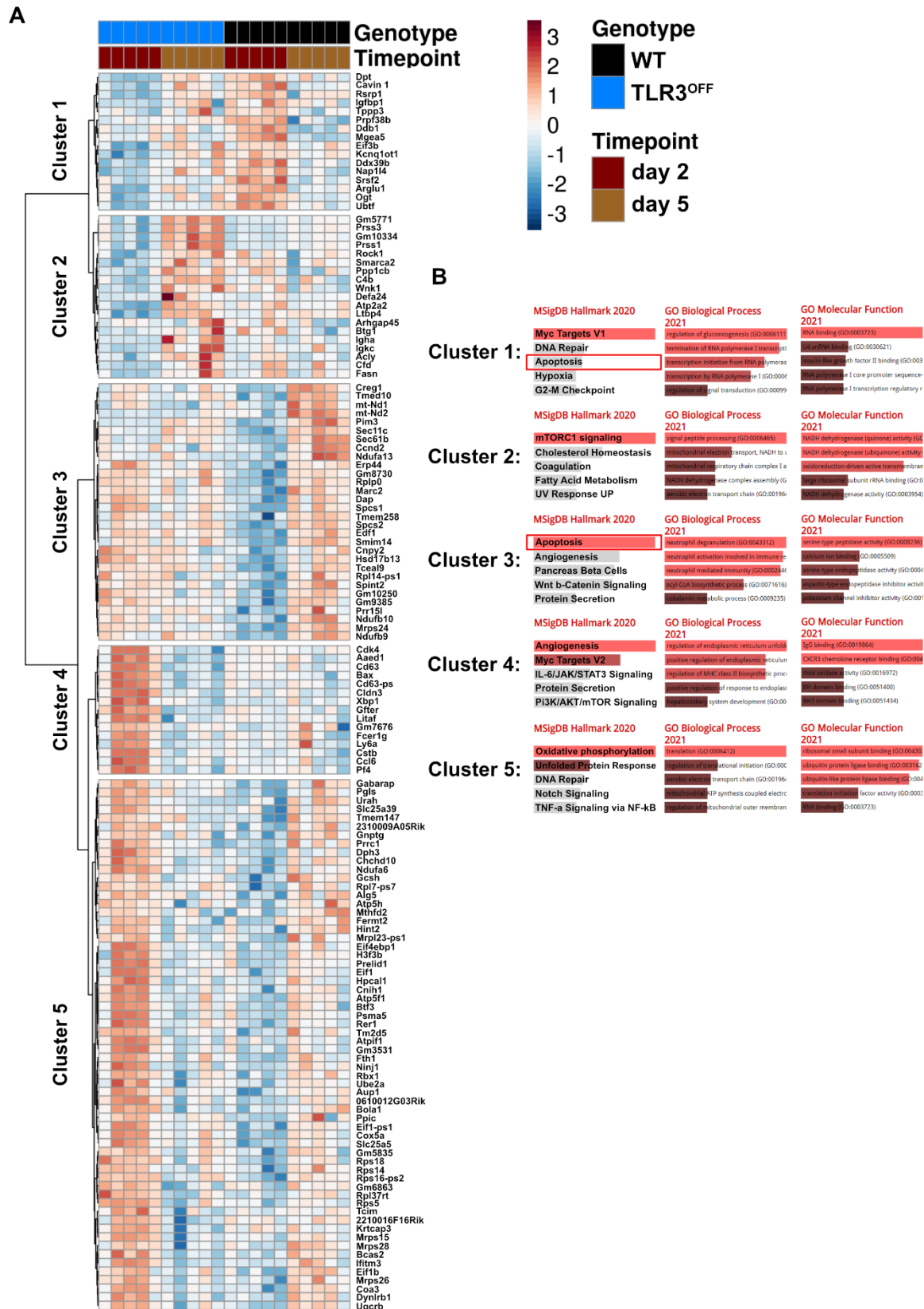


Figure 15: Bulk pancreas RNA sequencing confirms the TLR3-dependent induction of cell death pathways in the late phase of tissue regeneration after AP. (A) Hierarchically clustered heatmap of differentially expressed genes in the pancreas of TLR3^{OFF} (blue) and WT (black) mice at day 2 (red) and day 5 (brown) after AP induction. **(B)** Pathway analysis of differentially expressed gene clusters using the online tool Enrichr (<https://maayanlab.cloud/Enrichr/>). RNA Sequencing was performed in cooperation with Dr. Roland Rad (Klinikum rechts der Isar, Munich, Germany).

3.1.8 *Casp8* deficiency has no effect on pancreatic regeneration after acute pancreatitis in mice

TLR3 signaling in macrophages was shown to terminate the immune response after acute pancreatitis by inducing the cell death of macrophages, involving the formation of cleaved caspase 8. To examine a potential function of caspase 8 in pancreatic regeneration, AP was induced in mice with myeloid cell-specific deletion of *Casp8* (*Casp8^{Myc}*) by LysM-Cre-mediated inactivation of the *loxP*-flanked exon 3 in the gene locus of *Casp8*. Mice that were homozygous for the *loxP*-flanked *Casp8* allele (*Casp8^{fl/fl}*) were used as a control group.

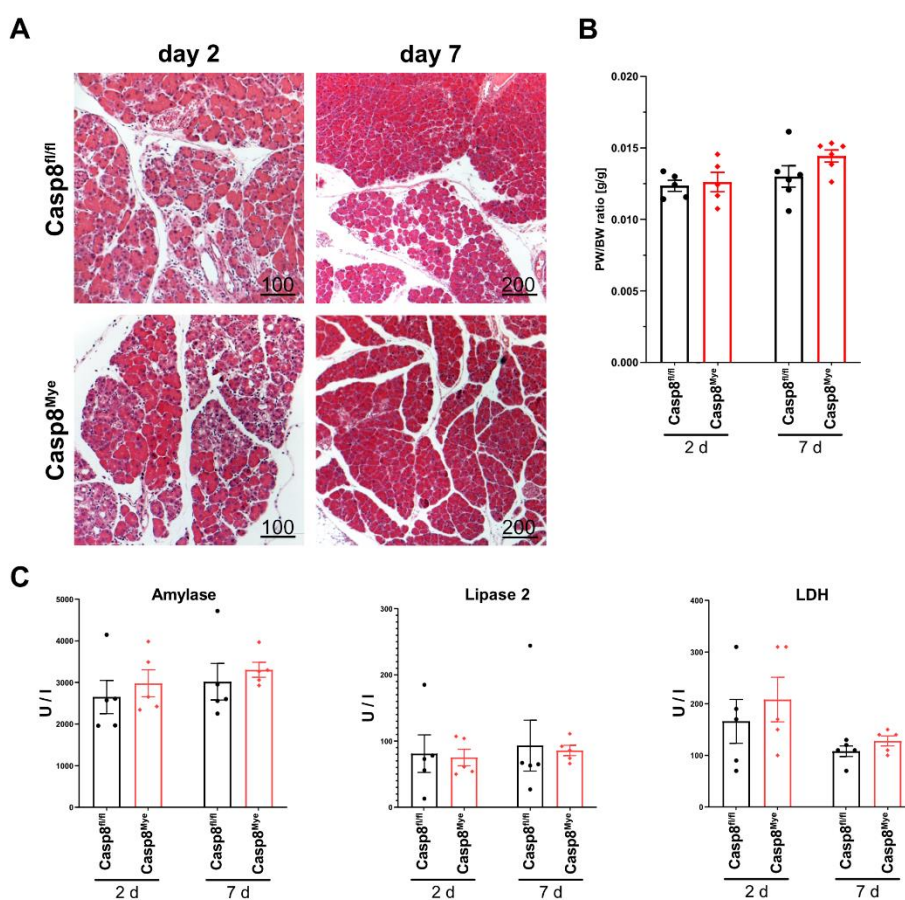


Figure 16: Myeloid cell *Casp8* deficiency does not affect pancreatic regeneration after acute pancreatitis in mice. (A) Representative H&E pictures of pancreas sections from *Casp8^{fl/fl}* and *Casp8^{Myc}* mice on day 2 and day 7 after the induction of acute pancreatitis by 6 hourly i.p. injections of caerulein on day -2 and day 0. Scale bars indicate 100 μ m (left panels, day 2) or 200 μ m (right panels, day 7). **(B)** Pancreas-to-body weight ratio of *Casp8^{fl/fl}* and *Casp8^{Myc}* mice at day 2 and day 7 after AP induction. **(C)** Serum levels of the pancreatitis-associated serum markers amylase, lipase 2, and LDH of *Casp8^{Myc}* mice compared to *Casp8^{fl/fl}* mice at day 2 and day 7. Data are presented as mean \pm SEM.

At day 2 after AP induction, pancreatic regeneration of *Casp8^{fl/fl}* mice was associated with ADM formation and high immune cell infiltration, as shown by H&E staining (Fig. 16A). At

day 7, the pancreas of *Casp8^{fl/fl}* mice was fully regenerated with no signs of ADM, combined with the clearance of immune cells, indicative of the proper termination of the AP-induced immune response. Pancreatic regeneration of *Casp8^{fl/fl}* mice was equal to WT mice, with no apparent effect caused by the *loxP*-sites (data not shown).

Mice with myeloid cell-specific deletion of *Casp8* were healthy until the time point of AP induction, with no evident signs of immunological defects. At day 2 and day 7 after AP induction, the pancreatic regeneration was histologically unaffected by myeloid cell-specific deletion of *Casp8* (Fig. 16A). The pancreas-to-body weight ratio (Fig. 16B) and the examination of the pancreatitis-associated serum markers amylase, lipase 2, and LDH (Fig. 16C) also showed no effect of myeloid cell-specific *Casp8* deficiency.

The results demonstrate that deficiency of *Casp8* in myeloid cells is not sufficient to impair pancreatic regeneration after AP.

3.1.9 TLR3 induces cell death of macrophages alternatively via induction of caspase-dependent or RIPK1-dependent pathways

Next, the TLR3-dependent cell death of macrophages was mechanistically characterized by poly(I:C) stimulation in the presence of the pan-caspase inhibitor Z-VAD-FMK or the RIPK1 inhibitor Necrostatin-1 (Nec-1).

Immunoblot analysis demonstrated that Z-VAD-FMK led to a dose-dependent reduction of the poly(I:C)-induced formation of cleaved caspase 8, confirming the functionality of the caspase inhibitor (Fig. 17A). The presence of 10 μ M Z-VAD-FMK efficiently blocked the formation of cleaved caspase 8 by poly(I:C).

To investigate the potential dependency of TLR3-mediated cell death on caspase activation, macrophage viability was analyzed after stimulation with a combination of poly(I:C) and Z-VAD-FMK. Z-VAD-FMK was able to inhibit the formation of cleaved caspase 8 but had no consequence for the poly(I:C)-induced reduction of cell viability (Fig. 17B).

To test whether the remaining caspase activity, caused by an incomplete inhibition, is sufficient to induce cell death, a *Casp8*-deficient Hoxb8-ER/FL immune progenitor cell line was generated from femoral bone marrow cells of mice with deletion of *Casp8* in myeloid cells (*Casp8^{Mye}*). *Casp8* deficiency did not affect the differentiation of *in vitro* generated macrophages (data not shown). Genetic *Casp8* deficiency had no effect on the proportion of an-

nexin V⁺/PI⁺ macrophages after poly(I:C) stimulation (Fig. 17C). The results demonstrate that TLR3-mediated induction of cell death in macrophages can occur in a CASP8-independent manner.

To test for CASP8-independent, alternative mechanisms involved in TLR3-mediated cell death, the effect of the selective RIPK1 inhibitor Necrostatin-1 (Nec-1) was investigated by annexin V/PI staining (Fig. 17D). Inhibition of RIPK1 by Nec-1 did not affect poly(I:C)-induced cell death of macrophages. Neither Z-VAD-FMK nor Nec-1 were separately able to reduce poly(I:C)-dependent cell death. Interestingly, the simultaneous inhibition of caspases by Z-VAD-FMK and RIPK1 by Nec-1 blocked the induction of cell death by poly(I:C).

Both the RIPK1 signaling pathway and the caspase signaling pathway needed to be inhibited simultaneously to prevent TLR3-dependent cell death of macrophages. The results indicate the existence of two alternative signaling pathways for TLR3-mediated cell death.

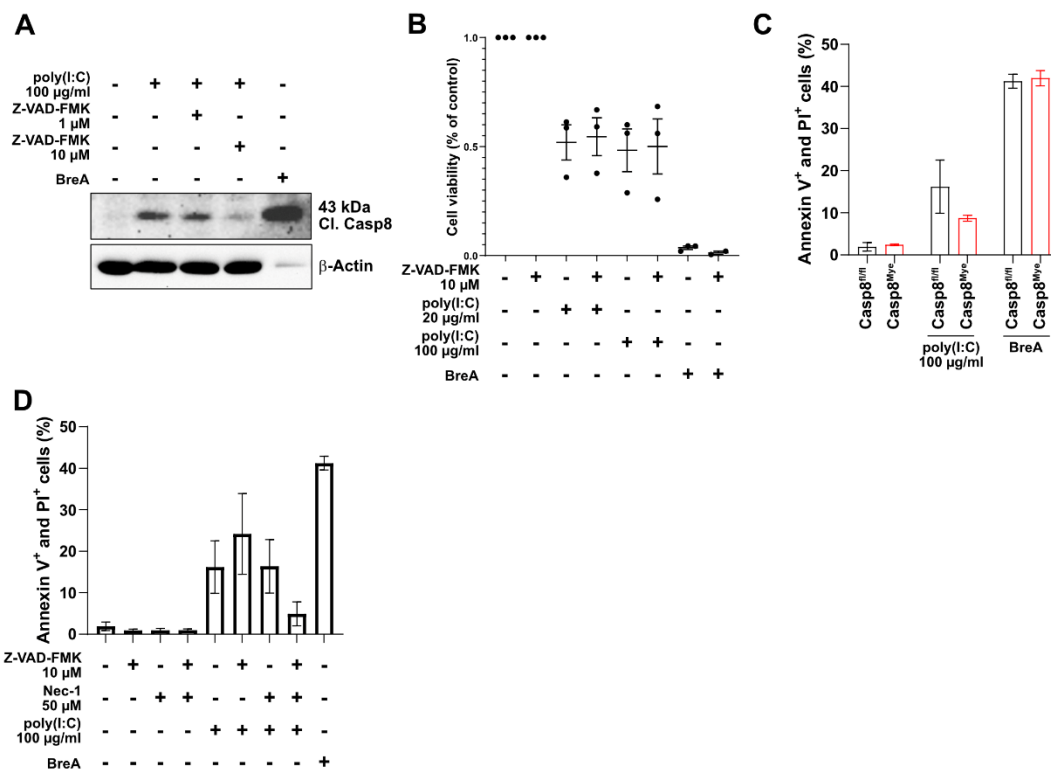


Figure 17: Mechanistic characterization of TLR3-mediated cell death in macrophages. (A) Representative immunoblot of cleaved caspase 8 formation in macrophages and (B) MTT-based quantification of the cell viability after 48 h of stimulation with poly(I:C) in presence of the pan-caspase inhibitor Z-VAD-FMK (10 µM). The cell viability was normalized to the corresponding controls. (C) Flow cytometry-based quantification of annexin V⁺/PI⁺ macrophages from Casp8^{fl/fl} and Casp8^{Mye} mice after 48 h of stimulation with poly(I:C) (100 ng/µl). (D) Cell viability and (E) quantification of annexin V⁺/PI⁺ WT macrophages after 48 h of stimulation with poly(I:C) (100 ng/µl) in combination with Z-VAD-FMK (10 µM) and the RIPK1 inhibitor Nec-1 (50 µM). Data are presented as mean ± SEM.

3.1.10 Exosomal dsRNA as a new potential ligand for TLR3 activation

TLR3 can be activated not only by viral dsRNA but also by dsRNA liberated from necrotic cells (Karikó et al., 2004). Acute pancreatitis involves necrosis of acinar cells, which are correspondingly assumed to be the source of TLR3 ligands. In addition, cells can actively secrete dsRNA in exosomes to induce paracrine TLR3 signaling (Seo et al., 2016). To investigate the origin of TLR3 ligands in AP and pancreatic carcinogenesis, a dsRNA-specific antibody was used to determine the localization of dsRNA in acinar cells, as well as in pancreatic lesions and *in vitro* cultured tumor cell lines (Fig. 18A). dsRNA was ubiquitously present in non-transformed exocrine and endocrine cells of the pancreas, as well as in preinvasive lesion areas and tumor cells.

High-resolution microscopy of *in vitro* cultured tumor cell lines (isolated from mice with the genotype *Pdx1-Flp; FSF-Kras^{G12D}; Trp53^{FRT/FRT}* (KPPF)) showed that dsRNA was localized diffusely in the nucleus and in a granular manner in the cytosol, indicating the presence of dsRNA in vesicles (Fig. 18A).

To test whether acinar cells are able to secrete exosomes to communicate with cells in the microenvironment, murine non-transformed acinar cells were isolated and cultured in 3D with daily medium changes. After 1 day and 3 days in culture, exosomes were isolated from the cell culture supernatant and quantified. PDAC cells are known to secrete high quantities of exosomes (Chen et al., 2021). Therefore, the quantification of secreted exosomes from *in vitro* cultured pancreatic tumor cells (KPPF) was included as a positive control.

Quantification of exosomes revealed that both acinar cells on day 1 and transdifferentiated acinar cells on day 3 secreted high amounts of exosomes in culture (Fig. 18B). Accordingly, in addition to dsRNA released from necrotic cells, exosomal dsRNA represents a potential way to activate TLR3 signaling. This makes it conceivable that acinar cells specifically activate TLR3 signaling of immune cells in the microenvironment to orchestrate the immune response. A similar mechanism is reported for the activation of TLR3 in stellate cells by exosomal dsRNA after liver injury (Seo et al., 2016). The controlled activation of TLR3 could be of versatile importance for the regeneration of the pancreas after acute pancreatitis as well as for pancreatic carcinogenesis.

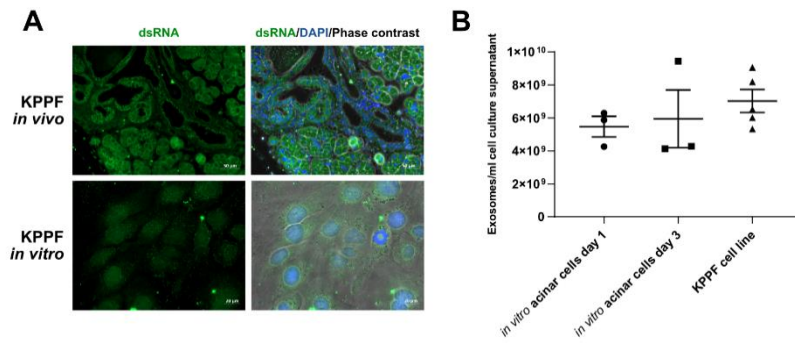


Figure 18: Exosomal dsRNA represents a potential source of TLR3 ligands. (A) Representative immunofluorescence pictures of dsRNA in the pancreas of mice with pancreas-specific homozygous deletion of *Trp53* and activation of oncogenic *Kras^{G12D}* (KPPF, upper panels, scale bar = 50 μm) and in isolated KPPF tumor cells *in vitro* (lower panels, scale bar = 20 μm). **(B)** Quantification of isolated exosomes from the supernatant of 3D cultured acinar cells at different time points and *in vitro* cultured KPPF tumor cells. Data are presented as mean ± SEM.

In summary, it was demonstrated that dsRNA was ubiquitously present in acinar cells and pancreatic lesions and that *in vitro* cultured acinar cells secreted high quantities of exosomes.

3.2 Myeloid cell TLR3 limits inflammation-induced carcinogenesis but does not affect oncogene-driven carcinogenesis in the pancreas

3.2.1 Oncogene-driven pancreatic carcinogenesis is unaffected by *Tlr3* deficiency

3.2.1.1 *Flp* activity depends on paternal inheritance

Due to the key importance of myeloid cell-specific expression of *Tlr3* for pancreatic regeneration after acute pancreatitis, we next investigated the cell-specific function of TLR3 for pancreatic carcinogenesis. The recently developed dual recombinase system (Schönhuber et al., 2014) enables the pancreas-specific activation of oncogenic *FSF-Kras^{G12D}* and the deletion of *FRT*-flanked *Trp53* by *Pdx1-Flp* (KPF), as well as the independent cell type-specific rescue of *Tlr3* expression by Cre-mediated recombination.

Despite the genetic presence of *Pdx1-Flp* and *FSF-Kras^{G12D}*, 55.02% of the experimental mice developed no signs of pancreatic carcinogenesis. In these mice, the test for pancreas-specific recombined *FSF-Kras^{G12D}* via PCR confirmed the inactivity of Flp. To illuminate the underlying mechanism, the correlation between the presence of active Flp, the gender of the experimental mice, and the gender of the *Pdx1-Flp* inheriting parental mice were analyzed. Overall, 49.06% of the male and 40.67% of the female experimental animals had active Flp (Table 10), demonstrating a marginal dependence of the gender of the experimental mice on Flp activity.

Table 10: Correlation of the Flp activity and the gender of the experimental mice. Flp activity was proven by PCR detection of recombined *FSF-Kras^{G12D}*.

| Gender of experimental mouse | Flp activ | Flp inactive | Percentage |
|------------------------------|-----------|--------------|---------------|
| ♂ | 78 | 81 | 49.06% |
| ♀ | 61 | 89 | 40.67% |

When *Pdx1-Flp* was inherited paternally for two generations, 56.59% of the male and 50.43% of the female experimental mice had active Flp (Table 11). When *Pdx1-Flp* was inherited maternally in the penultimate generation and inherited paternally to the experimental mice, the percentage of mice with active Flp decreased to 33.33% for males and 30.00% for females. Strikingly, when *Pdx1-Flp* of the experimental mice was inherited from the maternal side, Flp was inactive irrespective of the gender of the experimental mice and the previous

inheritance. The statistical evaluation clearly demonstrates the dependency of Flp activity on the gender of the *Pdx1-Flp* inheriting parents. Only paternal inheritance maintained the Flp activity. For the following experiments, only mice with confirmed Flp activity were included, proven by the PCR detection of recombined *FSF-Kras^{G12D}* in pancreas biopsies.

Table 11: Correlation of the Flp activity and the gender of the Flp inheriting parents.

| Gender of experimental mouse | Gender of <i>Pdx1-Flp</i> inheriting parent | Gender of <i>Pdx1-Flp</i> inheriting parent (penultimate Generation) | Flp activ | Flp inactive | Percentage |
|------------------------------|---|--|-----------|--------------|---------------|
| ♂ | ♂ | ♂ | 73 | 56 | 56.59% |
| ♀ | ♂ | ♂ | 58 | 57 | 50.43% |
| ♂ | ♂ | ♀ | 5 | 10 | 33.33% |
| ♀ | ♂ | ♀ | 3 | 7 | 30.00% |
| ♂ | ♀ | ♂ | 0 | 6 | 0% |
| ♀ | ♀ | ♂ | 0 | 8 | 0% |
| ♂ | ♀ | ♀ | 0 | 9 | 0% |
| ♀ | ♀ | ♀ | 0 | 17 | 0% |

3.2.1.2 *Tlr3* deficiency has no effect on pancreatic carcinogenesis in the KPF mouse model

First, the oncogene-driven pancreatic carcinogenesis was analyzed in mice with pancreas-specific expression of *Kras^{G12D}* and heterozygous deletion of *Trp53* (KPF, Fig. 19A). The cell-specific role of TLR3 was investigated by using KPF mice with global *Tlr3* deficiency (KPFT^{OFF}) or myeloid cell-specific rescue of *Tlr3* expression (KPFT^{Mye}, Fig. 19B).

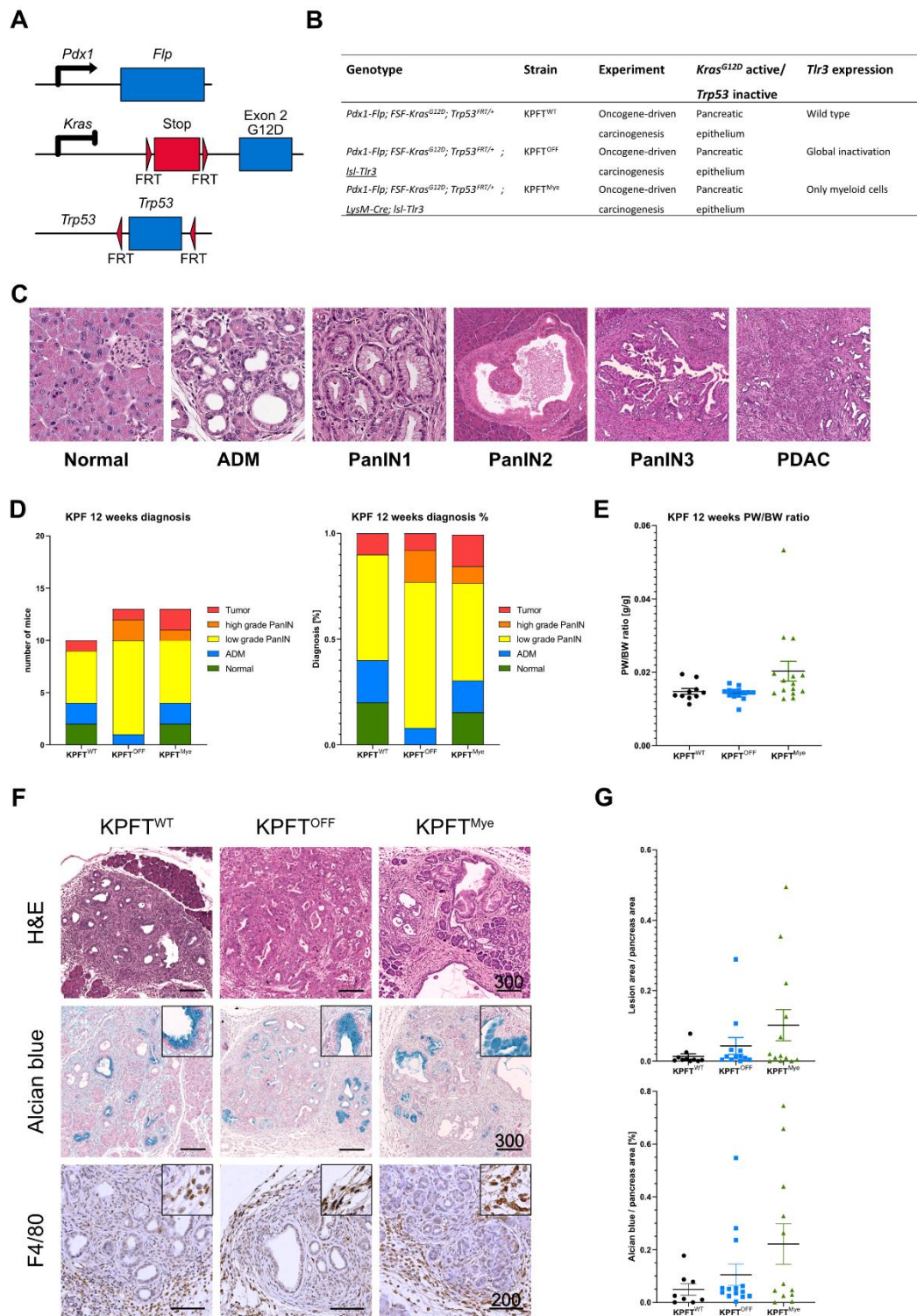


Figure 19: Global or partial *Tlr3* deficiency had no effect on oncogene-driven pancreatic carcinogenesis in the KPF model. (A) Schematic representation of the KPF mouse model for pancreatic carcinogenesis. The pancreas-specific expression of *Flp* is mediated by the promoter of *Pdx1*. The induction of *Kras*^{G12D} expression in the pancreas is regulated by Flp-mediated deletion of the *FRT*-site flanked transcriptional termination element and the heterozygous pancreas-specific inactivation of *Trp53* by Flp-mediated deletion of the *FRT*-flanked *Trp53* allele. (B) Overview of the KPF mouse lines used to study the cell-specific function of TLR3 on oncogene-driven carcinogenesis. (C) Representative H&E-stained pancreas sections at different stages of carcinogenesis observed in KPF mice at 12 weeks of age. (D) Stage of the most advanced pancreatic lesion of KPFT^{OFF} and KPFT^{Myc} mice compared to KPFT^{WT} mice at the age of 12 weeks. The graphs display the total number of mice (left graph), as well as the percentage of mice (right graph) with the respective diagnosis. (E) Pancreas-to-body weight ratio of KPFT^{WT}, KPFT^{OFF}, and KPFT^{Myc} mice at the age of 12 weeks. (F) Representative pictures of H&E, Alcian blue, and F4/80-stained pancreatic sections of 12-week-old KPFT^{WT}, KPFT^{OFF}, and KPFT^{Myc} mice. Scale bars indicate 300 μm (H&E staining, Alcian blue) or 200 μm (F4/80). (G) Quantification of lesion area (upper graph) and Alcian blue⁺ area (lower graph) of 12-week-old KPFT^{WT}, KPFT^{OFF}, and KPFT^{Myc} mice, each normalized to the total area of the pancreas. Data are presented as mean ± SEM.

Mice of the KPF model were sacrificed at the age of 12 weeks. Pancreatic carcinogenesis was evaluated histologically, based on the most advanced stage of lesions and the total lesion area. The KPF mouse model recapitulated the full spectrum of PDAC carcinogenesis (Fig. 19C). Preinvasive PanIN lesions resembled those of human patients including the expression of ductal markers (*Krt19*) and Alcian blue⁺ mucins.

In general, there was a high variance of diagnoses, ranging from lesion-free pancreases to ADM, low-grade PanIN, high-grade PanIN, and invasive PDAC (Fig. 19C). At the age of 12 weeks, most mice of the KPF model were diagnosed with low-grade PanIN lesions (PanIN1, PanIN2, Fig. 19D). Two animals of both the KPFT^{WT} and KPFT^{Mye} lines had no pancreatic lesion at this time point, despite evidence of active Flp and recombined *FSF-Kras*^{G12D} in the pancreas biopsy. All KPFT^{OFF} mice had pancreatic lesions with ADM as the lowest stage of carcinogenesis in one KPFT^{OFF} mouse. One mouse each from the KPFT^{WT} and KPFT^{OFF} lines, as well as two mice from the KPFT^{Mye} line, were diagnosed with invasive PDAC. None of these mice had metastases at this time point.

Overall, there was no correlation between the carcinogenesis stage and the expression of *Tlr3* observed in the KPF model at this time point. Likewise, the pancreas-to-body weight ratio was not significantly different between the cohorts (Fig. 19E). Quantification of the total lesion area normalized to the total area of the pancreas showed no differences between the lines (Fig. 19F, Fig. 19G).

Alcian blue staining was used to stain acidic mucopolysaccharides expressed by PanIN lesions. Accordingly, Alcian blue staining served as a marker for advanced stages of carcinogenesis. The Alcian blue⁺ area was unaffected by global or partial *Tlr3* deficiency. Pancreatic infiltration of F4/80⁺ cells was independent of the *Tlr3* expression.

To analyze the effect of TLR3 on carcinogenesis-associated inflammation and protumorigenic signal transduction, the expression of inflammatory markers and the activation of carcinogenesis-associated signaling pathways was investigated by RT-qPCR and immunoblot analysis (Fig. 20).

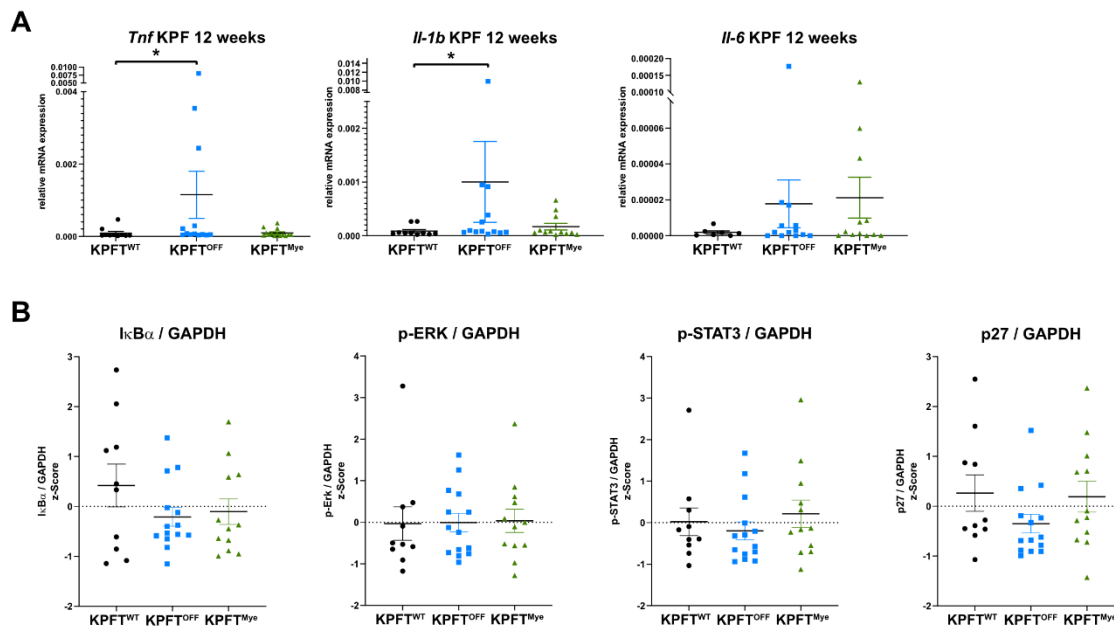


Figure 20: *Tlr3* deficiency did not affect the activation of tumor-relevant signal transduction pathways. (A) RT-qPCR-based quantification of *Tnf*, *Il-1b*, and *Il-6* expression in 12-weeks old KPFT^{WT}, KPFT^{OFF}, and KPFT^{Mye} mice. Data were analyzed using the Mann-Whitney test and presented as mean \pm SEM. * $p < 0.05$. **(B)** z-Scores calculated based on the quantification of immunoblot staining for I κ B α , p-ERK, p-STAT3, and p27, normalized to the staining intensity of Gapdh. The z score was calculated to compare protein expression on different membranes.

The different stages of carcinogenesis in mice are reflected by the highly deviating expression of the proinflammatory markers *Tnf*, *Il-1 β* , and *Il-6*. KPFT^{OFF} mice had a significantly up-regulated pancreatic expression of *Tnf* and *Il-1 β* , whereas the expression in KPFT^{Mye} mice did not differ significantly from KPFT^{WT} mice. *Il-6* was unaffected by *Tlr3* expression.

The immunoblot analysis of I κ B α , p-ERK, p-STAT3, and p27 revealed no effect of *Tlr3* deficiency on the regulation of tumor-associated signal transduction pathways.

Collectively, global or partial *Tlr3* deficiency had no effect on carcinogenesis in KPF mice at the age of 12 weeks. Neither lesion area, lesion stage, immune cell infiltration nor tumorigenic signal transduction was affected by *Tlr3* deficiency.

3.2.1.3 Myeloid *Tlr3* has no effect on the survival of KPPF mice but modulates the tumor microenvironment

Next, the function of global *Tlr3* deficiency or myeloid cell-specific rescue of *Tlr3* expression on pancreatic carcinogenesis in mice with pancreas-specific activation of *Kras*^{G12D} and homozygous deletion of *Trp53* (KPPF) was investigated (Fig. 21A, Fig. 21B). The health status of the mice was monitored daily by visual inspection and at least twice a week by scoring. A survival curve was generated based on the time point when the health status of the mice reached predefined termination criteria.

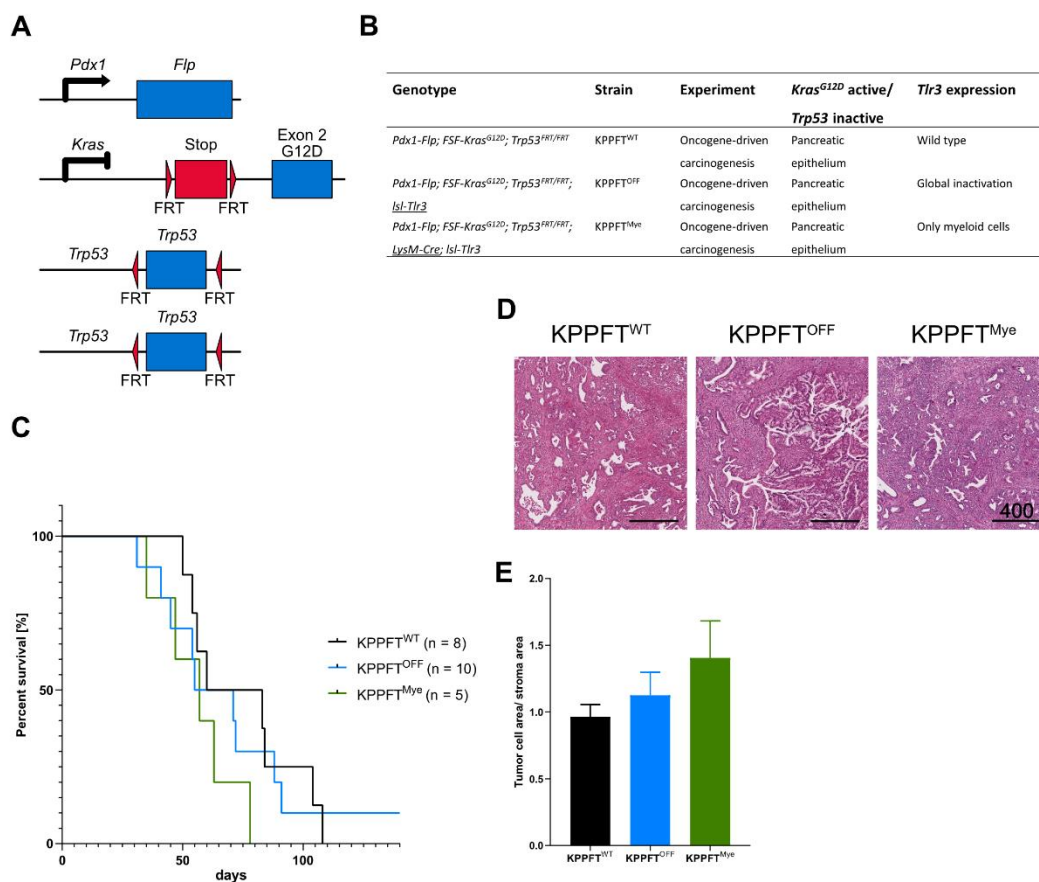


Figure 21: *Tlr3* deficiency did not affect oncogene-driven carcinogenesis in the KPPF model. (A) Schematic representation of the KPPF mouse model for pancreatic carcinogenesis. Pdx1-Flp induces pancreas-specific activation of *Kras*^{G12D} expression and the homozygous deletion of FRT-site flanked *Trp53*. **(B)** Overview of the KPPF mouse cohorts used to investigate the cell-specific function of TLR3 on oncogene-driven carcinogenesis. **(C)** Kaplan Meier survival curves of KPPFT^{WT}, KPPFT^{OFF}, and KPPFT^{Myc} mice. **(D)** Representative H&E-stained pancreatic ductal adenocarcinomas from the KPPF mouse lines. Scale bars indicate 400 μ m. **(E)** Tumor cell-to-stroma ratio of KPPF tumors, quantified by Zen 3.0 software. Data are presented as mean \pm SEM.

Compared to the previously described KPF model, homozygous deletion of *Trp53* substantially accelerated pancreatic carcinogenesis. The median survival time was 71.5 days for

KPPFT^{WT} mice, 63 days for KPPFT^{OFF} mice, and 57 days for KPPFT^{Mye} mice (Fig. 21C). All mice developed pancreatic tumors within the observation period of 140 days. Only 1 mouse did not reach the termination criteria within the observation period but still had a pancreatic tumor. Partial or global *Tlr3* deficiency had no significant effect on the survival of KPPF mice.

Histologically, tumors from the KPPF model were characterized by a highly desmoplastic stroma, associated with a low tumor cell-to-stroma ratio and a high number of tumor-associated fibroblasts (Fig. 21D). Tumors of the classical/ pancreatic progenitor subtype as well as tumors of the mesenchymal/squamous subtype were diagnosed independently of the *Tlr3* expression in all KPPF cohorts. The histological characterization of the tumor morphology showed no influence of *Tlr3* deficiency on the tumor subtype. Similarly, computer-based quantification of the tumor cell-to-stroma ratio revealed no differences between the mouse lines (Fig. 21E).

RT-qPCR characterization of the tumors showed significantly increased expression of the T cell marker *Cd3* and the Treg cell marker *Foxp3* in KPPFT^{OFF} tumors compared to tumor samples from KPPFT^{WT} mice (Fig. 22). The expression of *Cd3* and *Foxp3* in KPPFT^{Mye} tumors did not differ significantly from KPPFT^{WT} tumors.

The results indicate a negative regulation of the recruitment of T cells and FOXP3⁺ Treg cells into the tumor microenvironment by myeloid cell TLR3. The expression of other lineage markers for immune cells (*Adgre1*, *Mpo*) did not differ between the cohorts. Similarly, the expression of EMT markers (*Zeb1*, *Snai1*), inflammatory markers (*Il-6*, *Il-10*) and tumor subtype-specific markers (*Hnf4*, *Krt7*; Puleo et al., 2018) was unaffected by *Tlr3* deficiency.

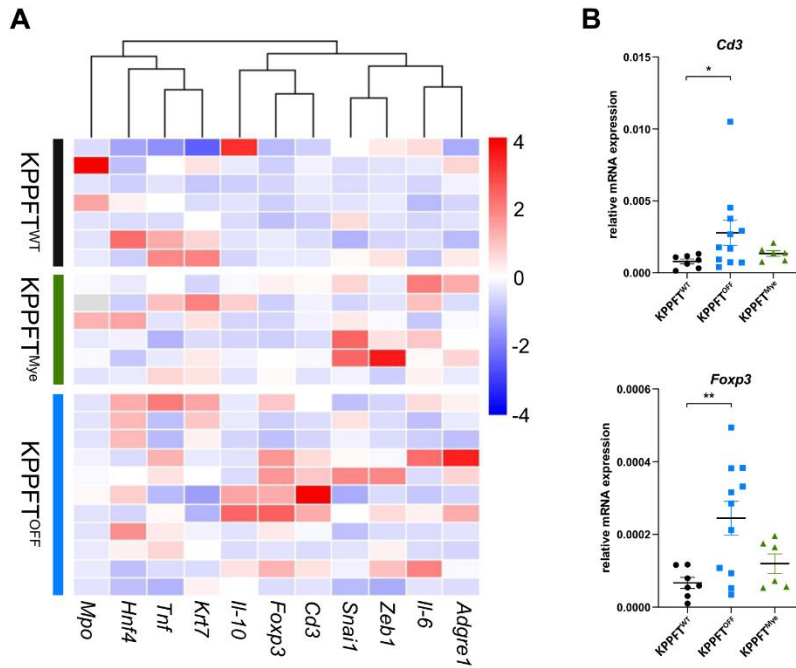


Figure 22: TLR3 signaling in myeloid cells limits expression of *Cd3* and *Foxp3* in KPPF tumors. (A) RT-qPCR-based characterization of tumors from KPPFT^{OFF} and KPPFT^{Mye} mice, compared to KPPFT^{WT} tumors. Data are represented as a heatmap with hierarchical clustering of the genes. **(B)** Graph of the *Cd3* and *Foxp3* expression. Data were analyzed using the Mann-Whitney test (*Cd3*) or the unpaired t-test (*Foxp3*). Data are presented as mean \pm SEM. * $p < 0.05$, ** $p < 0.01$.

3.2.2 Myeloid cell-specific TLR3 signaling inhibits pancreatitis-driven carcinogenesis

3.2.2.1 Global *Tlr3* deficiency enhances inflammation-induced carcinogenesis

Myeloid cell-specific TLR3 signaling was shown to have a key role in the termination of the immune response after acute pancreatitis. Sustaining inflammation represents a hallmark of carcinogenesis (Hanahan and Weinberg). Next, the cell-specific function of TLR3 in inflammation-driven carcinogenesis was investigated.

Inflammation was induced by 6 hourly injections of caerulein at day -2 and day 0 in mice with pancreas-specific expression of oncogenic *Kras*^{G12D}. KF mice with wild-type *Tlr3* expression (KFT^{WT}) were compared to KF mice with global *Tlr3* deficiency (KFT^{OFF}) or rescue of *Tlr3* expression exclusively in myeloid cells (KFT^{Mye}) or pancreatic epithelial cells (KFT^{Epi}, Fig. 23A, Fig. 23B). The pancreas was analyzed on day 7 and day 21 after caerulein treatment.

Expression of oncogenic *Kras*^{G12D} blocked pancreatic regeneration after pancreatitis and evoked a substantially enhanced lesion formation and persistence of lesion areas compared to mice with WT *Kras*.

At day 7, the lesions were mainly composed of ADM structures and some low-grade PanIN structures, combined with fibrosis and a high immune cell infiltrate (Fig. 23C).

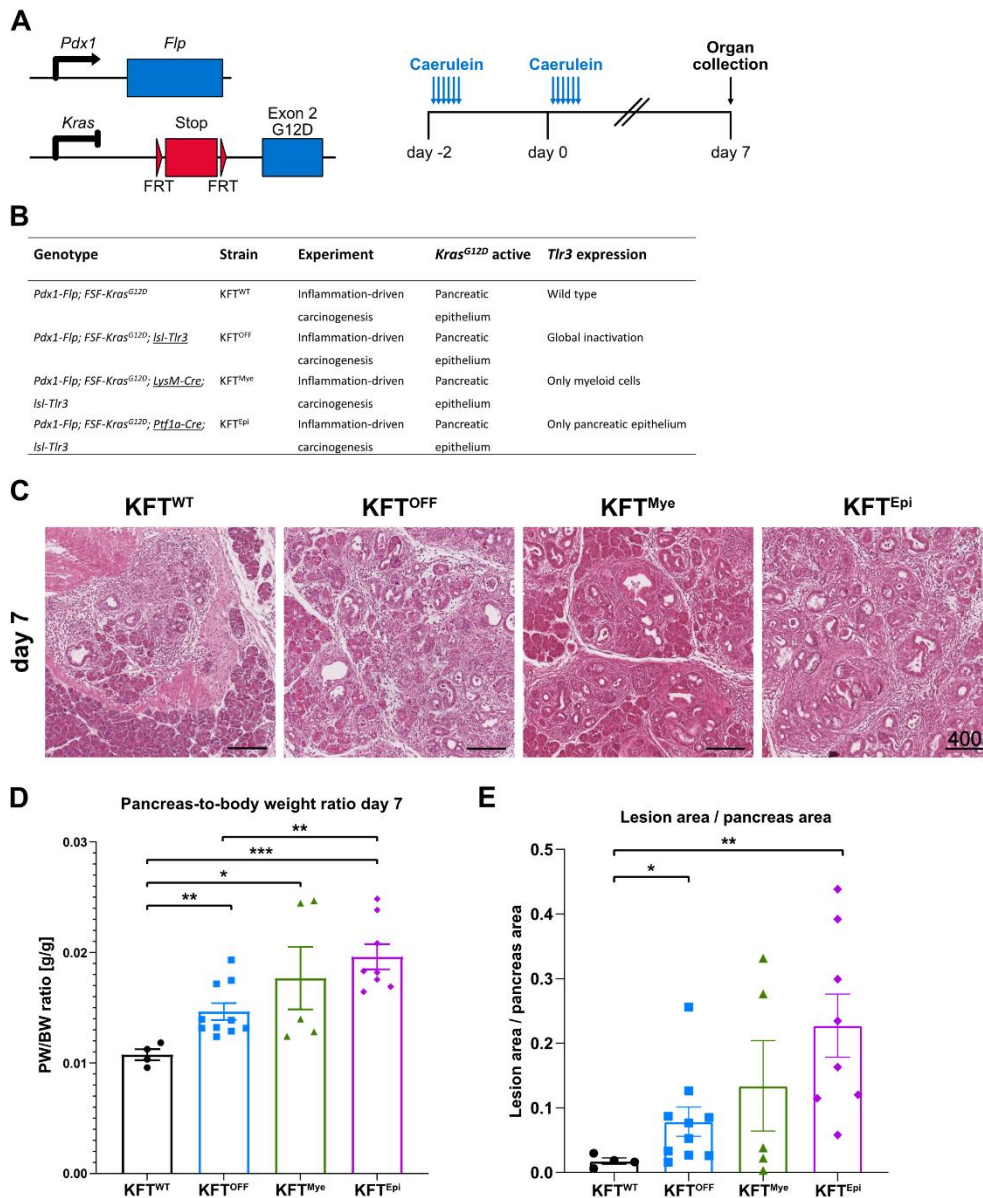


Figure 23: *Tlr3* deficiency promotes lesion formation at day 7 after pancreatitis induction in the KF mouse model. (A, B) Schematic representation of the key genetic elements in the KF model and overview of the mouse lines used to investigate the function of TLR3 in inflammation-driven carcinogenesis. Inflammation was induced in mice with pancreas-specific expression of oncogenic *Kras*^{G12D} by six hourly injections of caerulein at day -2 and day 0. To study the cell-specific effect of TLR3, lesion formation in mice with exclusively rescued *Tlr3* expression in myeloid cells (KFT^{Mye}) or in cells of the pancreatic epithelium (KFT^{Epi}) was compared to global *Tlr3*-deficient mice (KFT^{OFF}) and mice with wild-type *Tlr3* expression (KFT^{WT}). **(C)** Representative H&E-stained lesions at day 7 after caerulein treatment. Scale bars indicate 400 μm. **(D)** Pancreas-to-body weight ratio of KF mouse cohorts at day 7 after inflammation induction. Data were analyzed using the unpaired t-test or the Mann-Whitney test. **(E)** Quantification of the lesion area normalized to the total area of the pancreas on day 7. Data were analyzed using the Mann-Whitney test. Data are presented as mean ± SEM. * *p* < 0.05, ** *p* < 0.01, *** *p* < 0.001.

At day 7, KFT^{OFF}, KFT^{Mye}, and KFT^{Epi} mice had an increased pancreas-to-body weight ratio compared to KFT^{WT} mice (Fig. 23D). The pancreas-to-body weight ratio of mice with an epithelial rescue of *Tlr3* expression was higher compared to global *Tlr3*-deficient mice.

The lesion area in KFT^{OFF} and KFT^{Epi} mice was significantly elevated compared to KFT^{WT} mice (Fig. 23E). Interestingly, lesion areas of KFT^{Mye} mice did not differ significantly from KFT^{WT} mice, showing the importance of myeloid cell TLR3 for limiting inflammation-driven pancreatic carcinogenesis.

The constitutively active $KRAS^{G12D}$ causes persistence of the lesions and promotes pancreatic carcinogenesis after inflammation. Accordingly, the lesion areas of KF mice persisted at day 21. At day 21, the lesions had a characteristically high degree of extracellular matrix and were mainly composed of low-grade PanIN structures, indicative of the progressed carcinogenesis compared to the lesions at day 7 (Fig. 24A, Fig. 24B). None of the mice developed high-grade PanIN structures or an invasive carcinoma within this time frame.

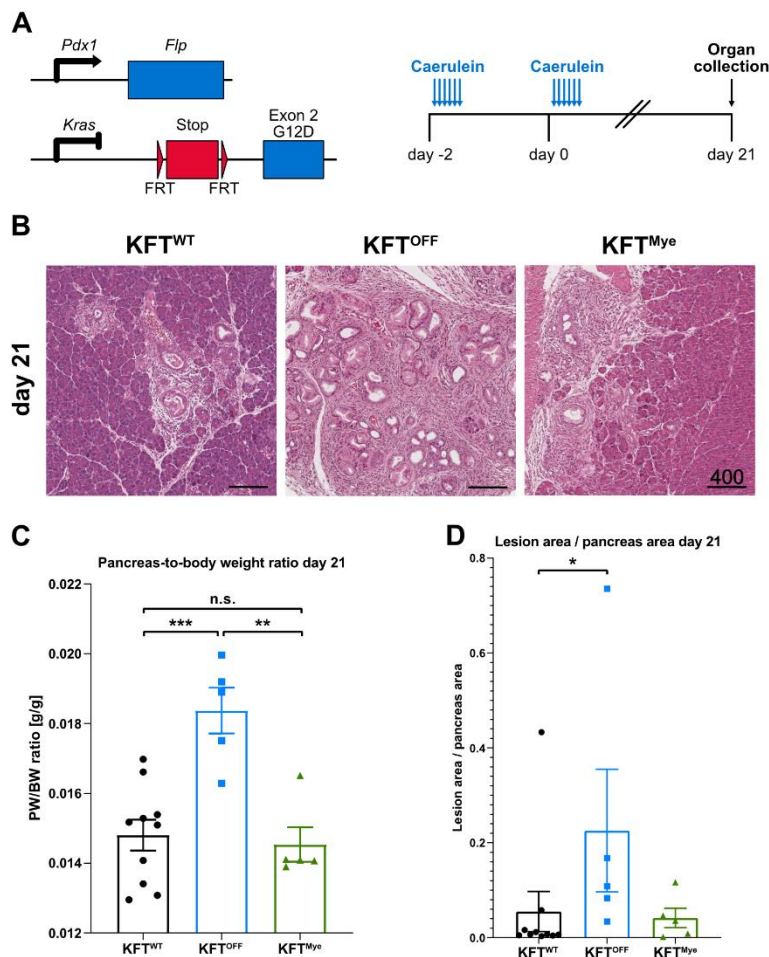


Figure 24: Myeloid cell-specific TLR3 signaling inhibits pancreatitis-driven carcinogenesis at day 21. (A) Schematic representation of the mouse model used to analyze the cell-specific function of TLR3 in inflammation-driven carcinogenesis at day 21. (B) Representative H&E staining of pancreatic lesions from KFT^{WT} , KFT^{OFF} , and KFT^{Mye} mice at day 21 after caerulein treatment. Scale bars indicate 400 μ m. (C) Pancreas-to-body weight ratio of systemic *Tlr3*-deficient mice compared to KFT^{Mye} and KFT^{WT} mice. Data were analyzed using the unpaired t-test. (D) Quantification of the lesion area normalized to the total area of the pancreas at day 21 after inflammation induction. Data were analyzed using the Mann-Whitney test. Data are presented as mean \pm SEM. * $p < 0.05$, ** $p < 0.01$, *** $p < 0.001$.

At day 21, The pancreas-to-body weight ratio was significantly increased in KFT^{OFF} mice compared to KFT^{WT} mice and KFT^{Mye} mice (Fig. 24C). In accordance, global *Tlr3*-deficient mice had a significantly increased lesion area compared to mice with wild-type *Tlr3* expression (Fig. 24B, Fig. 24D). The lesion area of KFT^{Mye} mice was equal to KFT^{WT} mice, highlighting the importance of myeloid TLR3 for limiting pancreatitis-induced carcinogenesis.

Global *Tlr3* deficiency was shown to enhance lesion formation at day 7 and day 21 of inflammation-driven carcinogenesis, while myeloid cell exclusive expression of *Tlr3* limited the lesion formation.

Pancreatitis-associated serum markers were quantified on day 7 and day 21 (Fig. 25). At day 7, KFT^{Epi} mice had significantly elevated serum levels of amylase compared to KFT^{WT} mice, as a sign of increased pancreatic inflammation. Lipase 2 and LDH levels did not differ between the groups. After 21 days, there was no difference in the serum concentrations of amylase, lipase 2, and LDH.

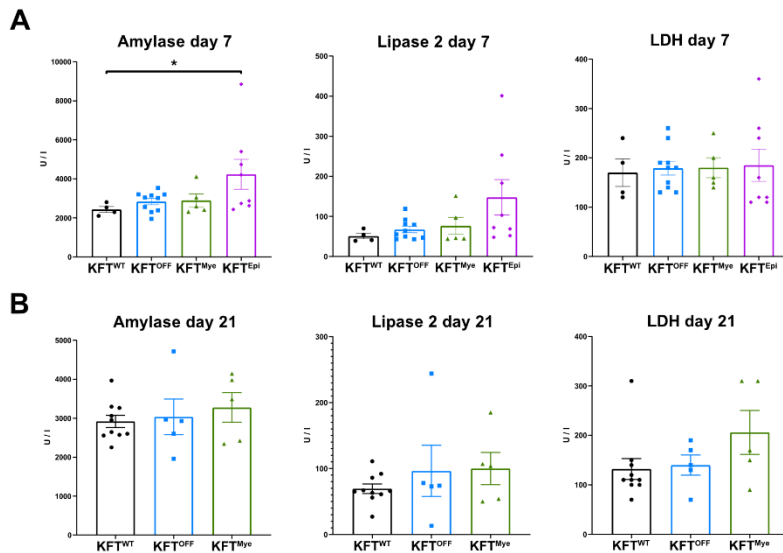


Figure 25: Pancreatitis-associated serum marker levels are unaffected by global or partial *Tlr3* deficiency. (A, B) Serum levels of amylase, lipase 2, and LDH at day 7 (A) and day 21 (B) after inflammation induction in the KF mouse model. Data were analyzed using the Mann-Whitney test. Data are presented as mean \pm SEM. * $p < 0.05$.

3.2.2.2 Myeloid cell TLR3 limits the immune cell infiltration in the early phase of inflammation-driven carcinogenesis

Immune cells are of decisive importance in inflammation-driven carcinogenesis (Guerra et al., 2011; Kong et al., 2018). The immune cell infiltration was analyzed by IHC staining (Fig. 26A) and by RT-qPCR-based expression analysis of characteristic cell lineage markers (Fig. 26B).

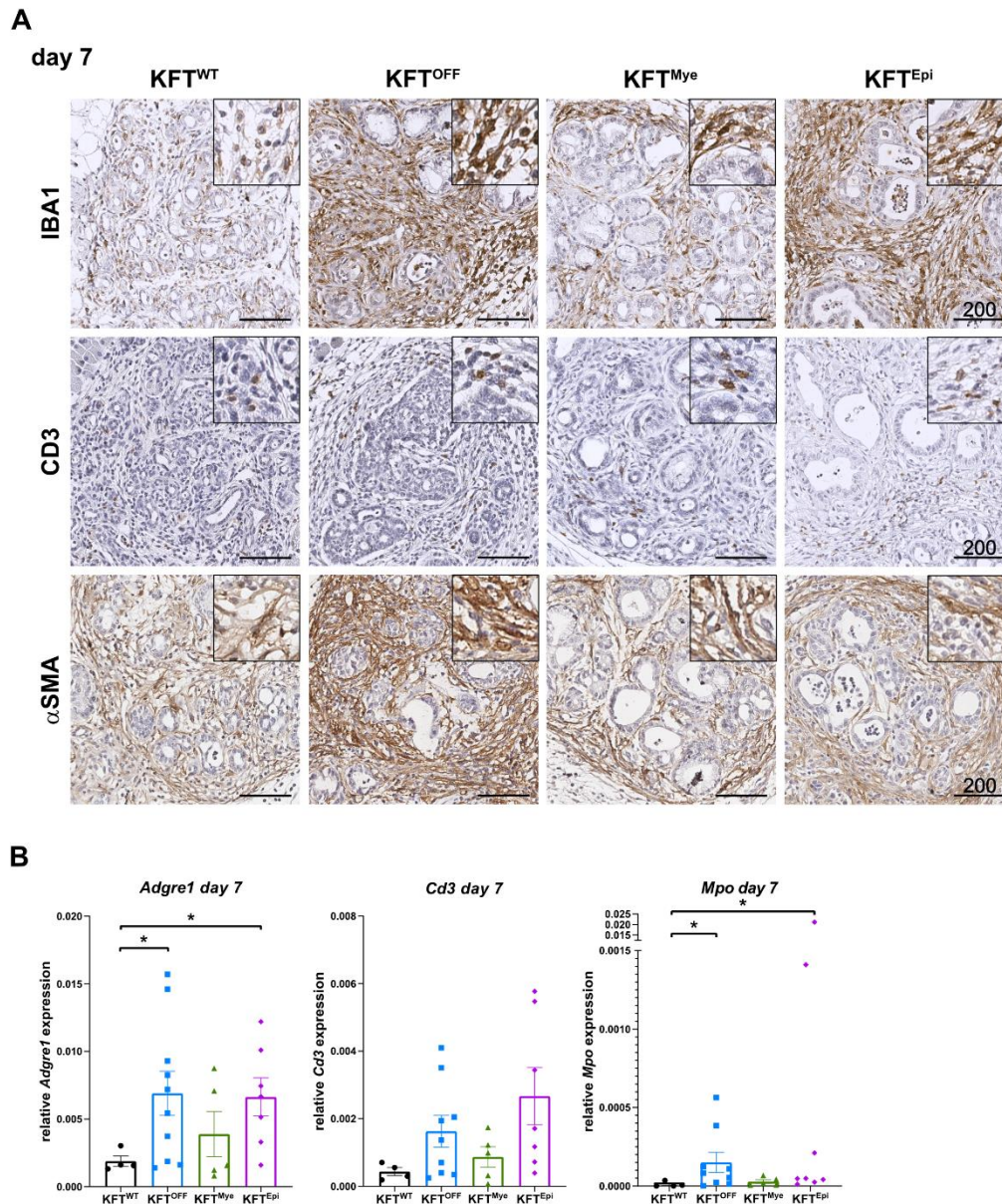


Figure 26: Myeloid cell TLR3 limits the infiltration of macrophages and neutrophils at day 7 of pancreatitis-driven carcinogenesis. (A) Representative IHC staining of IBA1, CD3, and α SMA in pancreatic sections of KFT^{WT}, KFT^{OFF}, KFT^{Mye}, and KFT^{Epi} mice at day 7 after caerulein treatment. Scale bars indicate 200 μ m. **(B)** RT-qPCR-based expression analysis of the cell lineage marker *Adgre1*, *Cd3*, and *Mpo*. Data were analyzed using the Mann-Whitney test and presented as mean \pm SEM. * $p < 0.05$.

The number of IBA1⁺ cells in the lesion microenvironment was increased in KFT^{OFF} and KFT^{Epi} mice compared to KFT^{WT} mice. Accordingly, the expression of the macrophage-specific marker *Adgre1* and the neutrophil-specific marker *Mpo* was significantly elevated in KFT^{OFF} and KFT^{Epi} mice, compared to KFT^{WT} mice. Strikingly, there was no significant difference between KFT^{Mye} and KFT^{WT} mice, showing the influence of myeloid cell-specific TLR3 signaling for limiting the total number of tissue-resident macrophages and neutrophils. The expression of *Cd3* and the number of infiltrating CD3⁺ or α SMA⁺ cells was not influenced by global or partial *Tlr3* deficiency.

3.2.2.3 Induction of pro-proliferative signal transduction pathways caused by *Tlr3* deficiency

To characterize the consequence of the increased immune cell infiltration at day 7 caused by *Tlr3* deficiency, the activation of carcinogenesis-associated cellular signal transduction pathways and the expression of inflammatory markers was investigated by immunoblot analysis (Fig. 27A, Fig. 27B) and by RT-qPCR (Fig. 27C).

The phosphorylation of ERK is a key signal transduction pathway regulating cell proliferation. At day 7, KF mice with global *Tlr3* deficiency or exclusive epithelial expression of *Tlr3* had a significantly higher p-ERK/total ERK ratio compared to KFT^{WT} mice. The p-ERK/total ERK ratio did not differ between KFT^{Mye} and KFT^{WT} mice. The increased p-ERK/total ERK ratio in KFT^{OFF} and KFT^{Epi} mice was associated with a significantly higher number of Ki67⁺, proliferating exocrine cells in pancreatic lesions (Fig. 27D, Fig. 27E). The ratio of p-STAT3/total STAT3 was significantly increased in KFT^{Epi} mice compared to KFT^{WT} mice. Consistently, KFT^{Epi} mice had a significantly enhanced expression of *Il-6*. The expression of *Il-10*, *Ccl5*, or *Ccnb1* did not vary between the mouse lines.

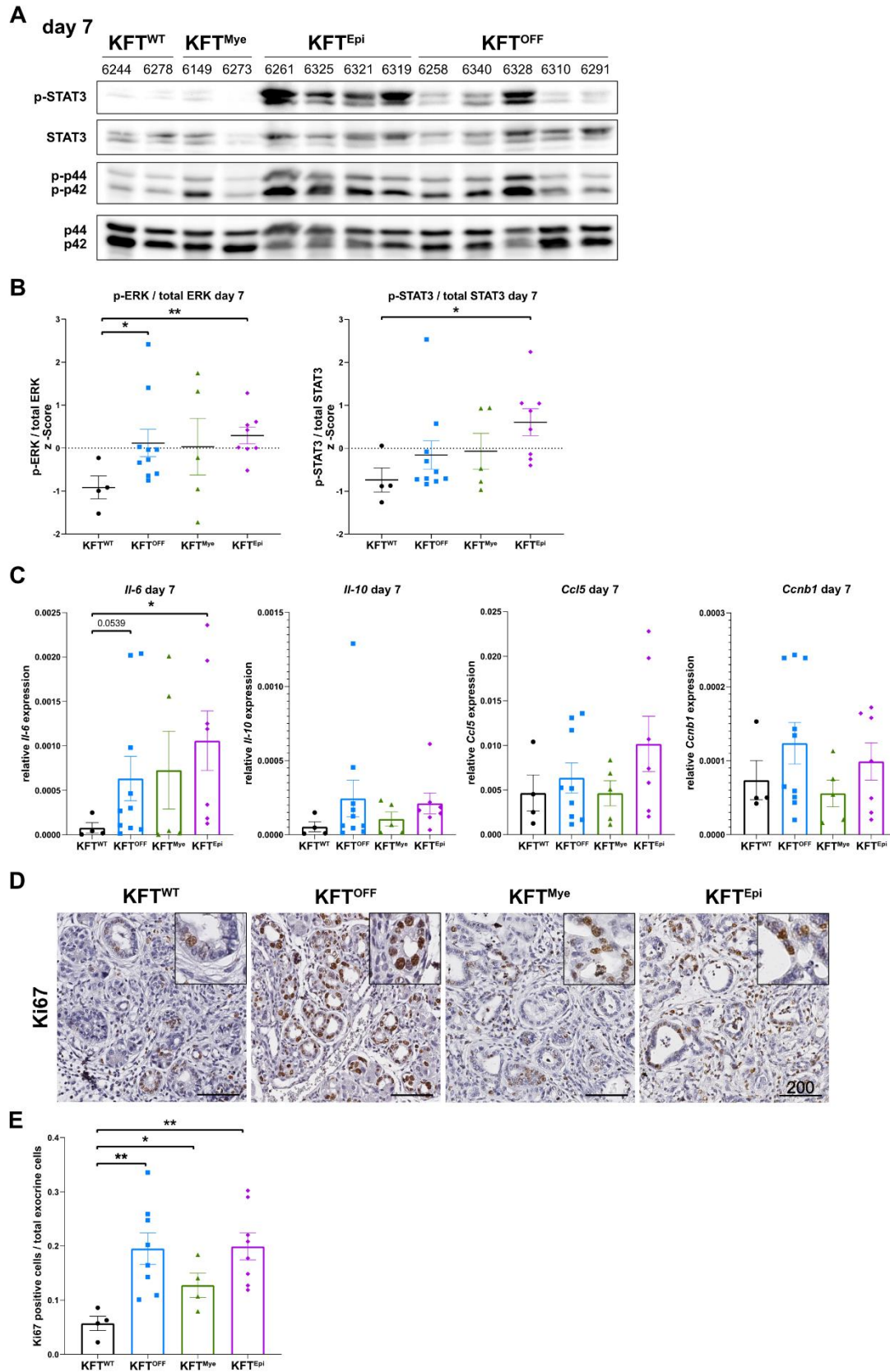


Figure 27: Activation of pro-tumorigenic signal transduction pathways by *Tlr3* deficiency at day 7 of pancreatitis-induced carcinogenesis. (A, B) Representative immunoblot analysis and densitometric quantification of p-STAT3, total STAT3, p-ERK (p-p44 + p-p42), and total ERK (p44 + p42) in KFT^{WT}, KFT^{OFF}, KFT^{Mye}, and KFT^{Epi} mice at day 7 after caerulein-induced pancre-

atitis. Data were analyzed using the unpaired t-test. **(C)** RT-qPCR-based quantification of *Il-6*, *Il-10*, *Ccl5*, and *Ccnb1* expression. Data were analyzed using the Mann-Whitney test and are presented as mean \pm SEM. **(D)** Representative IHC staining of Ki67 in pancreatic sections at day 7 after pancreatitis induction. Scale bars indicate 200 μ m. **(E)** Quantification of Ki67⁺ exocrine cells normalized to the total number of exocrine cells in pancreatic lesions at day 7. Data were analyzed using the unpaired t-test and are presented as mean \pm SEM. * $p < 0.05$, ** $p < 0.01$.

In summary, global *Tlr3* deficiency or exclusive expression of *Tlr3* in pancreatic epithelial cells caused enhanced lesion formation at day 7 of inflammation-driven carcinogenesis in mice with pancreas-specific expression of oncogenic *Kras*^{G12D}. The increased lesion area in KFT^{OFF} and KFT^{Epi} mice was associated with an elevated infiltration of macrophages and neutrophils, the induction of the pro-carcinogenic p-ERK signal transduction pathway, and increased proliferation of exocrine cells in the lesion areas. Notably, lesion formation in mice with myeloid cell-specific rescue of *Tlr3* expression was not different from KFT^{WT} mice, showing a partial rescue of the phenotype by TLR3 in myeloid cells. Myeloid cell-specific TLR3 signaling reduced the number of macrophages and neutrophils in the pancreas and reduced the activation of p-ERK signaling. The results suggest a limiting function of myeloid TLR3 on pancreatic carcinogenesis after inflammation.

3.2.2.4 Increased expression of lesion markers caused by systemic *Tlr3* deficiency at day 21 after inflammation induction

Next, the cell-specific effect of TLR3 at day 21 after pancreatitis induction in KF mice was characterized by IHC staining. The ductal marker KRT19 was highly present in the pancreas of the KF mouse lines, characteristic of the pronounced lesion areas (Fig. 28A). Compared to KFT^{WT} mice, global *Tlr3*-deficient mice had a significantly increased KRT19⁺ area (Fig. 28B). KRT19⁺ area in mice with myeloid cell-specific rescue of *Tlr3* expression equaled KFT^{WT} mice, indicative of the limiting role of myeloid *Tlr3* for the formation of ductal lesions. Equally, the Alcian blue-stained area was significantly increased in KFT^{OFF} compared to KFT^{WT}, with no significant difference between KFT^{WT} and KFT^{Mye} (Fig. 28A, Fig. 28B).

The quantification of the KRT19⁺ and Alcian blue⁺ area underlines the increased lesion formation and progression of carcinogenesis in global *Tlr3*-deficient mice. The rescue by myeloid cell-specific re-expression of *Tlr3* demonstrates the causative role of TLR3 signaling in myeloid cells for the formation of ductal lesion areas in the context of inflammation-driven carcinogenesis.

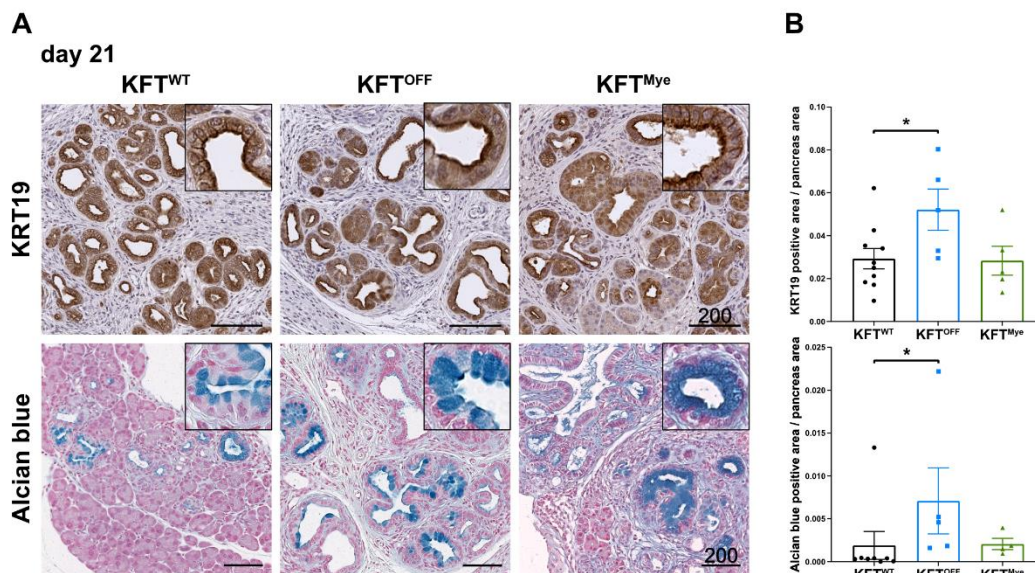


Figure 28: Myeloid TLR3 limits the formation and progression of pancreatic lesions at day 21 of inflammation-driven carcinogenesis. (A) Representative pictures of KRT19-stained and Alcian blue-stained lesions at day 21 after caerulein treatment of KF mouse cohorts. Scale bars indicate 200 μ m. **(B)** Quantification of KRT19- and Alcian blue-stained area normalized to the total area of the pancreas. Data were analyzed using the Mann-Whitney test and are presented as mean \pm SEM. * $p < 0.05$.

In accordance with the increased lesion area, KFT^{OFF} mice had significantly reduced expression of the acinar cell markers *Cpa1* compared to KFT^{WT} and KFT^{Mye} mice (Fig. 29A). The expression of *Ptf1a* was reduced in KFT^{OFF}, while there was no difference between KFT^{WT} and KFT^{Mye} mice. The difference in the expression of the ductal marker *Sox9* was not significant.

To elucidate the cause of the increased lesion area in globally *Tlr3*-deficient mice, the expression of proliferative markers was examined (Fig. 29B). KFT^{OFF} mice had an increased expression of *Ccnb1* compared to KFT^{WT} and an increased expression of *Cdk1* compared to KFT^{Mye}. This result supports the conclusion that enhanced lesion formation is associated with the proliferation of metaplastic cells within the lesions.

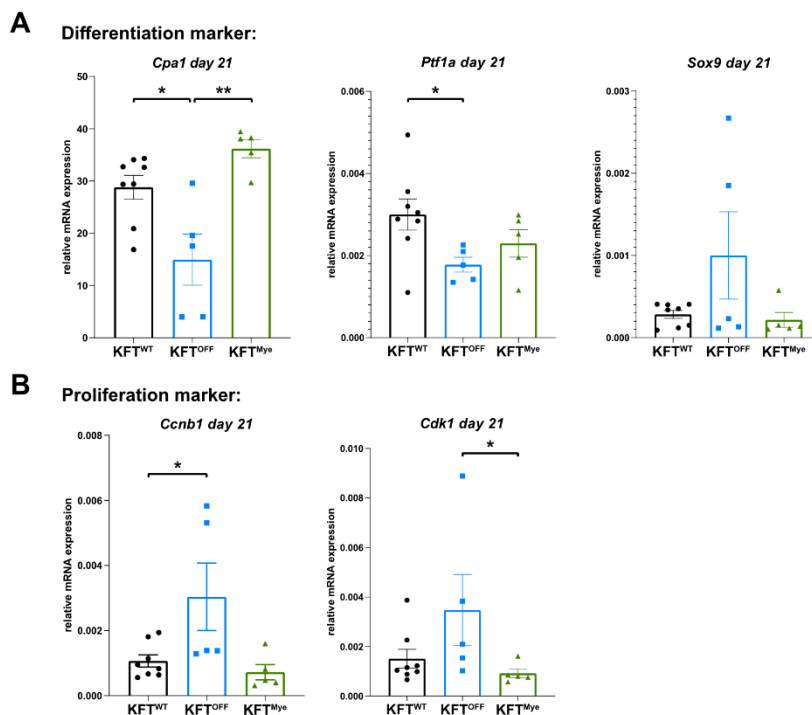


Figure 29: Global *Tlr3*-deficient mice express low levels of acinar lineage markers and high levels of proliferative markers at day 21 of pancreatitis-induced carcinogenesis. (A, B) Expression of the acinar cell-specific markers (*Cpa1*, *Ptf1a*), the ductal marker *Sox9*, and proliferative markers (*Ccnb1*, *Cdk1*) in the pancreas of KF mouse lines at day 21 after pancreatitis induction, quantified via RT-qPCR. Data were analyzed using the unpaired t-test or Mann-Whitney test and are presented as mean \pm SEM. * $p < 0.05$, ** $p < 0.01$.

3.2.2.5 The lesion microenvironment is not influenced by *Tlr3* deficiency at day 21 of pancreatitis-induced carcinogenesis

At day 7 after the induction of inflammation, enhanced pancreatic infiltration of macrophages and neutrophils was detected in KFT^{OFF} and KFT^{Epi} mice. To test whether these differences persisted at day 21, the cells in the lesion microenvironment were quantified via IHC staining

and the total pancreatic immune cells were examined by RT-qPCR expression analysis of lineage markers (Fig. 30).

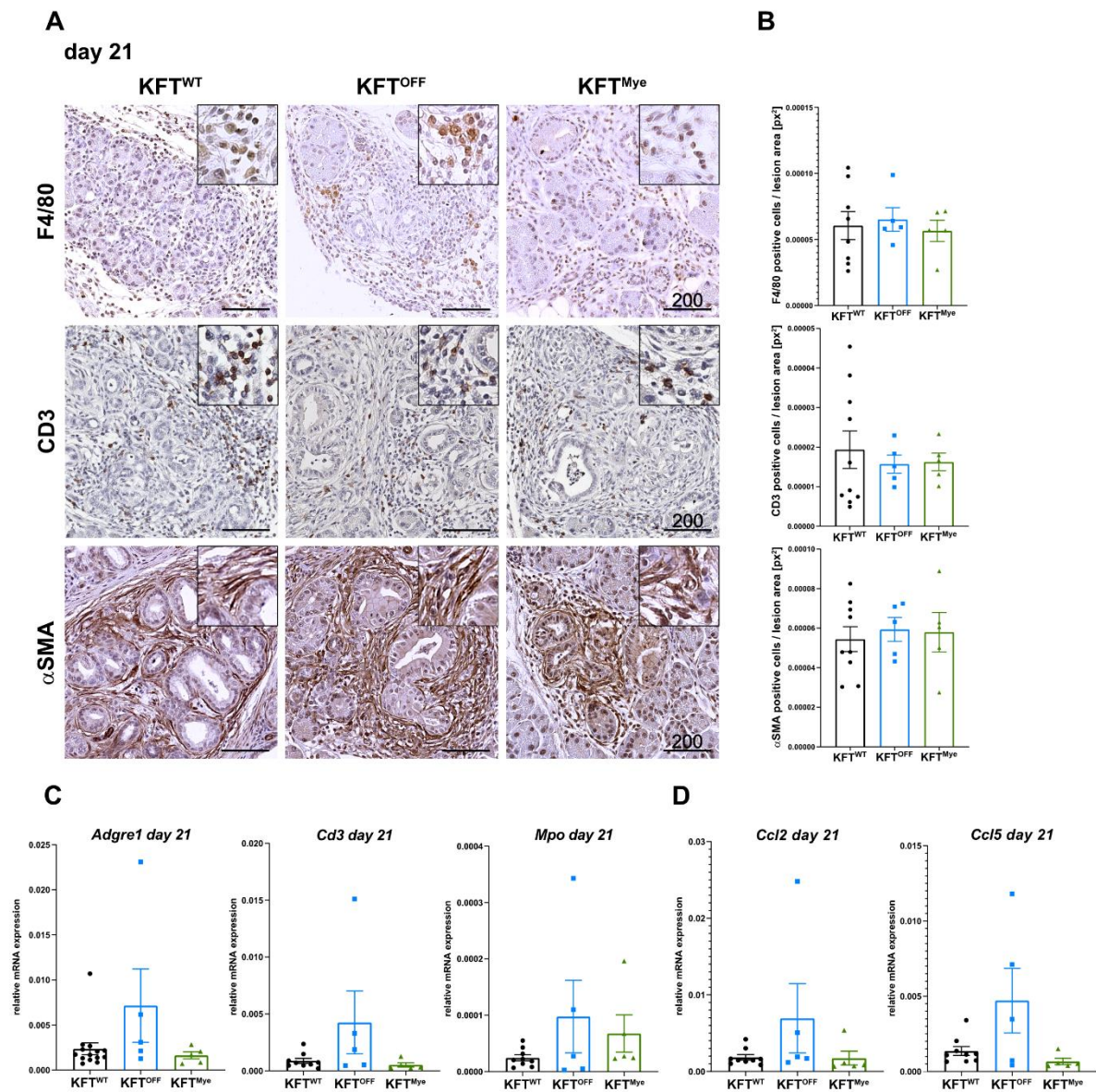


Figure 30: The regulatory effect of myeloid TLR3 on the lesion microenvironment does not persist until day 21 of pancreatitis-driven carcinogenesis. (A) Representative IHC staining of F4/80, CD3, and α SMA in pancreatic sections of KFT^{WT}, KFT^{OFF}, and KFT^{Mye} mice at day 21 after caerulein treatment. Scale bars indicate 200 μm . **(B)** Quantification of F4/80⁺ (upper graph), CD3⁺ (middle graph), and α SMA⁺ (lower graph) cells in pancreatic lesions, normalized to the area of the quantified lesions. **(C, D)** Expression analysis of cell lineage-specific markers (*Adgre1*, *Cd3*, *Mpo*) and cytokines (*Ccl2*, *Ccl5*) via RT-qPCR. Data are presented as mean \pm SEM.

Neither the IHC analysis of macrophages (F4/80⁺), T cells (CD3⁺), and myofibroblasts (α SMA⁺) in the lesion microenvironment, nor the quantification of the lineage markers *Adgre1*, *Cd3*, and *Mpo* indicated an influence of global or partial *Tlr3* deficiency on the lesion microenvironment at day 21 after caerulein treatment. The expression of the cytokines *Ccl2* and *Ccl5*

was not affected either by *Tlr3* deficiency.

The differences in immune cell infiltration regulated by myeloid cell-specific TLR3 signaling at day 7 did not persist until day 21.

3.2.2.6 *Tlr3* in myeloid cells counteracts pro-tumorigenic signaling pathways

Despite the similar quantities of tissue-resident immune cells at day 21 after pancreatitis induction, we next examined whether *Tlr3* deficiency affects the activity of immune cells in the microenvironment. Therefore, the expression of inflammatory markers and the activation of cellular signal transduction pathways was analyzed. The pancreatic expression of *Il-6* was significantly increased in global *Tlr3*-deficient mice compared to KFT^{WT} mice (Fig. 31A). The *Il-6* expression of KFT^{Mye} mice equaled the expression of KFT^{WT} mice, highlighting the importance of *Tlr3* in myeloid cells for the regulation of the pancreatic expression of *Il-6*. In contrast, the expression of *Tnf* and *Il-1b* was unaffected by *Tlr3* deficiency. Consistent with the increased *Il-6* expression, KFT^{Off} mice had a significantly increased activation of p-STAT3 signaling compared to KFT^{WT} and KFT^{Mye} mice (Fig. 31B, Fig. 31C). The findings highlight the negative regulation of the IL-6/STAT3 pathway by TLR3 in myeloid cells. Myeloid cell-mediated activation of the IL-6/STAT3 pathway is a well-established mechanism for inflammation-dependent carcinogenesis (Lesina et al., 2011). Correspondingly, global *Tlr3*-deficient mice had a significantly increased p-ERK/ERK ratio compared to KFT^{WT} and KFT^{Mye} mice. The advanced carcinogenesis in KFT^{Off} mice was associated with the reduction of the protein level of p27 compared to KFT^{WT} mice, indicating the overcoming of cellular senescence barriers. Compared to KFT^{Mye} mice, KFT^{Off} mice had reduced protein levels of I κ B α , suggesting an increased activation of the NF- κ B signal transduction pathway.

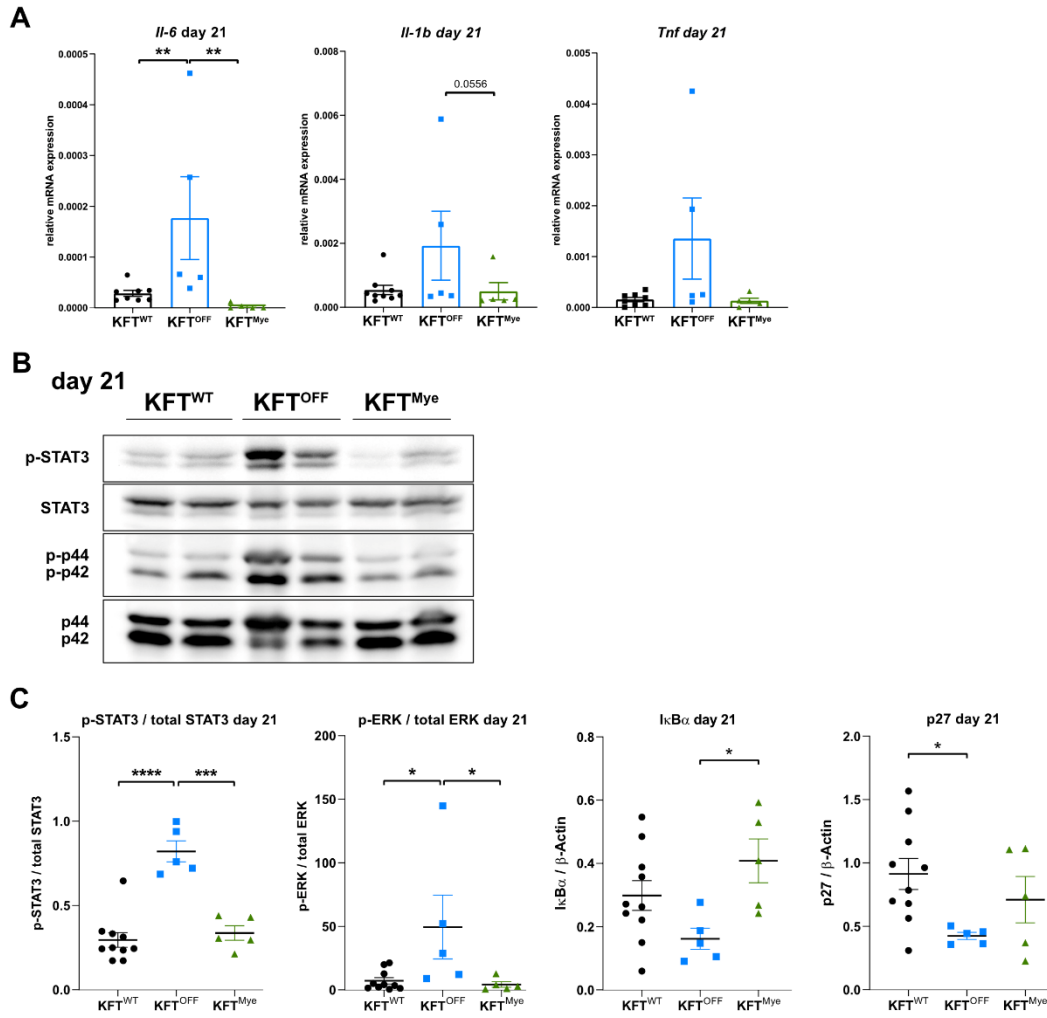


Figure 31: Myeloid TLR3 inhibits activation of pro-tumorigenic signal transduction pathways. (A) RT-qPCR-based quantification of the expression of proinflammatory cytokines (*Il-6*, *Il-1b*, *Tnf*) in the pancreas of KF mouse lines at day 21 after pancreatitis induction. Data were analyzed using the Mann-Whitney test. **(B)** Representative immunoblot showing the induction of p-STAT3 and p-ERK (p-p44 + p-p42) caused by systemic *Tlr3* deficiency. **(C)** Activation of pro-tumorigenic (p-STAT3, p-ERK, NF- κ B) signaling pathways and the reduction of cellular senescence barriers (p27) were analyzed by densitometrical quantification of the immunoblot signals and normalized to the respective total protein or β -Actin. Data were analyzed using the unpaired t-test or Mann-Whitney test. Data are presented as mean \pm SEM. * $p < 0.05$, ** $p < 0.01$, *** $p < 0.001$, **** $p < 0.0001$.

3.3 TLR3 in human PDAC

In the mouse model, myeloid cell TLR3 was shown to influence pancreatitis-induced carcinogenesis, while epithelial TLR3 had no influence on oncogene- or inflammation-driven carcinogenesis. To confirm the relevance of the animal studies for human patients, the function of TLR3 in human PDAC was investigated.

Data analysis from online databases revealed that high RNA expression levels of *TLR3* correlate with reduced survival of patients with PDAC (Fig. 32A, Nagy et al., 2021). According to mutation analysis of *TLR3* in human pancreatic cancer, *TLR3* is mutated in 6% of the patients (Fig. 32B, Witkiewicz et al., 2015). Components of the TLR3 signal transduction pathway are mutated in up to 39% of patients with pancreatic cancer.

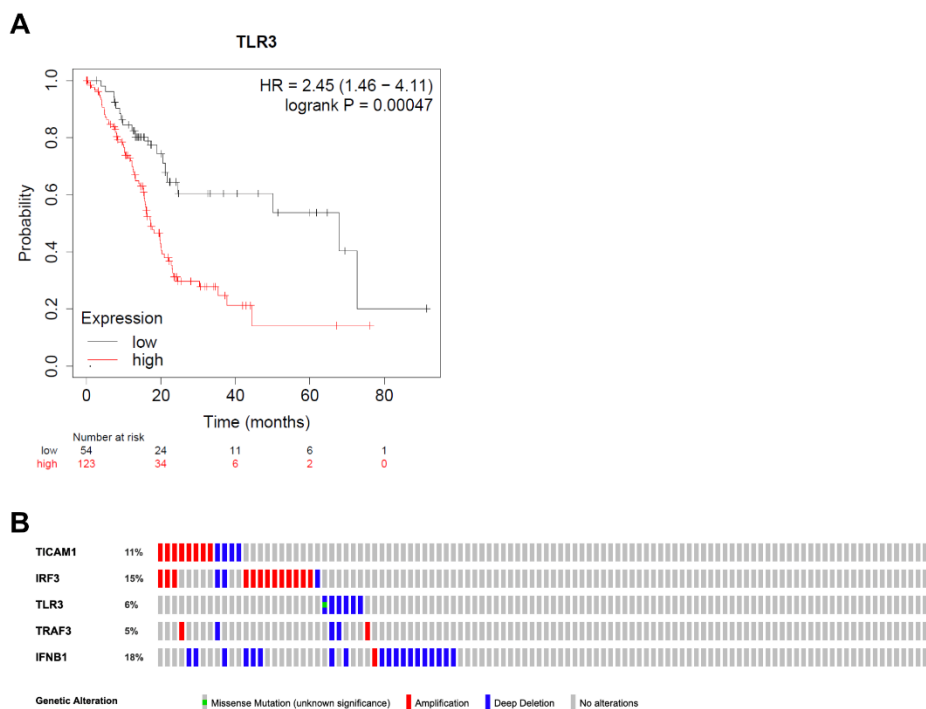


Figure 32: TLR3 in human PDAC. (A) Bulk RNA sequencing-based Kaplan Meier survival curve showing the correlation of *TLR3* expression and the survival of patients with PDAC. The data was analyzed using the log-rank test (Nagy et al., 2021). **(B)** Mutation frequency (missense mutations, amplifications, deep deletions) of components of the TLR3 signaling pathway in human pancreatic cancer samples (Witkiewicz et al., 2015).

3.3.1 Generation of a *TLR3*-deficient human tumor cell line using the CRISPR/Cas9 system

The relevance of epithelial *TLR3* in human PDAC was characterized using PDAC cell lines. First, the expression of *TLR3* in different PDAC cell lines was examined via RT-qPCR to select a suitable line with high *TLR3* expression (Fig. 33A). Based on the expression of *TLR3* and the existence of established transfection protocols for genetic manipulation, the cell line AsPC-1 was selected. AsPC-1 cells were infected using a lentiviral delivery system to enable the Cas9-mediated knock-out of *TLR3*. To minimize off-target effects, two different sgRNAs were used independently. The pre-screening of *TLR3*-deficient AsPC-1 clones was done by detection of genetic variation in the *TLR3* locus using the T7 endonuclease assay. To this end, the sgRNA targeted region of the *TLR3* locus was amplified by PCR and hybridized with the PCR product of *TLR3* from wild-type AsPC-1 cells. Heteroduplex regions were formed in case of CRISPR/Cas9-mediated genetic variation, enabling the digestion by T7 endonuclease. The digestion approach was analyzed by gel electrophoresis, to identify additional bands caused by T7 endonuclease-mediated digestion (Fig. 33B). *TLR3* deficiency of the pre-screened clones was proven by next-generation sequencing of the gene locus. *TLR3* deficiency was verified for two clones for each sgRNA (sgRNA1: AsPC-1 #1, AsPC-1 #9; sgRNA2: AsPC-1 #66, AsPC-1 #67).

For the functional verification of *TLR3* deficiency, the poly(I:C)-induced regulation of target genes was tested. Poly(I:C) promoted the expression of *CXCL1* and *TNF* in WT AsPC-1 cells. In *TLR3*-deficient AsPC-1 clones, expression of *CXCL1* and *TNF* was unaffected by poly(I:C) stimulation. The lack of responsiveness to poly(I:C) confirmed the absence of functional *TLR3* in the AsPC-1 clones. The cell morphology of AsPC-1 cells was unaffected by *TLR3* deficiency.

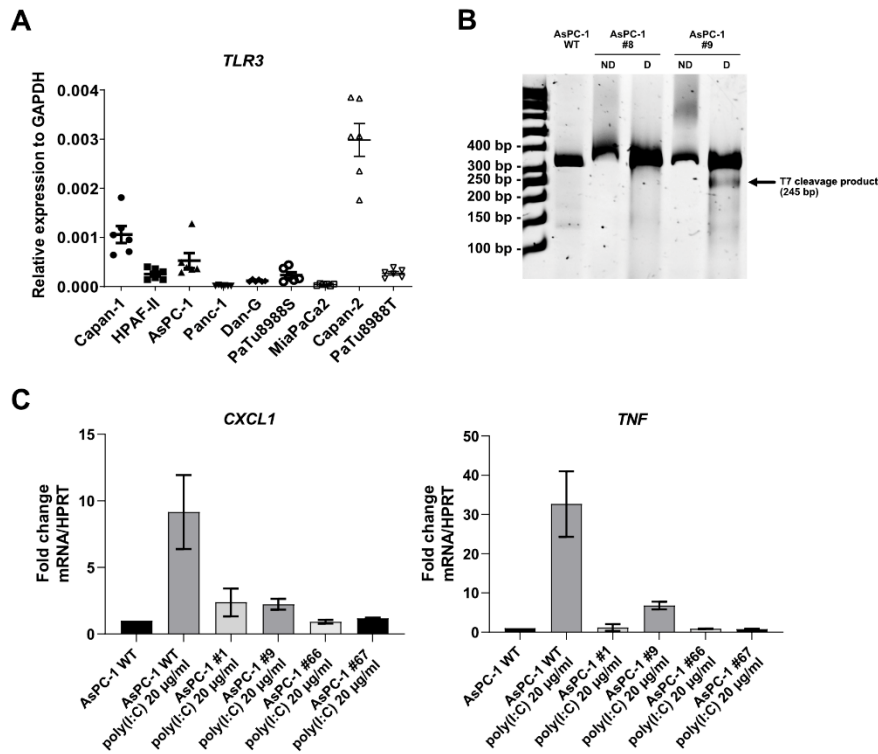


Figure 33: Generation of *TLR3*-deficient AsPC-1 cells by CRISPR/Cas9. (A) Validation of *TLR3* expression in different pancreatic tumor cell lines via RT-qPCR. **(B)** Representative DNA-PAGE showing the pre-screening of CRISPR/Cas9 targeted AsPC-1 clones by T7 endonuclease assay. ND = not digested, D = incubated with T7 endonuclease. **(C)** Functional verification of *TLR3* deficiency by RT-qPCR-based quantification of cytokine expression (*CXCL1*, *TNF*) after poly(I:C) stimulation (20 µg/ml, 6 h) of AsPC-1 clones. Data are presented as mean ± SEM.

3.3.2 *TLR3* is unable to induce cell death of AsPC-1 cells *in vitro*

Resistance to cell death is a hallmark of cancer (Hanahan and Weinberg, 2011). *TLR3* signaling was proven to be able to induce cell death of murine macrophages (3.1.6). To test for a similar effect of *TLR3* on tumor cells, the cell viability of AsPC-1 cells and *TLR3*-deficient clones was analyzed after stimulation with different doses of poly(I:C) (Fig. 34A, Fig. 34B). The presence of FCS did not influence the cell viability upon poly(I:C) stimulation. Even high doses of poly(I:C) were insufficient to reduce the cell viability of AsPC-1 cells, regardless of their *TLR3* expression, demonstrating the resistance of AsPC-1 cells to *TLR3*-mediated cell death.

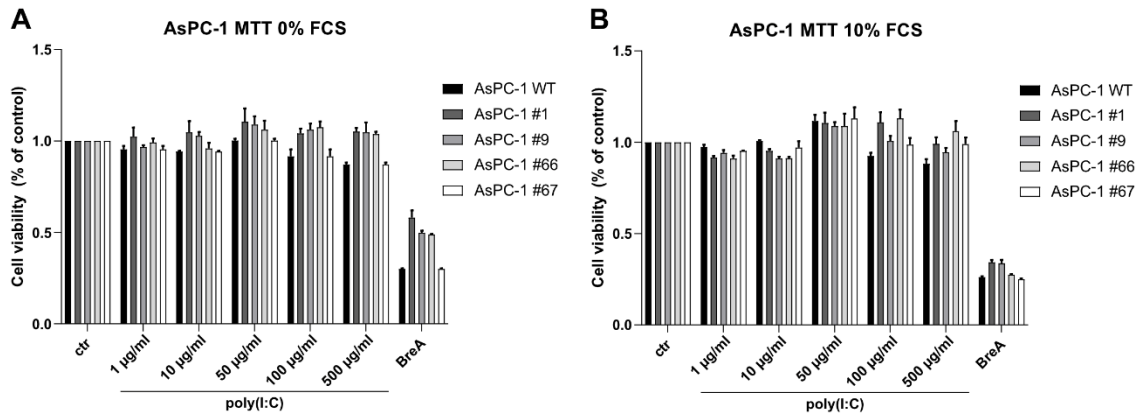


Figure 34: TLR3 signaling has no effect on cell viability of AsPC-1 cells. (A, B) Cell viability of WT and *TLR3*-deficient (#1, #9, #66, #67) AsPC-1 cells measured by MTT assay after 48 h of stimulation with indicated concentrations of poly(I:C). The stimulation was performed in absence of FCS (A) or in media supplemented with 10% FCS (B). Brefeldin A (4.5 µg/ml) was used as a positive control for the induction of apoptosis. Data are presented as mean ± SEM.

3.3.3 TLR3 regulates cytokine expression in human tumor cell lines

Manipulation of the immune cell infiltrate to generate an immunosuppressive, desmoplastic, pro-tumorigenic microenvironment is another core aspect of PDAC (Knudsen et al., 2017; Siret et al., 2019; Storz and Crawford, 2020). The expression of proinflammatory cytokines and interferons to modulate the immune response is a tumor-relevant potential effect of TLR3. The absence of functional TLR3 had no remarkable influence on the basal cytokine expression of AsPC-1 cells (data not shown). RT-qPCR-based expression analysis showed that poly(I:C) stimulation led to a pronounced induction of the expression of proinflammatory cytokines (*IL-1α*, *IL-1β*, *IL-6*, *TNF*) and chemokines (*IL-8*, *CCL1*, *CCL17*, *CXCL1*, *CXCL5*) in tumor cells (Fig. 35).

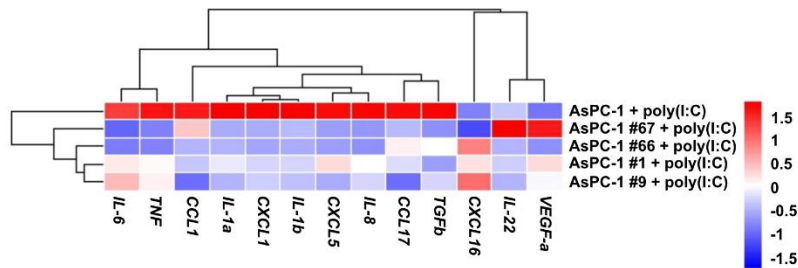


Figure 35: TLR3 signaling induces cytokine expression in AsPC-1 cells. (A) Hierarchically clustered heatmap showing the fold change of cytokine expression in WT and *TLR3*-deficient (#1, #9, #66, #67) AsPC-1 cells induced by poly(I:C) (20 µg/ml, 6 h), compared to unstimulated controls.

Collectively, it was demonstrated that components of the TLR3 signaling pathway are frequently mutated in human PDAC and that high expression of TLR3 correlates with reduced survival of PDAC patients. *In vitro*, TLR3 signaling was incapable of inducing cell death in the PDAC cell line AsPC-1, but the induction of TLR3 signaling substantially altered the cytokine expression of tumor cells. Accordingly, the results demonstrate a potential modulation of the tumor microenvironment by TLR3-induced cytokine expression in PDAC cells.

4 Discussion

4.1 Myeloid cell TLR3 is important for pancreatic regeneration after acute pancreatitis

4.1.1 Immunoregulatory function of myeloid cell TLR3 in pancreatic regeneration

Acute pancreatitis is the most common reason for hospitalization among gastrointestinal diseases (Peery et al., 2012). In recent years, the incidence of AP has risen rapidly (Krishna et al., 2017). The overall mortality in acute pancreatitis is 5%, especially necrotizing pancreatitis is associated with high mortality (Banks and Freeman, 2006). The main reason for AP-associated mortality is a multi-organ failure caused by the uncontrolled activation of the inflammatory cascade (Veit et al., 2014). Tissue necrosis in AP leads to the liberation of DAMPS, like nucleic acids (Kang et al., 2014). dsRNA from necrotic tissue can thereby activate TLR3 in immune cells and acinar cells (Karikó et al., 2004; Regel et al., 2019). Additionally, it has been demonstrated in this thesis that acinar cells secrete high amounts of exosomes, which can potentially stimulate TLR3 as well (3.1.10, Seo et al., 2016). The pro-regenerative function of TLR3 after tissue damage has previously been demonstrated for partial hepatectomy (Stöß et al., 2020), myocardial infarction (Wang et al., 2018), or skin neogenesis (Nelson et al., 2015). In the present study, the myeloid cell-specific function of TLR3 for pancreatic regeneration after caerulein-induced acute pancreatitis in mice was analyzed.

Global *Tlr3* deficiency led to increased formation and persistence of ADM structures, thereby preventing pancreatic regeneration after AP. This was associated with a persistently high immune cell infiltration, especially by macrophages. Exclusive expression of *Tlr3* in myeloid cells resulted in a partial rescue of the phenotype on days 2 and 5 and completely rescued the regenerative defect on day 7 after AP induction. Consistently, *in vitro* poly(I:C) stimulation of WT acinar cells confirmed that epithelial TLR3 signaling has no direct effect on the transdifferentiation of acinar cells. TLR3 in myeloid cells was shown to be important for the clearance of immune cells and the termination of the immune response after AP, thus enabling tissue regeneration. TLR3 signaling was demonstrated to induce cell death of murine macrophages *in vitro*. The results from RNA sequencing revealed the high expression of apoptotic markers at day 5 after AP in WT mice, while *Tlr3*-deficient mice expressed genes associated with tissue regeneration and inflammation at this time point. Mechanistically, the

TLR3-dependent induction of macrophage cell death could lead to the clearance of macrophages and the resolution of the immune response after AP. Thereby, TLR3 was identified as a central regulatory element for pancreatic regeneration.

Notably, *Tlr3* deficiency did not affect the early phase of acute pancreatitis. The recently published study by Regel et al. 2019 reported increased edema and necrosis in the early phase of AP (10 h after the first injection, AP was induced by 10 injections of 50 µg/kg body weight caerulein) due to global *Tlr3* deficiency, through increased NF-κB regulated induction of acinar cell necrosis (Regel et al., 2019). In contrast, we did not observe an effect of TLR3 on the severity of acute pancreatitis at 8 h and 24 h after caerulein-induced AP, in terms of edema formation, immune cell infiltration, necrosis, and hemorrhage. The deviating results may be attributed to the different mouse models which were used as well as the different protocols for the induction of acute pancreatitis. Our results are consistent with the observations of Hoque et al. 2011, who also found no effect of *Tlr3* deficiency at 24 h after caerulein-induced AP in mice (Hoque et al., 2011). Both groups did not investigate the function of TLR3 in the late phase of acute pancreatitis.

The enhanced formation and persistence of ADM in TLR3^{OFF} mice was associated with sustained high numbers of macrophages, neutrophils, and T cells in the pancreas. Neutrophils play an important role in AP (Gukovskaya et al., 2002; Zheng et al., 2013). In caerulein-induced AP in mice, neutrophils lead to NADPH oxidase-mediated activation of pancreatic digestive enzymes and systemic depletion of neutrophils was shown to reduce the severity of AP (Gukovskaya et al., 2002). On day 2, an increased number of neutrophils was detected in the pancreas of TLR3^{OFF} mice, correlating with the enhanced formation of ADM structures.

Macrophages function as key immune cells in pancreatic regeneration after AP (Zheng et al., 2013; Xue et al., 2014). The extent of macrophage activation directly correlates with the severity of AP (Zheng et al., 2013). Macrophages secreted proinflammatory cytokines such as TNF, IL-6, CCL2, and MCP1 recruit other immune cells and thus regulate the immune response (Xue et al., 2014). In accordance with the high number of pancreatic macrophages, TLR3^{OFF} mice had an increased expression of proinflammatory cytokines (*Tnf*, *Il-6*, *Ccl2*) in the pancreas compared to WT and TLR3^{Mye} mice. The high secretion of chemoattractant cytokines provides a potential explanation for the increased number of neutrophils and T cells in

the pancreas of TLR3^{OFF} mice.

Macrophages are able to directly induce ADM formation by the secretion of CCL5 and TNF (Liou et al., 2013). Accordingly, it is reported that *in vivo* depletion of macrophages reduces ADM formation and the severity of AP, thereby improving pancreas regeneration (Liou et al., 2013; Folias et al., 2014). At all time points examined after AP, macrophages were the predominant type of immune cells in the pancreas, highlighting their key role in AP. The persistent ADM structures of TLR3^{OFF} mice correlated with a persistently high number of pancreatic macrophages. Interestingly, myeloid cell-exclusive expression of *Tlr3* was sufficient to decrease the number of macrophages to WT levels and to rescue pancreatic regeneration. Accordingly, we focused on potential factors responsible for the resolution of pancreatic macrophages by TLR3 in the late phase of AP. *In vitro* generated macrophages had a high expression of *Tlr3*, associated with a strong responsiveness to poly(I:C)-induced TLR3 signaling. The results of the present study demonstrate that TLR3 signaling specifically promotes cell death of macrophages. TLR3-induced resolution of the immune response by clearance of macrophages represents a so far unknown, potential mechanism for the termination of inflammatory responses in tissue regeneration.

The resolution of the immune response is not a passive process after the elimination of the injurious agent, but a tightly regulated, active process (Serhan et al., 2007; Fullerton and Gilroy, 2016). It is well documented that macrophages play a central role in this process by removing cell debris and apoptotic immune cells from the tissue and subsequently leave the tissue themselves by lymphatic drainage, reverse migration, or apoptosis, thereby terminating the immune response (Gilroy et al., 2003; Serhan et al., 2007; Sugimoto et al., 2019). Our data provide evidence for a previously unknown mechanism for the termination of the immune response in the late phase of AP. Our results from bulk RNA sequencing demonstrated that pro-apoptotic pathways were activated in WT mice at day 5 after AP induction, while TLR3^{OFF} mice persistently expressed regeneration-associated and proinflammatory genes, proving the defective, sustaining pancreatic regeneration process. TLR3-induced cell death of macrophages could contribute to the clearance of immune cells from tissue and ultimately lead to the resolution of ADM and pancreatic regeneration after AP. Our data on globally *Tlr3*-deficient mice demonstrate that dysregulation of the TLR3-dependent tissue clearance of macrophages could cause persistent inflammation. This provides new possibilities for

therapeutic interventions in AP based on the direct TLR3-dependent induction of pro-resolution pathways.

It is well documented in the literature that the initiation of inflammation in AP depends on the activation of pattern recognition receptors by DAMPs released from injured acinar cells (reviewed in Hoque et al., 2012). In this thesis, we exemplified the pivotal role of the myeloid PRR TLR3 for tissue regeneration after AP by the termination of the inflammatory response.

4.1.2 Mechanism for TLR3-dependent induction of macrophage cell death

The pivotal role of macrophages in the immune response, as well as their high sensitivity to TLR3 signaling, places macrophages in the focus of potential therapeutic interventions for the modulation of the immune reaction. TLR3-dependent clearance of macrophages could be induced to resolve persisting inflammations. Specific TLR3-based therapeutic modulation of the immune response requires a profound knowledge of the mechanism of TLR3 signaling in macrophages.

Short-term poly(I:C) stimulation of murine macrophages induced NF- κ B signaling via nuclear translocation of p65/RelA and the expression of proinflammatory cytokines. At 48 h, poly(I:C) resulted in TLR3-dependent induction of macrophage cell death associated with the formation of cleaved caspase 8. The absent effect of poly(I:C) on the cell viability of *Tlr3*-deficient macrophages confirmed the selectivity of this effect for TLR3. Neither inhibition of caspase activity by Z-VAD-FMK nor genetic *Casp8* deficiency blocked the effect of poly(I:C) on the cell viability of macrophages. Interestingly, inhibition of RIPK1 by Nec-1 was also insufficient to inhibit the TLR3-dependent cell death. Strikingly, only combined inhibition of caspase activity by Z-VAD-FMK and RIPK1 by Nec-1 efficiently blocked poly(I:C)-induced cell death of macrophages. The results provide evidence for the existence of parallel, alternative signaling pathways of TLR3-regulated cell death of macrophages.

The mechanism for the induction of cell death by TLR3 is described in the literature for various human cancer cell lines (Feoktistova et al., 2011; Estornes et al., 2012). Estornes et al reported the poly(I:C)-induced formation of an atypical death complex consisting of TLR3, TRIF, RIPK1, CASP8, CASP10, and FADD in human lung cancer cell lines, regulated by cIAP1/2-dependent ubiquitinylation of RIPK1 (Estornes et al., 2012). In these cell lines, poly(I:C)-

dependent cell death could be inhibited by knockdown of *CASP8* (Estornes et al., 2012). In contrast, our results showed no influence of pharmacological inhibition of *CASP8* by Z-VAD-FMK or genetic *Casp8* deficiency on the induction of cell death by poly(I:C) in murine macrophages.

Feoktistova et al. characterized in HaCaT cells the TLR3-dependent formation of the so-called ripoptosome complex, consisting of TLR3, TRIF, RIPK1, *CASP8*, *CASP10*, FADD, and cFLIP isoforms (Feoktistova et al., 2011). Depending on the composition of the ripoptosome, cFLIP_L leads to *CASP8*-dependent induction of apoptosis or cFLIP_S leads to RIPK-dependent necrosis (Feoktistova et al., 2011). HaCaT cells were protected from poly(I:C)-induced cell death only in case of parallel inhibition of caspase activity by Z-FMK-VAD and RIPK1 by Nec-1 (Feoktistova et al., 2011). Our results replicate the observations of this group. In the murine macrophage lines, combined inhibition of caspases and RIPK1 was necessary to block poly(I:C)-mediated cell death. Accordingly, we assume a similar mechanism of TLR3-dependent cell death in macrophages as described by Feoktistova et al for HaCaT cells (Feoktistova et al., 2011).

Caspase-induced apoptosis is a central mechanism for immune cell clearance (Sugimoto et al., 2019). In human patients, homozygous *CASP8* deficiency is manifested by defective apoptosis of lymphocytes, combined with impaired activation of T cells, B cells, and NK cells, causing immunodeficiency (Chun et al., 2002). Two other patients with the identical homozygous *CASP8* mutation were characterized by multiorgan lymphocyte infiltration, granulomas, and immune dysregulation (Niemela et al., 2015).

TLR3 signaling in macrophages led to the activation of *CASP8*. To test whether *CASP8*-dependent cell death of macrophages is functionally involved in the clearance of immune cells after acute pancreatitis, we examined AP in mice with exclusive deletion of *Casp8* in myeloid cells. Pancreatic regeneration was unaffected by partial *Casp8* deficiency. Accordingly, we assume that in case of blocked caspase signaling, alternative mechanisms for the clearance of immune cells are existent. The *in vitro* characterization of TLR3-dependent induction of cell death showed that TLR3 induces RIPK1-mediated cell death in case of blocked caspase activity (Feoktistova et al., 2011). Accordingly, equivalent mechanisms may have occurred for the pancreatic regeneration of myeloid cell-specific *Casp8*-deficient mice. The results are consistent with our *in vitro* experiments by supporting the assumption of parallel,

alternative pathways for the induction of TLR3-dependent cell death. To verify this hypothesis, the activation of RIPK-dependent signaling pathways needs to be inhibited simultaneously in the late phase of acute pancreatitis.

4.2 Cell-specific function of TLR3 in oncogene-driven and pancreatitis-driven carcinogenesis

The 5-year survival rate of PDAC patients (9%) is one of the lowest of all cancer types, highlighting the urgent need for novel, innovative therapeutic strategies (Rawla et al., 2019; Miller et al., 2020). PDAC is rapidly progressive and early metastatic but is often asymptomatic in its early stages (Hidalgo et al., 2015). To enable early detection and to develop efficient therapies, the investigation of early, preinvasive stages of carcinogenesis is of outstanding importance.

In the regeneration of the pancreas after acute pancreatitis, we were able to demonstrate the role of myeloid cell TLR3 for limiting ADM formation and the importance of TLR3 for the regeneration of the pancreas. ADM represents the initial step of PDAC carcinogenesis (Schmid, 2002; Kopp et al., 2012; Reichert et al., 2016). Defective regeneration and incomplete termination of the immune response can progress to chronic pancreatitis and PDAC (Lowenfels et al., 1993; Kirkegård et al., 2017). Therefore, we next analyzed the cell-specific function of TLR3 on oncogene-driven and pancreatitis-induced carcinogenesis using a genetically engineered mouse model.

GEMMs enable the *ab initio* examination of the full spectrum of carcinogenesis *in vivo* (Gabriel et al., 2020). Since tumor development occurs in the presence of an intact immune system, GEMMs mimic clinical features like immunoediting and tumor heterogeneity. GEMMs can also be used to investigate mechanisms of immune cell recruitment and activation as well as mechanisms of immune evasion (Lee et al., 2016; Ischenko et al., 2021). To investigate the cell-specific function of TLR3 on oncogene-driven carcinogenesis, we used the recently published dual-recombinase system (Schönhuber et al., 2014). The system was generated by nuclear injection of the *Pdx1-Flp-o* transgene into C57BL/6 zygotes, followed by random integration of the transgene into the genome (Schönhuber et al., 2014).

4.2.1 Maternal imprinting of the *Pdx1*-Flp transgene in the dual recombinase system

For many experimental mice, we observed the absence of Flp-mediated recombination despite the genetic presence of the alleles for *Pdx1-Flp* and *FSF-Kras^{G12D}*. We found a strong correlation between the inactivity of flippase and maternal inheritance of the *Pdx1-Flp* allele. Genomic imprinting describes the reversible, epigenetic inactivation of mammalian alleles depending on whether they were inherited maternally or paternally (Sapienza et al., 1989; Bartolomei et al., 1993; Ruvinsky, 1999). Imprinting represents a compromise between contradictory fetal and maternal demands (Ruvinsky, 1999). We assume that maternal imprinting of the *Pdx1* promoter caused the observed recombinational inactivity of Flp.

4.2.2 Myeloid cell TLR3 in oncogene-driven carcinogenesis

In the KPF mouse model, global or partial *Tlr3* deficiency did not affect the mere oncogene-driven PDAC carcinogenesis concerning progression, lesion area, immune infiltrate, cytokine expression, or the activation of cellular signal transduction pathways. Similar to the Cre-dependent KPC model, ductal lesions in the KPF mouse cohorts recapitulated all stages of PDAC carcinogenesis (ADM, PanIN1, PanIN2, PanIN3, PDAC) combined with a pronounced desmoplastic response and infiltrating fibroblasts and immune cells (Hingorani et al., 2005).

In general, 12-week-old KPF mice had a high deviation concerning tumor progression and the formation of lesion areas. A high genomic instability is reported for the KPC model in the literature (Hingorani et al., 2005; Niknafs et al., 2019). Hingorani et al. characterized the loss of heterozygosity (LOH) of the *Trp53* allele as a fundamental step in the progression to invasive PDAC, which occurs spontaneously in all KPC mice with PDAC (Hingorani et al., 2005). Depending on the time point when this step stochastically takes place, carcinoma develops at an earlier or later time point. Accordingly, the spontaneous LOH in PDAC carcinogenesis in the KPC model could cover a potential effect of *Tlr3* deficiency and lead to the high deviation of the results.

Further evidence for the high genomic instability in the KPC model is provided by recently published whole exon sequencing data from KPC-derived tumors (Niknafs et al., 2019). The results showed an average of 13 ± 7 somatic mutations per KPC tumor with $32 \pm 13\%$ of the genes that were affected by copy gains or losses (Niknafs et al., 2019). Similar to spontane-

ous LOH, the high number of additional random mutations could compensate for the effect of partial or global *Tlr3* deficiency and explains the high deviation of results.

Analogously, the Kaplan-Meier survival curve of KPPF mouse cohorts displayed high deviation in survival time with no influence of *Tlr3* deficiency on the survival. Again, the high genomic instability of the mouse model could mask potential effects of *Tlr3* deficiency. At the same time, homozygous deletion of *Trp53* in combination with pancreas-specific expression of *Kras^{G12D}* has a strong oncogenic potential and covers thereby the potentially weaker effects of partial or global *Tlr3* deficiency.

KPPF mice reproduced characteristic symptoms of PDAC patients including cachexia, jaundice, ascites, and abdominal distension. No distant metastases were observed in the mice. The lack of metastases is also reported in the literature for the corresponding KPPC model (Gabriel et al., 2020). The tremendously rapid tumor growth in the KPPC/KPPF model leads to early-on pronounced pathologies caused by the high volume of the primary tumor, evoking a strong decline in general well-being, even before distant metastases can be formed in time.

KPPFT^{OFF} mice had significantly increased expression of the immune cell lineage markers *Cd3* and *Foxp3* compared to tumors from the KPPFT^{WT} and KPPFT^{Mye} cohorts. We conclude a limitation of intratumoral infiltration by T cells and specifically Treg cells, caused by myeloid cell TLR3. While high infiltration of CD4⁺ and CD8⁺ T cells generally correlates with longer survival of PDAC patients, infiltration with immunosuppressive FOXP3⁺ Treg cells correlates with reduced overall survival (Hiraoka et al., 2006; Ino et al., 2013; Wang et al., 2017).

Treg cells create an immunosuppressive microenvironment in PDAC by suppressing the activity of proinflammatory immune cells and by the activation of anti-inflammatory pathways (Whiteside, 2015; Jang et al., 2017; Siret et al., 2019). In a mouse model, depletion of Tregs was proven to reduce PDAC growth and to prolong the overall survival, dependent on the increased activity of cytotoxic CD8⁺ T cells (Jang et al., 2017). Our results indicate that TLR3-dependent modulation of T cell infiltration in the KPPF model was insufficient to manifest in altered overall survival of the mice. Likewise, the tumor cell-to-stroma ratio and tumor morphology were unaffected by the altered T cell infiltrate. The missing effect of the modified microenvironment in the KPPF model is most likely caused by the extremely rapid progression of tumor growth in this model, which can hardly be influenced by external factors.

4.2.3 Myeloid cell TLR3 limits inflammation-driven carcinogenesis

Inflammation is a core aspect of PDAC initiation and progression (Garcea et al., 2005). The carcinogenesis of pancreatic acinar cells to invasive carcinoma requires the overcoming of cellular senescence barriers through the deletion of tumor suppressor genes or inflammation (Hingorani et al., 2005; Guerra et al., 2007; Guerra et al., 2011; Di Magliano and Logsdon, 2013). Due to the central role of myeloid cell TLR3 for the termination of inflammation after acute pancreatitis (Chapter 3.1), we next investigated the effect of global or partial *Tlr3* deficiency on inflammation-driven carcinogenesis by caerulein-mediated induction of pancreatitis in mice with pancreas-specific expression of oncogenic *Kras*^{G12D}.

While the pancreas of mice with wild-type *Kras* was entirely regenerated at day 7 and day 21 after pancreatitis induction, all mice with pancreas-specific expression of *Kras*^{G12D} had pronounced, persistent lesions in the pancreas. Oncogenic KRAS^{G12D} blocks the recovery of the pancreas after inflammation (Morris et al., 2010; Kong et al., 2018). Morris et al. demonstrated that KRAS^{G12D} inhibits the expression of the differentiation factor β -catenin (Morris et al., 2010). Thereby, KRAS^{G12D} prevents the redifferentiation of ductal-like progenitor cells into acinar cells and impairs pancreatic regeneration (Morris et al., 2010). Alternatively, tissue damage is hypothesized to activate adult stem cells in the pancreas, which are susceptible to oncogenic transformation by KRAS^{G12D}, thus promoting pancreatic carcinogenesis (Pérez-Mancera et al., 2012).

The lesions at day 21 were predominantly composed of mucinous, proliferative PanIN structures surrounded by a fibrotic environment with high infiltration of α SMA⁺ cells. Thus, the lesions showed characteristic histological core aspects of early pancreatic carcinogenesis. Invasive PDAC structures were not expected at this early time point since they are reported to emerge in about 80 days after caerulein treatment (Carrière et al., 2009).

Tlr3 deficiency led to significantly elevated lesion size and to an increased pancreas-to-body weight ratio at day 7 after pancreatitis induction in the KF cohorts. KFT^{OFF} and KFT^{Epi} mice had an increased pancreatic infiltration of macrophages and neutrophil granulocytes compared to KFT^{WT} mice, while infiltration in KFT^{Mye} mice was not significantly different from KFT^{WT} mice. In accordance with the immunoregulatory function of myeloid TLR3 in acute pancreatitis in WT mice (Chapter 3.1), we were able to show that myeloid cell-specific TLR3 signaling limited the number of pancreatic macrophages and neutrophils in inflammation-

driven carcinogenesis. In contrast, exclusive *Tlr3* expression in pancreatic epithelial cells did not rescue the increased immune cell infiltration caused by global *Tlr3* deficiency.

Macrophages and neutrophils are both reported to promote the severity of pancreatitis (McKay et al., 1996; Gukovskaya et al., 2002; Bhatia et al., 2005; Abdulla et al., 2011; Liou et al., 2013; Merza et al., 2015). The increased infiltration of immune cells on day 7 was associated with the activation of the p-ERK signaling pathway in the pancreas and increased proliferation of exocrine cells within the lesions. The results at day 7 demonstrate the inhibitory effect of myeloid cell TLR3 on the early phase of pancreatitis-induced carcinogenesis, by restricting the immune cell infiltration and thereby limiting pro-proliferative, tumor-promoting inflammation.

The enhanced proliferation at day 7 was manifested at day 21 by the increased lesion area and pancreas-to-body weight ratio of KFT^{OFF} mice. Exclusive expression of *Tlr3* in myeloid cells was sufficient to fully rescue the pancreas-to-body weight ratio and to partially rescue the lesion area at day 21, demonstrating the dependence of this phenotype on TLR3 in myeloid cells. Consistent with the increased lesion area at day 21, KFT^{OFF} mice had an enlarged KRT19⁺ ductal lesion area and decreased pancreatic expression of the acinar cell markers *Ptf1a* and *Cpa1* compared to KFT^{WT} mice.

PanIN structures are characterized by the high expression of mucins and hence can be detected by Alcian blue staining (Distler et al., 2014). The elevated proportion of Alcian blue⁺ area in KFT^{OFF} mice reflects the increased occurrence of PanIN structures and thus indicates the progression of carcinogenesis compared to KFT^{WT} mice.

While AP in mice with WT *Kras* is terminated by the clearance of immune cells as part of the pancreatic regeneration process (Chapter 3.1), pancreatitis in mice with KRAS^{G12D} leads to continuous infiltration of immune cells as part of a non-resolving, tumor-promoting immune response (Kong et al., 2018). Accordingly, we assume that the TLR3-dependent induction of cell death in macrophages does not affect the inflammation-induced carcinogenesis due to missing phases of immune cell clearance and continuous immune cell recruitment.

The difference in immune cell infiltration observed at day 7 did not persist until day 21. Independent of the number of infiltrating immune cells, the enhanced expression of proinflammatory *Il-6* in KFT^{OFF} mice revealed an amplified immune cell activity compared to KFT^{WT} and KFT^{Mye} mice. Consistently, the increased expression of *Il-6* in KFT^{OFF} mice was associated with a significantly enhanced activation of the protumorigenic p-STAT3 pathway compared

to KFT^{WT} and KFT^{Mye} mice.

The IL-6/p-STAT3 pathway is a key regulator of pancreatitis severity and pancreatic carcinogenesis (Corcoran et al., 2011; Fukuda et al., 2011; Lesina et al., 2011; Zhang et al., 2013). In pancreatitis, myeloid cells secrete IL-6 to enhance inflammation (Zhang 2013). Fukuda et al. demonstrated that p-STAT3 is activated in pancreatitis-induced carcinogenesis of KC mice and promotes the proliferation of acinar cells and ductal cells, thus driving the expansion of lesion areas (Fukuda et al., 2011). Accordingly, KC mice with pancreas-specific deletion of *Stat3* exhibit reduced lesion areas in pancreatitis-induced carcinogenesis (Fukuda et al., 2011). Consistently, the enlarged lesion area of KFT^{OFF} mice correlated with significantly increased expression of *Il-6* and enhanced activation of p-STAT3. The induction of p-STAT3 in KFT^{OFF} mice was linked to increased activation of p-ERK signaling compared to KFT^{WT} and KFT^{Mye} mice and enhanced RNA expression of proliferation markers (*Ccnb1*, *Cdk1*). The complete rescue of p-STAT3 activation by myeloid TLR3 highlights the inhibitory influence of myeloid cell TLR3 signaling on the secretion of *Il-6* and thus on activation of the p-STAT3 and the p-ERK pathway. It is currently unknown whether this effect is mediated by direct regulation of the IL-6/p-STAT3 pathway or by indirect regulation of the secretion of anti-inflammatory cytokines.

The group of Hana Algül showed in the KC model that macrophage-derived IL-6 was able to induce p-STAT3 in preinvasive pancreatic lesions via trans-signaling and thus enhanced pancreatic carcinogenesis, whereas genetic *Il-6* deficiency or pancreas-specific inactivation of STAT3 impaired progression of PanIN lesions and blocked PDAC development (Lesina et al., 2011). Progression of ADM and preinvasive low-grade PanIN structures to carcinoma *in situ* and PDAC depends on the overcoming of cellular senescence barriers (Guerra et al., 2007; Guerra et al., 2011). Consistent with the central function of p-STAT3 in PDAC pathogenesis, the increased activation of the IL-6/p-STAT3 pathway in KFT^{OFF} mice correlated with an elevated proportion of mucinous PanIN structures, combined with reduced protein levels of the senescence factor p27. p27 is a well-established factor for the induction of oncogene-dependent stress-induced premature senescence and is frequently downregulated in PDAC carcinogenesis to overcome senescence (Diersch et al., 2013; Flores et al., 2014; Jeannot et al., 2015; Li et al., 2018). Our results revealed the correlation between reduced p27 protein levels and the progression of carcinogenesis in KFT^{OFF} mice.

While *Tlr3* deficiency had no effect on oncogene-driven carcinogenesis in the KPF and KPPF model, the results of pancreatitis-driven carcinogenesis showed that TLR3 signaling in myeloid cells was able to inhibit immune cell activity, thereby limiting the expansion and progression of preinvasive lesion areas.

The myeloid cell-specific function of TLR3 in acute pancreatitis and pancreatitis-induced carcinogenesis in absence of an effect of TLR3 on mere oncogene-driven carcinogenesis demonstrate that the highly inflammatory context of pancreatitis was mandatory for the manifestation of TLR3-dependent effects. Pancreatitis causes tissue necrosis and thereby provokes the liberation of DAMPs like dsRNA, as ligands of TLR3 (Karikó et al., 2004; Kang et al., 2014). Thus, pancreatitis is able to induce strong TLR3 signaling. In contrast, early preinvasive stages of oncogene-driven PDAC carcinogenesis are associated with only limited occurrence of necrosis and liberation of dsRNA. The activation of TLR3 signaling is correspondingly lower, thus providing a possible explanation for the lack of TLR3-dependent effects in the KPF and KPPF model.

4.3 TLR3 in human PDAC

It was shown that myeloid cell TLR3 promotes inflammation-associated pancreatic regeneration and inhibits inflammation-mediated carcinogenesis. A similar effect of TLR3 in human AP and PDAC carcinogenesis cannot be verified due to the lack of suitable model systems.

The Kaplan Meier survival curve of human PDAC patients revealed the correlation between high *TLR3* expression and low survival of the patients. It is important to note that the data were obtained by bulk RNA sequencing of cDNA derived from the whole tumor (Bailey et al., 2016). The percentage of neoplastic cells in PDAC is only 5-20% due to the high desmoplastic reaction and the infiltration of fibroblasts and immune cells into the microenvironment (Wood and Hruban, 2012). Accordingly, the immune cell infiltrate contributes critically to the pancreatic expression of *TLR3* and thus influences the bulk RNA sequencing-based survival analysis. Bianchi et al., for example, showed by IHC staining of human NSCLC sections that high expression of *TLR3* by tumor cells correlates with longer patient survival, whereas high *TLR3* expression in infiltrating immune cells correlates with poor prognosis (Bianchi et al., 2019). Lanki et al. determined by IHC staining of human PDAC samples that the absence of *TLR3* expression in tumor cells correlates with low patient survival (Lanki et al., 2019). Thus,

the cell-specific expression analysis is necessary to unequivocally determine the cell type-dependent influence of *TLR3* expression on the survival of PDAC patients.

The function of TLR3 in human PDAC cells was investigated by CRISPR/Cas9-mediated gene knock-out of *TLR3*. To exclude off-target effects, two independent sgRNAs were used and two clones per sgRNA were examined. Sequencing of the *TLR3* locus and the lack of responsiveness to poly(I:C) confirmed the absence of functional TLR3.

TLR3 deficiency did not affect the morphology of AsPC-1 cells, nor the basal expression of cytokines. The TLR3-dependent induction of cell death is described for various human cancer cell lines (Salaun et al., 2006; Paone et al., 2008; Estornes et al., 2012). However, the stimulation of AsPC-1 cells with poly(I:C) was not sufficient to induce cell death via TLR3. TLR3-dependent cell death is a highly regulated process, which can be blocked by diverse cellular inhibitors. For example, human melanoma cell lines were shown to be resistant to TLR3-mediated cell death despite their high expression of *TLR3*, due to the presence of cIAP1/cIAP2 as negative regulators (Weber et al., 2010). Consistently, IAP antagonists were proven to sensitize HaCaT cells for poly(I:C)-induced cell death (Feoktistova et al., 2011). A similar dysregulation of negative regulators could be responsible for the missing regulation of cell viability of AsPC-1 cells by TLR3, despite their high expression of *TLR3*.

Cytokines facilitate PDAC development and progression but also have antitumoral effects (Bhatia et al., 2022). While in the early phase of carcinogenesis mainly proinflammatory signals promote tumor progression, immunosuppressive factors are important to inhibit the antitumoral immunosurveillance in advanced tumor stages (Roshani et al., 2014; Padoan et al., 2019). Cytokines are secreted not only by immune cells in the tumor microenvironment but also directly by tumor cells (Padoan et al., 2019). The cytokine expression profile after poly(I:C) stimulation of AsPC-1 cells compared to *TLR3*-deficient clones revealed the TLR3-dependent regulation of cytokine expression in the PDAC cell line. TLR3 signaling induced the expression of various proinflammatory cytokines (*IL-1 α* , *IL-1 β* , *IL-6*, *TNF*), chemokines (*IL-8*, *CCL1*, *CCL17*, *CXCL1*, *CXCL5*), and *TGF- β* .

Tumor-derived cytokines like TGF- β and IL-6 are able to remodel the tumor microenvironment and thereby exert wide-ranging effects on tumor progression (Bellone et al., 2006). TLR3 signaling can lead to modulation of the tumor microenvironment (Bellone et al., 2006; Chew et al., 2012b; Azuma et al., 2016). In hepatocellular carcinoma cells, TLR3 induces the

expression of *CCL2*, *CCL5*, and *CXCL10*, resulting in the infiltration of NK cells and T cells and prolonged patient survival (Chew et al., 2012b). In clear-cell renal carcinoma, high expression of *TLR3* correlates with increased infiltration of B cells, CD4⁺ and CD8⁺ T cells, macrophages, neutrophils, and dendritic cells (Liao et al., 2021).

In the KPPF model, an immunomodulatory effect of myeloid cell TLR3 was demonstrated by limiting the intratumoral infiltration of CD3⁺ and FOXP3⁺ cells (Chapter 3.2.1.3). Further, we demonstrated the extensive effects of myeloid cell TLR3 on immune cell infiltration in the context of pancreatic regeneration after acute pancreatitis, as well as in inflammation-driven PDAC carcinogenesis. The TLR3-induced modulation of the cytokine expression by human PDAC cells supports our findings of a regulatory influence of TLR3 on the tumor microenvironment.

PDAC is associated with a highly immunosuppressive microenvironment (Zheng et al., 2013; Knudsen et al., 2017; Carpenter et al., 2021). Numerous research efforts are aimed at adapting immunotherapy for the treatment of PDAC patients to specifically restore the endogenous anti-tumor immune surveillance function (Smith et al., 2018; Deutsch et al., 2019; Le Naour et al., 2020). The TLR3-mediated modulation of cytokine expression, in combination with TLR3-mediated induction of cell death in tumor cells, highlights the potential versatile therapeutic effects of TLR3 agonists in highly immunosuppressive tumors.

5 Conclusion and Outlook

Work of the present thesis shows that the pro-regenerative function of myeloid cell TLR3 after AP is characterized by the resolution of the inflammatory response, potentially by TLR3-induced clearance of macrophages. Mechanistically, TLR3 induced cell death of macrophages via combined caspase- and RIPK1-dependent pathways. Consistently, myeloid cell-specific *Casp8* deficiency was not sufficient to cause regenerative defects after AP.

Persistent, chronic pancreatitis represents an important risk factor for PDAC (Lowenfels et al., 1993; Kirkegård et al., 2017). Since causal treatments are missing, patients with acute or chronic pancreatitis are treated solely symptomatic by analgesia, fluid substitution, and close monitoring (Carroll et al., 2007). Huang et al. demonstrated that i.p. application of poly(I:C) was sufficient to reduce the severity of AP in a mouse model by limiting the recruitment of neutrophils, inhibiting the generation of ROS, and thereby reducing inflammation (Huang et al., 2019). Our results support the findings of Huang et al by demonstrating the pro-regenerative function of myeloid cell TLR3 in AP. We demonstrated the anti-inflammatory effect of TLR3 signaling in AP, highlighting the therapeutic potential of poly(I:C) for the treatment of AP and CP.

Tlr3 deficiency had no obvious effect on the mere oncogene-driven carcinogenesis in the KPF and KPPF mouse models. In the highly inflammatory context of pancreatitis-induced carcinogenesis, however, myeloid cell TLR3 limited the recruitment and activation of immune cells and thereby prevented the progression of carcinogenesis. In human tumor cells, TLR3 signaling was shown to induce cytokine expression, demonstrating a potential modulation of the tumor microenvironment by tumor cell TLR3. In the KPPF model, TLR3 in myeloid cells had an inhibitory effect on the recruitment of FOXP3⁺ Tregs to the tumor microenvironment. In this thesis, the pro-regenerative effect of TLR3 after acute pancreatitis and its antitumorigenic effect on inflammation-driven PDAC carcinogenesis was demonstrated.

Despite immense research efforts and numerous clinical studies, current therapies for PDAC are still largely ineffective. Standard chemotherapies with FOLFIRINOX or gemcitabine hardly extend patient survival but lead to massive side effects and an impaired quality of life for patients (Conroy et al., 2011). PDAC is characterized by a highly immunosuppressive microenvironment (Zheng et al., 2013; Carpenter et al., 2021). Accordingly, the specific reactivation of the endogenous anti-tumoral immune response by immunotherapy offers a promis-

ing therapeutic concept (Smith et al., 2018; Deutsch et al., 2019; Le Naour et al., 2020).

Previous trials of immunotherapy for PDAC patients failed due to low response rates associated with high toxicity and severe side effects (Royal et al., 2010; Brahmer et al., 2012; O'Reilly et al., 2019; Principe et al., 2021). The efficient reactivation of the endogenous, anti-tumoral immune defense requires improvement of the current therapeutic approaches.

Conventional chemotherapy or radiotherapy causes the release of DAMPs by necrotic tumor cells (Deutsch et al., 2019). DAMPs can be recognized by PRRs of the innate immune system and induce the local immune reaction (Deutsch et al., 2019). Accordingly, there is a focus on the development of PRR agonists as therapeutic adjuvants for tumor therapy to enhance the PRR-mediated activation of the immune response (Smith et al., 2018; Le Naour et al., 2020).

One example involves the cytosolic DNA sensor STING. The combination of conventional radiotherapy and agonists of STING as an immune adjuvant displayed synergistic effects in the treatment of PDAC in mice, through induction of a systemic T cell response and modulation of cytokine expression by macrophages, leading to significantly increased survival of the mice (Baird et al., 2016). The example demonstrates the efficient complementation of conventional therapeutic approaches with modulators of the endogenous anti-tumoral immune response.

dsRNA structures were originally developed for the therapeutic stimulation of interferon secretion against viral infections (Lampson et al., 1967). Recently, several clinical studies demonstrated the efficient usage of TLR3 agonists in tumor therapy (Okada et al., 2011; Mehrotra et al., 2017; Smith et al., 2018; Le Naour et al., 2020). TLR3 agonists serve as an immune adjuvant by stimulating the secretion of proinflammatory interferons and cytokines to trigger the endogenous anti-tumoral immune response. Simultaneously, TLR3 has direct anti-tumor effects by inducing cell death of tumor cells (Chang et al., 2021).

Okada et al. demonstrated in glioblastoma patients that poly-ICLC (poly(I:C) conjugated with lysine and carboxymethylcellulose) as an immunoadjuvant effectively potentiated the immune response in α DC1-based immunotherapy (Okada et al., 2011). The pre-administration of poly(I:C) prior to radiotherapy was documented to cause TLR3-dependent tumor growth retardation by inducing the infiltration of anti-tumoral cytotoxic T cells and stimulation of macrophages (Yoshida et al., 2018). Mehrotra et al. treated patients with pancreatic cancer with peptide-pulsed autologous dendritic cells in combination with poly-ICLC as an immuno-

adjuvant (Mehrotra et al., 2017). The combination therapy was proven to effectively produce tumor-specific T cell populations (Mehrotra et al., 2017).

The studies demonstrate that the efficiency of conventional therapies can be potentiated synergistically by the combinatorial use of TLR3 agonists as immune adjuvants to reactivate cancer immunosurveillance. This enables the effective treatment of highly immunosuppressive tumors like PDAC.

In this thesis, the pro-regenerative effect of TLR3 in myeloid cells in acute pancreatitis, as well as the myeloid cell-specific inhibitory function of TLR3 on inflammation-induced carcinogenesis, was revealed. Further, it was shown that myeloid cell TLR3 modulates the tumor microenvironment in advanced PDAC. The findings presented in this thesis may therefore provide important information for further understanding the mechanisms underlying potential therapeutic effects of TLR3 agonists in the treatment of cancer. Moreover, the results of this project represent a further basic step toward understanding the complex, versatile role of the immune system in tissue regeneration, in the early steps of carcinogenesis, as well as in advanced PDAC. The research results are intended to help develop new therapeutic approaches based on the specific modulation of the immune response.

6 References

- Abdulla, A., Awla, D., Thorlacius, H., and Regnér, S. (2011). Role of neutrophils in the activation of trypsinogen in severe acute pancreatitis. *Journal of leukocyte biology* *90*, 975-982. <https://doi.org/10.1189/jlb.0411195>.
- Alexopoulou, L., Holt, A.C., Medzhitov, R., and Flavell, R. (2001). Recognition of double-stranded RNA and activation of NF- κ B by Toll-like receptor 3. *Nature*.
- Almoguera, C., Shibata, D., Forrester, K., Martin, J., Arnheim, N., and Perucho, M. (1988). Most human carcinomas of the exocrine pancreas contain mutant c-K-ras genes. *Cell* *53*, 549-554. [https://doi.org/10.1016/0092-8674\(88\)90571-5](https://doi.org/10.1016/0092-8674(88)90571-5).
- Azuma, M., Takeda, Y., Nakajima, H., Sugiyama, H., Ebihara, T., Oshiumi, H., Matsumoto, M., and Seya, T. (2016). Biphasic function of TLR3 adjuvant on tumor and spleen dendritic cells promotes tumor T cell infiltration and regression in a vaccine therapy. *Oncoimmunology* *5*, e1188244. <https://doi.org/10.1080/2162402X.2016.1188244>.
- Bachem, M.G., Schünemann, M., Ramadani, M., Siech, M., Beger, H., Buck, A., Zhou, S., Schmid-Kotsas, A., and Adler, G. (2005). Pancreatic carcinoma cells induce fibrosis by stimulating proliferation and matrix synthesis of stellate cells. *Gastroenterology* *128*, 907-921. <https://doi.org/10.1053/j.gastro.2004.12.036>.
- Bailey, P., Chang, D.K., Nones, K., Johns, A.L., Patch, A.-M., Gingras, M.-C., Miller, D.K., Christ, A.N., Bruxner, T.J.C., and Quinn, M.C., et al. (2016). Genomic analyses identify molecular subtypes of pancreatic cancer. *Nature* *531*, 47-52. <https://doi.org/10.1038/nature16965>.
- Baird, J.R., Friedman, D., Cottam, B., Dubensky, T.W., Kanne, D.B., Bambina, S., Bahjat, K., Crittenden, M.R., and Gough, M.J. (2016). Radiotherapy Combined with Novel STING-Targeting Oligonucleotides Results in Regression of Established Tumors. *Cancer research* *76*, 50-61. <https://doi.org/10.1158/0008-5472.CAN-14-3619>.
- Banks, P.A., and Freeman, M.L. (2006). Practice guidelines in acute pancreatitis. *The American journal of gastroenterology* *101*, 2379-2400. <https://doi.org/10.1111/j.1572-0241.2006.00856.x>.

Bartolomei, M.S., Webber, A.L., Brunkow, M.E., and Tilghman, S.M. (1993). Epigenetic mechanisms underlying the imprinting of the mouse H19 gene. *Genes & Development* 7, 1663-1673.

Basturk, O., Hong, S.-M., Wood, L.D., Adsay, N.V., Albores-Saavedra, J., Biankin, A.V., Brosens, L.A.A., Fukushima, N., Goggins, M., and Hruban, R.H., et al. (2015). A Revised Classification System and Recommendations From the Baltimore Consensus Meeting for Neoplastic Precursor Lesions in the Pancreas. *The American journal of surgical pathology* 39, 1730-1741. <https://doi.org/10.1097/PAS.0000000000000533>.

Beatty, G.L., Winograd, R., Evans, R.A., Long, K.B., Luque, S.L., Lee, J.W., Clendenin, C., Gladney, W.L., Knoblock, D.M., and Guirnalda, P.D., et al. (2015). Exclusion of T Cells From Pancreatic Carcinomas in Mice Is Regulated by Ly6C(low) F4/80(+) Extratumoral Macrophages. *Gastroenterology* 149, 201-210. <https://doi.org/10.1053/j.gastro.2015.04.010>.

Bedrosian, A.S., Nguyen, A.H., Hackman, M., Connolly, M.K., Malhotra, A., Ibrahim, J., Cieza-Rubio, N.E., Henning, J.R., Barilla, R., and Rehman, A., et al. (2011). Dendritic cells promote pancreatic viability in mice with acute pancreatitis. *Gastroenterology* 141, 1915-26.e1-14. <https://doi.org/10.1053/j.gastro.2011.07.033>.

Beisner, D.R., Ch'en, I.L., Kolla, R.V., Hoffmann, A., and Hedrick, S.M. (2005). Cutting edge: innate immunity conferred by B cells is regulated by caspase-8. *Journal of immunology (Baltimore, Md. : 1950)* 175, 3469-3473. <https://doi.org/10.4049/jimmunol.175.6.3469>.

Bellone, G., Carbone, A., Smirne, C., Scirelli, T., Buffolino, A., Novarino, A., Stacchini, A., Bertetto, O., Palestro, G., and Sorio, C., et al. (2006). Cooperative induction of a tolerogenic dendritic cell phenotype by cytokines secreted by pancreatic carcinoma cells. *Journal of immunology (Baltimore, Md. : 1950)* 177, 3448-3460. <https://doi.org/10.4049/jimmunol.177.5.3448>.

Bhatia, M., Ramnath, R.D., Chevali, L., and Guglielmotti, A. (2005). Treatment with bindarit, a blocker of MCP-1 synthesis, protects mice against acute pancreatitis. *American journal of physiology. Gastrointestinal and liver physiology* 288, G1259-65. <https://doi.org/10.1152/ajpgi.00435.2004>.

- Bhatia, R., Bhyravbhatla, N., Kisling, A., Li, X., Batram S.K., and Kumar, S. (2022). Cytokines chattering in pancreatic ductal adenocarcinoma tumor microenvironment. *Seminars in Cancer Biology*, 499-510.
- Bianchi, F., Milione, M., Casalini, P., Centonze, G., Le Noci, V.M., Storti, C., Alexiadis, S., Truini, M., Sozzi, G., and Pastorino, U., et al. (2019). Toll-like receptor 3 as a new marker to detect high risk early stage Non-Small-Cell Lung Cancer patients. *Scientific reports* 9, 14288. <https://doi.org/10.1038/s41598-019-50756-2>.
- Bockman, D.E., Boydston, W.R., and Anderson, M.C. (1982). Origin of tubular complexes in human chronic pancreatitis. *American journal of surgery* 144, 243-249. [https://doi.org/10.1016/0002-9610\(82\)90518-9](https://doi.org/10.1016/0002-9610(82)90518-9).
- Bos, J.L., Rehmann, H., and Wittinghofer, A. (2007). GEFs and GAPs: critical elements in the control of small G proteins. *Cell* 129, 865-877. <https://doi.org/10.1016/j.cell.2007.05.018>.
- Braganza, J.M., Lee, S.H., McCloy, R.F., and McMahon, M.J. (2011). Chronic pancreatitis. *The Lancet* 377, 1184-1197. [https://doi.org/10.1016/S0140-6736\(10\)61852-1](https://doi.org/10.1016/S0140-6736(10)61852-1).
- Brahmer, J.R., Tykodi, S.S., Chow, L.Q.M., Hwu, W.-J., Topalian, S.L., Hwu, P., Drake, C.G., Camacho, L.H., Kauh, J., and Odunsi, K., et al. (2012). Safety and activity of anti-PD-L1 antibody in patients with advanced cancer. *The New England Journal of Medicine* 366, 2455-2465. <https://doi.org/10.1056/NEJMoa1200694>.
- Bsibsi, M., Persoon-Deen, C., Verwer, R.W.H., Meeuwssen, S., Ravid, R., and van Noort, J.M. (2006). Toll-like receptor 3 on adult human astrocytes triggers production of neuroprotective mediators. *Glia* 53, 688-695. <https://doi.org/10.1002/glia.20328>.
- Burnet, F.M. (1970). The Concept of Immunological Surveillance. *Progr. exp. Tumor Res.*, 1-27.
- Caroll, J.K., Herrick, B., and Gipson, T. (2007). Acute Pancreatitis: Diagnosis, Prognosis, and Treatment. *American Family Physician*.
- Carpenter, E., Nelson, S., Bednar, F., Cho, C., Nathan, H., Sahai, V., Di Magliano, M.P., and Frankel, T.L. (2021). Immunotherapy for pancreatic ductal adenocarcinoma. *Journal of surgical oncology* 123, 751-759. <https://doi.org/10.1002/jso.26312>.
- Carrière, C., Young, A.L., Gunn, J.R., Longnecker, D.S., and Korc, M. (2009). Acute pancreatitis markedly accelerates pancreatic cancer progression in mice expressing oncogenic Kras. *Bio-*

chemical and Biophysical Research Communications 382, 561-565.
<https://doi.org/10.1016/j.bbrc.2009.03.068>.

Cavassani, K.A., Ishii, M., Wen, H., Schaller, M.A., Lincoln, P.M., Lukacs, N.W., Hogaboam, C.M., and Kunkel, S.L. (2008). TLR3 is an endogenous sensor of tissue necrosis during acute inflammatory events. *The Journal of experimental medicine* 205, 2609-2621.
<https://doi.org/10.1084/jem.20081370>.

Cerami, E., Gao, J., Dogrusoz, U., Gross, B.E., Sumer, S.O., Aksoy, B.A., Jacobsen, A., Byrne, C.J., Heuer, M.L., and Larsson, E., et al. (2012). The cBio cancer genomics portal: an open platform for exploring multidimensional cancer genomics data. *Cancer discovery* 2, 401-404.
<https://doi.org/10.1158/2159-8290.CD-12-0095>.

Chan, W.M., Siu, W.Y., Lau, A., and Poon, R.Y.C. (2004). How many mutant p53 molecules are needed to inactivate a tetramer? *Molecular and Cellular Biology* 24, 3536-3551.
<https://doi.org/10.1128/MCB.24.8.3536-3551.2004>.

Chang, E.H., Gonda, M.A., Ellis, R.W., Scolnick, E.M., and Lowy, D.R. (1982). Human genome contains four genes homologous to transforming genes of Harvey and Kirsten murine sarcoma viruses. *Proceedings of the National Academy of Sciences of the United States of America* 79, 4848-4852. <https://doi.org/10.1073/pnas.79.16.4848>.

Chang, S.-C., Zhang, B.-X., Su, E.C.-Y., Wu, W.-C., Hsieh, T.-H., Salazar, A.M., Lin, Y.-K., and Ding, J.L. (2021). Hiltonol Cocktail Kills Lung Cancer Cells by Activating Cancer-Suppressors, PKR/OAS, and Restraining the Tumor Microenvironment. *International journal of molecular sciences* 22. <https://doi.org/10.3390/ijms22041626>.

Chen, K., Wang, Q., Kornmann, M., Tian, X., and Yang, Y. (2021). The Role of Exosomes in Pancreatic Cancer From Bench to Clinical Application: An Updated Review. *Frontiers in oncology* 11, 644358. <https://doi.org/10.3389/fonc.2021.644358>.

Chew, V., Chen, J., Lee, D., Loh, E., Lee, J., Lim, K.H., Weber, A., Slankamenac, K., Poon, R.T.P., and Yang, H., et al. (2012a). Chemokine-driven lymphocyte infiltration: an early intratumoural event determining long-term survival in resectable hepatocellular carcinoma. *Gut* 61, 427-438. <https://doi.org/10.1136/gutjnl-2011-300509>.

Chew, V., Tow, C., Huang, C., Bard-Chapeau, E., Copeland, N.G., Jenkins, N.A., Weber, A., Lim, K.H., Toh, H.C., and Heikenwalder, M., et al. (2012b). Toll-like receptor 3 expressing tumor

parenchyma and infiltrating natural killer cells in hepatocellular carcinoma patients. *Journal of the National Cancer Institute* *104*, 1796-1807. <https://doi.org/10.1093/jnci/djs436>.

Chin, A.I., Miyahira, A.K., Covarrubias, A., Teague, J., Guo, B., Dempsey, P.W., and Cheng, G. (2010). Toll-like receptor 3-mediated suppression of TRAMP prostate cancer shows the critical role of type I interferons in tumor immune surveillance. *Cancer research* *70*, 2595-2603. <https://doi.org/10.1158/0008-5472.CAN-09-1162>.

Cho, Y., Gorina, S., Jeffrey, P.D., and Pavletich, N.P. (1994). Crystal structure of a p53 tumor suppressor-DNA complex: Understanding tumorigenic mutations. *Science* *265*.

Choe, J., Kelker, M.S., and Wilson, I.A. (2005). Crystal Structure of Human Toll-like Receptor 3 (TLR3) Ectodomain. *Science* *309*, 581-585.

Chun, H.J., Zheng, L., Ahmad, M., Wang, J., Speirs, C.K., Siegel, R.M., Dale, J.K., Puck, J., Davis, J., and Hall, C.G., et al. (2002). Pleiotropic defects in lymphocyte activation caused by caspase-8 mutations lead to human immunodeficiency. *Nature* *419*, 395-399. <https://doi.org/10.1038/nature01063>.

Clause, B.E., Burkhardt, C., Reith, W., Renkawitz, R., and Förster, I. (1999). Conditional gene targeting in macrophages and granulocytes using LysMcre mice. *Transgenic Research* *8*, 265-277.

Conroy, T., Desseigne, F., Ychou, M., Bouché, O., Guimbaud, R., Bécouarn, Y., Adenis, A., Raoul, J.-L., Gourgou-Bourgade, S., and La Fouchardière, C. de, et al. (2011). FOLFIRINOX versus Gemcitabine for Metastatic Pancreatic Cancer. *The New England Journal of Medicine* *364*, 1817-1825.

Corcoran, R.B., Contino, G., Deshpande, V., Tzatsos, A., Conrad, C., Benes, C.H., Levy, D.E., Settleman, J., Engelman, J.A., and Bardeesy, N. (2011). STAT3 plays a critical role in KRAS-induced pancreatic tumorigenesis. *Cancer research* *71*, 5020-5029. <https://doi.org/10.1158/0008-5472.CAN-11-0908>.

Coussens, L.M., and Werb, Z. (2002). Inflammation and cancer. *Nature* *420*, 860-867.

Crippa, S., Salvia, R., Warshaw, A.L., Domínguez, I., Bassi, C., Falconi, M., Thayer, S.P., Zamboni, G., Lauwers, G.Y., and Mino-Kenudson, M., et al. (2008). Mucinous cystic neoplasm of the pancreas is not an aggressive entity: lessons from 163 resected patients. *Annals of surgery* *247*, 571-579. <https://doi.org/10.1097/SLA.0b013e31811f4449>.

Criscimanna, A., Coudriet, G.M., Gittes, G.K., Piganelli, J.D., and Esni, F. (2014). Activated macrophages create lineage-specific microenvironments for pancreatic acinar- and β -cell regeneration in mice. *Gastroenterology* *147*, 1106-18.e11. <https://doi.org/10.1053/j.gastro.2014.08.008>.

Das, A., Sinha, M., Datta, S., Abas, M., Chaffee, S., Sen, C.K., and Roy, S. (2015). Monocyte and macrophage plasticity in tissue repair and regeneration. *The American journal of pathology* *185*, 2596-2606. <https://doi.org/10.1016/j.ajpath.2015.06.001>.

Demols, A., Le Moine, O., Desalle, D., Quertinmont, E., van Laethem, J.-L., and Devière, J. (2000). CD4+ T Cells Play an Important Role in Acute Experimental Pancreatitis in Mice. *Gastroenterology*, 582-590.

Deutsch, E., Chargari, C., Galluzzi, L., and Kroemer, G. (2019). Optimising efficacy and reducing toxicity of anticancer radioimmunotherapy. *The Lancet. Oncology* *20*, e452-e463. [https://doi.org/10.1016/S1470-2045\(19\)30171-8](https://doi.org/10.1016/S1470-2045(19)30171-8).

Di Magliano, M.P., and Logsdon, C.D. (2013). Roles for KRAS in pancreatic tumor development and progression. *Gastroenterology* *144*, 1220-1229. <https://doi.org/10.1053/j.gastro.2013.01.071>.

Diersch, S., Wenzel, P., Szameitat, M., Eser, P., Paul, M.C., Seidler, B., Eser S., Messer, M., Reichert, M., and Pagel, P., et al. (2013). Efemp1 and p27Kip1 modulate responsiveness of pancreatic cancer cells towards a dual PI3K/mTOR inhibitor in preclinical models. *Oncotarget* *4*, 277-288.

Distler, M., Aust, D., Weitz, J., Pilarsky, C., and Grützmann, R. (2014). Precursor lesions for sporadic pancreatic cancer: PanIN, IPMN, and MCN. *BioMed research international* *2014*, 474905. <https://doi.org/10.1155/2014/474905>.

Distler, M., Kersting, S., Niedergethmann, M., Aust, D.E., Franz, M., Rückert, F., Ehehalt, F., Pilarsky, C., Post, S., and Saeger, H.-D., et al. (2013). Pathohistological subtype predicts survival in patients with intraductal papillary mucinous neoplasm (IPMN) of the pancreas. *Annals of surgery* *258*, 324-330. <https://doi.org/10.1097/SLA.0b013e318287ab73>.

Doyle, S.E., Vaidya, S.A., O'Connell, R., Dodgostar, H., Dempsey, P.W., Wu, T.T., Rao, G., Sun, R., Haberland, M.E., and Modlin, R.L., et al. (2002). IRF3 Mediates a TLR3/TLR4-Specific Antiviral Gene Program. *Immunity*, 251-263.

- Dvorak, H.F. (1986). Tumors: Wounds That Do Not Heal. *The New England Journal of Medicine*, 1650-1659.
- Ebihara, T., Azuma, M., Oshiumi, H., Kasamatsu, J., Iwabuchi, K., Matsumoto, K., Saito, H., Taniguchi, T., Matsumoto, M., and Seya, T. (2010). Identification of a polyI:C-inducible membrane protein that participates in dendritic cell-mediated natural killer cell activation. *The Journal of experimental medicine* 207, 2675-2687. <https://doi.org/10.1084/jem.20091573>.
- Elsässer, H.P., Adler, G., and Kern, H.F. (1986). Time Course and Cellular Source of Pancreatic Regeneration Following Acute Pancreatitis in the Rat. *Pancreas*.
- Estornes, Y., Toscano, F., Virard, F., Jacquemin, G., Pierrot, A., Vanbervliet, B., Bonnin, M., Lalaoui, N., Mercier-Gouy, P., and Pachéco, Y., et al. (2012). dsRNA induces apoptosis through an atypical death complex associating TLR3 to caspase-8. *Cell death and differentiation* 19, 1482-1494. <https://doi.org/10.1038/cdd.2012.22>.
- Feldmann, K., Maurer, C., Peschke, K., Teller, S., Schuck, K., Steiger, K., Engleitner, T., Öllinger, R., Nomura, A., and Wirges, N., et al. (2021). Mesenchymal Plasticity Regulated by Prrx1 Drives Aggressive Pancreatic Cancer Biology. *Gastroenterology* 160, 346-361.e24. <https://doi.org/10.1053/j.gastro.2020.09.010>.
- Feoktistova, M., Geserick, P., Kellert, B., Dimitrova, D.P., Langlais, C., Hupe, M., Cain, K., MacFarlane, M., Häcker, G., and Leverkus, M. (2011). cIAPs block Ripoptosome formation, a RIP1/caspase-8 containing intracellular cell death complex differentially regulated by cFLIP isoforms. *Molecular cell* 43, 449-463. <https://doi.org/10.1016/j.molcel.2011.06.011>.
- Ferreira, R.M.M., Sancho, R., Messal, H.A., Nye, E., Spencer-Dene, B., Stone, R.K., Stamp, G., Rosewell, I., Quaglia, A., and Behrens, A. (2017). Duct- and Acinar-Derived Pancreatic Ductal Adenocarcinomas Show Distinct Tumor Progression and Marker Expression. *Cell reports* 21, 966-978. <https://doi.org/10.1016/j.celrep.2017.09.093>.
- Figura, G. von, Fahrenkrog-Petersen, L., Hidalgo-Sastre, A., Hartmann, D., Hüser, N., Schmid, R.M., Hebrok, M., Roy, N., and Esposito, I. (2017). Atypical flat lesions derive from pancreatic acinar cells. *Pancreatology : official journal of the International Association of Pancreatology (IAP) ... [et al.]* 17, 350-353. <https://doi.org/10.1016/j.pan.2017.04.014>.

Figura, G. von, Morris, J.P., Wright, C.V.E., and Hebrok, M. (2014). Nr5a2 maintains acinar cell differentiation and constrains oncogenic Kras-mediated pancreatic neoplastic initiation. *Gut*.

Flores, J.M., Martín-Caballero, J., and García-Fernández, R.A. (2014). p21 and p27 a shared senescence history. *Cell cycle (Georgetown, Tex.)* 13, 1655-1656. <https://doi.org/10.4161/cc.29147>.

Folias, A.E., Penaranda, C., Su, A.L., Bluestone, J.A., and Hebrok, M. (2014). Aberrant innate immune activation following tissue injury impairs pancreatic regeneration. *PloS one* 9, e102125. <https://doi.org/10.1371/journal.pone.0102125>.

Forte, G., Rega, A., Morello, S., Luciano, A., Arra, C., Pinto, A., and Sorrentino, R. (2012). Poly-inosinic-polycytidylic acid limits tumor outgrowth in a mouse model of metastatic lung cancer. *Journal of immunology (Baltimore, Md. : 1950)* 188, 5357-5364. <https://doi.org/10.4049/jimmunol.1103811>.

Freed-Pastor, W.A., and Prives, C. (2012). Mutant p53: one name, many proteins. *Genes & Development* 26, 1268-1286. <https://doi.org/10.1101/gad.190678.112>.

Fukuda, A., Wang, S.C., Morris, J.P., Folias, A.E., Liou, A., Kim, G.E., Akira, S., Boucher, K.M., Firpo, M.A., and Mulvihill, S.J., et al. (2011). Stat3 and MMP7 contribute to pancreatic ductal adenocarcinoma initiation and progression. *Cancer cell* 19, 441-455. <https://doi.org/10.1016/j.ccr.2011.03.002>.

Fullerton, J.N., and Gilroy, D.W. (2016). Resolution of inflammation: a new therapeutic frontier. *Nature reviews. Drug discovery* 15, 551-567. <https://doi.org/10.1038/nrd.2016.39>.

Gabriel, A., Jiao, Q., Yvette, U., Yang, X., Al-Ameri, S.A., Du, L., Wang, Y.-S., and Wang, C. (2020). Differences between KC and KPC pancreatic ductal adenocarcinoma mice models, in terms of their modeling biology and their clinical relevance. *Pancreatology : official journal of the International Association of Pancreatology (IAP) ... [et al.]* 20, 79-88. <https://doi.org/10.1016/j.pan.2019.11.006>.

Gao, J., Aksoy, B.A., Dogrusoz, U., Dresdner, G., Gross, B., Sumer, S.O., Sun, Y., Jacobsen, A., Sinha, R., and Larsson, E., et al. (2013). Integrative analysis of complex cancer genomics and clinical profiles using the cBioPortal. *Science signaling* 6, pl1. <https://doi.org/10.1126/scisignal.2004088>.

- Garbe, C., Eigentler, T.K., Keilholz, U., Hauschild, A., and Kirkwood, J.M. (2011). Systematic review of medical treatment in melanoma: current status and future prospects. *The oncologist* 16, 5-24. <https://doi.org/10.1634/theoncologist.2010-0190>.
- Garcea, G., Dennison, A.R., Steward, W.P., and Berry, D.P. (2005). Role of Inflammation in Pancreatic Carcinogenesis and the Implications for Future Therapy. *Pancreatology* 5, 514-529.
- Garcia-Cattaneo, A., Gobert, F.-X., Müller, M., Toscano, F., Flores, M., Lescure, A., Del Nery, E., and Benaroch, P. (2012). Cleavage of Toll-like receptor 3 by cathepsins B and H is essential for signaling. *Proceedings of the National Academy of Sciences of the United States of America* 109, 9053-9058. <https://doi.org/10.1073/pnas.1115091109>.
- Gillen, S., Schuster, T., zum Meyer Büschenfelde, C., Friess, H., and Kleeff, J. (2010). Preoperative/neoadjuvant therapy in pancreatic cancer: a systematic review and meta-analysis of response and resection percentages. *PLoS medicine* 7, e1000267. <https://doi.org/10.1371/journal.pmed.1000267>.
- Gilroy, D.W., Colville-Nash, P.R., McMaster, S., Sawatzky, D.A., Willoughby, D.A., and Lawrence, T. (2003). Inducible cyclooxygenase-derived 15-deoxy Δ 12-14PGJ2 brings about acute inflammatory resolution in rat pleurisy by inducing neutrophil and macrophage apoptosis. *The FASEB Journal*, 2269-2271.
- Gocheva, V., Wang, H.-W., Gadea, B.B., Shree, T., Hunter, K.E., Garfall, A.L., Berman, T., and Joyce, J.A. (2010). IL-4 induces cathepsin protease activity in tumor-associated macrophages to promote cancer growth and invasion. *Genes & Development* 24, 241-255. <https://doi.org/10.1101/gad.1874010>.
- Guerra, C., Collado, M., Navas, C., Schuhmacher, A.J., Hernández-Porrás, I., Cañamero, M., Rodríguez-Justo, M., Serrano, M., and Barbacid, M. (2011). Pancreatitis-induced inflammation contributes to pancreatic cancer by inhibiting oncogene-induced senescence. *Cancer cell* 19, 728-739. <https://doi.org/10.1016/j.ccr.2011.05.011>.
- Guerra, C., Schuhmacher, A.J., Cañamero, M., Grippo, P.J., Verdaguer, L., Pérez-Gallego, L., Dubus, P., Sandgren, E.P., and Barbacid, M. (2007). Chronic pancreatitis is essential for induction of pancreatic ductal adenocarcinoma by K-Ras oncogenes in adult mice. *Cancer cell* 11, 291-302. <https://doi.org/10.1016/j.ccr.2007.01.012>.

Gukovskaya, A.S., Vaquero, E., Zaninovic, V., Gorelick, F.S., Lusic, A.J., Brennan, M.-L., Holland, S., and Pandol, S.J. (2002). Neutrophils and NADPH oxidase mediate intrapancreatic trypsin activation in murine experimental acute pancreatitis. *Gastroenterology* *122*, 974-984. <https://doi.org/10.1053/gast.2002.32409>.

Habbe, N., Shi, G., Meguid, R.A., Fendrich, V., Esni, F., Chen, H., Feldmann, G., Stoffers, D.A., Konieczny, S.F., and Leach, S.D., et al. (2008). Spontaneous induction of murine pancreatic intraepithelial neoplasia (mPanIN) by acinar cell targeting of oncogenic Kras in adult mice. *Proceedings of the National Academy of Sciences of the United States of America* *105*, 18913-18918. <https://doi.org/10.1073/pnas.0810097105>.

Habtezion, A. (2015). Inflammation in acute and chronic pancreatitis. *Current opinion in gastroenterology* *31*, 395-399. <https://doi.org/10.1097/MOG.0000000000000195>.

Hanahan, D., and Weinberg, R.A. (2011). Hallmarks of cancer: the next generation. *Cell* *144*, 646-674. <https://doi.org/10.1016/j.cell.2011.02.013>.

Hidalgo, M., Cascinu, S., Kleeff, J., Labianca, R., Löhr, J.-M., Neoptolemos, J., Real, F.X., van Laethem, J.-L., and Heinemann, V. (2015). Addressing the challenges of pancreatic cancer: future directions for improving outcomes. *Pancreatology : official journal of the International Association of Pancreatology (IAP) ... [et al.]* *15*, 8-18. <https://doi.org/10.1016/j.pan.2014.10.001>.

Hidalgo-Sastre, A., Kuebelsbeck, L.A., Jochheim, L.S., Stauffer, L.M., Altmayr, F., Johannes, W., Steiger, K., Ronderos, M., Hartmann, D., and Hüser, N., et al. (2021). Toll-like receptor 3 expression in myeloid cells is essential for efficient regeneration after acute pancreatitis in mice. *European journal of immunology* *51*, 1182-1194. <https://doi.org/10.1002/eji.202048771>.

Hingorani, S.R., Petricoin, E.F., Maitra, A., Rajapakse, V., Kinf, C., Jacobetz, M.A., Ross, S., Conrads, T.P., Veenstra, T.D., and Hitt, B.A., et al. (2003). Preinvasive and invasive ductal pancreatic cancer and its early detection in mouse. *Cancer cell*, 437-450.

Hingorani, S.R., Wang, L., Multani, A.S., Combs, C., Deramaudt, T.B., Hruban, R.H., Rustgi, A.K., Chang, S., and Tuveson, D.A. (2005). Trp53R172H and KrasG12D cooperate to promote chromosomal instability and widely metastatic pancreatic ductal adenocarcinoma in mice. *Cancer cell* *7*, 469-483. <https://doi.org/10.1016/j.ccr.2005.04.023>.

- Hiraoka, N., Onozato, K., Kosuge, T., and Hirohashi, S. (2006). Prevalence of FOXP3+ regulatory T cells increases during the progression of pancreatic ductal adenocarcinoma and its premalignant lesions. *Clinical cancer research : an official journal of the American Association for Cancer Research* *12*, 5423-5434. <https://doi.org/10.1158/1078-0432.CCR-06-0369>.
- Hoque, R., Malik, A.F., Gorelick, F., and Mehal, W.Z. (2012). Sterile inflammatory response in acute pancreatitis. *Pancreas* *41*, 353-357. <https://doi.org/10.1097/MPA.0b013e3182321500>.
- Hoque, R., Sohail, M., Malik, A., Sarwar, S., Luo, Y., Shah, A., Barrat, F., Flavell, R., Gorelick, F., and Husain, S., et al. (2011). TLR9 and the NLRP3 Inflammasome Link Acinar Cell Death With Inflammation in Acute Pancreatitis. *Gastroenterology* *1*, 358-369.
- Hruban, R.H., Adsay, N.V., Albores-Saavedra, J., Compton, C., Garrett, E.S., Goodman, S.N., Kern, S.E., Klimstra, D.S., Klöppel, G., and Longnecker, D.S., et al. (2001). Pancreatic Intraepithelial Neoplasia. *The American journal of surgical pathology*, 579-586.
- Huang, C., Chen, S., Zhang, T., Li, D., Huang, Z., Huang, J., Qin, Y., Chen, B., Cheng, G., and Ma, F., et al. (2019). TLR3 Ligand PolyI:C Prevents Acute Pancreatitis Through the Interferon- β /Interferon- α/β Receptor Signaling Pathway in a Caerulein-Induced Pancreatitis Mouse Model. *Frontiers in immunology* *10*, 980. <https://doi.org/10.3389/fimmu.2019.00980>.
- Huang, L., Guo, Z., Wang, F., and Fu, L. (2021). KRAS mutation: from undruggable to druggable in cancer. *Signal transduction and targeted therapy* *6*, 386. <https://doi.org/10.1038/s41392-021-00780-4>.
- Huang, P.-W., and Chang, J.W.-C. (2019). Immune checkpoint inhibitors win the 2018 Nobel Prize. *Biomedical journal* *42*, 299-306. <https://doi.org/10.1016/j.bj.2019.09.002>.
- Ino, Y., Yamazaki-Itoh, R., Shimada, K., Iwasaki, M., Kosuge, T., Kanai, Y., and Hiraoka, N. (2013). Immune cell infiltration as an indicator of the immune microenvironment of pancreatic cancer. *British journal of cancer* *108*, 914-923. <https://doi.org/10.1038/bjc.2013.32>.
- Ischenko, I., D'Amico, S., Rao, M., Li, J., Hayman, M.J., Powers, S., Petrenko, O., and Reich, N.C. (2021). KRAS drives immune evasion in a genetic model of pancreatic cancer. *Nature communications* *12*, 1482. <https://doi.org/10.1038/s41467-021-21736-w>.
- Jang, J.-E., Hajdu, C.H., Liot, C., Miller, G., Dustin, M.L., and Bar-Sagi, D. (2017). Crosstalk between Regulatory T Cells and Tumor-Associated Dendritic Cells Negates Anti-tumor Immuni-

ty in Pancreatic Cancer. *Cell reports* 20, 558-571. <https://doi.org/10.1016/j.celrep.2017.06.062>.

Jeannot, P., Callo, C., Baer, R., Duquesnes, N., Guerra, C., Guillermet-Guibert, J., Bachs, O., and Arnaud, B. (2015). Loss of p27Kip1 promotes metaplasia in the pancreas via the regulation of Sox9 expression. *Oncotarget* 6, 35880-35892.

Jensen, J.N., Cameron, E., Garay, M.V.R., Starkey, T.W., Gianani, R., and Jensen, J. (2005). Recapitulation of elements of embryonic development in adult mouse pancreatic regeneration. *Gastroenterology* 128, 728-741. <https://doi.org/10.1053/j.gastro.2004.12.008>.

Johnson, C.D., and Abu-Hilal, M. (2004). Persistent organ failure during the first week as a marker of fatal outcome in acute pancreatitis. *Gut* 53, 1340-1344. <https://doi.org/10.1136/gut.2004.039883>.

Julier, Z., Park, A.J., Briquez, P.S., and Martino, M.M. (2017). Promoting tissue regeneration by modulating the immune system. *Acta biomaterialia* 53, 13-28. <https://doi.org/10.1016/j.actbio.2017.01.056>.

Kang, J., Hwang, I., Yoo, C., Kim, K.-P., Jeong, J.H., Chang, H.-M., Lee, S.S., Park, D.H., Song, T.J., and Seo, D.W., et al. (2018). Nab-paclitaxel plus gemcitabine versus FOLFIRINOX as the first-line chemotherapy for patients with metastatic pancreatic cancer: retrospective analysis. *Investigational new drugs* 36, 732-741. <https://doi.org/10.1007/s10637-018-0598-5>.

Kang, R., Lotze, M.T., Zeh, H.J., Billiar, T.R., and Tang, D. (2014). Cell death and DAMPs in acute pancreatitis. *Molecular medicine (Cambridge, Mass.)* 20, 466-477. <https://doi.org/10.2119/molmed.2014.00117>.

Karamitopoulou, E. (2019). Tumour microenvironment of pancreatic cancer: immune landscape is dictated by molecular and histopathological features. *British journal of cancer* 121, 5-14. <https://doi.org/10.1038/s41416-019-0479-5>.

Karikó, K., Ni, H., Capodici, J., Lamphier, M., and Weissman, D. (2004). mRNA is an endogenous ligand for Toll-like receptor 3. *The Journal of biological chemistry* 279, 12542-12550. <https://doi.org/10.1074/jbc.M310175200>.

Kawaguchi, Y., Cooper, B., Gannon, M., Ray, M., MacDonald, R.J., and Wright, C.V.E. (2002). The role of the transcriptional regulator Ptf1a in converting intestinal to pancreatic progenitors. *Nature genetics* 32, 128-134. <https://doi.org/10.1038/ng959>.

- Kirkegård, J., Mortensen, F.V., and Cronin-Fenton, D. (2017). Chronic Pancreatitis and Pancreatic Cancer Risk: A Systematic Review and Meta-analysis. *The American journal of gastroenterology* 112, 1366-1372. <https://doi.org/10.1038/ajg.2017.218>.
- Kleeff, J., Whitcomb, D.C., Shimosegawa, T., Esposito, I., Lerch, M.M., Gress, T., Mayerle, J., Drewes, A.M., Rebours, V., and Akisik, F., et al. (2017). Chronic pancreatitis. *Nature reviews. Disease primers* 3, 17060. <https://doi.org/10.1038/nrdp.2017.60>.
- Knudsen, E.S., Vail, P., Balaji, U., Ngo, H., Botros, I.W., Makarov, V., Riaz, N., Balachandran, V., Leach, S., and Thompson, D.M., et al. (2017). Stratification of Pancreatic Ductal Adenocarcinoma: Combinatorial Genetic, Stromal, and Immunologic Markers. *Clinical cancer research : an official journal of the American Association for Cancer Research* 23, 4429-4440. <https://doi.org/10.1158/1078-0432.CCR-17-0162>.
- Kong, B., Bruns, P., Behler, N.A., Chang, L., Schlitter, A.M., Cao, J., Gewies, A., Ruland, J., Fritzsche, S., and Valkovskaya, N., et al. (2018). Dynamic landscape of pancreatic carcinogenesis reveals early molecular networks of malignancy. *Gut* 67, 146-156. <https://doi.org/10.1136/gutjnl-2015-310913>.
- Kopp, J.L., Figura, G. von, Mayes, E., Liu, F.-F., Dubois, C.L., Morris, J.P., Pan, F.C., Akiyama, H., Wright, C.V.E., and Jensen, K., et al. (2012). Identification of Sox9-dependent acinar-to-ductal reprogramming as the principal mechanism for initiation of pancreatic ductal adenocarcinoma. *Cancer cell* 22, 737-750. <https://doi.org/10.1016/j.ccr.2012.10.025>.
- Krah, N.M., La O, J.-P. de, Swift, G.H., Hoang, C.Q., Willet, S.G., Chen Pan, F., Cash, G.M., Bronner, M.P., Wright, C.V., and MacDonald, R.J., et al. (2015). The acinar differentiation determinant PTF1A inhibits initiation of pancreatic ductal adenocarcinoma. *eLIFE* 4. <https://doi.org/10.7554/eLife.07125>.
- Krishna, S.G., Kamboj, A.K., Hart, P.A., Hinton, A., and Conwell, D.L. (2017). The Changing Epidemiology of Acute Pancreatitis Hospitalizations: A Decade of Trends and the Impact of Chronic Pancreatitis. *Pancreas* 46, 482-488. <https://doi.org/10.1097/MPA.0000000000000783>.
- Kuzmickiene, I., Everatt, R., Virviciute, D., Tamosiunas, A., Radisauskas, R., Reklaitiene, R., and Milinaviciene, E. (2013). Smoking and other risk factors for pancreatic cancer: a cohort

study in men in Lithuania. *Cancer epidemiology* 37, 133-139. <https://doi.org/10.1016/j.canep.2012.10.001>.

Lampel, M., and Kern, H.F. (1977). Acute interstitial pancreatitis in the rat induced by excessive doses of a pancreatic secretagogue. *Virchows Arch A Pathol Anat Histol.* 373, 97-117.

Lampson, G.P., Tytell, A.A., Field, A.K., Nemes, M., and Hilleman, M.R. (1967). Inducers of interferon and host resistance, I. double-stranded RNA from extracts of *penicillium funiculosum*. *Biochemistry*, 782-789.

Lanki, M., Seppänen, H., Mustonen, H., Hagström, J., and Haglund, C. (2019). Toll-like receptor 1 predicts favorable prognosis in pancreatic cancer. *PloS one* 14, e0219245. <https://doi.org/10.1371/journal.pone.0219245>.

Le Naour, J., Galluzzi, L., Zitvogel, L., Kroemer, G., and Vacchelli, E. (2020). Trial watch: TLR3 agonists in cancer therapy. *Oncoimmunology* 9, 1771143. <https://doi.org/10.1080/2162402X.2020.1771143>.

Lee, J.W., Komar, C.A., Bengsch, F., Graham, K., and Beatty, G.L. (2016). Genetically Engineered Mouse Models of Pancreatic Cancer: The KPC Model (LSL-Kras(G12D/+); LSL-Trp53(R172H/+); Pdx-1-Cre), Its Variants, and Their Application in Immuno-oncology Drug Discovery. *Current protocols in pharmacology* 73, 14.39.1-14.39.20. <https://doi.org/10.1002/cpph.2>.

Lee, P.J., and Papachristou, G.I. (2019). New insights into acute pancreatitis. *Nature reviews. Gastroenterology & hepatology* 16, 479-496. <https://doi.org/10.1038/s41575-019-0158-2>.

Lerch, M.M., and Gorelick, F.S. Models of Acute and Chronic Pancreatitis. *Gastroenterology* 2014.

Lerch, M.M., and Gorelick, F.S. (2000). Early trypsinogen activation in acute pancreatitis. *Medical Clinics of North America* 3, 549-563. [https://doi.org/10.1016/S0016-5085\(99\)70205-2](https://doi.org/10.1016/S0016-5085(99)70205-2).

Lesina, M., Kurkowski, M.U., Ludes, K., Rose-John, S., Treiber, M., Klöppel, G., Yoshimura, A., Reindl, W., Sipos, B., and Akira, S., et al. (2011). Stat3/Socs3 activation by IL-6 transsignaling promotes progression of pancreatic intraepithelial neoplasia and development of pancreatic cancer. *Cancer cell* 19, 456-469. <https://doi.org/10.1016/j.ccr.2011.03.009>.

- Li, D., Morris, J., Liu, H., Hassan, M.M., Day, R.S., Bondy, M.L., and Abbruzzese, J.L. (2009). Body Mass Index and Risk, Age of Onset and Survival in Patients With Pancreatic Cancer. *JAMA* 301, 2553-2562.
- Li, Z., Tao, Y., Wang, X., Jiang, P., Li, J., Peng, M., Zhang, X., Chen, K., Liu, H., and Zhen, P., et al. (2018). Tumor-Secreted Exosomal miR-222 Promotes Tumor Progression via Regulating P27 Expression and Re-Localization in Pancreatic Cancer. *Cellular physiology and biochemistry : international journal of experimental cellular physiology, biochemistry, and pharmacology* 51, 610-629. <https://doi.org/10.1159/000495281>.
- Liao, G., Lv, J., Ji, A., Meng, S., and Chen, C. (2021). TLR3 Serves as a Prognostic Biomarker and Associates with Immune Infiltration in the Renal Clear Cell Carcinoma Microenvironment. *Journal of oncology* 2021, 3336770. <https://doi.org/10.1155/2021/3336770>.
- Ligorio, M., Sil, S., Malagon-Lopez, J., Nieman, L.T., Misale, S., Di Pilato, M., Ebright, R.Y., Karabacak, M.N., Kulkarni, A.S., and Liu, A., et al. (2019). Stromal Microenvironment Shapes the Intratumoral Architecture of Pancreatic Cancer. *Cell* 178, 160-175.e27. <https://doi.org/10.1016/j.cell.2019.05.012>.
- Liou, G.-Y., Bastea, L., Fleming, A., Döppler, H., Edenfield, B.H., Dawson, D.W., Zhang, L., Bardeesy, N., and Storz, P. (2017). The Presence of Interleukin-13 at Pancreatic ADM/PanIN Lesions Alters Macrophage Populations and Mediates Pancreatic Tumorigenesis. *Cell reports* 19, 1322-1333. <https://doi.org/10.1016/j.celrep.2017.04.052>.
- Liou, G.-Y., Döppler, H., Necela, B., Edenfield, B., Zhang, L., Dawson, D.W., and Storz, P. (2015). Mutant KRAS-induced expression of ICAM-1 in pancreatic acinar cells causes attraction of macrophages to expedite the formation of precancerous lesions. *Cancer discovery* 5, 52-63. <https://doi.org/10.1158/2159-8290.CD-14-0474>.
- Liou, G.-Y., Döppler, H., Necela, B., Krishna, M., Crawford, H.C., Raimondo, M., and Storz, P. (2013). Macrophage-secreted cytokines drive pancreatic acinar-to-ductal metaplasia through NF- κ B and MMPs. *The Journal of cell biology* 202, 563-577. <https://doi.org/10.1083/jcb.201301001>.
- Liu, L., Botos, I., Wang, Y., Leonard, J.N., Shiloach, J., Segal, D.M., and Davies, D.R. (2008). Structural Basis of Toll-Like Receptor 3 Signaling with Double-Stranded RNA. *Science* 320, 376-379. <https://doi.org/10.1126/science.1154994>.

Löhr, M., Klöppel, G., Maisonneuve, P., Lowenfels, A.B., and Lüttges, J. (2005). Frequency of K-ras mutations in pancreatic intraductal neoplasias associated with pancreatic ductal adenocarcinoma and chronic pancreatitis: a meta-analysis. *Neoplasia (New York, N.Y.)* 7, 17-23. <https://doi.org/10.1593/neo.04445>.

Lowenfels, A.B., Maisonneuve, P., Cavallini, G., Ammann, R.W., Lankisch, P.G., Andersen, J.R., Dimagno, E.P., Andren-Sandberg, A., and Domellof, L. (1993). Pancreatitis and the Risk of Pancreatic Cancer. *The New England Journal of Medicine* 328, 1433-1437.

Malkin, D., Li, F.P., Strong, L.C., Fraumeni, J.F., Nelson, C.E., Kim, D.H., Kassel, J., Gryka, M.A., Bischoff, F.Z., and Tainsky, M.A., et al. (1990). Germ Line p53 Mutations in a Familial Syndrome of Breast Cancer, Sarcomas, and Other Neoplasms. *Science*, 1233-1238.

Marik, P.E., and Zaloga, G.P. (2004). Meta-analysis of parenteral nutrition versus enteral nutrition in patients with acute pancreatitis. *BMJ (Clinical research ed.)* 328, 1407. <https://doi.org/10.1136/bmj.38118.593900.55>.

McKay, C., Imrie, C.W., and Baxter, J.N. (1996). Mononuclear Phagocyte Activation and Acute Pancreatitis. *Gastroenterology*, 32-36.

Mehrotra, S., Britten, C.D., Chin, S., Garrett-Mayer, E., Cloud, C.A., Li, M., Scurti, G., Salem, M.L., Nelson, M.H., and Thomas, M.B., et al. (2017). Vaccination with poly(IC:LC) and peptide-pulsed autologous dendritic cells in patients with pancreatic cancer. *Journal of hematology & oncology* 10, 82. <https://doi.org/10.1186/s13045-017-0459-2>.

Merza, M., Hartman, H., Rahman, M., Hwaiz, R., Zhang, E., Renström, E., Luo, L., Mörgelin, M., Regner, S., and Thorlacius, H. (2015). Neutrophil Extracellular Traps Induce Trypsin Activation, Inflammation, and Tissue Damage in Mice With Severe Acute Pancreatitis. *Gastroenterology* 149, 1920-1931.e8. <https://doi.org/10.1053/j.gastro.2015.08.026>.

Miller, K.D., Fidler-Benaoudia, M., Keegan, T.H., Hipp, H.S., Jemal, A., and Siegel, R.L. (2020). Cancer statistics for adolescents and young adults, 2020. *CA: a cancer journal for clinicians* 70, 443-459. <https://doi.org/10.3322/caac.21637>.

Missirlis, P.I., Smailus, D.E., and Holt, R.A. (2006). A high-throughput screen identifying sequence and promiscuity characteristics of the loxP spacer region in Cre-mediated recombination. *BMC genomics* 7, 73. <https://doi.org/10.1186/1471-2164-7-73>.

- Morris, J.P., Cano, D.A., Sekine, S., Wang, S.C., and Hebrok, M. (2010). Beta-catenin blocks Kras-dependent reprogramming of acini into pancreatic cancer precursor lesions in mice. *The Journal of clinical investigation* *120*, 508-520. <https://doi.org/10.1172/JCI40045>.
- Mounzer, R., and Whitcomb, D.C. (2013). Genetics of acute and chronic pancreatitis. *Current opinion in gastroenterology* *29*, 544-551. <https://doi.org/10.1097/MOG.0b013e3283639383>.
- Murakami, Y., Fukui, R., Motoi, Y., Kanno, A., Shibata, T., Tanimura, N., Saitoh, S., and Miyake, K. (2014). Roles of the cleaved N-terminal TLR3 fragment and cell surface TLR3 in double-stranded RNA sensing. *Journal of immunology (Baltimore, Md. : 1950)* *193*, 5208-5217. <https://doi.org/10.4049/jimmunol.1400386>.
- Murtaugh, L.C., and Keefe, M.D. (2015). Regeneration and repair of the exocrine pancreas. *Annual review of physiology* *77*, 229-249. <https://doi.org/10.1146/annurev-physiol-021014-071727>.
- Murtaugh, L.C., and Leach, S.D. (2007). A case of mistaken identity? Nonductal origins of pancreatic "ductal" cancers. *Cancer cell* *11*, 211-213. <https://doi.org/10.1016/j.ccr.2007.02.020>.
- Muzio, M., Bosisio, D., Polentarutti, N., D'amico, G., Stoppacciaro, A., Mancinelli, R., van't Veer, C., Penton-Rol, G., Ruco, L.P., and Allavena, P., et al. (2000). Differential expression and regulation of toll-like receptors (TLR) in human leukocytes: selective expression of TLR3 in dendritic cells. *Journal of immunology* *164*, 5998-6004. <https://doi.org/10.4049/jimmunol.164.11.5998>.
- Nagy, Á., Munkácsy, G., and Gyórfy, B. (2021). Pancancer survival analysis of cancer hall-mark genes. *Scientific reports* *11*, 6047. <https://doi.org/10.1038/s41598-021-84787-5>.
- Nelson, A.M., Reddy, S.K., Ratliff, T.S., Hossain, M.Z., Katseff, A.S., Zhu, A.S., Chang, E., Resnik, S.R., Page, C., and Kim, D., et al. (2015). dsRNA Released by Tissue Damage Activates TLR3 to Drive Skin Regeneration. *Cell stem cell* *17*, 139-151. <https://doi.org/10.1016/j.stem.2015.07.008>.
- Niemela, J., Kuehn, H.S., Kelly, C., Zhang, M., Davies, J., Melendez, J., Dreiling, J., Kleiner, D., Calvo, K., and Oliveira, J.B., et al. (2015). Caspase-8 Deficiency Presenting as Late-Onset Multi-Organ Lymphocytic Infiltration with Granulomas in two Adult Siblings. *Journal of clinical immunology* *35*, 348-355. <https://doi.org/10.1007/s10875-015-0150-8>.

Niknafs, N., Zhong, Y., Moral, J.A., Zhang, L., Shao, M.X., Lo, A., Makohon-Moore, A., Iacobuzio-Donahue, C.A., and Karchin, R. (2019). Characterization of genetic subclonal evolution in pancreatic cancer mouse models. *Nature communications* 10, 5435. <https://doi.org/10.1038/s41467-019-13100-w>.

Nowell, P.C. (1976). The Clonal Evolution of Tumor Cell Populations. *Science* 194, 23-28.

Offield, M.F., Jetton, T.L., Labosky, P.A., Ray, M., Stein, R.W., Magnuson, M.A., Hogan, B., and Wright, C. (1996). PDX-1 is required for pancreatic outgrowth and differentiation of the rostral duodenum. *Development (Cambridge, England)*, 983-995.

Okada, H., Kalinski, P., Ueda, R., Hoji, A., Kohanbash, G., Donegan, T.E., Mintz, A.H., Engh, J.A., Bartlett, D.L., and Brown, C.K., et al. (2011). Induction of CD8+ T-cell responses against novel glioma-associated antigen peptides and clinical activity by vaccinations with {alpha}-type 1 polarized dendritic cells and polyinosinic-polycytidylic acid stabilized by lysine and carboxymethylcellulose in patients with recurrent malignant glioma. *Journal of clinical oncology : official journal of the American Society of Clinical Oncology* 29, 330-336. <https://doi.org/10.1200/JCO.2010.30.7744>.

O'Reilly, E.M., Oh, D.-Y., Dhani, N., Renouf, D.J., Lee, M.A., Sun, W., Fisher, G., Hezel, A., Chang, S.-C., and Vlahovic, G., et al. (2019). Durvalumab With or Without Tremelimumab for Patients With Metastatic Pancreatic Ductal Adenocarcinoma: A Phase 2 Randomized Clinical Trial. *JAMA Oncology*.

Oshiumi, H., Matsumoto, M., Funami, K., Akazawa, T., and Seya, T. (2003). TICAM-1, an adaptor molecule that participates in Toll-like receptor 3-mediated interferon-beta induction. *Nature immunology* 4, 161-167. <https://doi.org/10.1038/ni886>.

Özdemir, B.C., Pentcheva-Hoang, T., Carstens, J.L., Zheng, X., Wu, C.-C., Simpson, T.R., Laklai, H., Sugimoto, H., Kahlert, C., and Novitskiy, S.V., et al. (2014). Depletion of carcinoma-associated fibroblasts and fibrosis induces immunosuppression and accelerates pancreas cancer with reduced survival. *Cancer cell* 25, 719-734. <https://doi.org/10.1016/j.ccr.2014.04.005>.

Padoan, A., Plebani, M., and Basso, D. (2019). Inflammation and Pancreatic Cancer: Focus on Metabolism, Cytokines, and Immunity. *International journal of molecular sciences* 20. <https://doi.org/10.3390/ijms20030676>.

- Paone, A., Starace, D., Galli, R., Padula, F., Cesaris, P. de, Filippini, A., Ziparo, E., and Riccioli, A. (2008). Toll-like receptor 3 triggers apoptosis of human prostate cancer cells through a PKC-alpha-dependent mechanism. *Carcinogenesis* 29, 1334-1342. <https://doi.org/10.1093/carcin/bgn149>.
- Pardoll, D. (2015). Cancer and the Immune System: Basic Concepts and Targets for Intervention. *Seminars in oncology* 42, 523-538. <https://doi.org/10.1053/j.seminoncol.2015.05.003>.
- Peery, A.F., Dellon, E.S., Lund, J., Crockett, S.D., McGowan, C.E., Bulsiewicz, W.J., Gangarosa, L.M., Thiny, M.T., Stizenberg, K., and Morgan, D.R., et al. (2012). Burden of gastrointestinal disease in the United States: 2012 update. *Gastroenterology* 143, 1179-1187.e3. <https://doi.org/10.1053/j.gastro.2012.08.002>.
- Peng, J., Sun, B.-F., Chen, C.-Y., Zhou, J.-Y., Chen, Y.-S., Chen, H., Liu, L., Huang, D., Jiang, J., and Cui, G.-S., et al. (2019). Single-cell RNA-seq highlights intra-tumoral heterogeneity and malignant progression in pancreatic ductal adenocarcinoma. *Cell research* 29, 725-738. <https://doi.org/10.1038/s41422-019-0195-y>.
- Pérez-Mancera, P.A., Guerra, C., Barbacid, M., and Tuveson, D.A. (2012). What we have learned about pancreatic cancer from mouse models. *Gastroenterology* 142, 1079-1092. <https://doi.org/10.1053/j.gastro.2012.03.002>.
- Petrov, M.S., and Yadav, D. (2019). Global epidemiology and holistic prevention of pancreatitis. *Nature reviews. Gastroenterology & hepatology* 16, 175-184. <https://doi.org/10.1038/s41575-018-0087-5>.
- Pförringer, S. (1899). Ueber die Selbstverdauung des Pankreas. *Archiv für pathologische Anatomie und Physiologie und für klinische Medicin*, 126-147.
- Polireddy, K., Singh, K., Pruski, M., Jones, N.C., Manisundaram, N.V., Ponnella, P., Ouellette, M., van Buren, G., Younes, M., and Bynon, J.S., et al. (2019). Mutant p53R175H promotes cancer initiation in the pancreas by stabilizing HSP70. *Cancer letters* 453, 122-130. <https://doi.org/10.1016/j.canlet.2019.03.047>.
- Pradere, J.-P., Dapito, D.H., and Schwabe, R.F. (2014). The Yin and Yang of Toll-like receptors in cancer. *Oncogene* 33, 3485-3495. <https://doi.org/10.1038/onc.2013.302>.

- Principe, D.R., Korc, M., Kamath, S.D., Munshi, H.G., and Rana, A. (2021). Trials and tribulations of pancreatic cancer immunotherapy. *Cancer letters* 504, 1-14. <https://doi.org/10.1016/j.canlet.2021.01.031>.
- Provenzano, P., Cuevas, C., Chang, A.E., Goel, V.K., Hoff, D.D. von, and Hingorani, S.R. (2012). Enzymatic targeting of the stroma ablates physical barriers to treatment of pancreatic ductal adenocarcinoma. *Cancer cell* 21, 418-429.
- Puleo, F., Nicolle, R., Blum, Y., Cros, J., Marisa, L., Demetter, P., Quertinmont, E., Svrcek, M., Elarouci, N., and Iovanna, J., et al. (2018). Stratification of Pancreatic Ductal Adenocarcinomas Based on Tumor and Microenvironment Features. *Gastroenterology* 155, 1999-2013.e3. <https://doi.org/10.1053/j.gastro.2018.08.033>.
- Rahib, L., Smith, B.D., Aizenberg, R., Rosenzweig, A.B., Fleshman, J.M., and Matrisian, L.M. (2014). Projecting cancer incidence and deaths to 2030: the unexpected burden of thyroid, liver, and pancreas cancers in the United States. *Cancer research* 74, 2913-2921. <https://doi.org/10.1158/0008-5472.CAN-14-0155>.
- Rawla, P., Sunkara, T., and Gaduputi, V. (2019). Epidemiology of Pancreatic Cancer: Global Trends, Etiology and Risk Factors. *World journal of oncology* 10, 10-27. <https://doi.org/10.14740/wjon1166>.
- Redecke, V., Wu, R., Zhou, J., Finkelstein, D., Chaturvedi, V., High, A.A., and Häcker, H. (2013). Hematopoietic progenitor cell lines with myeloid and lymphoid potential. *Nature methods* 10, 795-803. <https://doi.org/10.1038/nmeth.2510>.
- Regel, I., Raulefs, S., Benitz, S., Mihaljevic, C., Rieder, S., Leinenkugel, G., Steiger, K., Schlitter, A.M., Esposito, I., and Mayerle, J., et al. (2019). Loss of TLR3 and its downstream signaling accelerates acinar cell damage in the acute phase of pancreatitis. *Pancreatology* 19, 149-157. <https://doi.org/10.1016/j.pan.2018.12.005>.
- Reichert, M., Blume, K., Kleger, A., Hartmann, D., and Figura, G. von (2016). Developmental Pathways Direct Pancreatic Cancer Initiation from Its Cellular Origin. *Stem cells international* 2016. <https://doi.org/10.1155/2016/9298535>.
- Reynolds, A.E., Murray, A.W., and Szostak, J. (1987). Roles of the 2 μ m Gene Products in Stable Maintenance of the 2 μ m Plasmid of *Saccharomyces cerevisiae*. *Molecular and Cellular Biology* 7, 3566-3573.

- Rhim, A.D., Oberstein, P.E., Thomas, D.H., Mirek, E.T., Palermo, C.F., Sastra, S.A., Dekleva, E.N., Saunders, T., Becerra, C.P., and Tattersall, I.W., et al. (2014). Stromal elements act to restrain, rather than support, pancreatic ductal adenocarcinoma. *Cancer cell* 25, 735-747. <https://doi.org/10.1016/j.ccr.2014.04.021>.
- Roshani, R., McCarthy, F., and Hagemann, T. (2014). Inflammatory cytokines in human pancreatic cancer. *Cancer letters* 345, 157-163. <https://doi.org/10.1016/j.canlet.2013.07.014>.
- Royal, R.E., Levy, C., Turner, K., Mathur, A., Hughes, M., Kammula, U.S., Sherry, R.M., Topalian, S.L., Yang, J.C., and Lowy, I., et al. (2010). Phase 2 trial of single agent Ipilimumab (anti-CTLA-4) for locally advanced or metastatic pancreatic adenocarcinoma. *Journal of immunotherapy* (Hagerstown, Md. : 1997) 33, 828-833. <https://doi.org/10.1097/CJI.0b013e3181eec14c>.
- Ruvinsky, A. (1999). Basics of Gametic Imprinting. *Journal of Animal Science*, 228-237.
- Salaun, B., Coste, I., Rissoan, M.-C., Lebecque, S.J., and Renno, T. (2006). TLR3 can directly trigger apoptosis in human cancer cells. *Journal of immunology* 176, 4894-4901. <https://doi.org/10.4049/jimmunol.176.8.4894>.
- Saluja, A.K., Bhagat, L., Lee, H.S., Bhatia, M., Frossard, J.L., and Steer, M.L. (1999). Secretagogue-induced digestive enzyme activation and cell injury in rat pancreatic acini. *The American journal of physiology* 276, G835-42. <https://doi.org/10.1152/ajpgi.1999.276.4.G835>.
- Sapienza, C., Paquette, J., Tran, T.H., and Peterson, A. (1989). Epigenetic and genetic factors affect transgene methylation imprinting. *Development (Cambridge, England)* 107, 165-168. <https://doi.org/10.1242/dev.107.1.165>.
- Sarkar, S.N., Elco, C.P., Peters, K.L., Chattopadhyay, S., and Sen, G.C. (2007). Two tyrosine residues of Toll-like receptor 3 trigger different steps of NF-kappa B activation. *The Journal of biological chemistry* 282, 3423-3427. <https://doi.org/10.1074/jbc.C600226200>.
- Sarles, H., Lebreuil, G., Tasso, F., Figarella, C., Clemene, F., Devaux, M.A., Fagonde, B., and Payan, H. (1971). A comparison of alcoholic pancreatitis in rat and man. *Gut*, 377-388.
- Scarpa, A., Capelli, P., Mukai, K., Zamboni, G., Oda, T., Iacono, C., and Hirohash, S. (1993). Pancreatic Adenocarcinomas Frequently Show p53 Gene Mutations. *American Journal of Pathology* 142, 1534-1543.

Schadendorf, D., Hodi, F.S., Robert, C., Weber, J.S., Margolin, K., Hamid, O., Patt, D., Chen, T.-T., Berman, D.M., and Wolchok, J.D. (2015). Pooled Analysis of Long-Term Survival Data From Phase II and Phase III Trials of Ipilimumab in Unresectable or Metastatic Melanoma. *Journal of clinical oncology : official journal of the American Society of Clinical Oncology* 33, 1889-1894. <https://doi.org/10.1200/JCO.2014.56.2736>.

Schlesinger, Y., Yosefov-Levi, O., Kolodkin-Gal, D., Granit, R.Z., Peters, L., Kalifa, R., Xia, L., Nasereddin, A., Shiff, I., and Amran, O., et al. (2020). Single-cell transcriptomes of pancreatic preinvasive lesions and cancer reveal acinar metaplastic cells' heterogeneity. *Nature communications* 11, 4516. <https://doi.org/10.1038/s41467-020-18207-z>.

Schmid, R.M. (2002). Acinar-to-ductal metaplasia in pancreatic cancer development. *J. Clin. Invest.* 109, 1403-1404. <https://doi.org/10.1172/JCI200215889>.

Schönhuber, N., Seidler, B., Schuck, K., Veltkamp, C., Schachtler, C., Zukowska, M., Eser, S., Feyerabend, T.B., Paul, M.C., and Eser, P., et al. (2014). A next-generation dual-recombinase system for time- and host-specific targeting of pancreatic cancer. *Nature medicine* 20, 1340-1347. <https://doi.org/10.1038/nm.3646>.

Sendler, M., Weiss, F.-U., Golchert, J., Homuth, G., van den Brandt, C., Mahajan, U.M., Par-tecke, L.-I., Döring, P., Gukovsky, I., and Gukovskaya, A.S., et al. (2018). Cathepsin B-Mediated Activation of Trypsinogen in Endocytosing Macrophages Increases Severity of Pan-creatitis in Mice. *Gastroenterology* 154, 704-718.e10. <https://doi.org/10.1053/j.gastro.2017.10.018>.

Seo, W., Eun, H.S., Kim, S.Y., Yi, H.-S., Lee, Y.-S., Park, S.-H., Jang, M.-J., Jo, E., Kim, S.C., and Han, Y.-M., et al. (2016). Exosome-mediated activation of toll-like receptor 3 in stellate cells stimulates interleukin-17 production by $\gamma\delta$ T cells in liver fibrosis. *Hepatology* 64, 616-631. <https://doi.org/10.1002/hep.28729>.

Serhan, C.N., Brain, S.D., Buckley, C.D., Gilroy, D.W., Haslett, C., O'Neill, L.A.J., Perretti, M., Rossi, A.G., and Wallace, J.L. (2007). Resolution of inflammation: state of the art, definitions and terms. *FASEB journal : official publication of the Federation of American Societies for Experimental Biology* 21, 325-332. <https://doi.org/10.1096/fj.06-7227rev>.

- Shankaran, V., Ikeda, H., Bruce, A.T., White, J.M., Swanson, P.E., Old, L.J., and Schreiber, R.D. (2001). IFN γ and lymphocytes prevent primary tumour development and shape tumour immunogenicity. *Nature*, 1107-1111.
- Shi, C., Daniels, J.A., and Hruban, R.H. (2008). Molecular Characterization of Pancreatic Neoplasms. *Adv Anat Pathol* 15, 185-195.
- Singh, V.P., and Chari, S.T. (2005). Protease inhibitors in acute pancreatitis: lessons from the bench and failed clinical trials. *Gastroenterology* 128, 2172-2174. <https://doi.org/10.1053/j.gastro.2005.03.087>.
- Siret, C., Collignon, A., Silvy, F., Robert, S., Cheyrol, T., André, P., Rigot, V., Iovanna, J., van de Pavert, S., and Lombardo, D., et al. (2019). Deciphering the Crosstalk Between Myeloid-Derived Suppressor Cells and Regulatory T Cells in Pancreatic Ductal Adenocarcinoma. *Frontiers in immunology* 10, 3070. <https://doi.org/10.3389/fimmu.2019.03070>.
- Smith, M., García-Martínez, E., Pitter, M.R., Fucikova, J., Spisek, R., Zitvogel, L., Kroemer, G., and Galluzzi, L. (2018). Trial Watch: Toll-like receptor agonists in cancer immunotherapy. *Oncoimmunology* 7, e1526250. <https://doi.org/10.1080/2162402X.2018.1526250>.
- Solomon, S., Das, S., Brand, R., and Whitcomb, D.C. (2012). Inherited pancreatic cancer syndromes. *Cancer journal (Sudbury, Mass.)* 18, 485-491. <https://doi.org/10.1097/PPO.0b013e318278c4a6>.
- Spormann, H., Sokolowski, A., and Letko, G. (1989). Effect of temporary ischemia upon development and histological patterns of acute pancreatitis in the rat. *Pathology - Research and Practice* 184, 507-513. [https://doi.org/10.1016/S0344-0338\(89\)80143-8](https://doi.org/10.1016/S0344-0338(89)80143-8).
- Sternberg, N. and Hamilton, D. (1981). Bacteriophage P1 Site-specific Recombination I. Recombination Between loxP sites. *J. Mol. Biol.*, 467-486.
- Storz, P., and Crawford, H.C. (2020). Carcinogenesis of Pancreatic Ductal Adenocarcinoma. *Gastroenterology* 158, 2072-2081. <https://doi.org/10.1053/j.gastro.2020.02.059>.
- Stöß, C., Laschinger, M., Wang, B., Lu, M., Altmayr, F., Hartmann, D., Hüser, N., and Holzmann, B. (2020). TLR3 promotes hepatocyte proliferation after partial hepatectomy by stimulating uPA expression and the release of tissue-bound HGF. *FASEB journal : official publication of the Federation of American Societies for Experimental Biology*. <https://doi.org/10.1096/fj.202000904R>.

- Sugimoto, M.A., Vago, J.P., Perretti, M., and Teixeira, M.M. (2019). Mediators of the Resolution of the Inflammatory Response. *Trends in immunology* 40, 212-227. <https://doi.org/10.1016/j.it.2019.01.007>.
- Sung, H., Ferlay, J., Siegel, R.L., Laversanne, M., Soerjomataram, I., Jemal, A., and Bray, F. (2021). Global Cancer Statistics 2020: GLOBOCAN Estimates of Incidence and Mortality Worldwide for 36 Cancers in 185 Countries. *CA: a cancer journal for clinicians* 71, 209-249. <https://doi.org/10.3322/caac.21660>.
- Veit, P., Steiner, J.M., and Algül, H. (2014). Early phase of acute pancreatitis: Assessment and management. *World journal of gastrointestinal pathophysiology* 5, 158-168. <https://doi.org/10.4291/wjgp.v5.i3.158>.
- Virchow, R. (1864-1865). *Die krankhaften Geschwülste*. Verlag von August Hirschwald.
- Visser, K.E. de, Eichten, A., and Coussens, L.M. (2006). Paradoxical roles of the immune system during cancer development. *Nature reviews. Cancer* 6, 24-37. <https://doi.org/10.1038/nrc1782>.
- Vogelstein, B., Fearon, E.R., Hamilton, S.R., Kern, S.E., Preisinger, A.C., Leppert, M., Smits, A., and Bos, J.L. (1988). Genetic Alterations during Colorectal-Tumor Development. *The New England Journal of Medicine* 319, 525-532.
- Wagner, M., Greten, F.R., Weber, C.K., Koschnick, S., Mattfeldt, T., Deppert, W., Kern, H., Adler, G., and Schmid, R.M. (2000). A murine tumor progression model for pancreatic cancer recapitulating the genetic alterations of the human disease. *Genes & Development*, 286-293.
- Wagner, R., and Hildt, E. (2019). Zusammensetzung und Wirkmechanismen von Adjuvanzen in zugelassenen viralen Impfstoffen. *Bundesgesundheitsblatt, Gesundheitsforschung, Gesundheitsschutz* 62, 462-471. <https://doi.org/10.1007/s00103-019-02921-1>.
- Wang, G.G., Calvo, K.R., Pasillas, M.P., Sykes, D.B., Häcker, H., and Kamps, M.P. (2006). Quantitative production of macrophages or neutrophils ex vivo using conditional Hoxb8. *Nature methods* 3, 287-293. <https://doi.org/10.1038/nmeth865>.
- Wang, X., Ha, T., Liu, L., Hu, Y., Kao, R., Kalbfleisch, J., Williams, D., and Li, C. (2018). TLR3 Mediates Repair and Regeneration of Damaged Neonatal Heart through Glycolysis Dependent YAP1 Regulated miR-152 Expression. *Cell death and differentiation* 25, 966-982. <https://doi.org/10.1038/s41418-017-0036-9>.

- Wang, X., Lang, M., Zhao, T., Feng, X., Zheng, C., Huang, C., Hao, J., Dong, J., Luo, L., and Li, X., et al. (2017). Cancer-FOXP3 directly activated CCL5 to recruit FOXP3+Treg cells in pancreatic ductal adenocarcinoma. *Oncogene* 36, 3048-3058. <https://doi.org/10.1038/onc.2016.458>.
- Watanabe, T., Kudo, M., and Strober, W. (2017). Immunopathogenesis of pancreatitis. *Mucosal immunology* 10, 283-298. <https://doi.org/10.1038/mi.2016.101>.
- Weber, A., Kirejczyk, Z., Besch, R., Potthoff, S., Leverkus, M., and Häcker, G. (2010). Proapoptotic signalling through Toll-like receptor-3 involves TRIF-dependent activation of caspase-8 and is under the control of inhibitor of apoptosis proteins in melanoma cells. *Cell death and differentiation* 17, 942-951. <https://doi.org/10.1038/cdd.2009.190>.
- Weiss, F.U., Laemmerhirt, F., and Lerch, M.M. (2019). Etiology and Risk Factors of Acute and Chronic Pancreatitis. *Visceral Medicine*, 73-81. <https://doi.org/10.1159/000499138>.
- Weniger, M., Honselmann, K.C., and Liss, A.S. (2018). The Extracellular Matrix and Pancreatic Cancer: A Complex Relationship. *Cancers* 10. <https://doi.org/10.3390/cancers10090316>.
- Werb, Z. (1999). Half the Secret of Life Is outside the Cell. *Cell* 96, 473-474. [https://doi.org/10.1016/S0092-8674\(00\)80644-3](https://doi.org/10.1016/S0092-8674(00)80644-3).
- Whitcomb, D.C. (2010). Genetic aspects of pancreatitis. *Annual review of medicine* 61, 413-424. <https://doi.org/10.1146/annurev.med.041608.121416>.
- Whiteside, T.L. (2015). The role of regulatory T cells in cancer immunology. *ImmunoTargets and therapy* 4, 159-171. <https://doi.org/10.2147/ITT.S55415>.
- Witkiewicz, A.K., McMillan, E.A., Balaji, U., Baek, G., Lin, W.-C., Mansour, J., Mollaei, M., Wagner, K.-U., Koduru, P., and Yopp, A., et al. (2015). Whole-exome sequencing of pancreatic cancer defines genetic diversity and therapeutic targets. *Nature communications* 6, 6744. <https://doi.org/10.1038/ncomms7744>.
- Wood, L.D., and Hruban, R.H. (2012). Pathology and Molecular Genetics of Pancreatic Neoplasms. *Cancer* 18, 492-501.
- Xiao, A.Y., Tan, M.L.Y., Wu, L.M., Asrani, V.M., Windsor, J.A., Yadav, D., and Petrov, M.S. (2016). Global incidence and mortality of pancreatic diseases: a systematic review, meta-analysis, and meta-regression of population-based cohort studies. *The Lancet Gastroenterology & Hepatology* 1, 45-55. [https://doi.org/10.1016/S2468-1253\(16\)30004-8](https://doi.org/10.1016/S2468-1253(16)30004-8).

- Xue, J., Sharma, V., and Habtezion, A. (2014). Immune cells and immune-based therapy in pancreatitis. *Immunologic research* 58, 378-386. <https://doi.org/10.1007/s12026-014-8504-5>.
- Yamamoto, K., Venida, A., Yano, J., Biancur, D.E., Kakiuchi, M., Gupta, S., Sohn, A.S.W., Mukhopadhyay, S., Lin, E.Y., and Parker, S.J., et al. (2020). Autophagy promotes immune evasion of pancreatic cancer by degrading MHC-I. *Nature* 581, 100-105. <https://doi.org/10.1038/s41586-020-2229-5>.
- Yoshida, S., Shime, H., Takeda, Y., Nam, J.-M., Takashima, K., Matsumoto, M., Shirato, H., Kasahara, M., and Seya, T. (2018). Toll-like receptor 3 signal augments radiation-induced tumor growth retardation in a murine model. *Cancer science* 109, 956-965. <https://doi.org/10.1111/cas.13543>.
- Yu, P., Lübben, W., Slomka, H., Gebler, J., Konert, M., Cai, C., Neubrandt, L., Da Prazeres Costa, O., Paul, S., and Dehnert, S., et al. (2012). Nucleic acid-sensing Toll-like receptors are essential for the control of endogenous retrovirus viremia and ERV-induced tumors. *Immunity* 37, 867-879. <https://doi.org/10.1016/j.immuni.2012.07.018>.
- Zhang, H., Neuhöfer, P., Song, L., Rabe, B., Lesina, M., Kurkowski, M.U., Treiber, M., Wartmann, T., Regnér, S., and Thorlacius, H., et al. (2013). IL-6 trans-signaling promotes pancreatitis-associated lung injury and lethality. *The Journal of clinical investigation* 123, 1019-1031. <https://doi.org/10.1172/JCI64931>.
- Zheng, L., Xue, J., Jaffee, E.M., and Habtezion, A. (2013). Role of immune cells and immune-based therapies in pancreatitis and pancreatic ductal adenocarcinoma. *Gastroenterology* 144, 1230-1240. <https://doi.org/10.1053/j.gastro.2012.12.042>.
- Zhou, Q., and Melton, D.A. (2018). Pancreas regeneration. *Nature* 557, 351-358. <https://doi.org/10.1038/s41586-018-0088-0>.
- Zhu, Y., Herndon, J.M., Sojka, D.K., Kim, K.-W., Knolhoff, B.L., Zuo, C., Cullinan, D.R., Luo, J., Bearden, A.R., and Lavine, K.J., et al. (2017). Tissue-Resident Macrophages in Pancreatic Ductal Adenocarcinoma Originate from Embryonic Hematopoiesis and Promote Tumor Progression. *Immunity* 47, 323-338.e6. <https://doi.org/10.1016/j.immuni.2017.07.014>.

Sanjana NE, Shalem O, Zhang F. (2014). Improved vectors and genome-wide libraries for CRISPR screening. *Nat Methods*. 11(8):783-4. doi: 10.1038/nmeth.3047. 10.1038/nmeth.3047 PubMed 25075903

7 Appendix

7.1 Description of preinvasive pancreatic lesions

| Preinvasive lesion | Description from Hruban et al. 2001 |
|---|---|
| Acinar-to-ductal metaplasia (ADM) | <ul style="list-style-type: none"> - Loss of acinar cell markers and expression of ductal, progenitor cell markers - Formation of tubular complexes - Involved in pancreatic regeneration and pancreatic carcinogenesis |
| Pancreatic intraepithelial neoplasia (PanIN1A) | <ul style="list-style-type: none"> - Flat epithelial lesions composed of tall columnar cells - Basally located, round to oval, small nuclei - Abundant supranuclear mucin |
| PanIN1B | <ul style="list-style-type: none"> - Papillary, micropapillary or basally pseudostratified architecture - Otherwise, identical to PanIN1A |
| PanIN2 | <ul style="list-style-type: none"> - Papillary, mucinous epithelial lesions - Nuclear abnormalities including loss of polarity, nuclear crowding, enlarged nuclei, pseudo stratification and hyperchromatism |
| PanIN3/Carcinoma <i>in situ</i> | <ul style="list-style-type: none"> - Usually papillary or micropapillary, cibriforming - Appearance of small epithelial clusters in the lumen and luminal necrosis - Loss of nuclear polarity, abnormal mitosis - Resemble carcinoma at the cytonuclear level, without invasion through the basement membrane |
| Intraductal papillary mucinous neoplasm (IPMN) | <ul style="list-style-type: none"> - Mucinous epithelial neoplasms involving the main pancreatic duct or the major branches - Larger than PanINs |

| | |
|--|--|
| Mucinous cystic neoplasm (MCN) | - Ovarian stroma surrounding the cyst - No connection to the main duct system |
| Atypical flat lesion (AFL) | - Highly proliferative, ductal lesions arising in ADM areas - Tubular structure - Loose but highly cellular stroma |

7.2 Chemicals

| Name | Supplier, Headquarter, Country |
|---|---|
| 4',6-Diamidin-2-phenylindol (DAPI) | Sigma-Aldrich, St. Louis, Missouri, USA |
| Acrylamide solution (30%) | Carl Roth, Karlsruhe, Germany |
| Agarose | Invitrogen, Carlsbad, Kalifornien, USA |
| Alcian blue 8GX | Sigma-Aldrich, St. Louis, Missouri, USA |
| Ammonium persulfate | Sigma-Aldrich, St. Louis, Missouri, USA |
| Antigen Unmasking Solution, Citrate-based | Vector Laboratories, Burlingame, California, USA |
| Biozym Blue S'Green qPCR Mix | Biozym Scientific, Hessisch Oldendorf, Germany |
| Bovine serum albumin | Carl Roth, Karlsruhe, Germany |
| Bromophenol blue | Merck, Darmstadt, Germany |
| Caerulein | Bachem, Bubendorf, Switzerland |
| Chloroform | Sigma-Aldrich, St. Louis, Missouri, USA |
| Cytoflex Daily QC Fluorospheres | Beckman Coulter, Brea, California, USA |
| Dimethylsulfoxid (DMSO) | Sigma-Aldrich, St. Louis, Missouri, USA |
| DirectPCR Lysis Reagent | Viagen Biotech, Los Angeles, California, USA |
| Dithiothreitol (DTT) | Sigma-Aldrich, St. Louis, Missouri, USA |
| DNA Gel Loading Dye, blue 6 x | Thermo Fisher Scientific, Waltham, Massachusetts, USA |
| dNTP-Mix | Thermo Fisher Scientific, Waltham, Massachusetts, USA |
| ECL Western Blotting Substrate | Pierce, Bonn, Germany |
| Eosin Y | Sigma-Aldrich, St. Louis, Missouri, USA |
| Ethanol absolute | Merck, Darmstadt, Germany |
| Ethidium bromide | Carl-Roth, Karlsruhe, Germany |
| Ethylendiamintetraacetat (EDTA) | Carl-Roth, Karlsruhe, Germany |
| Eukitt | Sigma-Aldrich, Stammheim, Germany |
| Formaldehyde (3,5%-3,7%) | Fischar, Saarbrücken, Germany |

| | |
|--|---|
| GeneRuler 1 kb DNA ladder | Thermo Fisher Scientific, Waltham, Massachusetts, USA |
| GeneRuler 100 bp DNA ladder | Thermo Fisher Scientific, Waltham, Massachusetts, USA |
| Hematoxylin | Sigma-Aldrich, St. Louis, Missouri, USA |
| Hydrogenperoxide (H ₂ O ₂ , 30%) | Merck, Darmstadt, Germany |
| Methanol | Merck, Darmstadt, Germany |
| NP-40 | Thermo Fisher Scientific, Waltham, Massachusetts, USA |
| Nuclear Fast Red | Vector Laboratories, Burlingame, California, USA |
| PageRuler Prestained Protein Ladder (10-180 kDa) | Thermo Fisher Scientific, Waltham, Massachusetts, USA |
| PBS powder without Ca ²⁺ | Merck, Darmstadt, Germany |
| Phosphatase inhibitor cocktail, PhosSTOP | Roche, Basel, Switzerland |
| Protease inhibitor cocktail, <i>cOmplete</i> | Roche, Basel, Switzerland |
| RiboLock RNase Inhibitor | Thermo Fisher Scientific, Waltham, Massachusetts, USA |
| RNAlater solution | Thermo Fisher Scientific, Waltham, Massachusetts, USA |
| ROTI GelStain | Carl Roth, Karlsruhe, Germany |
| ROTICLEAR | Carl Roth, Karlsruhe, Germany |
| Sodium chloride | Sigma-Aldrich, St. Louis, Missouri, USA |
| Sodium deoxycholate | Sigma-Aldrich, St. Louis, Missouri, USA |
| Sodium dodecyl sulfate (SDS) | Carl Roth, Karlsruhe, Germany |
| Tetramethylethylenediamine (TEMED) | Bio-Rad Laboratories, Hercules, Kalifornien, USA |
| Tris(hydroxymethyl)-aminomethane | Carl Roth, Karlsruhe, Germany |
| Triton X-100 | Bio-Rad Laboratories, Hercules, Kalifornien, USA |
| TRIzol Reagent | Thermo Fisher Scientific, Waltham, Massachusetts, USA |
| TWEEN-20 | Merck, Darmstadt, Germany |
| β-mercaptoethanol | Sigma-Aldrich, St. Louis, Missouri, USA |

7.3 Enzymes

| Name | Supplier, Headquarter, Country |
|--------------------------------------|---|
| GoTaq G2 Hot Start Green Master Mix | Promega, Madison, Wisconsin, USA |
| Phusion Hot Start II DNA Polymerase | Thermo Fisher Scientific, Waltham, Massachusetts, USA |
| Proteinase K, recombinant, PCR grade | Sigma-Aldrich, St. Louis, Missouri, USA |
| T7 Endonuclease I | New England Biolabs, Ipswich, Massachusetts, USA |

7.4 Buffer

| Name | Composition |
|--------------------------------------|---|
| Laemmli buffer (5x) | Tris-HCl (pH 6.8) 1.5 M SDS 10% (w/v) Glycerol 50% (v/v) DTT 77 mg/ml Bromphenol blue 0.01% (w/v) |
| Lysis Buffer for MTT Assay | HCl 0.1 M SDS 10% |
| PBS-Tw | PBS Tween-20 0.1% (v/v) |
| RIPA buffer | Tris-HCl (pH 7.4) 50 mM NaCl 150 mM NP-40 1% (v/v) Sodium deoxycholate 0.25% (v/v) EDTA (pH 8) 1 mM SDS 0.1% (v/v) |
| SDS-PAGE buffer (5x) | Tris-HCl (pH 7.5) 1.5 M Glycin 0.96 M SDS 0.5% |
| Transfer buffer | Tris-HCl (pH 7.5) 48 mM Glycin 39 mM Methanol 20% |
| TRIS-Acetate-EDTA (TAE) buffer (50x) | Tris-Base (pH 8.0) 2 M Acetic acid 1 M |

| | |
|---|--|
| | EDTA 0.05 M |
| TRIS-Boric acid-EDTA (TBE) buffer (10x) | Tris-Base 0.89 M Boric acid 0.89 M EDTA 0.02 M |

7.5 Commercial kits

| Name | Supplier, Headquarter, Country |
|---|---|
| Annexin V FITC / PI Dead Cell Apoptosis Kit | Thermo Fisher Scientific, Waltham, Massachusetts, USA |
| Avidin Biotin Complex Kit, VECTASTAIN | Vector Laboratories, Burlingame, California, USA |
| DAB substrate Kit | Vector Laboratories, Burlingame, California, USA |
| EnVision + Dual Link System-HRP (DAB+) Kit | Dako, Jena, Germany |
| ExoCET, exosome quantification Kit | System Biosciences, Palo Alto, California, USA |
| ExoQuick, exosome isolation Kit | System Biosciences, Palo Alto, California, USA |
| KAPA Express Extract Kit | Roche, Basel, Switzerland |
| LightCycler 480 SYBR Green I Master | Roche, Basel, Switzerland |
| Mouse on mouse Immunodetection Kit | Vector Laboratories, Burlingame, California, USA |
| Pierce BCA Protein Assay Kit | Thermo Fisher Scientific, Waltham, Massachusetts, USA |
| RevertAid RT Reverse Transcription Kit | Thermo Fisher Scientific, Waltham, Massachusetts, USA |
| RNeasy Mini Kit | Qiagen, Venlo, Netherlands |
| Streptavidin/Biotin blocking Kit | Vector Laboratories, Burlingame, California, USA |

7.6 Consumables

| Name | Supplier, principal office, Country |
|---|--|
| Amersham Protran 0.45 µm nitrocellulose Western blotting membrane | GE Healthcare, Little Chalfont, UK |
| Cell culture plates | Corning, Corning, New York, USA |

| | |
|-----------------------------------|---|
| Cell scraper | Biochrom, Berlin, Germany |
| Cell strainer 100 µm | Corning, Corning, New York, USA |
| Hydrophobic Barrier PAP Pen | Vector Laboratories, Burlingame, California, USA |
| Microvette serum tubes | Sarstedt, Nümbrecht, Germany |
| Pipette tips | BD Biosciences, Franklin Lakes, New Jersey, USA |
| Reaction tubes | Eppendorf, Hamburg, Germany |
| Safe Lock Reactiontubes | Eppendorf, Hamburg, Germany |
| Serological pipettes | Sarstedt, Nürnberg, Germany |
| Superfrost Plus Microscope Slides | Thermo Fisher Scientific, Waltham, Massachusetts, USA |
| Syringe filter, PVDF, 0.22 µm | Starlab, Hamburg, Germany |
| Whatman Blotting Paper | GE Healthcare, Little Chalfont, UK |

7.7 Technical equipment

| Name | Supplier, Headquarter, Country |
|---------------------------------|--|
| Analytical balance BP210S | Sartorius, Göttingen, Germany |
| Autoklav D-65 | Systec, Linden, Germany |
| AxioCam MRm | Carl Zeiss, Jena, Germany |
| AxioObserver Z1 microscope | Carl Zeiss, Jena, Germany |
| Axiovert 100 microscope | Carl Zeiss, Jena, Germany |
| BBD 6220 cell culture incubator | Heraeus, Hanau, Germany |
| Biometra P25T | Analytik Jena, Jena, Germany |
| Bioruptor Sonicator | Diagenode, Liege, Belgium |
| Cell counting chamber | Brand, Wertheim, Germany |
| Cobas 8000 modular analyzer | Roche, Basel, Switzerland |
| Cryostat CM3050S | Leica, Wetzlar, Germany |
| CytoFLEX flow cytometer | Beckman Coulter, Brea, California, USA |
| Electrophoresis chamber | Biometra, Göttingen, Germany |

| | |
|--------------------------------------|---|
| Gel Doc XR | Bio-Rad Laboratories, Hercules, California, USA |
| Herasafe biological safety cabinet | Thermo Fisher Scientific, Waltham, Massachusetts, USA |
| LightCycler 480 Instrument II | Roche, Basel, Switzerland |
| Megafuge centrifuge | Heraeus, Hanau, Germany |
| Microplate reader MRX | Dynex technologies, Chantilly, Virginia, USA |
| Multifuge 35-R | Heraeus, Hanau, Germany |
| NanoDrop ND-1000 | Nanodrop-Technologies, Wilmington, Delaware, USA |
| Sonopuls | Bandelin, Berlin, Germany |
| T3 Thermocycler | Biometra, Göttingen, Germany |
| TissueLyser II | Qiagen, Venlo, Netherlands |
| Trans-Blot SD semi-dry transfer cell | Bio-Rad Laboratories, Hercules, California, USA |
| UVP ChemStudio | Analytik Jena, Jena, Germany |
| UVP GelSolo | Analytik Jena, Jena, Germany |
| Vortex Genie 2 | Scientific Industries, Bohemia, New York, USA |

7.8 Cell culture reagents

| Name | Supplier, Headquarter, Country |
|---------------------------------|---|
| A83-01 | Tocris Bioscience, Bristol, UK |
| Advanced DMEM / F12 | Gibco life technologies, Carlsbad, California, USA |
| Attractene Transfection Reagent | Qiagen, Venlo, Netherlands |
| Biocoll (density 1.090) | Biochrom, Berlin, Germany |
| Blasticidin S | Santa Cruz Biotechnology, Santa Cruz, California, USA |
| Brefeldin A | BD Biosciences, Franklin Lakes, New Jersey, USA |
| Collagen type 1, Rat tail | Corning, Corning, New York, USA |
| Collagenase P, lyophilized | Sigma-Aldrich, St. Louis, Missouri, USA |
| Dexamethasone | Sigma-Aldrich, St. Louis, Missouri, USA |

| | |
|---|---|
| Dulbecco's Modified Eagle Medium (DMEM) | Gibco life technologies, Carlsbad, California, USA |
| Dulbecco's Phosphate Buffered Saline | Gibco life technologies, Carlsbad, California, USA |
| EGF | PeproTech, Rocky Hill, New Jersey, USA |
| Fetal calf serum (FCS) | Gibco life technologies, Carlsbad, California, USA |
| FGF10 | PeproTech, Rocky Hill, New Jersey, USA |
| Fibronectin, human | Roche, Basel, Switzerland |
| Gastrin | Sigma-Aldrich, St. Louis, Missouri, USA |
| Geneticin (G418) | Merck, Darmstadt, Germany |
| HBSS | Gibco life technologies, Carlsbad, California, USA |
| HEPES buffer, 1 M, pH 7.5 | Jena Bioscience, Jena, Germany |
| L-glutamine | Gibco life technologies, Carlsbad, California, USA |
| Lipofectamine Transfection Reagent | Thermo Fisher Scientific, Waltham, Massachusetts, USA |
| Matrigel Matrix, growth factor reduced | Corning, Corning, New York, USA |
| MTT Solution | Sigma-Aldrich, St. Louis, Missouri, USA |
| N-Acetyl cysteine | Sigma-Aldrich, St. Louis, Missouri, USA |
| Necrostatin-1 | Santa Cruz Biotechnology, Santa Cruz, California, USA |
| Nicotinamid | Sigma-Aldrich, St. Louis, Missouri, USA |
| Opti-MEM | Thermo Fisher Scientific, Waltham, Massachusetts, USA |
| Penicillin-Streptomycin | Gibco life technologies, Carlsbad, California, USA |
| poly(I:C) | Sigma-Aldrich, St. Louis, Missouri, USA |
| Puromycin | Sigma-Aldrich, St. Louis, Missouri, USA |
| RPMI 1640 Medium | Gibco life technologies, Carlsbad, California, USA |
| Soybean trypsin inhibitor | Sigma-Aldrich, St. Louis, Missouri, USA |
| Trypan blue solution | Sigma-Aldrich, St. Louis, Missouri, USA |
| Trypsin-EDTA | Gibco life technologies, Carlsbad, California, USA |
| Waymouth's medium | Gibco life technologies, Carlsbad, California, USA |

| | |
|--------------------|---|
| Y27632 | Sigma-Aldrich, St. Louis, Missouri, USA |
| z-VAD-FMK | Santa Cruz Biotechnology, Santa Cruz, California, USA |
| β -Estradiol | Sigma-Aldrich, St. Louis, Missouri, USA |

7.9 Oligonucleotides for RT-qPCR

| Target gene | Species | Sequence (5' → 3') |
|---------------|---------|---------------------------|
| <i>Ccl5</i> | Mouse | TGCAGAGGACTCTGAGACAGC |
| | | GAGTGGTGTCCGAGCCAT |
| <i>Tnf</i> | Mouse | TGCCTATGTCTCAGCCTCTTC |
| | | GAGGCCATTTGGGAACTTCT |
| <i>Tlr3</i> | Mouse | GATACAGGGATTGCACCCATA |
| | | TCCCCAAAGGAGTACATTAGA |
| <i>Il-6</i> | Mouse | GCTACCAAAGTGGATATAATCAGGA |
| | | CCAGGTAGCTATGGTACTCCAGAA |
| <i>Cpa1</i> | Mouse | TCCATCAATGTGCTGAAGT |
| | | GGATGCCAGTGTCAATCCA |
| <i>Krt19</i> | Mouse | ACCCTCCCAGATTACAACC |
| | | CAAGGCGTGTCTGTCTCAA |
| <i>Sox9</i> | Mouse | CCACGTGTGGATGTGGAAG |
| | | CTCAGCTGCTCCGTCTTGAT |
| <i>Il-1b</i> | Mouse | TGTAATGAAAGACGGCACACC |
| | | TCTTCTTTGGGTATTGCTTGG |
| <i>Adgre1</i> | Mouse | GGAGGACTTCTCCAAGCCTATT |
| | | AGGCCTCTCAGACTTCTGCTT |
| <i>Cd3</i> | Mouse | CTGTGCCTCAGCCTCCTAGC |
| | | CGTCACTGTCTAGAGGGCACG |
| <i>Mpo</i> | Mouse | CCCTTCCTAAACTGAACCTGAC |
| | | ATGGCCTCCGTCCTTCTC |
| <i>Ccl2</i> | Mouse | CATCCACGTGTTGGCTCA |
| | | GATCATCTTGCTGGTGAATGAGT |
| <i>Ccnb1</i> | Mouse | GCTTAGCGCTGAAAATTCTTG |
| | | TCTTAGCCAGGTGCTGCATA |
| <i>Cdk1</i> | Mouse | GGACCTCAAGAAGTACCTGGAC |

| | | |
|--------------|-------|---------------------------|
| | | CCCTGGAGGATTTGGTGTAAG |
| <i>Ptf1a</i> | Mouse | ACAAGCCGCTAATGTGCGAGA |
| | | TTGGAGAGGCGCTTTTCGT |
| <i>Il-10</i> | Mouse | CAGAGCCACATGCTCCTAGA |
| | | TGTCCAGCTGGTCCTTTGTT |
| <i>Zeb1</i> | Mouse | AGGTGATCCAGCCAAACG |
| | | GGTGGCGTGGAGTCAGAG |
| <i>Snai1</i> | Mouse | CTTGTGTCTGCACGACCTGT |
| | | CAGGAGAATGGCTTCTCACC |
| <i>Foxp3</i> | Mouse | GCGAAAGTGGCAGAGAGGTA |
| | | CCACAGCATGGGTCTGTCT |
| <i>Krt7</i> | Mouse | AGGAGATGGCCAACCACA |
| | | GGGCCTGGAGTGTCTCAA |
| <i>Hnf4</i> | Mouse | GTGTCAACTGTTTATGTGCCATC |
| | | GTTTCATTTTGACCGCTTCTTTT |
| <i>Gapdh</i> | Mouse | GGAGATTGTTGCCATCAACG |
| | | TTGGTGGTGCAGGATGCATT |
| <i>Rps13</i> | Mouse | TGGGCAAGAACACCATGATG |
| | | AGTTTCTCCAGAGCTGGGTTGT |
| <i>TLR3</i> | Human | AGAGTTGTCATCGAATCAAATTAAG |
| | | AATCTTCCAATTGCGTGAAAA |
| <i>CXCL1</i> | Human | CGAAAAGATGCTGAACAGTGA |
| | | GCCTCTGCAGCTGTGTCTC |
| <i>TNF</i> | Human | CAGCCTCTTCTCCTTCCTGA |
| | | GCCAGAGGGCTGATTAGAGA |
| <i>IL-6</i> | Human | GCCCAGCTATGAACTCCTTCT |
| | | GAAGGCAGCAGGCAACAC |
| <i>CCL1</i> | Human | TTGCTGCTAGCTGGGATGT |
| | | CTGGAGAAGGGTACCTGCAT |
| <i>IL-1a</i> | Human | GGTTGAGTTTAAGCCAATCCA |
| | | TGCTGACCTAGGCTTGATGA |
| <i>IL-1b</i> | Human | TACCTGTCCTGCGTGTTGAA |
| | | TCTTTGGGTAATTTTGGGATCT |
| <i>IL-8</i> | Human | GACCACACTGCGCCAACACA |
| | | CAGCCCTCTTCAAAACTTCCCA |

| | | |
|---------------|-------|---------------------------|
| <i>CCL17</i> | Human | GGCTTCTCTGCAGCACATC |
| | | GGAATGGCTCCCTTGAAGTA |
| <i>TGFb</i> | Human | ACTACTACGCCAAGGAGGTAC |
| | | TGCTTGAACTTGTCATAGATTTTCG |
| <i>CXCL16</i> | Human | TTCCTATGTGCTGTGCAAGAG |
| | | CAGGTATATAATGAACCGGCAGA |
| <i>IL-22</i> | Human | CAACAGGCTAAGCACATGTCA |
| | | ACTGTGTCCTTCAGCTTTTGC |
| <i>VEGFa</i> | Human | GAATGGGGAGCCCAGAGT |
| | | CCACTTCGTGATTCTGC |
| <i>HPRT</i> | Human | GAAAAGGACCCACGAAGTGT |
| | | AGTCAAGGGCATATCCTACAACA |

7.10 Primary and secondary antibodies

| Name | Conjugate | Clonality | origin | Application | Supplier, product number |
|---------------------------------|---------------|------------|--------|-------------|-------------------------------------|
| anti-CPA1 | Unconjugated | Polyclonal | Goat | IHC | RD Systems, AF2765 |
| anti-KRT19 | Unconjugated | Monoclonal | Rabbit | IHC | Abcam, ab133496 |
| anti-Clusterin 1 α | Unconjugated | Polyclonal | Goat | IHC | Santa Cruz, sc-6419 |
| anti-SOX9 | Unconjugated | Polyclonal | Rabbit | IHC | Millipore, AB5535 |
| anti-Ki67 | Unconjugated | Polyclonal | Rabbit | IHC | Abcam, ab833 |
| anti-cleaved caspase 8 (Asp387) | Unconjugated | Monoclonal | Rabbit | WB | Cell Signaling, D5B2 |
| anti-CD3 | Unconjugated | Monoclonal | Rabbit | IHC | Abcam, ab16669 |
| anti-MPO | Unconjugated | Monoclonal | Mouse | IHC | Santa Cruz Biotechnology, sc-390109 |
| anti-F4/80 | Unconjugated, | Monoclonal | Rat | IHC | Abcam, ab16911 |

| | PE | | | | |
|----------------------------|--------------|------------|--------|-----|-----------------------------------|
| anti-CD11b | PE, APC | Monoclonal | Rat | FC | Invitrogen, RM2805 |
| anti-CD115 | APC | Monoclonal | Rat | FC | eBioscience, AFS98 |
| anti-GAPDH | Unconjugated | Monoclonal | Rabbit | WB | Cell Signaling, 14C10 |
| anti- β -Actin | Unconjugated | Monoclonal | Rabbit | WB | Cell Signaling, 8457 |
| anti-IBA1 | Unconjugated | Monoclonal | Rabbit | IHC | Abcam, ab178846 |
| anti- α SMA | Unconjugated | Polyclonal | Rabbit | IHC | Abcam, ab5694 |
| anti-dsRNA | Unconjugated | Monoclonal | Mouse | IF | Jena Bioscience, RNT-SCI-10010200 |
| anti-p-STAT3 | Unconjugated | Monoclonal | Rabbit | WB | Cell Signaling, 9145 |
| anti-STAT3 | Unconjugated | Monoclonal | Rabbit | WB | Cell Signaling, 4904 |
| anti-p-ERK | Unconjugated | Polyclonal | Rabbit | WB | Cell Signaling, 9101 |
| anti--ERK | Unconjugated | Polyclonal | Rabbit | WB | Cell Signaling, 9102 |
| anti-HA | Unconjugated | Monoclonal | Mouse | WB | Cell Signaling, 2367 |
| anti-I κ B α | Unconjugated | Polyclonal | Rabbit | WB | Cell signaling, 9242 |
| anti-p27 | Unconjugated | Monoclonal | Rabbit | WB | Cell Signaling, 3688 |
| anti-p65/RelA | Unconjugated | Monoclonal | Rabbit | IF | Cell Signaling, 8242 |
| anti-TLR3 | Unconjugated | Polyclonal | Rabbit | IF | Novus Biologicals, NBP100-56571 |
| anti-Rabbit IgG (H+L) | HRP | | Goat | WB | Jackson 111-035-144 |

| | | | | | |
|-------------------------|-----------------|------------|-------|-----|----------------------------------|
| anti-Mouse IgG (H+L) | HRP | | Goat | WB | Jackson 115-035-003 |
| anti-Rat IgG (H+L) | HRP | | Mouse | WB | Jackson, 212-036-102 |
| anti-Mouse IgG | Alexa Fluor 488 | | Goat | IF | Thermo Fisher Scientific, A32723 |
| anti-Rabbit IgG | Alexa Fluor 488 | | Goat | IF | Thermo Fisher Scientific, A11008 |
| Anti-Rabbit IgG | Cy3 | | Goat | IF | Jackson, 115-165-003 |
| Anti-CD16/CD32 Fc-Block | | Polyclonal | Rat | IHC | BD Pharmingen, 553141 |

7.11 Optimized genotyping PCR protocols

The optimized PCR protocols used for the genotyping of *Ptf1a-Cre*, *LysM-Cre*, *recombined FSF-Kras^{G12D}*, *LSL-Tlr3*, *WT/LSL-Tlr3* and *Casp8* are listed below:

Ptf1a-Cre:

| | Step | Temperature | Time |
|-----|----------------------|--------------------|--------------|
| | Initial denaturation | 94 °C | 5 min |
| 40x | Denaturation | 94 °C | 30 sec |
| | Annealing | 58 °C | 30 sec |
| | Elongation | 72 °C | 1 min 30 sec |
| | Final elongation | 72 °C | 10 min |
| | Storage | 4 °C | ∞ |

LysM-Cre:

| | Step | Temperature | Time |
|-----|----------------------|--------------------|-------------|
| | Initial denaturation | 94 °C | 5 min |
| 34x | Denaturation | 94 °C | 1 min |
| | Annealing | 58 °C | 1 min |
| | Elongation | 72 °C | 2 min |
| | Final elongation | 72 °C | 10 min |
| | Storage | 4 °C | ∞ |

Recombined FSF-Kras^{G12D}:

| | Step | Temperature | Time |
|-----|----------------------|--------------------|--------------|
| | Initial denaturation | 95 °C | 3 min |
| 40x | Denaturation | 95 °C | 45 sec |
| | Annealing | 60 °C | 1 min |
| | Elongation | 72 °C | 1 min 30 sec |
| | Final elongation | 72 °C | 10 min |
| | Storage | 4 °C | ∞ |

LSL-Tlr3 and WT/LSL-Tlr3:

| | Step | Temperature | Time |
|-----|----------------------|--------------------|-------------|
| | Initial denaturation | 94 °C | 5 min |
| 40x | Denaturation | 94 °C | 30 sec |
| | Annealing | 60 °C | 30 sec |
| | Elongation | 72 °C | 1 min |
| | Final elongation | 72 °C | 10 min |
| | Storage | 4 °C | ∞ |

Casp8

| | Step | Temperature | Time |
|-----|----------------------|--------------------|-------------|
| | Initial denaturation | 94 °C | 3 min |
| 34x | Denaturation | 94 °C | 30 sec |

| | | |
|------------------|-------|--------|
| Annealing | 62 °C | 30 sec |
| Elongation | 72 °C | 30 sec |
| Final elongation | 72 °C | 10 min |
| Storage | 4 °C | ∞ |

Abbreviations

| | |
|--------|---|
| APC | Allophycocyanin |
| ADM | Acinar-to-ductal metaplasia |
| AFL | Atypical flat lesion |
| AP | Acute pancreatitis |
| BreA | Brefeldin A |
| BSA | Bovine serum albumin |
| Cas9 | CRISPR-associated endonuclease 9 |
| CDK | Cyclin-dependent kinase |
| cDNA | Complementary Deoxyribonucleic acid |
| CP | Chronic pancreatitis |
| Cre | Causes recombination |
| CRISPR | Clustered regularly interspaced short palindromic repeats |
| CXCL | CXC motif chemokine ligand |
| DAPI | 4',6-Diamidino-2-Phenylindole |
| DMEM | Dulbecco's modified Eagle medium |
| DMSO | Dimethyl sulfoxide |
| DNA | Deoxyribonucleic acid |
| dNTP | Deoxyribonucleotide triphosphate |
| dsRNA | Double-stranded RNA |
| ECM | Extracellular matrix |
| EDTA | Ethylenediaminetetraacetic acid |
| EGF | Epidermal growth factor |
| EGFR | Epidermal growth factor receptor |
| EMT | Epithelial-to-mesenchymal transition |
| ER | Estrogen receptor |
| ERK | Extracellular signal-regulated kinase |

| | |
|-------|--|
| EtOH | Ethanol |
| FCS | Fetal calf serum |
| FITC | Fluorescein isothiocyanate |
| Flp | Flippase |
| FRT | Flippase recognition target |
| FSF | FRT-stop-FRT |
| GAP | GTPase activating protein |
| GDP | Guanosine-5'-diphosphate |
| GEF | Guanin nucleotide exchange factor |
| GEMM | Genetic engineered mouse model |
| GTP | Guanosine-5'-triphosphate |
| H&E | Hematoxylin and eosin |
| HA | Hemagglutinin |
| Hoxb8 | Homeobox protein 8 |
| HPF | High power field |
| HRP | Horseradish Peroxidase |
| IFN | Interferon |
| IHC | Immunohistochemistry |
| IL | Interleukin |
| IPMN | Intraductal papillary mucinous neoplasm |
| IRF | Interferon regulated factor |
| KRAS | Kirsten rat sarcoma viral oncogene homolog |
| LOH | Loss of heterozygosity |
| loxP | Locus of crossing over P1 |
| LSL | Lox-stop-lox |
| MCN | Mucinous cystic neoplasm |
| mRNA | Messenger RNA |
| mTOR | Mammalian target of rapamycin |

| | |
|----------------|--|
| Nec-1 | Necrostatin 1 |
| NF- κ B | Nuclear factor kappa B |
| PanIN | Pancreatic intraepithelial neoplasia |
| PBS | Phosphate buffered saline |
| PCR | Polymerase chain reaction |
| PDAC | Pancreatic ductal adenocarcinoma |
| Pdx1 | Pancreatic and duodenal homeobox 1 |
| PE | Phycoerythrin |
| PI3K | Phosphoinositide 3-kinase |
| Poly(I:C) | Polyinosinic-polycytidylic acid |
| Ptf1a | Pancreas-specific transcription factor 1 α |
| qPCR | Quantitative polymerase chain reaction |
| RIPK | Receptor-interacting serine/threonine-protein kinase |
| RNA | Ribonucleic acid |
| SDS | Sodium dodecyl sulfate |
| TGF | Transforming growth factor |
| TLR | Toll-like receptor |
| TNF | Tumor necrosis factor |
| TRIF | TIR-domain-containing adapter-inducing interferon- β |
| WT | Wilde-type |
| Z-VAD-FMK | N-Benzyloxycarbonyl-Val-Ala-Asp(O-Me)-Fluoromethylketon |
| α SMA | α smooth muscle actin |

Acknowledgment

First, I would like to thank Prof. Dr. Bernhard Holzmann, Prof. Dr. Guido von Figura, and Prof. Dr. Anglika Schnieke for the supervision of my doctorate and the very helpful and constructive scientific feedback, as well as PD Dr. Daniel Hartmann and Prof. Dr. Norbert Hüser for providing me with a laboratory space.

I would like to thank Leonie Jochheim and Ana Hidalgo-Sastre for their important work on the function of TLR3 in acute pancreatitis.

I would like to express a special gratitude to Thorsten Neuß and Suyang Zhong for the numerous scientific discussions, constructive criticisms, and ideas during my doctorate.

In addition, I would like to thank Melanie Laschinger, Felicitas Altmayr, and Gabriela Holzmann for their manifold support in the laboratory.

I would like to thank Alexandra Berninger for providing the CASP8-deficient mice.

I would also like to thank my friends Ali Altaee, Kevin Schmid, Lina Stauer, and Andreas Sperlich for their help and for lightening the workday.

Finally, I would like to express my deepest gratitude to my beautiful wife Christiane for her support.